ON THE DEVELOPMENT AND EVOLUTION OF CARTILAGE WITHIN NON-CHORDATE METAZOA

by

Alison G. Cole

Submitted in partial fulfillment of the requirements
for the degree of Doctor of Philosophy
at
Dalhousie University
Halifax, Nova Scotia
August, 2004.

Your file Votre référence
ISBN: 0-612-94041-1
Our file Notre référence
ISBN: 0-612-94041-1

DALHOUSIE UNIVERSITY

To comply with the Canadian Privacy Act the National Library of Canada has requested that the following pages be removed from this copy of the thesis:

Preliminary Pages

Examiners Signature Page (pii)

Dalhousie Library Copyright Agreement (piii)

Appendices

Copyright Releases (if applicable)

This is dedicated to my family- for all their love and support through the years

-alison.

Table of Contents

List of Figures

List of Tables

Abstract

Cartilage is a type of connective tissue that is often considered restricted to vertebrates, however cartilaginous tissues are also found within invertebrates. Unfortunately, most definitions and classifications of cartilage suffer from a profound vertebrate bias. I find that cartilage is defined most precisely using histological criteria, considering as criteria the composition of the extracellular matrix and the presence of histologically distinct chondrocytes. I have undertaken a rigorous analysis of connective tissues from a number of representative invertebrate lineages using histology, immunochemistry, and developmental data. I find cartilage to be restricted to molluscs, polychaetes, and arthropods, whereas chondroid connective tissues (which have similar histological and structural properties to cartilage) are much more widespread amongst invertebrate lineages. I have expanded the classification system for cartilage to include a variety of vesicular cartilages, thereby accounting for the diversity of histologies exhibited by invertebrate cartilages.

The degree of homology between invertebrate and vertebrate cartilages has been unclear; phylogenetic relationships between metazoan lineages have undergone a series of revisions in recent years, making the evolutionary relationships between cartilage from different lineages difficult to discern from phylogeny alone. I discuss the relationships between cartilage and other related connective tissues using a supertree phylogeny I created from analysis of metazoan molecular systematics, concluding that cartilages from all lineages likely derived independently from a common chondroid connective tissue; thus forming a family of tissues that can be considered homologous at a tissue-level. Although the precise relationships between cartilages within different lineages remains obscured by the imprecision of current metazoan systematics, patterns in the evolution of cartilage as a tissue type can be elucidated through comparisons of histology and development of invertebrate cartilages.

I have identified a tendency within cephalopod molluscs and sabellid polychaetes towards reduction or loss of cartilages that accompanies decreases in body size. Developmental data collected from cephalopods – wherein cartilages are histologically most similar to vertebrate hyaline cartilage – illustrates that cartilage most often differentiates from uncondensed mesenchymal cells near the end of embryonic development. However, the earliest-forming cartilages differentiate from a cellular condensation in a manner reminiscent of vertebrate primary cartilage formation. Cartilages from sabellid polychaetes form during metamorphosis, and also differentiate from uncondensed mesenchymal cells. These animals can regenerate their cartilages at any stage post-metamorphosis. During regeneration, the growth of the new branchial tentacles mirrors their initial development, including differentiation of cartilage from uncondensed mesenchymal cells.

Further studies are merited to determine the full extent of homology (beyond the level of tissue types) between the various metazoan cartilages, and indeed between cartilages and other similar connective tissues (bone, chordoid, and chondroid), particularly with regards to their molecular composition and specification.

Acknowledgments

A number of people have been involved with various aspects of this thesis, to whom I would like to express my gratitude. Firstly, I wish to thank Eckhard Witten for teaching me much of what I know about histology; Matt Vickaryous for numerous discussion on the histology of skeletal tissues, putting me in contact with Olaf, and for walking me home so many times over the years; Olaf Bininda-Emonds for numerous discussions about supertree construction, and for running a number of analyses; Mike Hart for providing me a forum for phylogenetics discussions, and allowing me access to his computer and phylogenetics software; Brian Hall for introducing me to invertebrate cartilages, providing so much support over the past four years, and enabling me to bring the project to its current conclusion. Thank you; completion of this thesis would not have been possible without you all.

I gratefully acknowledge the following people for their assistance in supplying animal material used throughout the thesis: Matt Vickaryous supplied *Hymenochirus boettgeri* sections (Chapter 1); Dr. Chris Harvey-Clark collected *Terebratulina serpentrionalis* (Chapter 2) and *Myxicola infundibulum* (Chapters 2 and 6); Dr. Eckhard Witten and Andrew Gillis supplied *Salmo salar* sections (Chapter 2); Dr. Ron O'Dor supplied *Illex* specimens (Chapters 2 and 5); Leah Walsh and staff at the National Resource Center for Cephalopods (NRCC) in Galveston TX assisted in the collection of cephalopod species (Chapter 5); Maxine Westhead collected *Fabricia sabella* (Chapter 6). Donna Krailo supplied algae that fed the polychaetes, and Donna Krailo and Hollie Knoll assisted in feeding and caring for *Limulus polyphemus*.

Antibodies used in this work were obtained from the Developmental Studies Hybridoma Bank developed under the auspices of the NICHD and maintained by The University of Iowa, Department of Biological Science, Iowa City, IA 52242. Financial assistance supporting this work came from NSERC grants A5056, 44102 and 40519 to Dr. B.K. Hall and a Dalhousie graduate fellowship.

The following people provided valuable editorial comments on various drafts of the thesis: Tamara Franz-Odendaal, Matt Vickaryous, Tim Fedak, and my supervisor Brian Hall. I also graciously thank Jennifer Legere for translation assistance in creating table 5. Any errors or omissions remaining within the thesis are my own.

Finally, I would like to thank all the 'kids in the hall'-lab 2000 – 2004 for fostering a working environment that was always interesting. Special thanks go to the dear friends I've made in and around the lab – Matt, Tim, Andrew, Tamara, Eckhard, Fiona, Julie, Jae, Max, François, and of course H.H.T.R.H. Pope Rabbi Stone (a.k.a. Jon) – may you always remain part of my life.

Chapter 1: What is Cartilage?

1.1 Introduction[1]

Connective tissues are responsible for much of the variation in animal morphology. Connective tissues are most appropriately considered as a spectrum of tissue types that differ in the organizational complexity of their extracellular matrices, providing the characteristic features for distinguishing types.

At the most basic level, extracellular matrices are composed of two types of molecules: ground substance (glycosaminoglycans, proteoglycans), and fibrous proteins (largely but not exclusively collagen) (Junqueira *et al.* 1998). Much of the diversity in connective tissues arises from different relative amounts of these two components. The extracellular matrix of connective tissue is organized into three regions – the glycocalyx, which immediately surrounds the cell membrane; the pericellular matrix, which interacts with the glycocalyx; the rest of the matrix located outside the pericellular matrix. All animal cells have a glycocalyx and most have some degree of pericellular matrix, whereas more extensive extracellular matrices are largely restricted to connective tissues. The structural organization of the extracellular matrix allows further characterization of connective tissue into more specific types (Maclean and Hall, 1987).

Vertebrate connective tissue types can be distinguished in histological section by the relative amounts of the two different extracellular matrix components, and the orientation of fibrous proteins. For example, regular dense connective tissue (e.g. ligament or tendon) is identifiable by its parallel compact fibres (Ham and Cormack, 1979), distinguishable from irregular dense connective tissue by the directionality of the fibres, and from fibrocartilage by the cell morphology and pericellular matrix. Along this spectrum of connective tissues significant histological overlap exists between different tissue types, sometimes confounding

[1] The following is in press as part of: Cole, A.G. and Hall, B.K. 2004. Cartilage is a metazoan tissue; integrating data from invertebrate sources. – *Acta Zoologica* (Stockholm) **xx**:xxx-xxx

tissue identification. One type of connective tissue deserving further consideration is cartilage.

1.1.1 Cartilage

Cartilage is a tissue that within vertebrates serves important biomechanical and developmental functions: acting as the primary skeleton in elasmobranchs, scaffolding for endochondral bone formation in bony fishes and tetrapods, and forming the articulating surfaces of vertebrate joints. Various authors have identified an ostensibly similar tissue in non-vertebrate taxa (Person and Philpott, 1967, 1969a; Hall, 1978, 2004; Person, 1983; Robson *et al.*, 2000; Wright *et al.*, 2001; see section 1.2), thus cartilage is not a skeletal support tissue found exclusively among vertebrates.

Certain invertebrate cartilages are almost indistinguishable from vertebrate cartilage, but others demonstrate distinct histological morphologies (see Chapter 2). Designation of cartilage amongst invertebrates often has been based solely on the ability of this tissue to exhibit metachromatic staining properties (e.g. Reed and Cloney (1977) for the brachiopod *Terabratalia transversa*). At least amongst vertebrates this feature can be used reliably to identify cartilage due to the high amounts of acidic mucopolysaccharides (glycosaminoglycans) (Ham and Harris, 1950). However, taken alone this observation is insufficient to warrant the designation of "cartilage" to the invertebrate tissue in question, and a critical re-evaluation of these tissues at a histological level is merited.

In the pages that follow I summarize what is known about invertebrate cartilage-like tissues, address the question of defining cartilage and discuss whether or not current definitions are suitable for inclusion of particular invertebrate tissues.

1.2 Distribution of Cartilage-like tissues Amongst Invertebrate Taxa[2]

1.2.1 Cnidaria

Vesicular cells with a thin matrix are found as supporting structures in the umbrella of some medusae and the tentacles of some hydroid polyps (Person and Philpot, 1969a; Schaffer, 1930). Schaffer (1930) credits Koelliker (1864/65) with the first description of cartilage-like tissues in the cnidarians, citing him with reference to both the endodermal origin of these tissues and for stating that they are resistant to alkaline and weak acids, enabling them to be isolated from surrounding tissues. Cells comprising the tentacles of *Tubularia mesembryanthemum* are described as being bubble-like in appearance with the nucleus near the edge of the cell. The nucleus is surrounded by cytoplasm that sends thin extensions towards the cell membrane at the other side of the cell (Schaffer, 1930). These cells show a remarkable similarity in appearance to the notochordal tissues of chordates (Koelliker, cited in Schaffer, 1930). Person and Philpott (1969a) consider these cells to be similar in appearance to cartilage.

1.2.2 Brachiopoda

Stricker and Reed (1987) indicate the presence of a "fibro-cartilage"-like tissue in the proximal portion of the pedicle [fleshy protuberance attaching the animal to the substrate (Brusca and Brusca, 2002)] in adults of the brachiopod *Terabratalia transversa*. Reed and Cloney (1977) describe the connective tissue within the lophophore (feeding tentacles) of the same species as being metachromatic, thereby suggesting it to be cartilaginous.

1.2.3 Polychaeta

Sabellid polychaetes, commonly known as feather-duster worms, have elaborately branched feeding tentacles supported by internal cartilaginous tissue. This tissue begins at the base of the tentacles and extends into each of the branches, or radioles, of the feeding tentacles (Person, 1983). Previous analysis

---

[2] Parts of the following have been accepted for publication in *Zoology*, under the title: "The Nature and Significance of Invertebrate cartilages revisited: Distribution and histology of cartilage and cartilage-like tissues within the Metazoa"

of sectioned material revealed two distinct matrix components, described by the authors as a highly cellularized core (cartilage-like matrix) surrounded by a fibrous region (osteoid-like matrix) thought to be high in collagen (Person and Mathews, 1967). The cartilage-like matrix is reported to lack collagen fibers (Person, 1983). These tissues are reported to be mesodermal in origin (Marschall, 1907 as cited in Person, 1983). Although regeneration of this tissue has not been properly investigated, in *Sabellastarte magnifica* the branchial crown has been observed to regenerate in 11 to 14 days after autotomization with hydrochloric acid (Person, 1983).

Vestimentiferans and pogonophorans are tube dwelling worms that may be closely related to sabellid polychaetes (Rouse and Fauchald, 1997). Andersen *et al.* (2001) describe the extracellular matrix supporting the branchial plume (obteraculum) in the vestimentiferan worm, *Riftia pachyptila*, which includes a high amounts of collagen and mucopolysaccharides (likely chondroitin sulphate; Gaill *et al.*, 1994). Anderson *et al.* (2001) speculate that this tissue may fit Person's definition of invertebrate cartilage (Person and Mathews, 1967; see section 1.5), noting however that the cells residing within this matrix are spindle-shaped (similar to fibroblasts rather than cartilage cells) but surrounded by a basal lamina.

1.2.4 Arthropoda

Cartilage-like tissue has been recognized within arthropods, particularly amongst chelicerates (scorpions, spiders and mites) where it comprises the endosternite (Bitsch and Bitsch, 2002). Hyaline-like cartilaginous tissue also has been reported in the ejaculatory canal of a locust (Martoja and Bassot, 1965 as cited in Person, 1983).

The most thorough description of a cartilaginous endoskeleton within arthropods details that of the horseshoe crab *Limulus polyphemus*. *Limulus* is described as having three separate endoskeletal cartilages (Sekiguchi, 1988);

1) The endosternite, a rectangular plate that lies between the dorsal intestine and the ventral esophagus (also referred to as the supraneural plate (Packard, 1880) and thought to protect the brain);

2) Six opisthomatic endplates each of which underlies the ventral artery at the base of the corresponding opisthomatic appendage;

3) Six pairs of branchial cartilages nested between the opisthosomatic appendages and the entapophyses (in-pocketings of the chitinous exoskeleton).

Anterior to the branchial cartilages is a seventh pair of cartilaginous rods supporting the chilarium (Shultz, 2001; personal observation). The endosternite and branchial cartilages are not considered serially homologous structures, owing to the location of the branchial cartilages below the nerve cord (Bitsch and Bitsch, 2002).

The best-studied arthropod cartilages are those forming the gill bars – branchial cartilages – of horseshoe crabs. Each of these is surrounded by a PAS-negative perichondrium, indicating low glycosaminoglycan content (Person and Philpott, 1969b; Cowden, 1967). Much like the inner cartilaginous region of sabellid worms, *Limulus* cartilage is highly cellular. These cells are incorporated fully into the fibrous matrix as the horseshoe crab ages. Cell division in this tissue is similar to that seen in plants, with the formation of a phragmasome-like structure (Person and Philpott 1969b).

1.2.5 Mollusca

Cartilaginous tissues are abundant in the molluscs, found in two major groups: gastropods (snails and slugs) and cephalopods (squid, octopus and allies). There have been no reports of cartilaginous tissue within bivalves.

Gastropoda

Snails have a rasping organ, the radula, which is used in feeding. This organ is supported by extensive musculature and paired odontophore cartilages, whose evolution and functional significance is discussed by Guralnick and Smith (1999). The odontophore cartilage of the marine whelk, *Busycon canaliculatum* is the most studied histologically. Similar to *Limulus* gill cartilage, the odontophore cartilage consists of highly vacuolated cells with small amounts of matrix (Raven, 1958). The extracellular matrix that surrounds the cartilage cells contains

collagen; myoglobin is found within the cell bodies (Person, 1983). In vegetation-grazing molluscs (e.g. *Lymnea*) the odontophore cartilage contains both chondrocytes (cartilage cells) and muscle cells (Person and Philpott, 1969a).

Delsman (1912, as cited in Raven 1958) described the development of the odontophore cartilage in a snail of the genus *Littorina*. These cartilages arise from a layer of mesenchyme on the ventral side of the radular sac. During development, cells become columnar and are distinguishable from the remainder of the mesoderm. From a single layer, these cells go on to divide and give rise to a multi-layered structure. The cells then vacuolate to give rise to a tissue that appears cartilage-like (Raven, 1958). A similar proliferation of cells gives rise to the odontophorial cartilages of the marine snail *Polinices lewisii* (Page and Pederson, 1998).

Carriker *et al.* (1972) analyzed the regeneration of these cartilages in the marine gastropods *Urosalpinz cinerea, U. c. follyensis,* and *Eupleura caudata etterae*. After amputation, the cartilage and associated musculature regenerates from a blastema-like collection of cells, the cap cells. By eight days post-amputation the different tissue types are histologically differentiated, and the amputated proboscis is fully functional by day 11 (Carriker *et al.*, 1972).

Cephalopoda

An extensive list of the different cartilages within the cuttlefish is reported by Tompsett (1939). These include cartilages associated with the eye (scleral, equatorial, and horseshoe cartilages), mantle (dorsal, pallial, nuchal, and funnel cartilages), dermis (dermal and fin cartilages), and brain (cranial cartilage). The cranial cartilage is the most extensively studied element within cephalopods, likely due to its large size relative to the other cartilages.

The extracellular matrix of the cranial cartilage is extensive in comparison to those of arthropods and gastropods. Within vertebrates the cartilage organ is covered by a perichondrium, a lining of fibroblast-like cells that separates the cartilaginous extracellular matrix from the surrounding tissues. The structure of the cephalopod perichondrium has been most thoroughly studied in the cranial

cartilage of the octopus, *Octopus vulgaris*. Light and electron microscopy revealed the presence of cartilage lining cells (CLC), which separate cartilaginous extracellular matrix from surrounding connective tissue (Bairati *et al.*, 1995). The orbital region of the cranial cartilage has a distinct perichondrium, whereas in other regions of the cranial cartilage a single layer of these CLCs line muscle insertions and blood vessels (Bairati *et al.*, 1995). Chondrocyte morphology varies in accordance with their relative position within the organ.

The most comprehensive analysis of chondrocyte morphology is that of Bairati *et al.* (1998). Cells at the periphery of the cartilage organ are flattened and elongated, with their long axis parallel to the axis of the organ. Cells located internally are either round or irregular in shape, with extensive cellular processes extending into the extracellular matrix. The cell processes of irregular shaped cells show greater ramification than those of rounder cells. Cells within the matrix are comparable with differentiated chondrocytes, as indicated by the presence of microtubules, rough endoplasmic reticulum, and vesicles within the processes. These features are suggestive of embedded chondrocytes being the site of synthesis and transport activity of matrix molecules, contributing to the growth of the matrix (Bairati *et al.*, 1998). This postulation is further supported by the presence of junctions, or adhesion plaques, between cell processes and matrix as evidenced by TEM, rendering the entire organ a "functional syncytium" (Bairati *et al.*, 1998).

These data suggest that differentiated cells are those within the matrix, and not those at the periphery as suggested by Cowden (1967) based upon the compaction of cells at the periphery, the round shape of cells internally, and the presence of 'strings' of cells within this region. Compaction of cells, and nucleoli within the nuclei, are considered signs of differentiated cells, thus Cowden (1967) reasoned that cells were generated deep within the matrix and migrate towards the periphery where they differentiate fully. It is likely that growth of the matrix occurs via secretion of molecules from cells located internally, *and* addition of cells to the matrix from the periphery, allowing for the organ to continue increasing in size with growth of the organism.

Connections between chondrocytes as described for cephalopod cartilage are absent in vertebrates and have not been reported from other invertebrate cartilages. This may be a reflection of the fact that no one has studied these tissues in the other invertebrate groups with the electron microscope, suggesting that similar cell-cell connections may be present in other invertebrate cartilaginous tissues as well.

1.2.6 Hemichordata

Enteropneust hemichordates have cartilage-like skeletal tissue supporting their gills and proboscis (Kowalewsky, 1867), derived from hypertrophy of epidermal basement membranes (Benito and Pardos, 1997). Both of these structures are collagenous (Benito and Pardos, 1997). The gill bars and proboscis skeleton in *Saccoglossus pusillus* and *S. bromophenolosus* are reported to stain with Alcian Blue (Smith *et al.*, 2003) suggesting the presence of acidic mucopolysaccharides, possibly chondroitin sulphate.

1.2.7 Urochordata

Person and Philpott (1969a) indicate the presence of ectodermally derived cartilaginous elements in Urochordates. It is not clear which structures the authors are referring to, and to my knowledge these have not been investigated further.

Given the diversity of tissues described above, at what point should a connective tissue with cartilage-like extracellular matrix properties be identified as cartilage, and what does this mean for how we assess the homology of such tissues? The ability to identify cartilage and/or cartilage-like [chondroid] connective tissues reliably is a prerequisite to answering these questions.

1.3 What Is Cartilage?

Considering the diversity of tissues that have been called cartilage and their morphological and histological complexity, it comes as no surprise that working definitions and classifications of cartilage were developed in the context for which

they were employed (Moss and Moss-Salentijn, 1983). Vertebrate cartilage has been classified based upon positional (e.g. articular cartilage), developmental (e.g. primary vs. secondary cartilage), and histological (e.g. hyaline cartilage) criteria. Of these, the histological analyses are by far the most useful, since other classifications rely heavily on taxon-specific characters. Taylor *et al.* (1994) demonstrate the utility of using histological analyses for classifying previously undescribed skeletal tissues in the yellow perch (*Perca flavescens*) through comparisons of the histology of perch tissue with other vertebrate skeletal tissues.

1.3.1 Histological classification

On the basis of histology, mammalian cartilages can be classified as hyaline, fibrous, or elastic. Images of mammalian hyaline cartilage are prevalent in histology textbooks as typifying cartilage. Hyaline cartilage has an abundant metachromatic matrix, and the chondrocytes exhibit a spherical morphology (fig. 1a). Hyaline cartilage differs from elastic cartilage in that the extracellular matrix of the latter contains elastin in addition to fibrous protein (collagen) and glycosaminoglycan (chondroitin sulphate) (Ham and Cormack, 1979). Fibrocartilage is a tissue in which the extracellular matrix has a higher fibrous content, similar to dense connective tissue but with cells that exhibit a typical rounded chondrocyte morphology as opposed to the flattened morphology of fibrocytes (Beresford, 1981)

Detailed histological analysis of cartilages found in teleost fish led Benjamin (1990) to establish yet another broad category of cartilage. Cell-rich cartilages are cartilaginous tissue where >50% of the tissue volume is comprised of cells rather than extracellular matrix. Cell-rich cartilages can be further subdivided into a number of distinct classes, based upon histological features of the tissue. These include the hyaline-cell cartilages (having cells with chromophobic cytoplasm), *Zellknorpel* (having a more rigid matrix than hyaline-cell cartilages), and cell-rich cartilages that can be further categorized into hyaline, fibro- and

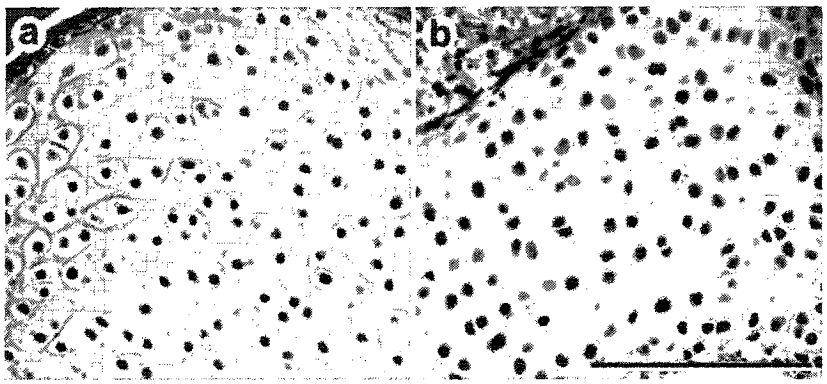

Figure 1: Histology of cartilage within vertebrates and cephalopods
Cartilage found within both vertebrate and cephalopod molluscs shows remarkable histological similarity. Masson's trichrome staining, scale bar = 100 µm. **a** Articulating cartilage in the hind limb of a dwarf African frog (*Hymenochirus boettgeri*). **b** Funnel cartilage in a squid of the genus *Illex.*

elastic cell-rich cartilages based upon matrix properties (Schaffer, 1930; Benjamin, 1990).

Classification of cartilaginous tissues into the aforementioned types should not be restricted to vertebrate tissues, given that many invertebrates have cartilage. Although consideration of tissue homology is important, the appearance of cartilage in two distinct groups says nothing of its qualities, only its origin. The primary concern here is the identification and categorization of connective tissues as cartilage based on histological properties, regardless of phylogenetic origin (which will be discussed later; Chapter 4). Restricting the definition of cartilage to include only tissues that can be clearly linked through common descent (homology) would disallow the notion of cephalopod "cartilage", thereby eliminating the ability to identify this tissue based solely upon histological criteria.

Cephalopod cartilage is largely indistinguishable from vertebrate hyaline cartilage at the light microscopic level (fig. 1b). However, at the ultrastructural level these tissues do demonstrate differences; cephalopod chondrocytes have cell processes that make cell-cell connections with neighbouring chondrocytes (Bairati *et al.*, 1998), similar to vertebrate osteocytes (Holtrop, 1990), whereas there are no reports of such cell-cell connections in any vertebrate cartilages (Kuettner and Pauli, 1983).

As terminally differentiated cells, vertebrate osteocytes and chondrocytes secrete different types and amounts of extracellular substances resulting in different extracellular matrices. Some invertebrate cartilages (e.g. those in sabellid polychaetes) can be distinguished from vertebrate cartilages by the presence of large vacuoles within the chondrocytes. This feature is more common in histological appearance to vertebrate notochordal or small adipose cells (Schaffer, 1930). However, such structural differences demonstrated by invertebrate non-mineralized endoskeletal tissues are not sufficient to warrant abandoning the designation "cartilage". Rather, they suggest current classification schemes need broadening to encompass the large spectrum of cartilaginous tissues.

1.4 Identifying Cartilage

1.4.1 Chondrocytes

Vertebrate chondrocytes are large round cells that differ morphologically from some connective tissue cell types such as fibrocytes and osteocytes, which are usually flat with elongate processes. This spherical cell morphology is critical for the production of cartilage-specific matrix molecules within vertebrates (see Benjamin *et al.*, 1994 for review). However, amongst vertebrate skeletal tissues there is considerable overlap in cell morphology relative to identified tissue type (e.g. Taylor *et al.*, 1994).

Often, designation of a tissue as a type of cartilage ultimately depends upon the presence of chondrocytes within the tissue (e.g. fibrocartilage). However, identification of a chondrocyte is based on what appear to be rather tautological principles. A chondrocyte is a cartilage cell, identifiable by the fact that it is found within a cartilaginous matrix. In culture, cells are designated as chondrocytes when they begin to secrete the matrix that ultimately forms the cartilage. Interestingly, even stromal cells (fibroblasts) from adipose tissue can be induced to produce cartilage matrix when cultured in conditions that support a three-dimensional cell morphology (Erickson *et al.*, 2002). Vertebrate chondrocytes secrete type II and X collagens and chondroitin sulphates whereas osteocytes secrete type I collagen, bone sialoprotein, osteonectin, osteocalcin and osteopontin. Therefore a cartilage cell (chondrocyte) is distinguishable from an osteocyte or fibroblast largely by the *combination* of molecules that it secretes into its extracellular matrix. Hall (1970a,b) even suggests that the composition of the extracellular matrix, in particular synthesis of chondroitin sulphates, regulates the fate of connective tissue stem cells as chondrocytes as opposed to becoming osteocytes.

1.4.2 Extracellular matrix

Although it has become apparent that some of the molecules that constitute the extracellular matrix of vertebrate cartilage are largely restricted to cartilage, these are in the minority, and in some cases their cartilage specificity is suspect.

Nonetheless, vertebrate cartilage has been, and continues to be, recognized by the synthesis of a handful of specific molecules. The most prominent member of this list is type II collagen, which is consistently used by tissue culture researchers as an indicator of chondrocyte differentiation (e.g. Erickson *et al.*, 2002). The rationale for this notion is that cells synthesize cell-specific molecules, and that production of these molecules is diagnostic for the cell type, even if other characteristics are not evident.

Collagen

Collagen molecules are composed of three polypeptide chains that form a triple helix. At least 42 collagen genes are present in the human genome, each producing a distinct polypeptide chain, and any three chains can be combined to make a functional collagen molecule (Myllyharju and Kivirikko, 2004). Collagen types are named according to the order in which they were discovered (Hay, 1981). To date, 27 different collagen types have been identified in vertebrates (Myllyharju and Kivirikko, 2004). These collagen types differ in polypeptide composition, with type I collagen composed of two α1(I) chains and a single α2(I) chain whereas type II collagen is composed of three α1(II) chains (Hay, 1981).

One distinction between cartilage and other skeletal tissues within vertebrates is that the former tissue has a high proportion of type II collagen; most other connective tissue predominantly use type I collagen. Although type II collagen is abundant in the cartilage of vertebrates, it is not restricted to this tissue type. Type II collagen is also found in the vitreous humour of the eye (Ayad and Weiss, 1984), the developing corneal epithelium (Hayashi *et al.*, 1988), and epithelial basement membranes during epithelial-mesenchyme interactions (Wood *et al.*, 1991). However, because type II collagen is much more abundant in vertebrate hyaline cartilage than in these other tissues, the practice of using abundant type II collagen as a marker for cartilage differentiation remains useful for studies of tetrapod cartilaginous tissues.

It is now known that abundant type II collagen is not a reliable marker outside of tetrapods. In many teleost fishes type II collagen antibodies fail to recognise all

cartilaginous tissues (Benjamin and Ralphs, 1991). Additionally, Benjamin and Ralphs (1991) report type II collagen antibody expression in bone of some teleost fish and three species showed extensive staining for collagen II throughout the dense connective tissue.

If type II collagen is regarded as exclusively a cartilage molecule, then its expression in bone or connective tissue is unexpected, indeed it is contra indicated. All cells from most vertebrates contain the gene for type II collagen and this fibrous protein is regularly expressed by osteoblasts during the early stages of bone formation (usually in association with initial deposition of osteoid) although it is rarely seen once the matrix mineralizes (Scott-Savage and Hall, 1979; Jacenko and Tuan, 1986). Whereas type II collagen is the defining feature of primary cartilage in terrestrial vertebrates, both secondary cartilage [cartilages arising on membrane bones relatively late in development (Beresford, 1981)] and shark cartilage contain high proportions of type I collagen in addition to type II collagen (Rama and Chandrakasan, 1984).

Amongst basal-most extant craniates, the so-called 'agnathans' (e.g. lamprey and hagfish), there are cartilages in which both collagen (in hagfish type 2 cartilage) or the lack of collagen (in hagfish types 1 and 3 cartilage, and all lamprey cartilage) may be featured (Wright *et al.*, 1998, 2001; Robson *et al.*, 2000). Despite the absence of type II collagen from the cartilages of 'agnathans', this molecule is expressed in the notochord. Robson *et al.* (2000) therefore suggest that type II collagen "originated as a notochord protein, and only became the predominant structural protein of cartilage matrix some time after the divergence of the jawless fish from the vertebrate ancestral line" (p. 290).

Following this assertion, should cartilage be found in other metazoan phyla, it would be expected to lack type II collagen. To date, type II collagen has not been found in any invertebrate. Whether or not type II collagen is also used in the notochord of other non-vertebrate chordates (e.g. Urochordata) is not known. Investigations considering the evolution of fibrillar collagens have revealed that vertebrate collagen types are more closely related to one-another than to their invertebrate counterparts, indicating that the diversity of collagen types found in

vertebrates evolved within the vertebrate lineage (Boot-Handford and Tuckwell, 2003). All the above points suggest type II collagen is not a prerequisite for cartilaginous tissues, and thus should not be used to define cartilage as a tissue. However, type II collagen remains useful for defining subtypes of cartilage such as vertebrate hyaline cartilage.

Invertebrate cartilage collagens

Because collagen sequences are absent from arthropod genomes, Boot-Handford and Tuckwell (2003) claim that arthropods have lost the fibrillar collagens. Arthropods are known to have cartilage and cartilage often uses collagen as its fibrous protein, thus it would be informative to determine which fibrillar protein is utilized in horseshoe crab cartilage. To date, the cranial cartilage of cephalopod molluscs is the only non-chordate cartilage for which collagen has been analyzed (see Kimura and Karasawa, 1985; Sivakumar and Chandrakasan, 1998; Bairati *et al.*, 1999; Sivakumar *et al.*, 2003).

Kimura and Karasawa (1985) compare skin and cranial cartilage collagens from the squid of the genus *Todarodes*, and suggest that collagen from both sources are derived from the same gene product, with post-translational modification of proline hydroxylation in the cartilage forms. Analysis of the collagen extract revealed two α chains, termed α1 and α2, with the structure $(\alpha1)_2(\alpha2)$. Homology to vertebrate type I collagen is proposed based on this structure and amino acid content (Kimura and Karasawa, 1985). Interestingly, the squid collagen has more glycosylated hydroxylysine than vertebrate type I collagen, and in this respect is more similar to vertebrate type II collagen (Kimura and Karasawa, 1985).

Bairati *et al.* (1999) investigate collagens in cranial cartilage of the cuttlefish *Sepia officinalis* using immunohistochemistry and note that antibodies against almost all vertebrate collagens give moderate reactivity with the extracellular matrix. The two exceptions are mammalian type I antibodies, which show no reactivity with cuttlefish cartilage, and rat type V antibodies, which show intensive immunoreactivity of the entire cartilage extracellular matrix that is comparable to expression patterns using antibodies raised against cuttlefish cartilage antigen

(Bairati *et al.*, 1999). The pepsin soluble collagen extract used as antigen to produce cuttlefish antibodies gives a similar electrophoretic pattern to that observed by Kimura and Karasawa (1985) and hence is also considered similar to vertebrate type I collagen (Bairati *et al.*, 1999).

Cross-reactivity between *S. officinalis* cartilage and the various vertebrate collagen antibodies, in particular a type V collagen antibody, suggests there is a cuttlefish collagen that is similar to vertebrate type V. Sivakumar and Chandrakasan (1998) and Sivakumar *et al.* (2003) purified collagen from *S. officinalis*, and report it to be similar to vertebrate type V or XI based upon the three isolated subunits of molecular weights 105, 115, and 130 kDa. *Sepia officinalis* cartilage also contains an additional collagen which is unlike any of the characterized vertebrate collagens (Rigo and Bairati, 2002).

The accumulation of biochemical work on the major collagens of *Sepia* cranial cartilage strongly suggests that more than one type of collagen molecule is present, and that at least one of these is similar to the minor collagens found associated with vertebrate bone (type V) and cartilage (type XI). Collagen isolated from the basal cnidarian *Veretillum cynomorium* (sea pen) is biochemically very similar to vertebrate type V collagen (Tillet *et al.*, 1996). A predominance of type V collagen within the cartilaginous tissues of arthropods and annelids would support strongly the notion that type II collagen is a molecule novel to the chordate lineage, which was subsequently co-opted into cartilage as the major collagen. Predominant type V collagen would also support Garrone's (1998) assertion that the minor collagens, such as type V, are ancestral (see also Exposito and Garrone, 1990). Collectively it seems the ancestral fibrillar collagen used in cartilage formation is similar in molecular composition to vertebrate collagen type V.

Chondroitin sulphate

Other important vertebrate cartilage extracellular matrix molecules are the sulphated glycosaminoglycans, in particular chondroitin sulphates. Within vertebrate cartilage the predominant chondroitin sulphates are chondroitin-4-

sulphate (CS-A) and chondroitin-6-sulphate (CS-C) (Lash and Vasan, 1983). A chondroitin sulphate similar to vertebrate chondroitin-6-sulphate has been found in polychaetes (Person, 1983). Horseshoe crab (*Limulus*)[3] branchial cartilage contains chondroitin 2,4-disulphate (CS-K) (Sugahara *et al.*, 1996). However when the authors analyzed the sulphation patterns, an additional sulphate group on the 3-C position was found that was undetectable following chondroitinase ABC digestion. Thus, *Limulus* chondroitin sulphate appears to be tri-sulphated.

Analysis of squid (species undefined) chondroitin sulphate by the same group of investigators reveals a similar tri-sulphated chondroitin sulphate variety (Kinoshita *et al.*, 1997). In contrast, Falshaw *et al.* (2000) analyzed the glycosaminoglycans of the squid *Nototodarus gouldi* and did not find any tri-sulphated chondroitin sulphate. There are at least two varieties of chondroitin sulphate in the cranial cartilage of the squid, a Ch4,6-diS (CS-E) and a minor unsulphated (Ch0-S; CS) variety (Falshaw *et al.*, 2000). An enzyme that transfers sulphate groups between the 4th and 6th position and will interact with both CS-A and CS-C also exists in squid cartilage (Inoue *et al.*, 1986; Ito and Habuchi, 2000), possibly explaining the discrepancies in chondroitin sulphate type found by different research groups. It is clear from these studies that sulphation patterns of chondroitin sulphate molecules predominant in cartilage are variable across species. However, it is also clear that sulphation at the 4th or 6th position is most common.

Core protein

Chondroitin sulphate chains are linked to a core protein, forming a proteoglycan. Core proteins within invertebrates appear to be different from any isolated from vertebrates. Vynios *et al.* (1985) showed that the protein core of the proteoglycan from the squid *Illex illecebrous coidentii* has a molecular weight of 150 kDa, and is high in threonine, serine, proline, and glycine content. Vynois and Tsiganos (1990) isolated three populations of proteoglycans from the squid

[3] Sugahara *et al.* (1996) do not use the species name nor do they refer to the horseshoe crab per se, but refer to the King Crab, which is an out-dated common name for the horseshoe crab *Limulus*.

of the genus *Illex* that differ in their protein core, the number of chondroitin sulphate chains, and the number and type of oligosaccharides. The ratio of galactosamine to uronic acid indicates the presence of proteoglycans other than chondroitin sulphate, suggesting squid cranial cartilage contains high amounts of non-collagenous protein. Of the three populations, the proteoglycan D1D1A contains five chondroitin sulphate chains on a 350 kDa protein core; D1D1B contains two or three chondroitin sulphate chains on a 290 kDa protein core; D1D2 contains two or three chondroitin sulphate chains on a 260 kDa protein core (Vynios and Tsiganos, 1990). This last fraction, D1D2, interacts with a squid link protein (Tsilemou *et al.*, 1998). These proteoglycans are sensitive to degradation by elastase, and two of them (D1D2 and D1D1A) interact strongly with type I collagen (Vynios *et al.*, 2000). This interaction is inhibited by degradation with either collagenase or chondroitinase ABC (Vynios *et al.*, 2001).

Tsilemou *et al.* (1998) isolated a squid link protein, which interacts with aggrecan (a vertebrate chondroitin sulphate-rich proteoglycan) and binds hyaluronan *in vitro*. Hyaluronan is an unique glycosaminoglycan because it does not form proteoglycans itself, but can interact with numerous other proteoglycans to form large aggregates of extracellular matrix material (Ayad *et al.*, 1994). To date, hyaluronan has not been isolated from the cartilage of any invertebrate, including cephalopods, and in culture large amounts must be present to achieve binding (Tsilemou *et al.*, 1998). However, proteoglycan staining of cartilages in the cuttlefish *Sepia officinalis* can be significantly reduced by pre-digestion of the cartilaginous matrix with testicular hyaluronidase (personal observation; see section 2.3.1), suggesting that small amounts of hyaluronan may be present in the cartilage of this species.

Additional extracellular matrix components

Many components of vertebrate cartilage matrices have not been sought from any invertebrate cartilage or chondroid connective tissue. These include small proteoglycans, (e.g. decorin, biglycan, chondroadherin, and fibromodulin), cartilage oligomeric matrix protein (COMP) and cartilage intermediate layer

protein (CILP) (Hedbom *et al.*, 1992; Lorenzo *et al.*, 1998). COMP and CILP have been studied only in mammalian cartilage, and thus neither the specificity of the molecules to cartilage, nor their ubiquity within vertebrate cartilages is known.

Apart from the diversity of molecules yet to be investigated, the extracellular matrix of invertebrate cartilages contains analogs of all major matrix molecules found within vertebrate cartilages. As would be expected, given the phylogenetic distance between vertebrates and the different invertebrate clades, these matrix components are not identical. Divergence in both the biochemical structure and histological appearance of any tissue would be expected over a long period of time. The use of abundant amounts of type II collagen in cartilage is a major change that occurred within the evolution of vertebrate cartilages.

1.5 Cartilage Defined

Despite numerous attempts to classify vertebrate cartilage types based upon histological organization, relatively little attention has been given to the definition of cartilage *in and of itself*. In fact, most authors do not offer a strict definition of cartilage. To quote the authors of the first chapter of the first volume in the authoritative three volume series *Cartilage*: "It is extremely difficult to define cartilage simply when attempting to encompass the complete spectrum of the types of this tissue existing at all ontogenetic states, in recent and fossil forms, throughout the vertebrates" (Moss and Moss-Salentijn, 1983, p.2).

Vertebrate researchers who study model systems where histological features of cartilage conform to that considered typical of cartilage have little need for a precise definition of cartilage. Confusion as to what vertebrate cartilage may or may not be is only an issue for those who study non-mammalian cartilages or other skeletal tissues at the transition between cartilage and tendon or bone, pathologists who may come across aberrant tissues that are intermediate in histology, or palaeohistologists who are interested in the relationships between skeletal tissues on an evolutionary time scale (Hall, 1978, 2002, 2004).

For those interested in cartilage and cartilage-like tissues in animals that fall outside the Vertebrata, a precise definition of cartilage is very important. Hall

(1978) provides a definition of cartilage taking into account the hierarchical nature of cartilage as a tissue, and addressing each aspect of cartilage classification found within the vertebrate literature:

> "Cartilage is an avascular, supporting, and articular skeletal tissue (although like bone, it may arise ectopically outside the skeleton), deposited by both chondroblasts and by chondrocytes, and removed by chondroclasts. Its extracellular matrix, primarily composed of glycosaminoglycans, contains a smaller collagen component of type $[\alpha I(II)]_3$ (type II collagen). Cartilage may or may not exist as a mineralized tissue. Cartilage functions as the primary embryonic skeletal tissue in many parts of the embryo and as the articular tissue at joints on both endochondral and membrane bones (in the latter case, the cartilage is known as secondary cartilage). Cartilage is found in both vertebrate and invertebrates." (p. 7).

Although recognising that cartilage can be found outside the vertebrate clade, Hall's definition shows strong biases towards vertebrate cartilage in two respects. There are no published studies on the development of most invertebrate cartilages (with the exception of gastropods: Delsman, 1912; Raven, 1958; Page and Pederson, 1998), therefore including references to embryonic function of cartilage and the classification of cartilages as "secondary" applies only to vertebrates. Second, and perhaps more importantly, Hall includes the presence of type II collagen as diagnostic for cartilage. As explored above (collagen: section 1.4.2), type II collagen is not unique to cartilage.

After spending the better part of two decades considering invertebrate cartilages, Philip Person came up with a general definition of cartilage. Person (1983) defines cartilage as:

> "an animal tissue, usually endoskeletal, but also exoskeletal... Physically, cartilages are gristle-like, relatively rigid, and resistant to forces of compression, shearing, and tension. As a skeletal support structure, cartilage aids in locomotion and in resisting the force of gravity. Histologically, it is a form of connective tissue composed of polymorphic cells suspended in highly hydrated, metachromatic colloidal gel matrices of varying rigidity, composition, and abundance. Chemically, cartilage is characterized by its high content of collagen, glycosaminoglycan complexes, and water." (pp. 33-34).

Person's definition was designed to be inclusive of all cartilage types in all animal groups, and as such is suitably generalized. In addition, Person and Mathews (1967) identified three criteria for the designation of cartilage:

1) Composed of cells suspended in a relatively rigid matrix of varying abundance;
2) Rich in acidic polysaccharides including chondroitin sulphates;
3) High in collagen content

1.5.1 Re-defining cartilage

It is not possible to use the above criteria to unequivocally recognize, in histological section, a previously undescribed tissue as cartilage. One such example is that illustrated by Andersen *et al.* (2001) for the vestimentiferan *Riftia pachyptila*, where the fibroblastic appearance of the cells rendered the authors unable to definitively answer their own question: "Could the obturaculum of *Riftia* be considered as a primitive 'cartilage'? ". I propose that the aforementioned criteria be modified to reflect the fact that morphologically distinct chondrocytes need to be present and distinguishable from other mesenchymal connective tissue cells (in 1 above). Additionally, the term "fibrous protein" should replace "collagen" in 3 above, to account for the lack of collagen in all lamprey cartilages (Wright *et al.*, 2001), types I and III hagfish cartilage (Wright *et al.*, 1998), and possibly arthropods including *Limulus* (Wright *et al.*, 2001). My revised definition of cartilage, as modified from Person and Matthews (1967) and Person (1983) is as follows:

> Cartilage is a rigid animal connective tissue that by virtue of its structure functions by resisting shearing, tension, and compression, thereby providing support and/or protection for the animal. Histologically, cartilage is composed of large cells (chondrocytes) that are morphology distinct from other connective tissue cells in the animal; these cells are embedded within an extracellular matrix of varying abundance that has high amounts

of fibrous protein (usually collagen or elastin), ground substance (usually chondroitin sulphate), and water.

Under this revised list of criteria, it would appear the vestimentiferan obturaculum does not qualify as cartilage because it lacks distinct chondrocytes, although the fibroblasts may be unique in that they are surrounded by a basal lamina (Andersen *et al.*, 2001).

1.6 Conclusions

The primary argument presented here is that cartilage is a metazoan tissue found in both vertebrates and invertebrates. It is important to note however, that the term cartilage does not necessarily imply homology of tissues. The diversity of invertebrate tissues described in the literature as cartilage makes it necessary to broaden the classification schemes and definitions currently used for vertebrates. Cartilage is defined structurally by the composition of its extracellular matrix and the presence of differentiated chondrocytes, both of which are distinct from other connective tissue cells and matrices. Because cartilage must be considered with reference to all forms found in all animal groups, new categories of cartilage are called for.

1.7 The Thesis

By presenting comparative data on the histological organization and immunoreactive properties of tissues from lineages previously reported to possess cartilage, the next chapter addresses whether or not all of these tissues have the required properties to be considered cartilage. Furthermore, based upon the histological structure of tissues that do merit the designation cartilage I expand current cartilage classification schemes so that invertebrate cartilages can be included.

In order to establish the evolutionary context of these data, I explore the phylogenetic relationships between major groups of metazoan animals. In Chapter 3 I present results from a supertree analyses of data derived from

in the following chapter as a basis for discussion of the evolution of cartilage amongst these groups.

How cartilage distribution and histology data impact on interpretations of cartilage origin and subsequent evolution is explored in Chapter 4, wherein the data presented in the previous chapters is combined with data collected from the literature about related skeletal tissues to update ideas of cartilage as a metazoan tissue. This chapter uses the phylogeny presented in the previous chapter as a tool to begin to analyze the evolution of cartilage as a tissue.

Skeletal biologists have largely disregarded invertebrate cartilages, and therefore little is known of their development. In Chapter 5 I present novel data concerning the differentiation of cartilage within cephalopod molluscs. Using the European cuttlefish *Sepia officinalis* as a starting point, I describe the basic mechanism of cephalopod cartilage formation, and explore differences in the timing of differentiation of cartilage formation in a number of other cephalopods.

These developmental data are then extended in Chapter 6 with data from a second invertebrate lineage, sabellid polychaetes. I compare the histological structure of the branchial cartilages of a number of sabellid polychaetes, and describe the development and regenerative abilities of *Potamilla*, with particular attention ascribed to the cartilaginous branchial skeleton.

In the final chapter I present a summary of the general trends described in this thesis with respect to building a connective tissue that is recognizable as cartilage within major bilaterian animal lineages.

Chapter 2: Histology and Distribution of Cartilage

2.1 Introduction

In order to determine the extent to which cartilage is found outside vertebrates, candidate invertebrate tissues must be subjected to rigorous histological analysis. Bearing in mind my revised definition of cartilage as a tissue type (see section 1.5.1), I extend previous reports of invertebrate cartilages (see section 1.2) through examination of histology and antigenic properties of cartilage and cartilage-like tissues using fresh material. According to my revised definition, to be considered cartilage a tissue must:

- function as a skeletal or developmental support and/or provide a protective function in the animal;
- be composed of cells with a morphology distinct from other connective tissue cells in the animal;
- have cells embedded within an extracellular matrix that has high amounts of fibrous protein (usually collagen or elastin), glycosaminoglycans (usually a mucopolysaccharide such as chondroitin sulphate), and water.

To re-evaluate the distribution and structural properties of a number of invertebrate tissues, I develop a new staining protocol for visualizing cartilage in histological sections, and use this and other protocols to characterize connective tissues from representatives of anthozoan cnidarians, echinoid echinoderms, urochordates, enteropneust hemichordates, cephalopod molluscs, chelicerate arthropods, serpulid polychaetes, sabellid polychaetes, and brachiopods. The previously known biochemical and histological properties of these tissues were presented in Chapter 1 (sections 1.2 and 1.4.2). I also survey the immunoreactivity of skeletal tissues in the brachiopod, hemichordate, cephalopod mollusc, horseshoe crab, and sabellid polychaete with a panel of antibodies raised against vertebrate connective tissue molecules.

I find that chondroid connective tissue (connective tissues with cartilage-like properties, but lacking chondrocytes) is common among invertebrates, and differs from invertebrate cartilage in the structure and organization of the cells

that comprise it. *Chondroid connective tissue* should not be confused with *chondroid bone*, an example of a tissue intermediate between vertebrate cartilage and bone (Beresford, 1981). I have found some groups to have extensive chondroid connective tissue: including brachiopods, polychaetes, and urochordates. My results indicate that cartilage is found within cephalopod molluscs, chelicerate arthropods and sabellid polychaetes. Skeletal tissues found within enteropneust hemichordates are unique in that the extracellular matrix shares many properties with vertebrate cartilage, yet these tissues are completely acellular.

2.2 Methods

2.2.1 Animals

Adult specimens of *Terebratalia transversa* (brachiopod) and *Potamilla* (sabellid polychaete) were collected off the west coast of Washington State near Friday Harbor. Adult specimens of *Terebratulina serpentrionalis* (brachiopod) and *Myxicola infundibullum* (sabellid polychaete) were collected by SCUBA by Dr. C. Harvey-Clark in the waters off the coast of Nova Scotia. Adult specimens of the following species were obtained from the Marine Resources Department at the Marine Biological Laboratories in Woods Hole, MA: *Saccoglossus kowalevski* (hemichordate), *Styella partita* (urochordate), *Strongylocentrotus droebachiensis* (echinoid echinoderm) and *Limulus polyphemus* (chelicerate arthropod). Adult and juvenile *Sepia officinalis* (cephalopod mollusc) were purchased from the National Resource Center for Cephalopods, in Galveston TX. Isolated cartilaginous tissues were dissected from adult *Limulus* and *Sepia*. A small specimen of *Metridium senile* (sea anemone) was collected from tubing of aquarium holding tanks after settling out from the water column and growing to a basal diameter of 3 cm. Sections of Atlantic salmon parr, collected under license from the Canadian Federal Department of Fisheries and Oceans, were prepared as described elsewhere (Witten and Hall, 2002). All specimens were fixed in 10% neutral buffered formal saline and stored in 70% ethanol until required.

2.2.2 Histology

Specimens were dehydrated in a graded series of ethanol, cleared in CitriSolve (Fisher No. 22-143975), and embedded in low melting paraffin wax at 54°C. Prior to embedding, specimens were decalcified in Cal-EX (Fisher No. CS510-1D) when necessary. Embedded tissues were sectioned at 5-7 µm, mounted on either Haupt's or Poly-L-lysine coated slides, and stored at room temperature until required. Following rehydration, most slides were stained with one of six histology protocols: Toluidine Blue (Presnell and Schreibman, 1997) Masson's Trichrome (Flint *et al.*, 1975), Hall-Brunt Quadruple (HBQ) stain (Hall, 1986), Mallory's trichrome (Presnell and Schreibman, 1997), or a new pentachrome protocol for distinguishing cartilage from other connective tissues (described below). Slides were mounted in DPX (Fluka No. 44581) and coverslipped.

2.2.3 Cartilage and connective tissue histology protocol

Slides were first stained in Verhoeff's stain [3 g haematoxylin (Sigma No. MSH-32) in 66 ml ethanol added to 24 ml of 10% ferric chloride and 24 ml of 4% potassium iodide and 2% iodine in distilled water (Presnell and Schreibman, 1997)] for 10 minutes, rinsed in running tap water for 1 minute followed by differentiation in 2% ferric chloride. If elastin distribution is not of interest, Verhoeff's stain can be replaced with Mayer's acid haematoxylin, and the ferric chloride differentiation step omitted. Sections were then stained in 1% aqueous Bismark Brown Y (Sigma No. B-2759) for 6-8 minutes, washed in tap water for 1 minute and processed through Masson's trichrome (Flint *et al.*, 1975) as follows: xylidine ponceau for 2 min [equal volumes of 0.5% xylidine ponceau 2R (C.I. no. 16150) in 1% acetic acid and 0.5% acid fuchsin (C.I. no. 42685) in 1% acetic acid], rinsed, 4 minutes in 1% phosphomolybdic acid, rinsed, and stained with light green for 1.5 minutes [2% light green (C.I. 42095) in 2% citric acid, diluted 1:10 with distilled water prior to use]. This protocol allows for visualization of five different histological components within a single section; elastin stains black, cell nuclei and cytoplasm stain purple, mucopolysaccharides stain orange/brown

stain orange/brown (Conn, 1973), low and high tensile fibres (collagen) stain green and red respectively (Flint, 1972; Flint *et al.*, 1975).

Bismark Brown Y was chosen over Alcian Blue for mucopolysaccharide staining because it gives greater contrast with the light green collagen staining. To verify specificity of the Bismark Brown Y mucopolysaccharide stain, sections were digested in 0.1M tris buffered saline (TBS) with 5 units/ml chondroitinase ABC (Sigma No. C2905) or 6 mg/ml hyaluronidase (Sigma No. He506) prior to incubation with staining reagents (Witten and Hall, 2002); 0.5 mg/ml Elastase (Sigma No. E-0127) was used to confirm specificity of Verhoeff's stain.

2.2.4 Immunohistochemistry

Following removal of paraffin, slides were immersed in 3% H_2O_2 in absolute methanol for 15 minutes to block endogenous peroxidases. Slides were rehydrated, and subjected to 10% trypsin in 0.1M TBS to retrieve masked antigen sites. Antibodies requiring that sections be reduced and alkylated [link protein (9/30/8-A4) and hyaluronic acid binding proteoglycan (12/21/1-C-6)] were incubated with Dithiothreitol [10 mg/ml (Sigma No. D-0632) in 0.1M TBS pH 8.0] for one hour, washed and incubated with Iodoacetic acid [60 mg/ml (Sigma No. I-4386) in TBS pH 8.0] for 30 minutes prior to the blocking step. Sections were blocked in 10% normal goat serum for 2 hours at room temperature, and incubated overnight in primary antibody supernatant. The following antibody supernatants (purchased from the Developmental Studies Hybridoma Bank (DSHB) at the University of Iowa) were used at a concentration of 1:20 in TBS: CB-1 (decorin), 9/30/8-A4 (link protein), I22 (keratan sulphate), 9BA12 (chondroitin sulphate proteoglycan), AON-1 (osteonectin), WVID1(9C5) (bone sialoprotein II) and X-AC9 (type X collagen). Other antibody supernatants tested did not yield positive immunoreactivity in any tissues in dilutions ranging from 1:20 to 1:1, and will not be discussed further (table 1). Slides were washed in TBS and incubated in secondary antibody (1:200 in TBS with 1% bovine serum albumin) for 2hrs at room temperature. The secondary antibody was visualized using fresh DAB/H2O2 solution (Sigma No. D-4293), and slides were counter-

Table 1: Antibodies tested in this study

Dilutions of quantified antibodies purchased from the Developmental Studies Hybridoma Bank (DSHB), in Tris Buffered Saline (TBS) with bovine serum albumin, were tested for immunoreactivity using sections of quail embryos. Antibodies requiring special treatment to reveal antigen sites are indicated (*). See text for details.

DSHB Antibody	Antigen	Special conditions	Ig quantitation (µg/ml)	Dilutions tested (in TBS + serum)	Expression in control slides? (quail)
9/30/8-A-4	link protein (rat)	reduced and alkylated*	47	1:20, 1:10	yes
X-AC9	type X collagen (chick)	none	>50	1:20, 1:10	yes
9BA12	chondroitin sulphate proteoglycan (chick)	none	>50	1:20, 1:10, 1:1	yes
AON-1	osteonectin (bovine)	none	46	1:20, 1:10	yes
WVID1(9C5)	bone sialoprotein II (rat)	none	>50	1:20, 1:10	yes
CB-1	decorin (chick)	none	27	1:20, 1:10	yes
I22	keratin sulphate (rabbit)	none	>50	1:20, 1:10	yes
MH27	cell-cell junctions from *C. elegans*	none	40	1:20, 1:10	no
12/21/1-C-6	hyaluronic acid binding proteoglycan (rat)	reduced and alkylated	>50	1:20, 1:10, 1:1	no
33	heparan sulphate proteoglycan (chick)	none	21	1:20, 1:10, 1:1	no
M3F7	type IV collagen (human)	none	45	1:20, 1:10, 1:1	no
MT4	fibronectin (newt)	none	45	1:20, 1:10, 1:1	no
C5	from plasma membrane vesicles shed from 48h culture of chick embryo breast muscle cells	none	>50	1:20, 1:10	no
MT1	tenascin (newt)	none	50	1:20, 1:10, 1:1	no

stained with haematoxylin, dehydrated, mounted in DPX (Fluka No. 44581), and coverslipped.

2.3 Results

2.3.1 Cartilage and connective tissue stain

The high collagen content in both vertebrate cartilage and unmineralized bone matrix results in green staining with Masson's trichrome protocol, which makes the differentiation between bone matrix and cartilage matrix difficult to discern. Although a number of staining compound combinations were examined to visualize collagen and mucopolysaccharides, I found that using light green for collagen staining (Flint *et al.*, 1975) and Bismark Brown Y for mucopolysaccharides (Conn, 1973) provided the best contrast.

Compared with Masson's trichrome staining (fig. 2a), addition of Bismark Brown Y changes the staining properties of cartilage (fig. 2b), but not that of bone or other fibrous connective tissues. The degree of mucopolysaccharide staining of the cartilage is affected by the method of decalcification. Specimens decalcified in EDTA (Witten and Hall, 2002) retain most of their mucopolysaccharides within the cartilage resulting in strong orange staining of the cartilage, easily distinguishable from the surrounding connective tissue (fig. 2c). Specimens decalcified with CalEx show a decreased amount of mucopolysaccharide staining within the cartilaginous matrix for both salmon and squid cartilages. In these cases, cartilage remains distinguishable from other connective tissue by the forest-green staining produced by the combination of collagen and mucopolysaccharide staining (fig. 2b and 3a). Salmon calcified cartilage retains higher amounts Bismark Brown staining in CalEx decalcified specimens (fig. 2b), allowing differentiation of hyaline and calcified cartilage that is not distinguishable in EDTA decalcified specimens or with Masson's trichrome stain alone (fig. 2a).

Figure 2: Analysis of cartilage and connective tissue stain using vertebrates
New cartilage and connective tissue stain (CCT stain) allows for increased differentiation of connective tissues and specific extracellular matrix components as demonstrated with Atlantic salmon parr sections, scale bars = 100 µm. **a** Hyaline cartilage (*hc*) and calcified cartilage (*cc*) cannot be differentiated using Masson's trichrome staining. **b** CCT staining of Cal-Ex decalcified specimens allows for differentiation between orange-brown staining calcified cartilage (*cc*) and forest green staining uncalcified hyaline cartilage (*hc*). **c** CCT staining of EDTA decalcified specimens allows for ready differentiation of cartilage (*orange-brown staining*) and non-cartilaginous connective tissues (*light green staining*), as well as identifying elastic components (*black staining*). **d** Elastase digestion eliminates black elastin staining as well as reducing mucopolysaccharide staining. Imaged is of a section adjacent to (c). **e-h** Chondroitinase reduces the amount of mucopolysaccharide staining significantly in ETDA decalcified sections. CCT staining before (**e**) and after (**f**) digestion with chondroitinase; Toluidine Blue staining before (**g**) and after (**h**) digestion with chondroitinase.

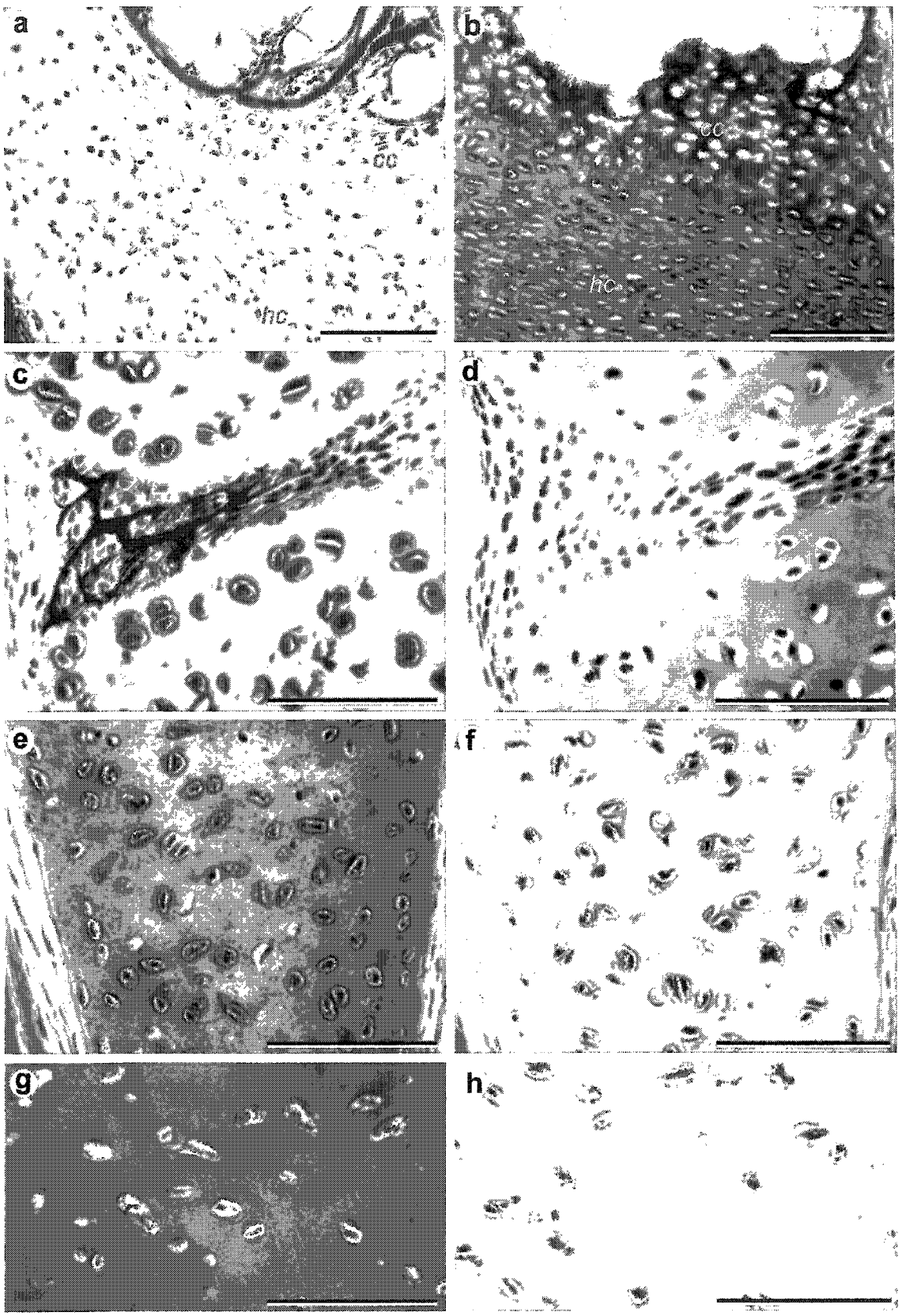

Figure 2

Elastin

Verhoeff's elastin stain is commonly used to visualize elastin fibres in histological section. In order to visualize elastin fibres in the same section as other connective tissue components, I combined Verhoeff's stain (Presnell and Schreibman, 1997) with Masson's trichrome protocol. When combined with Bismark Brown Y (see below), the resultant pentachrome stain allows for the differentiation of three important connective tissue components on a single slide: fibrous protein (collagen), mucopolysaccharides, and elastin (fig. 2c). The specificity of Verhoeff's stain for elastin fibres was confirmed by pre-digestion of the sections with elastase, eliminating the black staining of the elastin components (fig. 2d). Elastase treatment also alters the tensile collagen staining and reduces the amount of mucopolysaccharide staining in cephalopods and Salmon (fig. 2d). This is not surprising considering that elastase contains trypsin activity, and thus digests other proteins as well as elastin (Sigma No. E-0127; Windholz *et al.*, 1976).

Mucopolysaccharides

Pre-digestion of the mucopolysaccharides within the cartilage with chondroitinase ABC (fig. 2f and 3b) reduces the Bismark Brown Y mucopolysaccharide staining in EDTA decalcified specimens (fig. 2e), and eliminates staining in CalEx decalcified specimens (fig. 3). Sections stained with Toluidine Blue were used as a positive control, and showed similar reductions in staining intensity with enzyme digestion (fig. 2g,h and 3c,d). Digestion with hyaluronidase yields similar results for both squid and salmon cartilage.

2.3.2 Analysis of invertebrate cartilage and cartilage-like tissues

Cartilage is a tissue made up of cells that are morphologically distinct from other connective tissue cells, and that secrete extracellular matrix containing large amounts of fibrous protein and glycosaminoglycans (see section 1.5.1). After careful examination of cartilage-like tissues in representatives from the aforementioned groups, I find that these tissues represent a diversity of histologies, described below, surpassing even that described in fishes (Benjamin,

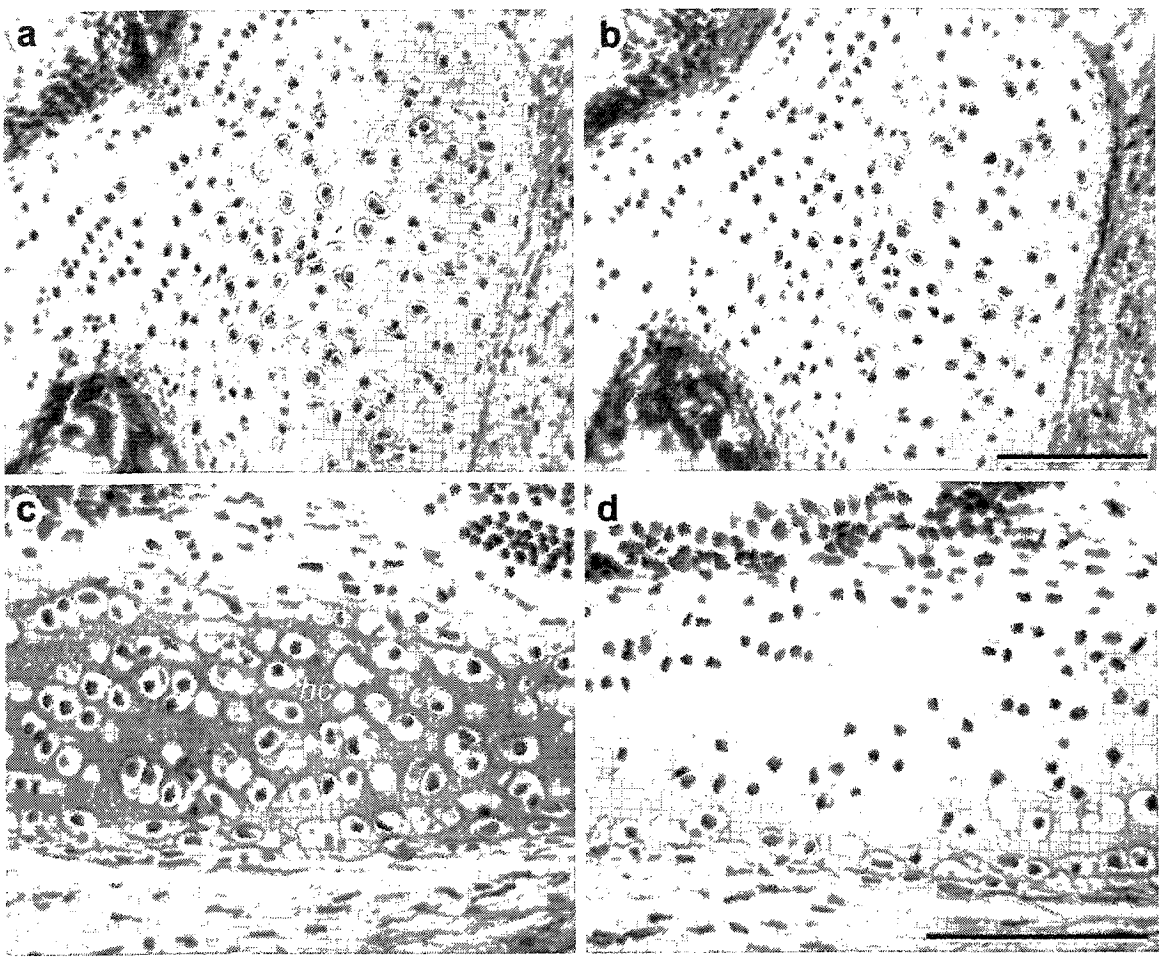

Figure 3: Analysis of cartilage and connective tissue stain using cephalopods
Chondroitinase eliminates mucopolysaccharide staining in sections of cartilage from immature squid of the genus *Illex*, scale bars = 100 µm. **a** Cartilage and connective tissue staining of Cal-Ex decalcified sections stains hyaline cartilage (*hc*) forest green. **b** Chondroitinase digestion eliminates mucopolysaccharide staining, resulting in light green staining of cartilage. **c** Toluidine Blue stains mucopolysaccharides metachromatically purple. **d** Chondroitinase digestion reduces mucopolysaccharide staining in an adjacent section.

1990). Although cartilage is found within a number of invertebrate groups, not all tissues previously reported to be cartilage have the appropriate properties to merit their distinction as cartilage.

Cnidaria

I investigated the mesoglea of the sea anemone *Metridium senile.* The mesoglea stains strongly for fibrous protein, but not for mucopolysaccharides (fig. 4). There are a number of heterogeneous cells within the mesoglea, some of which appear to contain large vacuoles. However, within this species the mesoglea does not appear to show any regional specialization with regards to distribution of these cells. Thus there are no cartilaginous tissues within the sea anemone *Metridium senile.* This does not mean that tissues with high mucopolysaccharide content and specialized cell morphology do not exist within the Cnidaria, however the specimen examined here lacks any connective tissue that can be considered cartilage.

Brachiopoda

The extracellular matrix of the lophophore in the brachiopods *Terebratalia transversa* and *Terebratulina serpentrionalis* stains for collagen and acidic mucopolysaccharides; discrete bundles of material stain histologically for elastin (fig. 5a). Collagen in the lophophore shows two different staining properties with both my cartilage and connective tissue stain and with Mallory's trichrome (fig. 5a,b). The collagen that surrounds the coelomic canals, which extend into the tentacles of the lophophore, stains more intensely than that in the adjacent tissue. This is similar to the difference in collagen staining seen between cartilage and bone in vertebrates (M. Vickaryous, personal communication, 2003).

Additionally, this intensely stained region of matrix is immunoreactive with antibodies against keratin sulphate (DSHB antibody l22: fig 5c). The matrix of the lophophore and the connective tissue with which it is continuous shows homogeneous immunoreactivity with antibodies against a chondroitin sulphate proteoglycan (DSHB antibody 9BA12: fig. 5d). Cells of the mature lophophore

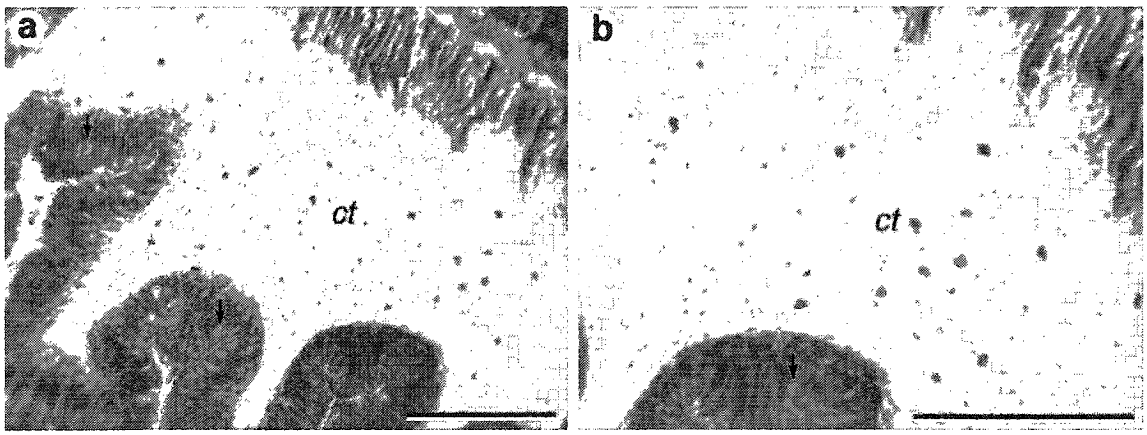

Figure 4: Histology of connective tissues from *Metridium senile* (Cnidaria)
The mesoglea of this sea anemone is an extensive fibrous connective tissue (*ct*). Although there is mucopolysaccharide staining within the epithelium (*arrowheads*), there is no staining within the mesoglea. Sections, imaged at low (**a**) and high (**b**) magnification, are stained with my new cartilage and connective tissue stain for mucopolysaccharides and fibrous protein; elastin staining was omitted from the protocol. Scale bars = 100 μm.

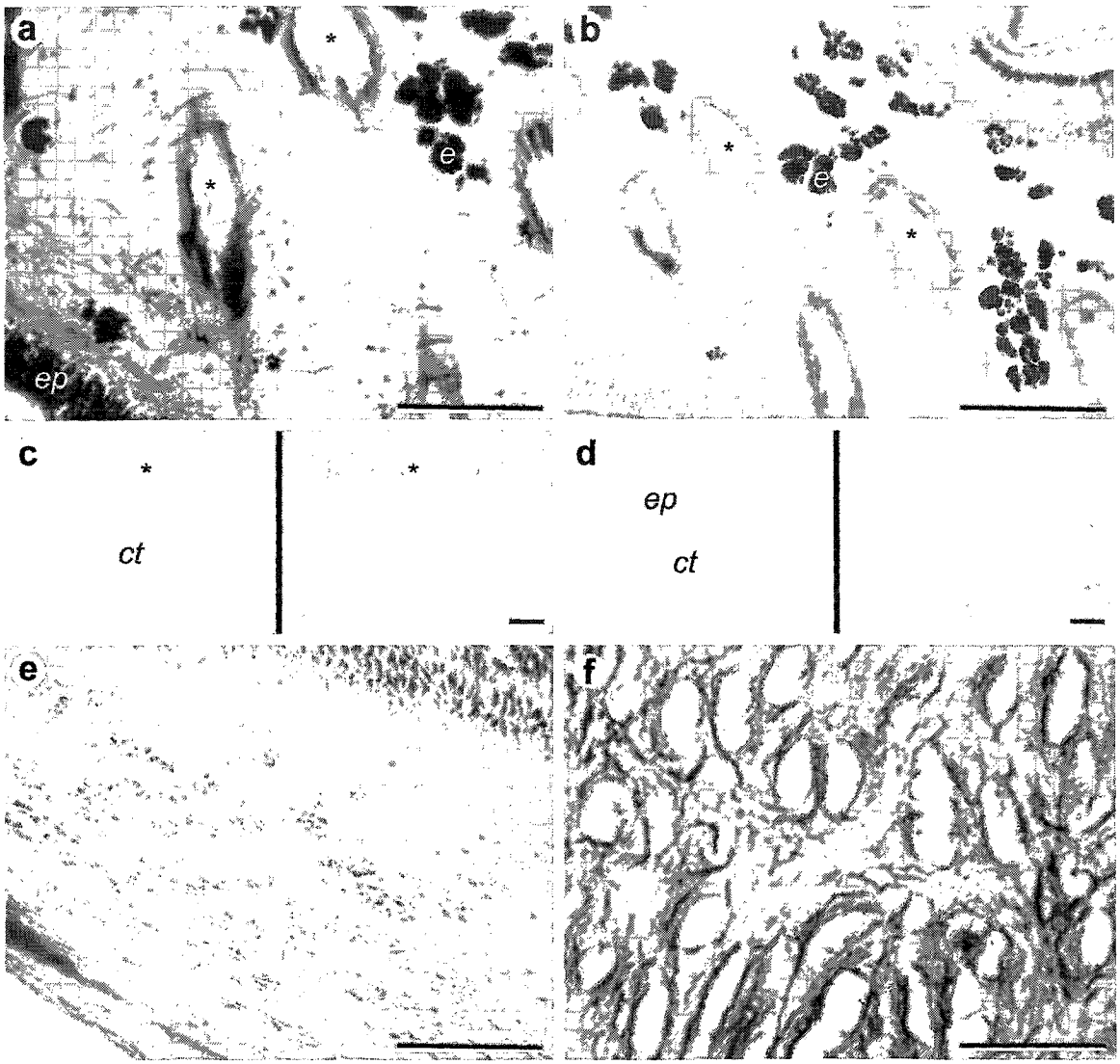

Figure 5: Histology and Immunoreactivity of connective tissues from *Terebratalia transversa* and *Terebratulina serpentrionalis* (Brachiopoda)

Connective tissues in brachiopods do not resemble cartilage in histological section. *Scale bar* = 100 µm; * = coelomic canals; *ct* = connective tissue; *e* = elastin bundles; *ep* = epithelium; a,b,e,f = *Terebratalia transversa*; c,d = *Terebratulina serpentrionalis* **a** Cartilage and connective tissue (CCT) staining of lophophore connective tissue shows mucopolysaccharides are distributed homogeneously, fibrous proteins are concentrated in regions surrounding the coelomic canals (*), and bundles of elastin (*e*) are seen throughout. **b** Mallory's trichrome staining reveals similar intense staining surrounding coelomic canals (*) **c,d** Lophophore connective tissue (*ct*) is immunoreactive with antibodies against the vertebrate molecules keratin sulphate (**c**) and chondroitin sulphate proteoglycan (**d**). **e** Masson's trichrome staining of connective tissue adjacent to pedicle shows similar staining properties and cellular histology as the lophophore connective tissue. **f** CCT staining identifies a mucopolysaccharide-rich tissue within the pedicle.

are usually very small and fibroblastic in appearance, however some vacuolated cells are present. The connective tissue of the lophophore is continuous with the rest of the connective tissues in the animal, with similar histological properties (fig. 5e). This connective tissue attaches to the pedicle, which stains strongly for mucopolysaccharides and appears to contain large numbers of vesicular cells (fig. 5f). Although the extracellular matrix of brachiopod connective tissue exhibits an interesting histology and immunoreactivity, the cells of this tissue do not exhibit any features that could be associated with being a distinct population of specialized cells– chondrocytes – and thus these tissues do not qualify as cartilage (Cole and Hall, 2004). Brachiopods therefore have extensive chondroid connective tissue, but not cartilage.

Polychaeta

All three matrix components (elastin, fibrous protein, and mucopolysaccharides) are found throughout the cartilaginous support of the branchial crown in sabellid polychaetes, but not homogeneously, particularly with reference to the cellular and acellular matrix regions. In *Potamilla sp.*, the staining pattern throughout all regions of the cartilage show both red and green parts of the spectrum (fig. 6a-c), indicating different tensile properties of the collagen (Flint, 1972; Flint *et al.*, 1975). The thin matrix between the cells stains for collagen, mucopolysaccharides and elastin (fig. 6c-e), whereas the thicker acellular matrix is devoid of elastin (fig. 6d) and has minimal mucopolysaccharides (fig. 6e).

The presumptive chondrocytes are large and contain a conspicuous vacuole, particularly evident in *Myxicola infundibulum* (fig. 6f). Chondrocytes within the pinnules are arranged in a "stack of coins" arrangement, similar to that of the pharyngeal cartilages described by Kimmel *et al.* (1998) in the zebrafish (*Danio rerio*). The acellular extracellular matrix surrounding the stacks of cells is continuous with the basement membrane of the overlying epithelium. This is more evident in *Myxicola* specimens (fig. 6f,g), where the tissue reacts with antibodies against chondroitin sulphate (DSHB antibody 9BA12: fig. 6h).

Figure 6: Histology and Immunoreactivity of branchial cartilage from *Potamilla* sp. and *Myxicola infundibulum* (Polychaeta)

Sabellid polychaete cartilages consist of an inner core of vacuolated cells (*cc*) surrounded by a thicker acelluar region of matrix (*arrows*), that is continuous with the basement membrane of the overlying epithelium (*ep*), and thicker in *Potamilla* (a-e) than in *Myxicola* (f-i). Scale bars = 100 µm; * = vacuolated cells; *cc* = cellular cartilage; *ep* = epithelium. **a,b** New cartilage and connective tissue (CCT) staining reveals that the acellular region contains fibrous protein with differential tensile properties (*green and red staining*). **c** Similar red and green staining occurs within the matrix of the cellular region, shown here with Masson's trichrome staining. **d,e,g** Staining for elastin (**d**) and mucopolysaccharides (**e,g**) is restricted to the cellular region (*cc*), although there is some Alcian Blue staining between the overlying epithelial layer and the acellular matrix (*arrows*) in *Potamilla*. **f** In *Myxicola*, the smaller pinnules are connected to the radiole by a single large vacuolated cell (*) that is supported by high tensile fibres (*red*) indicated with CCT staining. **h,i** Branchial skeletons show immunoreactivity with vertebrate antibodies; control sections shown to the left. **i** Polychaete cartilages are immunoreactive with antibodies against chondroitin sulphate proteoglycan, with most intense staining seen in fibrous tissue supporting the pinnule connections. **h** The overlying epithelium, but not the cartilage matrix is immunoreactive with vertebrate bone sialoprotein II antibodies.

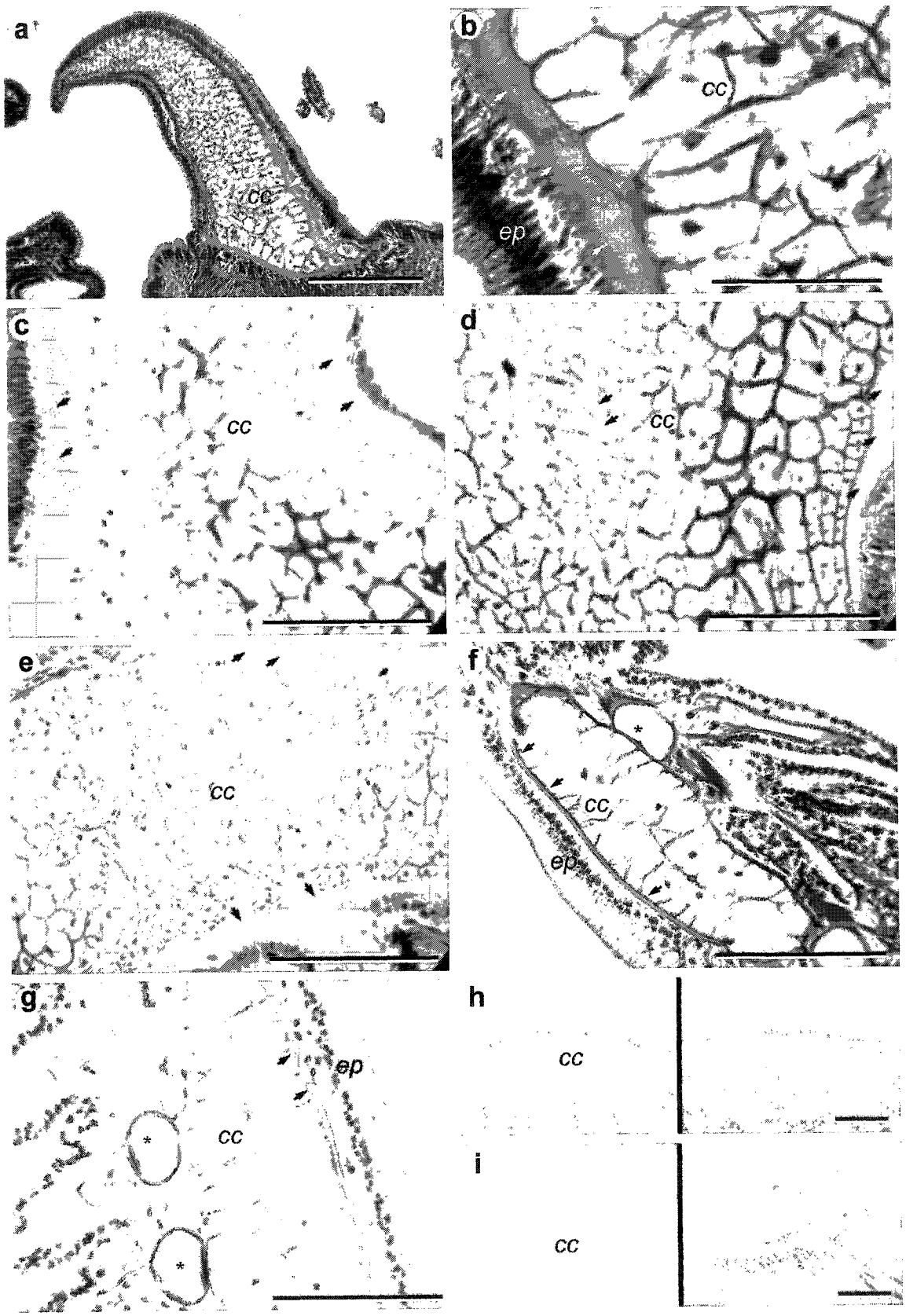

Figure 6

Interestingly, the cartilage matrix is also immunoreactive with antibodies against the vertebrate bone markers osteonectin (DSHB antibody AON-1), and the epithelium and internal matrix, but not the acellular matrix, are immunoreactive with bone sialoprotein II antibodies (DSHB antibody WVID1(9C5): fig. 6i).

Tissues supporting the tentacles within sabellid polychaetes show the cellular and extracellular matrix specialization required to be cartilage. The expanded region of acellular matrix likens this tissue to scleral cartilages, which are difficult to classify as either cell-rich or matrix-rich cartilages (Benjamin, 1990). Because this structural organization occurs within some vertebrate and cephalopod sclera (personal observation; see Chapter 5) in addition to sabellid polychaetes, it merits a classification of its own. I suggest naming this class of cartilage central cell-rich cartilage (CCRC), emphasizing the inner core of chondrocytes and by extension implying a cell-poor outer region.

Arthropoda

Within the opisthosome of the horseshoe crab *Limulus polyphemus*, cartilages of the opisthosomatic endplates and associated appendages (branchial and chilarium) (fig. 7b,d,f,i) are structurally very different from the cartilage that forms the endosternite (fig. 7a,c,e,g,h). The horseshoe crab thus has two histologically distinct cartilages in addition to extensive chondroid connective tissue.

The opisthosomatic cartilages are highly cellular, with large cells separated by a thin matrix. The matrix of this tissue stains strongly and homogenously for all three matrix components: high tensile collagen (fig. 7b,f), elastin (fig. 7i), and mucopolysaccharides (fig. 7d). The cells are large and spherical, and may also contain a large vacuole. Some chondrocytes are incorporated fully into the matrix by completely filling with extracellular matrix products. This new matrix is much higher in mucopolysaccharide content, and lacks elastin (fig. 7i).

The cartilage of the endosternite stains strongly for collagen and to a lesser extent for acidic mucopolysaccharides (fig. 7a,e vs. 7c). This tissue does not stain for elastin, and is highly fibrous peripherally. Cells of the endosternite vary

Figure 7: Histology and Immunoreactivity of cartilaginous tissues from *Limulus polyphemus* (Arthropoda)

Two distinct types of cartilage are present within the horseshoe crab: fibro-hyaline cartilage of the endosternite (a,c,e,g,h) and vesicular *Zellknorpel* opisthosomatic cartilages (b,d,f,i) – see text for discussion of these cartilage types. Scale bars = 100 μm; *fc* = fibrocartilage; *hc* = hyaline cartilage. **a** Mallory's trichrome staining reveals chondrocytes aligned in parallel rows between intensely staining fibrous bundles in peripheral regions of the endosternite. **b** The opisthosomatic cartilages are more cellular than the endosternite, and the extracellular matrix (ECM) between the cells stains yellow with Mallory's trichrome. **c** Alcian Blue positive mucopolysaccharide staining in the endosternite is diffuse throughout. **d** The opisthosomatic cartilages show Alcian Blue mucopolysaccharide staining in both the ECM and within the chondrocytes. **e** New cartilage and connective tissue (CCT) stain (elastin component omitted) reveals chondrocytes within the hyaline region (*hc*) of the endosternite cartilage are more spherical and spaced equidistant compared to the fibrocartilage regions (*fc*). **f** CCT staining (elastin staining omitted) reveals fibrous matrix within the opisthosomatic cartilages as high tensile fibres (*red staining*). Mucopolysaccharide staining (*forest green / brown staining*) is restricted to the chondrocytes and thicker regions of the ECM. The opisthosomatic cartilages are surrounded by fibrous connective tissue (*inset*) that is histologically similar to the endosternite. **g** CCT staining reveals that the opisthosomatic cartilage matrix also contains elastin-like protein (*black staining*). Opisthosomatic chondrocytes are sometimes seen to be replaced by ECM, resulting in larger regions of extracellular matrix that is mucopolysaccharide-rich (*orange-brown staining*). **h,i** The ECM of the endosternite stains with vertebrate connective tissue antibodies; control sections shown on the left. **h** Homogenous bone sialoprotein II immunostaining of the endosternite. **i** Homogenous chondroitin sulphate immunostaining.

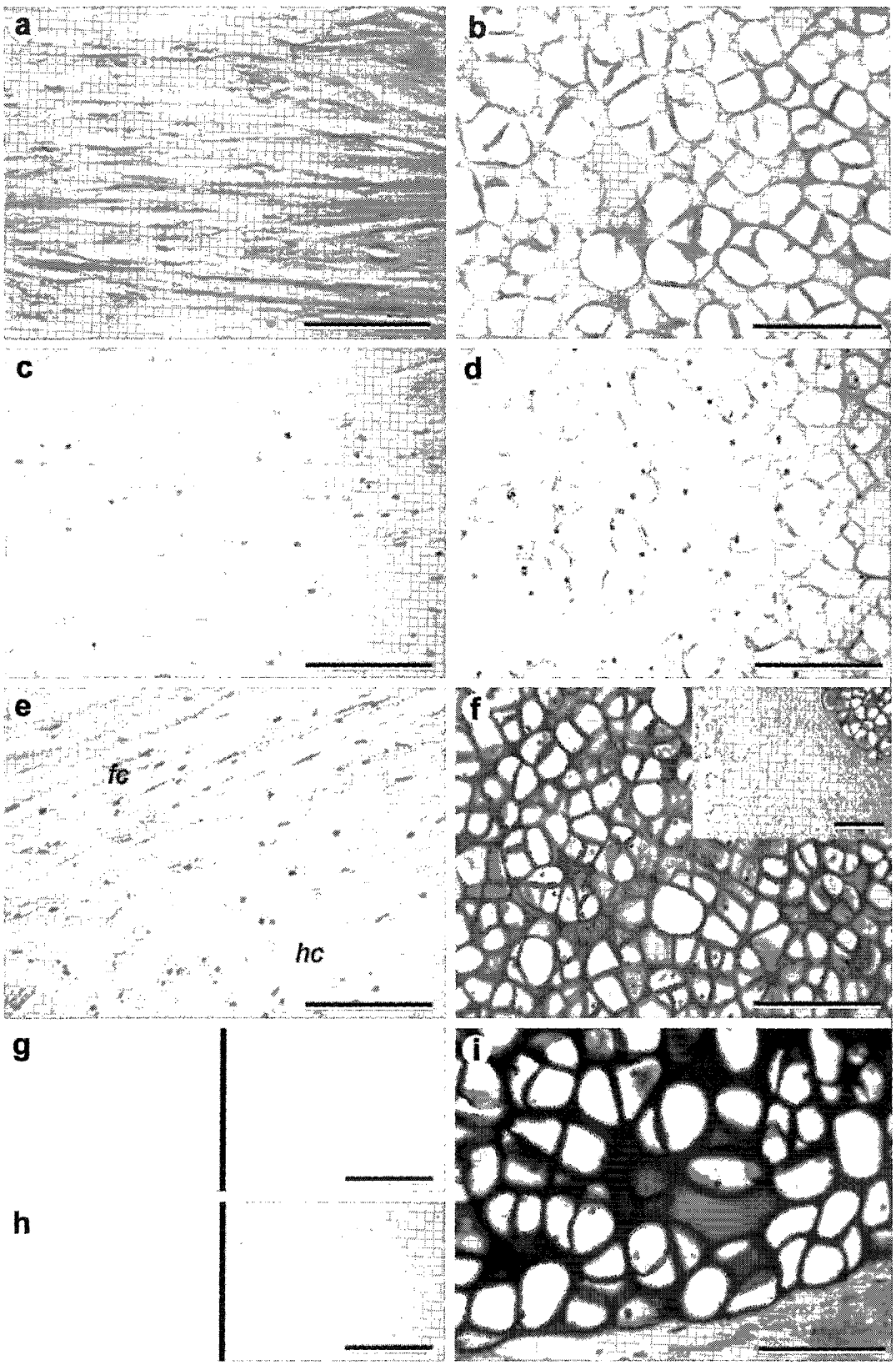

Figure 7

in shape, being more flattened and elongate in the fibrocartilaginous peripheral zones, and spherical within the central hyaline cartilage zone. Fibres within the fibrocartilaginous zone are irregularly arranged and stain differentially with both Mallory's trichrome (fig. 7a) and my cartilage and connective tissue stain (fig. 7e). A similar tissue is also present in the abdomen of the animal, in close association with the branchial cartilages (fig. 7f, inset). The highly cellular opisthosomatic endplate and branchial cartilages appear to derive from this adjacent fibrous tissue.

No positive immunoreactivity was found for any of the antibodies tested within the opisthosomatic cartilages, likely due to the nature of the material rather than absence of the molecules. Opisthosomatic cartilages are highly hydrophilic and sections often fail to remain on the slides, despite pre-coating slides with a variety of adhesive substances. The extracellular matrix of the endosternite reacts homogeneously with antibodies against bone sialoprotein II (DSHB antibody WVID1(9C5)) (fig. 7g) and chondroitin sulphate (DSHB antibody 9BA12) (fig. 7h).

The endosternite cartilage, which has homologues in other arthropods (Bitsch and Bitsch, 2002), contains regions of fibrocartilage and hyaline cartilage, thus is a large piece of fibro-hyaline cartilage. Fibro-hyaline cartilage has a much higher fibrous component than vertebrate hyaline cartilage, nonetheless has mucopolysaccharides that are immunoreactive with chondroitin sulphate antibodies, and the cells embedded within this matrix show the rounded morphology typical of chondrocytes. Whether or not the homologous tissues in other arthropods are also cartilaginous requires further investigations.

Mollusca

Of the invertebrate cartilages, cephalopod cranial cartilage most closely resembles vertebrate hyaline cartilage in histological section (fig. 2 vs. 8). Like the octopus cranial cartilage discussed in Chapter 1, the funnel and orbital cartilages in the cuttlefish *Sepia officinalis* are surrounded by a thin, but distinct, perichondrium. CalEx-resistant mucopolysaccharides are primarily localized in

Figure 8: Histology and Immunoreactivity of cartilages from *Illex* sp. and *Sepia officinalis* (Cephalopoda)

Cartilage within cephalopods resembles vertebrate cartilage in both matrix properties and organization of chondrocytes. Division of chondrocytes within the matrix results in formation of isogenous groups of cells (*) within lacunae. Juvenile cuttlefish (*Sepia*) cartilages show the same staining properties as those illustrated here for *Illex*. Scale bars = 100 µm; *hc* = hyaline cartilage; *pc* = peripheral cartilage; a-d = *Illex*; e-i = *Sepia officinalis*. **a** Acidic mucopolysaccharides are concentrated around the chondrocytes as evidenced by Alcian Blue staining of the orbital cartilage. **b** Homogeneous collagen staining is evident in Masson's trichrome staining of the nuchal cartilage (*light green staining*). **c** Mallory's trichrome staining of cranial cartilage also shows homogeneous fibrous protein (*blue staining*). **d** My new cartilage and connective tissue (CCT) stain reveals relatively homogenous concentration of mucopolysaccharides (*forest green staining*). **e** As cartilage matures, the distance between chondrocytes increases, and the perichondral region (*pc*) is expanded. The extracellular matrix (ECM) of the perichondrium stains light green with my new CCT stain, whereas the ECM surrounding the chondrocytes stains orange-brown in undecalcified sections. Deposition of new matrix, as indicated by proximity of chondrocytes and level of mucopolysaccharide staining, occurs peripherally. Extensive cellular processes are evident within this new matrix as small holes (*arrows*). **f** Mucopolysaccharide staining (*orange-brown staining*) is concentrated within the centre regions of the adult cartilage. **g-i** Fibrous tissues adjacent to the funnel cartilage within *Sepia officinalis* show immunoreactivity with a number of vertebrate antibodies. Control sections are shown on the left. **g** Bone Sialoprotein II; **h** Type X collagen; **i** Chondroitin sulphate proteoglycan.

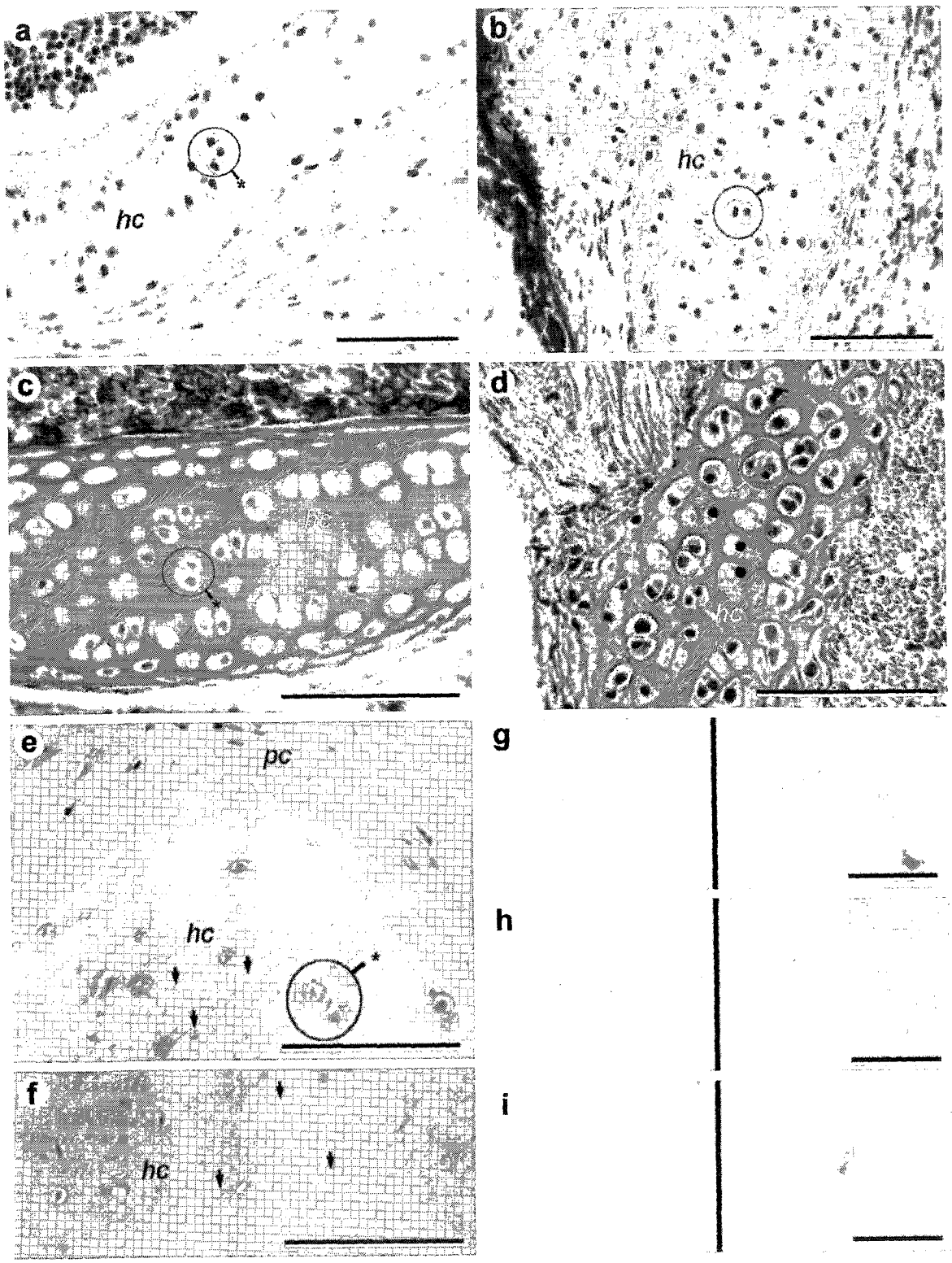

Figure 8

areas immediately surrounding the chondrocytes (fig. 8a). In contrast to the distance between chondrocytes in the adult funnel cartilage (fig. 8e,f), chondrocytes in juvenile cartilages are much closer together (fig. 8a-d; see also fig. 27e,f). The distribution of matrix components within this tissue strongly suggests growth from the periphery (where the matrix stains strongly for collagen, whereas the central cartilaginous matrix is mucopolysaccharide-rich; fig. 8e vs. 8f). Extensive cellular processes can be seen penetrating the extracellular matrix in older animals (fig. 8e,f). In senescent animals, regions of the fibrous connective tissue surrounding the funnel cartilage are immunoreactive with antibodies against vertebrate bone sialoprotein II (DSHB antibody WVID1(9C5): fig. 8g), type X collagen (DSHB antibody X-AC9: fig. 8h) and chondroitin sulphate proteoglycan (DSHB antibody 9BA12: fig. 8i). However due to the adhesive nature of cartilage, resulting in high non-specific background immunostaining, I was unable to confirm any positive immunoreactivity within the extracellular matrix of the *Sepia* cartilage.

Hemichordata

Histological analysis of the skeletal tissues in the hemichordate *Saccoglossus kowalevski* reveals them to be acellular, likely high in collagen but not in mucopolysaccharides (fig. 9a-c). The latter result is supported by the fact that this matrix is not immunoreactive with an antibody against chondroitin sulphate proteoglycan, and do not stain with Alcian Blue (fig. 9d). The acellular extracellular matrix of these skeletal structures in *S. kowalevski* are immunoreactive with antibodies against vertebrate bone sialoprotein II (DSHB antibody WVID1(9C5): fig. 9e), osteonectin (DSHB antibody AON-1: fig. 9f) and cartilage link protein (DSHB antibody 9/30/8-A-4: fig. 9g).

The lack of a cellular component within the hemichordate skeleton is in direct contrast with the working definition of cartilage set out at the beginning of this thesis, and therefore enteropneust hemichordates must be considered not to possess cartilage. However, the possibility that these tissues represent a new type of cartilage, acellular cartilage, is discussed below (section 2.4.4).

Figure 9: Histology and Immunoreactivity of skeletal tissues from *Saccoglossus kowalevski* (Hemichordata)

Hemichordate skeletal tissues are completely acellular extensions of epithelial (*ep*) basement membrane. Scale bars = 100 μm; *ac* = acellular skeleton; *ci* = ciliated epithelium; *mct* = mucoid connective tissue; a,c,d,f,g = gill bars; b,e = proboscis skeleton. **a** New cartilage and connective tissue (CCT) stain reveals the extracellular matrix (ECM) of the gill bars is high in collagen content. **b** CCT staining shows the acellular ECM of the proboscis skeleton contains both low (*green staining*) and high (*red staining*) fibrous protein. **c** High magnification of part of the section shown in (**a**). **d** Alcian Blue staining reveals no mucopolysaccharide staining within the acellular ECM (*ac*). Mucopolysaccharides (*bright blue staining*) are present in the mucoid loose connective tissue (*mct*) of the underlying mesenchyme. The overlying epithelial layer is ciliated (*ci*). **e-g** The acellular skeletal ECM shows immunostaining with vertebrate antibodies. Goblet cells within the epithelium react with the secondary antibody non-specifically (*arrows*). Control sections are shown on the left. **e** Bone sialoprotein II; **f** Osteonectin; **g** Link protein.

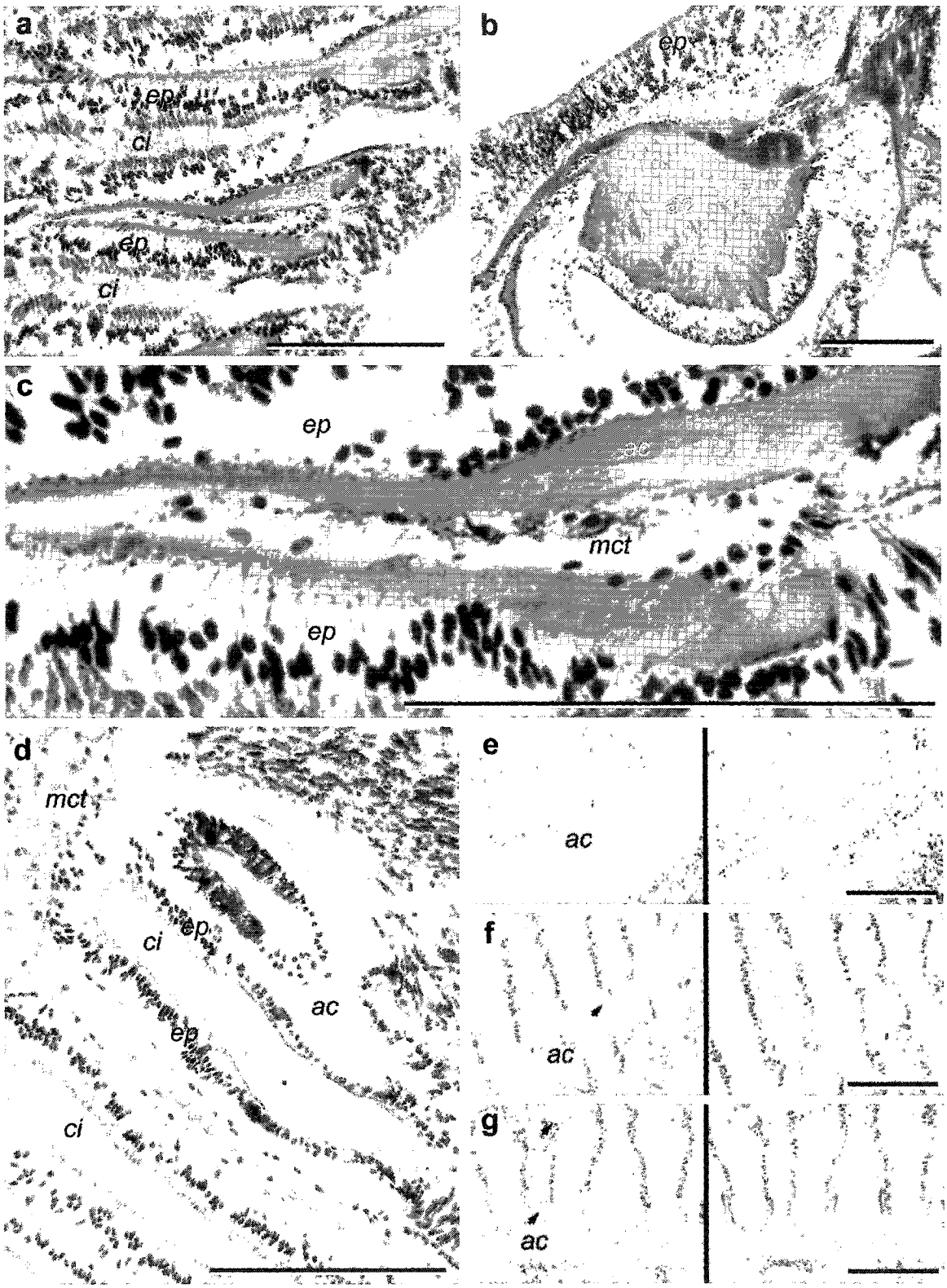

Figure 9

Echinodermata

I investigated the histological structure of the paradental tongues in juvenile *Strongylocentrotus droebachiensis* (3 mm and 10 mm test diameter). In both cases two cell types could be distinguished: those embedded in a mucopolysaccharide-rich matrix (fig. 10a), and those forming muscle fibres in the interior (fig. 10b). My initial examination of these tissues reveals that they are mucopolysaccharide rich, and also have a fibrous protein. Additionally they appear to have a distinct vacuolated cell type (Bonasoro and Carnevali, 1994a,b). Based upon histological features, these tissues fit my working definition of cartilage. Further investigations on the histology and molecular properties of these tissues are needed to fully resolve their position in the spectrum of connective tissues, although they have been postulated to be homologous with vertebrate notochords (Bonasoro and Carnevali, 1994a,b). These are interesting tissues that merit further investigations.

Urochordata

Histological analysis of adult *Styella partita* (with the outer tunic removed) reveals the presence of tissue associated with the siphons that is similar in appearance to the tissue found in the proximal portion of the pedicle of brachiopods. This tissue is highly reactive with stains for mucopolysaccharides (fig. 10c,d) but shows only diffuse staining in proximal regions for collagenous components. At least within *Styella partita*, there is no cartilage.

2.4 Discussion

2.4.1 Evaluation of cartilage and connective tissue stain

The ability to visualize all connective tissue components within a single section has several advantages over other commonly used histological stains, not the least of which is that fewer sections are required to get the same amount of information. My new cartilage and connective tissue staining protocol allows for visualization of elastin, tensile properties of fibrous proteins, mucopolysaccharides, and nuclear material within a single section. Differentiation

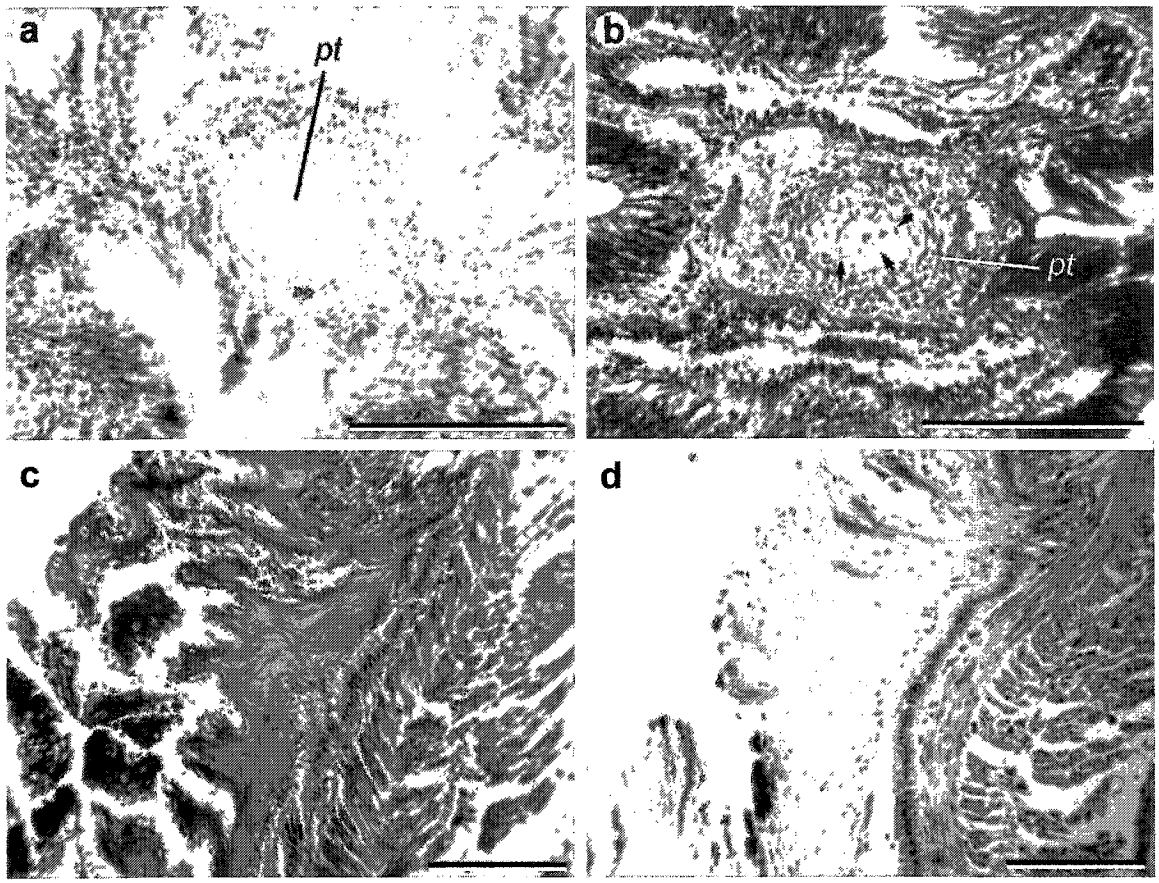

Figure 10: Histology and Immunoreactivity of connective tissues from *Strongylocentrotus droebachiensis* (Echinodermata) and *Styella partita* (Urochordata)

Echinoderms and urochordates possess tissues that are rich in mucopolysaccharides. Scale bars = 100 µm. **a** Paradental tongues (*pt*) in juvenile (2mm diameter) *Strongylocentrotus droebachiensis* show extensive acidic mucopolysaccharides, as evidenced by Alcian Blue staining (*bright blue staining*). **b** Two Fibres of muscle cells are distinguishable within the paradental tongues of juvenile (6mm diameter) urchins when stained with Masson's trichrome (*arrows*). **c** Siphonal tissues from the urochordate *Styella partita* are mucopolysaccharide rich as revealed by my new cartilage and connective tissue stain (*orange-brown staining*). **d** Alcian Blue staining (*bright blue*) also reveals mucopolysaccharides within the siphon.

of elastin staining can be difficult because it requires optimization for individual tissue types. Eliminating elastin staining from the protocol relieves this challenge, while retaining properties of the protocol for visualizing cartilage.

Interestingly, method of decalcification has major affects on staining properties of cartilage. Decalcification with CalEx (Fisher No. CS510-1D) has the advantage of distinguishing the boundary between calcified and uncalcified cartilage, not seen in ETDA decalcified specimens. In EDTA decalcified specimens the distinction between cartilage and other connective tissues is more apparent. However, the difference between cartilage and loose connective tissues remains distinguishable in CalEX specimens, including alligators and turtles (personal observation). The ability to detect calcified cartilage with this method will be a useful tool for continued histological investigations of invertebrate cartilages, where mineralization is not known to occur (Eliberg and Zuckerberg, 1975; Rabinowitz *et al.* 1976).

2.4.2 Immunoreactivity

Positive immunoreactivity of skeletal tissues was found for a variety of antibodies examined (table 2). Of particular interest are the antibodies against molecules thought to be specific to vertebrate cartilage (link protein), bone (osteonectin and bone sialoprotein II) and hypertrophic chondrocytes (type X collagen). Type X collagen antibodies showed positive immunoreactivity with only vertebrate hypertrophied cartilage and patches of acellular fibrous tissues within the connective tissues surrounding the cuttlefish cartilage. The function of type X collagen within hypertrophied vertebrate chondrocytes is not well understood, although it has been postulated to be involved with stabilization of the network of matrix proteoglycans within the cartilage (Luckman *et al.*, 2003).

The link protein antibody is reactive with only vertebrate cartilage and the hemichordate skeleton, possibly reflecting the closer phylogenetic affinities between hemichordates and vertebrates (see Chapter 3). Binding of this antibody suggests at the very least that a similar molecule is present within the hemichordate skeleton. Further characterization of the hemichordate link

Table 2: Immunoreactivity of invertebrate cartilaginous tissues with select vertebrate antibodies

Invertebrates, or isolated invertebrate tissues, were sectioned and stained with a panel of vertebrate antibodies from the Developmental Studies Hybridoma Bank (DSHB), using sections of quail embryos as positive controls. Tissues in which no positive expression was found are indicated "–".

DSHB Antibody	Control (quail) expression	*Sepia* Funnel cartilage	*Limulus* Endosternite	*Terebratulina*	*Potamilla*	*Saccoglossus*
Link protein (9/30/8-A-4)	cartilage matrix	–	–	–	–	skeletal matrix
Type X collagen (X-AC9)	Hypertrophied chondrocytes and cartilage matrix	Fibrous tissues surrounding cartilage, and possibly within chondrocytes*	–	–	–	–
Chondroitin sulphate proteoglycan (9BA12)	Cartilage, especially hypertrophied chondrocytes and matrix	Select connective tissue cells	Cartilage matrix	Homogenous expression throughout lophophore matrix	Branchial skeleton matrix	–
Osteonectin (AON-1)	Nuclei of all cells EXCEPT chondrocytes and osteocytes	Nuclei of most juvenile cells; no adult expression	–	– **	Branchial skeleton matrix	skeletal matrix
Bone Sialoprotein II (WVID1(9C5))	Most non-skeletal connective tissues; excluding cartilage and bone matrix	Select connective tissue cells and dispersed larger fibre bundles	Cartilage matrix and surrounding muscle	Shell matrix	Ciliated epithelium of branchial crown	skeletal matrix
Decorin (CB-1)	Blood cells and bone matrix	–	–	Shell matrix	–	–
Keratin Sulphate (I22)	Select chondrocytes	–	–	Fibrous regions surrounding the coelomic canals within lophophore	–	–

*Not confirmed due to high non-specific background staining
**Positive staining within parasites found within the lophophore

protein is needed to draw robust conclusions regarding the nature of these tissues.

Bone sialoproteins are involved in mineralization of vertebrate bone, probably acting as a crystal nucleator (Roach, 1994), and are reported to be restricted to mineralized connective tissues (Ayad *et al.*, 1994). Given the lack of mineralization of any invertebrate cartilages, the immunoreactivity with the bone sialoprotein II antibody in all invertebrate cartilages tested is particularly surprising. Two explanations present themselves for these expression patterns. The vertebrate antibody could be recognizing a similar epitope on a different molecule within the invertebrate lineages. Alternatively, bone sialoprotein II may have another function in these lineages that is not related to biomineralization. A second functional role is also suggested within vertebrates by the expression of bone sialoproteins during osteoblast differentiation in cell culture, and only later found associated with mineralization crystals (Nefussi *et al.*, 1997). Additionally, the widespread expression of this antibody within non-skeletal connective tissues of vertebrate control sections in this study is suggestive of either interpretation, and merits further investigation.

Osteonectin acts as a negative regulator of crystal growth in vertebrate skeletons, is expressed in high levels in bone matrices, and is thought to be involved in regulating the degree of bone mineralization (Roach, 1994). Expression of osteonectin within the non-mineralized matrices of some invertebrate cartilages (sabellid polychaetes and hemichordates) could suggest that this molecule may be involved in the lack of mineralization found in these tissues. However osteonectin has a number of other roles in many different tissue types involved in cell adhesion, cell cycling, cell shape, and cell differentiation (reviewed in Yan and Sage, 1999), some of which are associated with nuclear localization of this protein (Gooden *et al.*, 1999; also found here in quail and juvenile cuttlefish sections – table 2).

Along with some of the histological features, the immunoreactivity of those tissues examined with antibodies against molecules thought to be specific to

vertebrate bone suggests that these tissues are truly intermediate between vertebrate bone and cartilage.

2.4.3 Tissue distribution: Cartilage vs. chondroid connective tissue

Chondroid connective tissues – tissues that possess extracellular matrix properties of cartilage but lack distinctive chondrocytes – are common within metazoan taxa, being found within cnidarians, brachiopods, polychaetes, and urochordates (table 3). Chondroid connective tissues are likely very common throughout other invertebrate groups, supporting the notion that this is an ancient tissue type.

Of the invertebrates examined in this study, cephalopod molluscs, sabellid polychaetes, and chelicerate arthropods possess cartilage. Tissues described within echinoderms may also be cartilage, however further investigation of these tissues is required to assess this prospect. Within these invertebrate cartilages, those containing vacuoles within the chondrocytes are common. Because this is a common feature amongst invertebrate cartilages, it merits incorporation into cartilage classification systems.

2.4.4 Broadening cartilage classification

Vesicular cartilage

To facilitate the inclusion of all invertebrate cartilages into current schemes of cartilage classification, I propose adding a new category to Benjamin's (1990) cell-rich cartilages: *vesicular cell-rich cartilage*. The distinguishing feature of this type of cartilage is the presence of large vesicles or vacuoles within the chondrocytes, which augment the physical properties of the matrix. Within this new category are the cartilages within the tentacles of the sabellid polychaetes (Schaffer, 1930; Person and Philpott, 1967; Polychaeta section 2.3.2), the branchial cartilages of the horseshoe crabs (Person and Philpott, 1969a,b; Arthropoda section 2.3.2), the radular cartilages of molluscs (Raven, 1958; Person and Philpott, 1969a), and possibly the notochord of chordates (Olsson, 1965; Schmitz, 1998; see Chapter 4) to name just a few.

Table 3: Connective tissue types within select invertebrate groups
Comparative analysis of invertebrate connective tissues was undertaken to determine the histological composition of these tissues. Only tissues composed of mucopolysaccharides, fibrous protein, and morphologically distinct cells are classified as a type of cartilage. Tissues with only moderate expression are scored as +/–, absence: –, and presence: +. See text for discussion of the different connective tissue types.

	mucopolysaccharides	fibrous protein	unique cell type	tissue classification
Metridium (Cnidaria)	+	–	–	connective tissue
Terebratalia & *Terebratulina* (Brachiopoda)	+	+	–	chondroid connective tissue
Potamilla & *Myxicola* (Annelida, Polychaeta, Sabellidae)	+	+	+	vesicular central cell-rich cartilage*
Hydroides (Annelida, Polychaeta, Serpulidae)	+	+	–	chondroid connective tissue
Limulus (Endosternite) (Arthropoda, Chelicerata)	+	+	+	fibro-hyaline cell-rich cartilage*
Limulus (Branchial) (Arthropoda, Chelicerata)	+	+	+	vesicular *Zellknorpel* cartilage*
Illex & *Sepia* (Hyaline cartilages) (Mollusca, Cephalopoda)	+	+	+	cell-rich hyaline cartilage
Saccoglossus (Hemichordata)	+/–	+	–	acellular cartilage?*
Strongylocentrotus (paradental tongues) (Echinodermata)	+	+/–	+	vesicular cartilage?
Styella (Urochordata)	+	–	–	chondroid connective tissue

* see text for further discussion of these cartilage types.

This new category of cartilage can be further expanded to also take into account different features of the extracellular matrix. For example, I have described the cartilage of the sabellid polychaete branchial crown as a central cell-rich cartilage (see Polychaeta section 2.3.2). Because their chondrocytes are vacuolated, sabellid polychaete tentacle cartilage is a central cell-rich vesicular cartilage.

Within the opisthosomatic cartilages of the horseshoe crab, cells are large and spherical, and contain a large vesicle (or vacuole), making this tissue a vesicular cell-rich cartilage. The high cellularity and rigidity of the matrix is reminiscent of *Zellknorpel* cartilage described by Schaffer (1930) and Benjamin (1990), and therefore I conclude that *Limulus* branchial cartilages are vesicular *Zellknorpel* cartilages. To my knowledge the branchial cartilages do not have homologues within other extant arthropods. Furthermore, the branchial cartilages of the horseshoe crab are the only known examples of vesicular *Zellknorpel* cartilage – although the cartilage supporting the oral cirri of cephalochordates might also qualify (Ruppert, 1997; Wright *et al.*, 2001).

Expanding the classification of cartilage to include tissues of the central cell-rich vesicular cartilage type could permit the inclusion of some vertebrate notochords as a type of cell-rich cartilage, representing either a highly derived condition where the matrix separating the individual cells has been eliminated, or an ancestral condition indicating an epithelial origin for cartilage. Alternatively, the epithelial nature of the notochord could represent an example of a second, independent evolution of a cartilaginous tissue within the chordates. These ideas will be explored further in Chapter 4, within the context of cartilage evolution.

Acellular cartilage

Given that the extracellular matrix of the hemichordate skeleton is immunoreactive with antibodies against link protein (see Hemichordata, section 2.3.2) and type II collagen (as discussed by Swalla, 2004), the possibility that this tissue represents an acellular, epithelially derived cartilage should not be dismissed outright. Junqueira *et al.* (1983) describe an acellular cartilage found within the circulatory system of *Potamotrygon*, a fresh water stingray. This tissue

has no chondrocytes, and unlike other vertebrate cartilages, is perforated by vascular channels. Also of interest, this cartilage attaches to the basement membrane of an overlying squamous epithelium, and is not present in small specimens (Junqueira *et al.*, 1983). This stingray tissue and the skeletal tissues of hemichordates may be representatives of a new category of cartilage, acellular cartilage, located at the opposite end of the cartilage spectrum including cell-rich cartilages (Benjamin, 1990).

2.4.5 Cartilage and epithelia

Central cell-rich cartilage, as seen in sabellid polychaetes, may be thought to represent an intermediate phenotype between epithelial derived acellular skeletal tissues and cellular skeletal supports. In contrast to the minimal diversity in cellular skeletal supports present in extant lineages, most metazoan groups have expanded and elaborated the epithelial derived tissues as secreted skeletal support structures: for example molluscan shells and radulas; annelids have an external cuticle that is secreted by an epithelial layer (Brusca and Brusca, 2002); arthropods secrete an extensive exoskeleton from an epithelial layer; hemichordate skeletons derive from hypertrophy of an epithelial basement membrane (Benito and Pardos, 1997). Although epithelially derived cartilage may seem at odds with traditional wisdom, it becomes less so when one considers the molecular similarity between cartilage and some vertebrate notochords – epithelially derived skeletal tissues which exhibit cartilage specific proteoglycans within an acellular sheath (Eikenberry *et al.*, 1984; Welsch *et al.*, 1991, 1998; Schmitz, 1998; Cole and Hall, 2004; Chapter 4).

2.5 Conclusions

The data on invertebrate cartilaginous endoskeletons presented here offer unique insights into the evolution of vertebrate skeletal tissues. The ability to form cellular connective tissues structurally similar to cartilage without type II collagen is a feature that appeared before the evolution of vertebrates, supporting the notion that cartilage is not simply an embryonic adaptation (as per Romer, 1942),

but was present in vertebrates before calcification evolved (Denison, 1963; Donoghue and Sansom, 2002). Both vertebrate cartilage and bone likely arose from the same ancestral chondroid connective tissue that gave rise to the invertebrate cartilages, as evidenced by the fact that vertebrate bone shares features with invertebrate cartilages, such as cell-cell connections (Bairati *et al.*, 1998) and use of a type I collagen (Kimura and Karasawa, 1985; Bairati *et al.*, 1999). Additionally, positive immunoreactivity among various invertebrate cartilages and chondroid connective tissues with antibodies against molecules thought to be largely bone-specific within vertebrates further supports the notion that vertebrate bone and cartilage derive from a common chondroid connective tissue precursor.

The implications of the histological data presented here on the evolution of cartilage as a tissue type will be explored in Chapter 4. Prior to this discussion, in the chapter that follows I establish the evolutionary context for these tissues with an examination of metazoan phylogenetics.

Chapter 3: Clades and Grades in Molecular Phylogenetics

3.1 Introduction

In order to assess the evolution of cartilage as a tissue type, and thus the homology of invertebrate cartilages, it is necessary to have a robust phylogeny of the metazoa onto which cartilage distribution and features can be analyzed. In the following pages I evaluate the status of metazoan phylogenetics, and use maximum parsimony to create a supertree of the metazoa that reflects the current consensus from molecular systematics.

3.1.1 Phylogenetics and character evolution

The study of phylogenetics serves two main purposes. The most obvious is to determine relationships between organisms. However, phylogenetic hypotheses are also invaluable tools for many non-systematists whose interest lies in evolution of different features or characters of organisms. Analysis of character evolution relies heavily on having robust phylogenetic hypotheses available on which to map and polarize the characters in question. Use of a phylogeny or tree depicting false relationships between the organisms in question will inevitably lead to erroneous conclusions about the evolution of that feature (Symonds, 2002).

To study morphological character evolution, phylogenetic hypotheses based upon molecular evidence are particularly useful in that they are presumed to be completely independent of the character data being mapped. When the relationships between the taxa in question are established based upon a cladistic analysis of morphological characters, there is a possibility of confounding the evolution of the characters with evolution of the organisms because the two are no longer treated as independent. One might be lead to draw incorrect conclusions regarding character evolution if these characters, or aspects of the characters, are used to determine the phylogeny; the likelihood (and thus significance) of this happening has been debated (Brooks and McLennan, 1991; Maddison and Maddison, 1992; Swofford and Maddison, 1992).

Invertebrate zoologists interested in evolution of specific features, in this instance the evolution of cartilage, need to be careful in their choice of phylogenetic trees because of the amount of change that has recently taken place in the field of metazoan systematics. Metazoan phylogeneticists seek to determine the truth about the history of animal life. Over the years, there have been many fluctuations in the majority consensus of metazoan relationships. Whereas early studies of metazoan relationships were based (not surprisingly) solely on morphology, more recent efforts (beginning in 1988) have relied increasingly on molecular systematics. In particular small subunit ribosomal ribonucleic acid (18S rRNA) has been found to be a useful molecule for determining phylogenetic relationships within animal groups (Field 1988).

3.1.2 Molecular phylogenetics

There has been a substantial accumulation of molecular phylogenies in recent years. Initial analyses revealed metazoan relationships that disagreed with those established by traditional classification based on morphological characters (see Eernisse *et al.*, 1992; Nielsen, 2001). The most notable of changes is the detection of lophotrochozoan and ecdysozoan clades (see review by Adoutte *et al.*, 2000). Although these groups were detected based purely on molecular data, some morphological features have since been found that also unite animals within these newly established groups. Lophotrochozoa clusters animals with trochophore larvae (Mollusca, Annelida, Echiura, Pogonophora, Vestimentifera, Sipuncula, Nemertea, and Entoprocta) with those that possess a lophophore (the Lophophorates: Bryozoa (= Ectoprocta), Brachiopoda, and Phoronida; Halanych *et al.*, 1995). Ecdysozoa clusters animals that molt (Arthropoda, Nematoda, Tardigrada, Onychophora, Nematomorpha, Priapulida, Kinorhyncha, and Loricifera; Aguinaldo *et al.*, 1997; Aguinaldo and Lake 1998; Giribet *et al.*, 2000).

Ecdysozoa has been further supported by the discovery of horseradish peroxidase immunoreactivity within the neural tissues, to the exclusion of all other animal groups (Haase *et al.*, 2001). Platyzoa (Platyhelminthes, Gastrotricha, Gnathostomulida, Acanthocephala, Rotifera, and possibly

Cycliophera; Giribet *et al.*, 2000) also form a monophyletic clade often clustered with Lophotrochozoa in a clade termed Spiralia (Garey and Schmidt-Rhaesa, 1998), which finds support in HOX gene sequences (Bayascas *et al.*, 1998). Although some authors treat Platyzoa as members of Lophotrochozoa (Adoutte, *et al.*, 2000), for the purposes of this study Lophotrochozoa will be taken to exclude Platyzoa.

Although molecular data support the presence of three or four major bilaterian clades (Spiralia (= Lophotrochozoa + Platyzoa), Ecdysozoa, and Deuterostomia), the relationships within and between these groups remain largely unresolved. Additionally, it has been difficult to reliably place many of the lesser well-known animal groups within this general framework of metazoan phylogeny (e.g. Gnathostomulida: Littlewood *et al.*, 1998; Chaetognatha: Giribet *et al.*, 2000).

Despite initial hopes, the 18S molecule has fallen short of solving the riddle of evolution of animal forms, leading some researchers to push for increased investigations into other candidate molecules for use in molecular systematics (McHugh, 1998). Most recently, there has been a push in phylogenetic thinking towards a "total-evidence" approach to phylogenetics (*sensu* Kluge, 1989), resulting in a number of analyses that combine both molecular and morphological data (Giribet *et al.*, 2000; Peterson and Eernisse, 2001; Zrzavy *et al.*, 2001). A related phylogenetic tool is supertree methodology.

3.1.3 Supertrees

The supertree approach seeks to address the problem of combining phylogenetic hypotheses arising from different types of data. The history of this approach, its benefits, shortcomings, and uses can be found in Bininda-Emonds *et al.* (2002).

A supertree matrix is one step removed from the original (source) data. Each character represents a single node from a previously published source tree, rather than representing raw data. Not surprisingly this feature has drawn significant criticism (see Rodrigo, 1993, 1996; Springer and de Jong, 2001; Gatesy *et al.*, 2002). A supertree is then created from the matrix using a

Sanderson, 2001; Bininda-Emonds *et al.*, 2002). A redeeming feature of the supertree approach is the ability to combine phylogenetic hypotheses regardless of the taxa present. In order to be included in a supertree analysis, a source tree simply must contain a minimum of two taxa in common with other source trees included in the supertree data matrix. This results in a longer list of terminal taxa than present in any one original study.

Although most commonly used as a tool for generating novel phylogenetic hypotheses (Bininda-Emonds *et al.*, 1999; Liu *et al.*, 2001; Jones *et al.*, 2002; Pisani *et al.*, 2002), a supertree is also an epistemological device. A supertree is a reflection of the overall knowledge in the field because it combines multiple available hypotheses and determines the consensus, or lack thereof, between these studies. This feature of the supertree approach makes it an ideal tool for determining the current state of affairs in metazoan molecular phylogenetics.

Despite the plethora of molecular phylogenies that continue to accumulate within the literature, systematists have yet to reach a consensus on metazoan relationships. In order to evaluate the status of metazoan molecular phylogenetics from this mass of molecular literature in an objective way, I constructed a supertree of available molecular hypotheses. Because the main goal here is to evaluate molecular hypotheses, neither total-evidence studies, nor morphological studies are included in the supertree data matrix.

3.2 Methods

3.2.1 Source study selection

Metazoan phylogenetic hypotheses were selected from 62 analyses of molecular data, published between 1988 and early 2001 (Appendix 1). Of particular interest for this study was not the relationships of taxa within major metazoan clades, but rather the relationships between the clades. Therefore to be included in this study source trees had to include taxa from three or more higher-level taxonomic groups. In the event that any given source paper represented more than one molecular phylogeny derived from analyses of the same data set, only one tree was included in its entirety. From the remaining

same data set, only one tree was included in its entirety. From the remaining trees only nodes that differed from this original tree were included in the analysis, thereby creating a mini-supertree of the results depicted in the source paper. The source trees included were derived from analysis of the following molecules:

1. 18S,
2. elongation-factor alpha,
3. 12S rRNA (Ballard *et al.*, 1992; Wagele and Stanjek, 1995),
4. 16S rRNA (Schlegel *et al.*, 1996),
5. 23S rRNA (Odorico and Miller, 1997),
6. 28S rRNA (Christen *et al.*, 1991),
7. COI (Black *et al.*, 1997), and
8. beta-tubulin,
9. HSP70, and
10. protein kinase (Schutze *et al.*, 1999).

3.2.2 Taxon selection

Two data matrices were initially constructed, one where the terminal taxa used were genera (the *genera-grade* analysis) and another where more inclusive levels of classification were created by collapsing nodes within the source tree corresponding to monophyletic clades according to traditional classification schemes (the *class-grade* analysis). The validity of assuming monophyly of clades was determined from the topology of the tree from the genera-grade analysis. Most groups are represented as phyla, with the exception of the following:

- Mollusca (grouped as Polyplacophora, Bivalvia, Gastropoda, and Scaphopoda – no Cephalopoda data were available from any of the included studies)
- Annelida (grouped as Oligochaeta and Hirudina and Polychaete families)
- Arthropoda (grouped into traditional Classes)
- Platyhelminthes (grouped as Acoela, Catenulida, Nemertodermatida, and Rhabdocoela)
- Porifera (grouped as Calcaria and Demospongidae).

To facilitate analyses, and because monophyly of phyla-level grades is in most cases strongly supported by morphology (Nielsen, 2003), the condensed

matrices were further compressed to 39 phyla grade taxa (the *phyla-grade* analysis), regardless of whether or not this monophyly was supported by the genera-grade analysis.

3.2.3 Character coding

Character coding was completed manually; all taxa within the clade represented by the node received a coding of "1" and all other taxa represented in that particular source tree but outside the clade in question were coded as "0". Taxa not present within the source tree were coded as "?". For the class-grade analysis each collapsed node was inspected manually. In both instances, characters from within collapsed nodes were removed. In the phyla-grade analysis taxa were merged in MacClade, and inconsistencies with monophyly within the data matrix was reflected by a character state of "0&1".

The genera-grade analysis contained a total of 1585 characters and 430 terminal taxa (Appendix 2.1), whereas the class- and phyla-grade analyses included 959 characters and 72 (class) or 39 (phyla: see Appendix 2.2) terminal taxa derived from the same molecular source trees.

3.2.4 Phylogenetic analysis

Phyla- and class-grade analyses were conducted using PAUP* 3.1.1, using the heuristic search strategy, with TBR branch swapping and Maxtrees set at 10,000. As the genera-grade data set required specialized computing facilities, this analysis was conducted by Dr. Olaf Bininda-Emonds at the Technical University of Munich.

Decay indices, or Bremer support values (Bremer, 1988, 1994), were calculated for the phyla-grade tree by repeating the analysis with the tree score value increasing by 1 each repetition. The decay index represents how many extra steps, or character changes, are required within the matrix to collapse the clade. Therefore a high decay index indicates more robust support for that clade within the matrix.

A concern regarding these analyses is that a majority of the source data derives from analysis of the same 18S sequences, and are thus non-

independent. For the condensed class-grade analysis, a second matrix was created in collaboration with Bininda-Emonds, in which non-independence of the data was corrected for by first creating a two mini-supertrees from all source trees initially derived from 18S data (18S supertree) and elongation factor-α data (EF-α supertree). These mini-supertrees were then included in place of the original source trees within the supertree matrix. The resultant matrix is composed of 10 trees: 18S supertree, EF-α supertree, and eight source trees derived from other molecular data.

For both the 18S and EF-α supertree analyses, some taxa were represented poorly, such that they could cluster equally parsimoniously with almost every other taxon on the tree, thereby collapsing the resolution of the supertree. Thus, "safe taxonomic reduction" was used to identify and remove these taxa from the analysis (Wilkinson, 1995; Bininda-Emonds *et al.*, 1999). These taxa are then re-inserted into the resultant tree whenever possible based on their equivalent index taxa.

3.2.5 Evaluating supertree methodology

To confirm that collapsing terminal nodes does not adversely affect the topology of deeper nodes in the tree, a supertree methodology test was constructed wherein a fictitious "true" phylogeny was created consisting of three major clades, each clade consisting of three taxa (fig. 11a). A supertree matrix was compiled from 10 equally fictitious phylogenies, wherein not all terminal taxa of the "true" phylogeny were represented. The topology of six of these source trees reflected the "true" phylogeny (fig. 11b-g); two trees had topologies that were consistent with the "true" phylogeny, but contained some unresolved nodes (fig. 11h,i); the remaining two trees were inconsistent with the "true" phylogeny (fig. 11j,k). The matrix representing these trees was analysed with the same settings used for analysis of metazoan matrices. The effects on the resultant topology of collapsing the nodes within the three clades in the "true" phylogeny, was also examined.

Figure 11: Analysis of supertree methods and the effects of collapsing nodes
Supertree construction using maximum parsimony representation (MPR) accurately reconstructs relationships between clades. **a** A fictitious phylogeny was constructed representing the relationships between 9 taxa (*a-j*), comprising three clades. **b-k** Another ten fictitious source trees were arbitrarily created depicting the phylogenetic relationships of taxa found in (**a**). Of these, six phylogenies (**b-g**) are consistent with the original fictitious phylogeny, two are consistent with the original fictitious phylogeny, but show incomplete resolution (**h,i**), and the last two are incompatible with the original fictitious phylogeny (**j,k**). The topology of these source trees was coded into a matrix and subjected to MPR analysis in PAUP*, under a heuristic search strategy, TBR branch swapping, for 50 repetitions; see text for further details on supertree character coding. **l** Strict consensus of 30 most parsimonious trees reflects accurate topology of clade relationships represented in the original fictitious phylogeny (**a**).

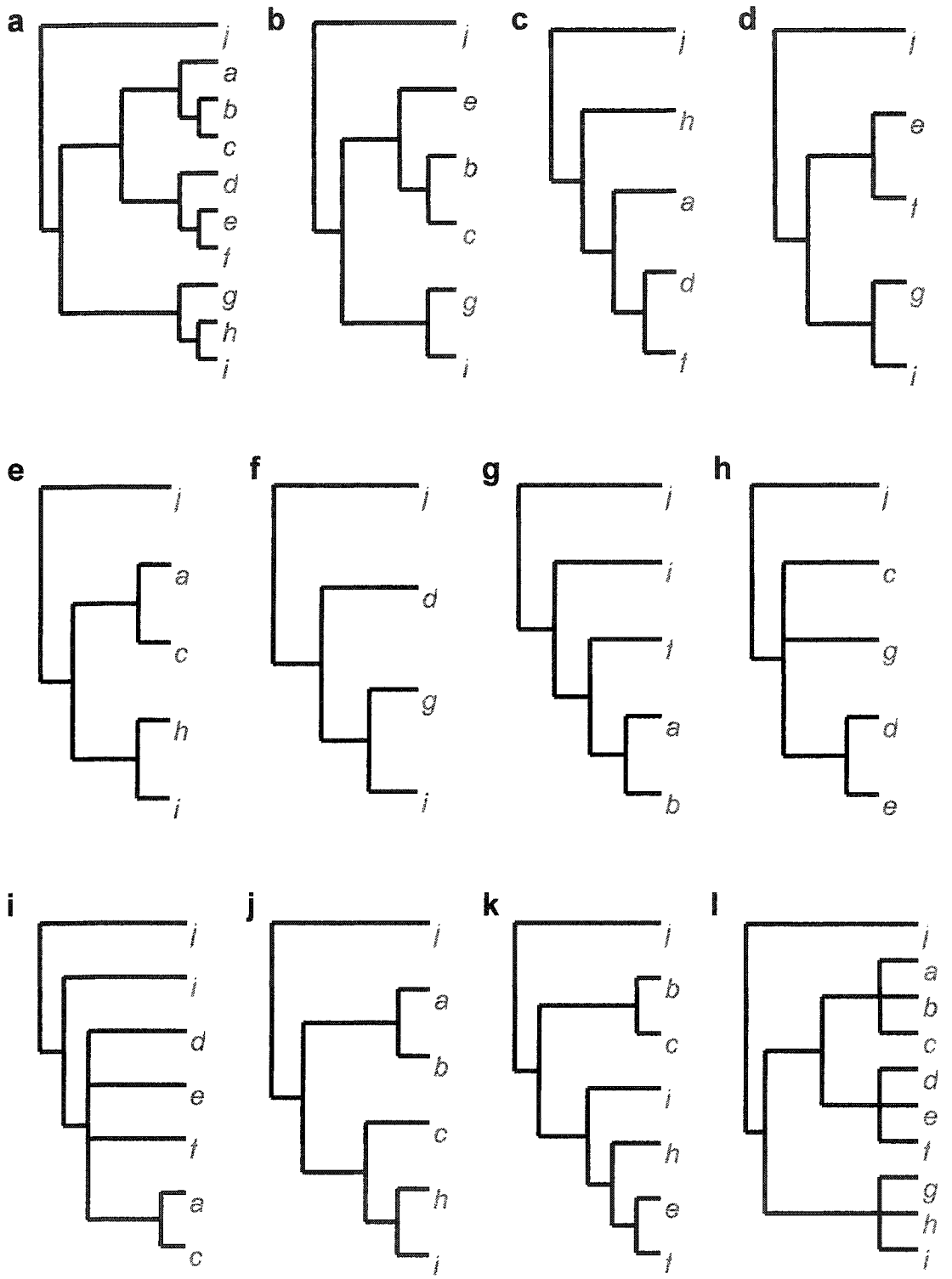
a
j
a
b
c
d
e
f
g
h
i
b
j
e
b
c
g
i
c
j
h
a
d
f
d
j
e
f
g
i
e
j
a
c
h
i
f
j
i
t
a
b
g
j
i
d
g
i
h
j
c
g
d
e
i
j
i
d
e
f
a
c
j
a
b
c
h
i
k
j
b
c
i
h
e
f
l
j
a
b
c
d
e
f
g
h
i

Figure 11

3.3 Results

3.3.1 Testing supertree methodology

The full matrix representing the fictitious tree topologies gives 34 most parsimonious trees, with the relationships between the three clades fully resolved (fig. 11l). However the method was unable to resolve the relationships within the clades. Collapsing nodes within the clades results in a single most parsimonious tree showing the same relationships between the clades as was resolved from the full matrix. The topology of these relationships accurately represents the topology of the "true" phylogeny (fig. 11a vs. l). This is taken as a demonstration that significant information reflecting the topology of deeper nested nodes is not lost by collapsing crown nodes, thereby supporting the utility of the class- and phyla-grade analyses presented below.

3.3.2 Genera-grade analysis

The final criteria for inclusion as a source tree are:

- studies published between 1990 and 2001;
- studies include only molecular data; and
- at least three phyletic grades are represented.

Although there is no full consensus from the genera-grade analysis, many of the taxa group together into traditional morphological grades (phyla) in >80% of the trees (Appendix 2.3) and thus I consider it safe to assume monophyly of these grades in creating the condensed matrix. In contrast, other morphological grades are distinctly paraphyletic in the supertree and therefore are collapsed into less inclusive taxonomic grades (sub-phylum or class) for the following analyses (table 4). Resolved within the majority rule tree are four recognized major bilaterian clades: Deuterostomia, Platyzoa, Lophotrochozoa, and Ecdysozoa (fig. 12).

Table 4: Taxonomic grades used for the condensed analyses
To facilitate analysis, taxa represented within source trees were condensed into more inclusive supraspecific taxa according to traditional classification schemes.

Taxonomic grouping	Supertree genera (#)	Estimated species numbers*
Cephalochordata	1	
Chordata	15	49,693
Urochordata	7	
Hemichordata	4	85
Enteropneusta	3	
Pterobranchia	1	
Echinodermata	22	7,000
Chaetognatha	2	100
Mollusca	38	93,195
Polyplacophora	7	
Gastropoda	17	
Bivalvia	14	
Scaphopoda	1	
Annelida	24	16,500
Polychaeta	14	
Polychaeta_Phyllodocida	5	
Polychaeta_Capitellida	2	
Polychaeta_Cheatopteridae	1	
Polychaeta_Cirratulida	1	
Polychaeta_Terebellidae	2	
Polychaeta_Spionida	1	
Polychaeta_Sabellida	1	
Polychaeta_Orbiniidae	1	
Hirudina	2	
Oligochaeta	8	
Nemertea	3	900
Nematoda	19**	25,000
Sipuncula	3	320
Brachipoda_Inarticulata	3	335
Brachipoda_Articulata	1	
Ectoprocta	3	4,500
	2	150
Entoprocta		
Phoronida	1	20
Echiura	3	135
Pogonophora	3	{annelid}
Vestimentifera	5	{annelid}
Gastrotricha	2	450
Gnathostomulida	1	80
Acoela	4	
Platyhelminthes	67	20,000
Onychophora	4	110
Pentastomida	1	
Tardigrada	30	800
Arthropoda	99	~1.097,289
Crustacea	30	
Insecta	29	
Myriapoda	14	
Chelicerata	16	
Pycnogonida	5	
Collembola	5	
Priapulida	1	16
Acanthocephala	11	1,100
Kinorhyncha	1	150
Nematomorpha	1	320
Rotifera	2	1,800
Cycliophora	1	1
Placozoa	1	1
Porifera	16	5,500
Porifera_Calcarea	4	
Porifera_Demospongiae	9	
Porifera_Hexacti	1	
Porifera_unclassified	2	
Cnidaria	38	10,000
Ctenophora	5	100
Myxozoa	3	na
Rhombozoa	1	70
Orthonectida	1	20

*from Brusca and Brusca (2002)
**13 long-branch taxa

Figure 12: Genera-grade supertree analysis
Colour coded cladogram showing the distribution of major metazoan phyla from analysis of a genera-level supertree analysis. Shown is the 50% majority rule tree (of 10,000 most parsimonious trees) illustrating relationships depicted in a parsimony analysis derived from 57 source trees; see text for details. Four major bilaterian clades resolve: Deuterostomia (D), Platyzoa (P), Lophotrochozoa (L), and Ecdysozoa (E). Dashed lines indicate branches leading to aberrantly placed taxa.

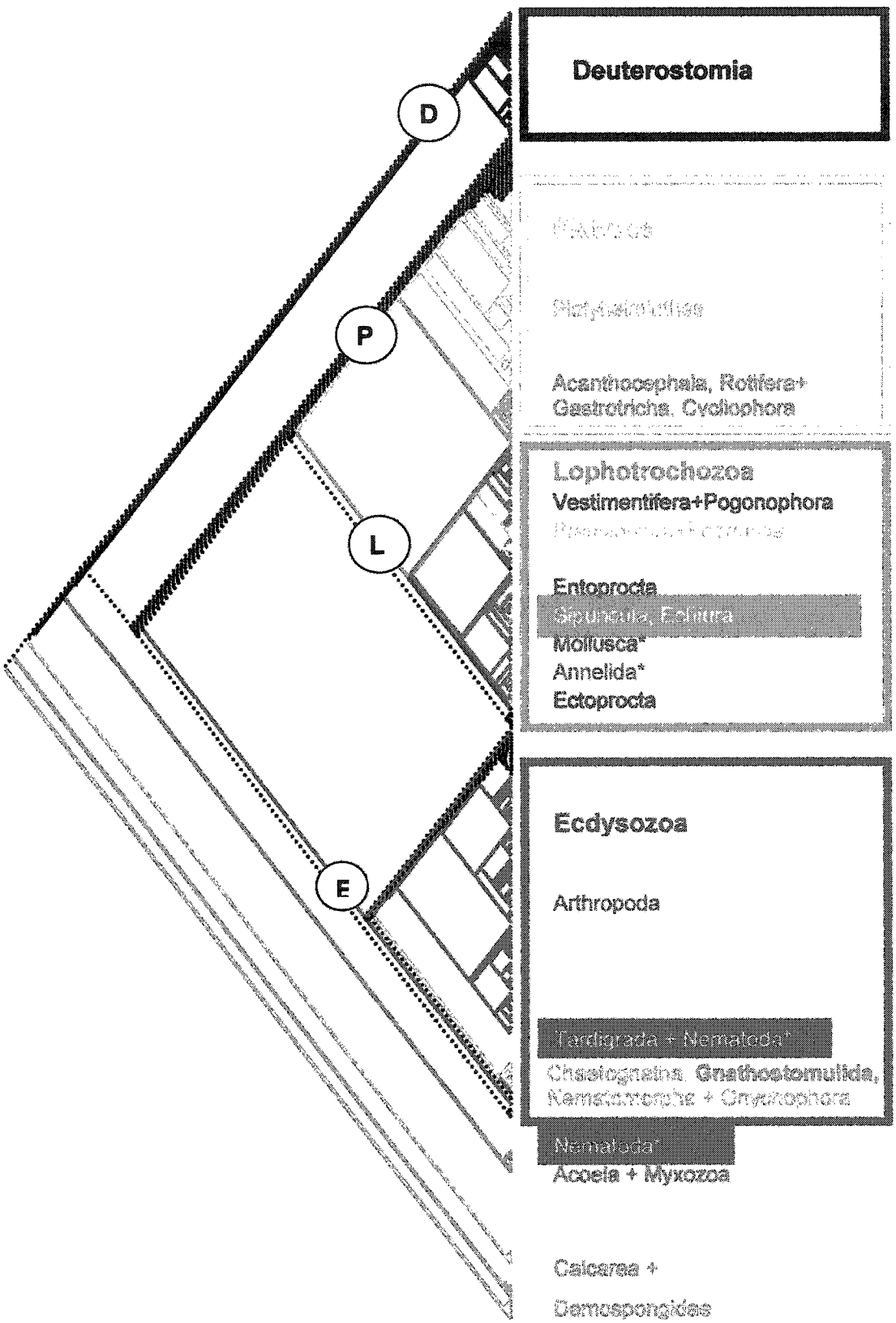
Deuterostomia
D
P
L
E
Acanthocephala, Rotifera+
Gastrotricha, Cycliophora
Lophotrochozoa
Vestimentifera+Pogonophora
Entoprocta
Mollusca*
Annelida*
Ectoprocta
Ecdysozoa
Arthropoda
Chaetognatha, Gnathostomulida,
Nematomorpha + Onychophora
Acoela + Myxozoa
Calcarea +
Demospongidae

Figure 12

3.3.3 Class-grade analyses

The main interest in this study is the deeper nodes (higher taxonomic level relationships) – how the different major animal lineages are related to one another. Therefore, I also created a smaller matrix analyzed at a class/phyla level. This subsequent analysis also included 7 additional studies not included in the initial genera-grade matrix (Appendix 1).

Three of the four bilaterian clades are represented in the consensus trees from the class-grade analysis: Deuterostomia, Lophotrochozoa, and Ecdysozoa. Platyzoa do not resolve in this analysis, nor do the relationships between the aforementioned major bilaterian groups (fig. 13).

3.3.4 Phyla-grade analysis

Traditional hypotheses about the relationships between different phyla are based upon morphological analyses. In morphology based cladistic analyses of phyla, characters are often coded at the most inclusive taxonomic units (viz., phyla: Nielsen, 2001; Brusca and Brusca, 2002), thereby predetermining the monophyly of these groups. In contrast, molecular phylogenetics works at the level of the individual, and thus gives hypotheses at the level of exemplar species. These relationships are often then extended to hypotheses of phyla-level relationships.

I have combined the approaches of using supraspecific taxa (terminal taxa that reflect multi-taxon assemblages, as in morphological analyses: Bininda-Emonds *et al.*, 1998), with data derived from exemplar taxa (single taxon representing an entire clade, as in molecular analyses) with the application of the supertree methodology to look at the consensus relationships at the level of phyla. An additional benefit of this approach is that it reduces analysis time and the number of most parsimonious trees. Parsimony analysis of a supertree matrix coded at the level of phyla results in only 4 most parsimonious trees with high resolution and a tree length score of 1256. The strict consensus tree of these 4 trees is shown in figure 14. The weakest portion of the tree, as indicated by decay index of 1, is found within the lophotrochozoan clade. Therefore it is not

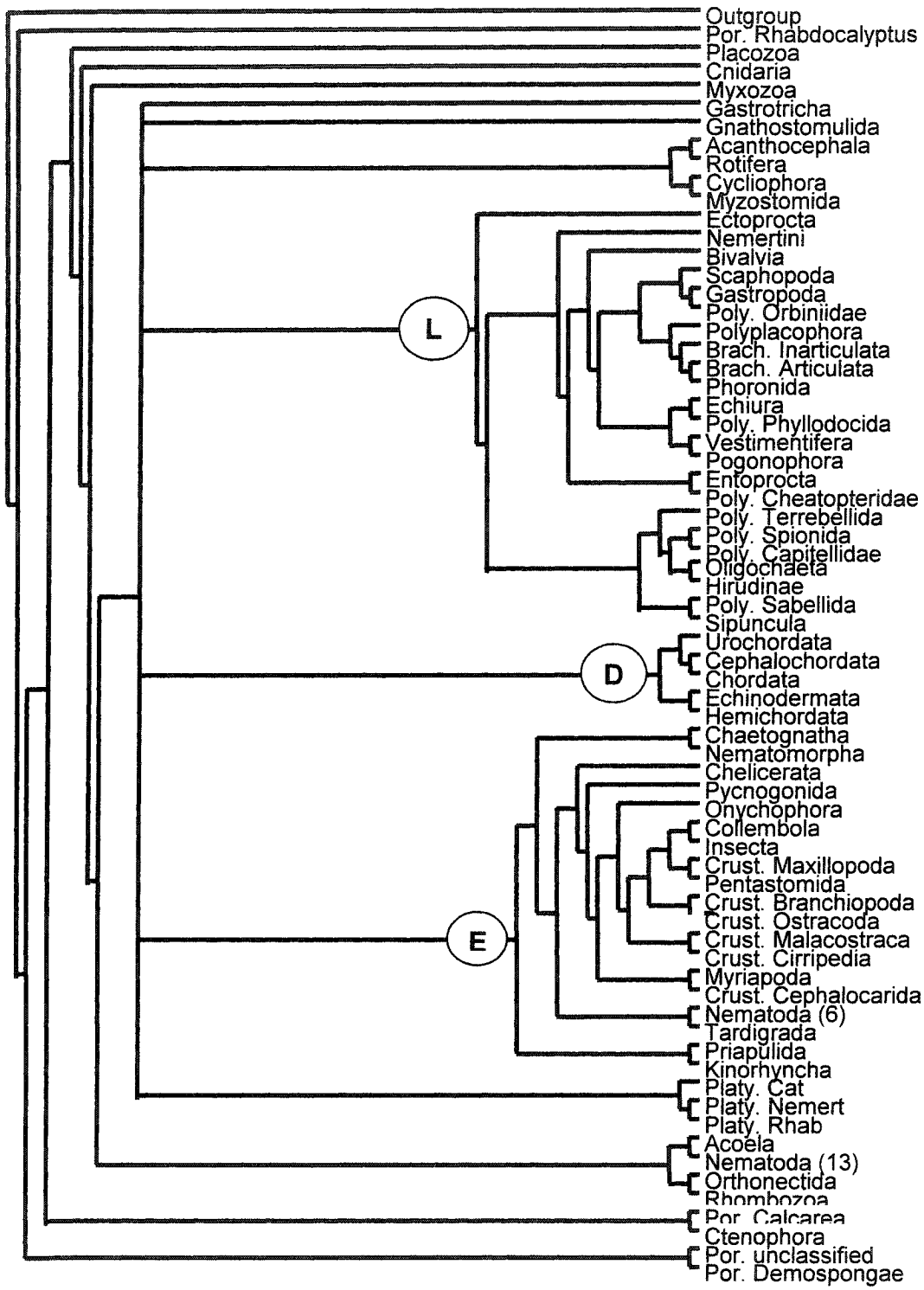

Figure 13: Molecular supertree of the metazoa at the class and phylum grade
Three of the four clades of metazoan lineages resolved at the genera-level are present in a supertree analysis coded at the level of class and phyla grade taxa. Strict consensus of 10,000 MP trees, derived from class-grade analysis of 64 molecular source trees. D = Deuterostomia; L = Lophotrochozoa; E = Ecdysozoa. Analysis is rooted with a hypothetical outgroup taxon.

Figure 14: Molecular supertree of the metazoa at the phylum grade
Supertree analysis, coded at phyla-level grades, resolves all four bilaterian clades that were found in the genera-level analysis (figure 12). Numbers at nodes represent decay indices (Bremmer support values). Nodes requiring greater than 12 steps to break down are not labelled. Strict consensus of 4 MP trees (tree score = 1256), derived from phyla-grade analysis of 62 molecular source trees. Four clades of bilaterian animals resolve: Deuterostomia (D), which includes Echinodermata, Hemichordata, Urochordata, Cephalochordata and Chordata; Platyzoa (P), which includes Rotifera, Acanthocephala, Cycliophera, Gastrotricha, Gnathostomulida, Myzostomida, and Platyhelminthes; Lophotrochozoa (L), which includes Annelida, Brachiopoda, Echiura, Entoprocta, Ectoprocta, Mollusca, Nemertea, Sipuncula, Phoronida, Pogonophora and Vestimentifera; Ecdysozoa (E), which includes Arthropoda, Chaetognatha, Kinorhyncha, Nematoda, Onychophora, Pentastomida, Priapulida, and Tardigrada.

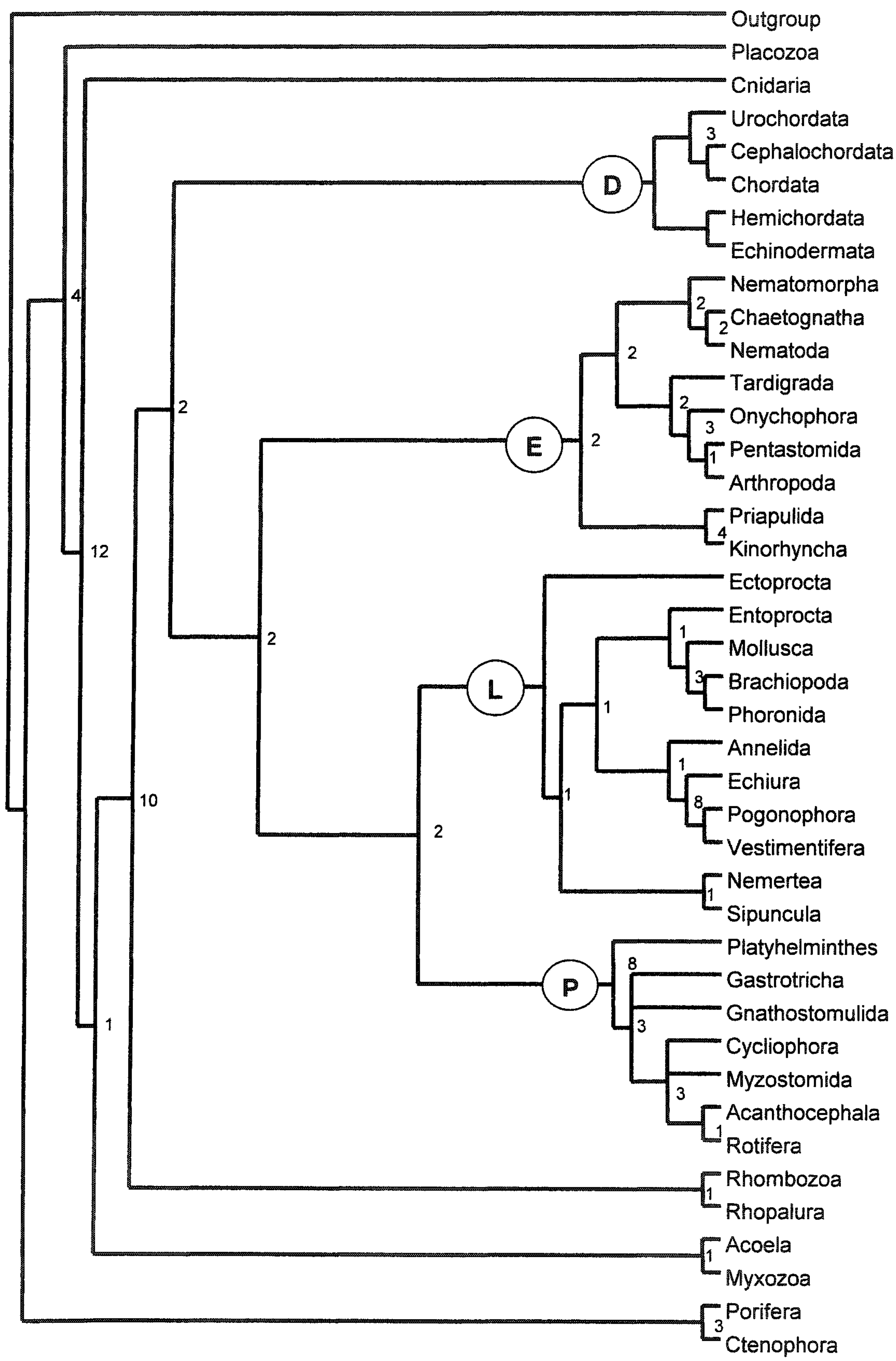
Outgroup
Placozoa
Cnidaria
Urochordata
Cephalochordata
Chordata
Hemichordata
Echinodermata
Nematomorpha
Chaetognatha
Nematoda
Tardigrada
Onychophora
Pentastomida
Arthropoda
Priapulida
Kinorhyncha
Ectoprocta
Entoprocta
Mollusca
Brachiopoda
Phoronida
Annelida
Echiura
Pogonophora
Vestimentifera
Nemertea
Sipuncula
Platyhelminthes
Gastrotricha
Gnathostomulida
Cycliophora
Myzostomida
Acanthocephala
Rotifera
Rhombozoa
Rhopalura
Acoela
Myxozoa
Porifera
Ctenophora
D
E
L
P

Figure 14

surprising that the relationships within this portion of the tree change depending upon how the different classes are condensed (see below). Despite the incongruency within Lophotrochozoa, the presence of this clade is very well supported with one of the highest decay index values (greater than 12 additional steps). In contrast Ecdysozoa dissolves with only two extra steps.

Monophyly of these traditional phyletic grades was not fully supported in the genera level analysis, therefore a select number of phyla were tested for monophyly and paraphyly (including some, but not all descendants) by allowing polyphyly. This is accomplished by coding different taxa in question as two or more grades at a lower taxonomic level (i.e. class or order). For several groups this test did not offer substantial changes to the tree topology: relaxing monophyly of the brachiopods results in the nesting of Phoronida within Brachiopoda; allowing polyphyly of the Platyhelminthes does not affect tree topology; separating Porifera illustrates that Calcarea clusters with Ctenophora, with other sponge groups holding a basal position within the tree. For others, discussed below, more significant changes result.

Nematoda

The nematodes form two distinct clades in the genera-grade analysis. One clade falls out basally in the tree [Nematoda (13)], associated with Acoela. The other [Nematoda (6)] is nested within Ecdysozoa, grouping with Tardigrada. Combining these two distinct nematode clades into a single grade clusters them with Chaetognatha within Ecdysozoa, as illustrated in the phyla-level tree. Relaxing monophyly of Nematoda changes the relationships between the four major bilaterian clades as follows (fig. 15).

Platyzoa move to a more basal position within the tree, outside of Lophotrochozoa, Ecdysozoa, and Deuterostomia. There are no changes in the topology within Lophotrochozoa, however within Platyzoa resolution increases, placing Gastrotricha in a basal-most position. Changes also occur within the more basal triploblast groups. Allowing the basal group of nematodes to fall out

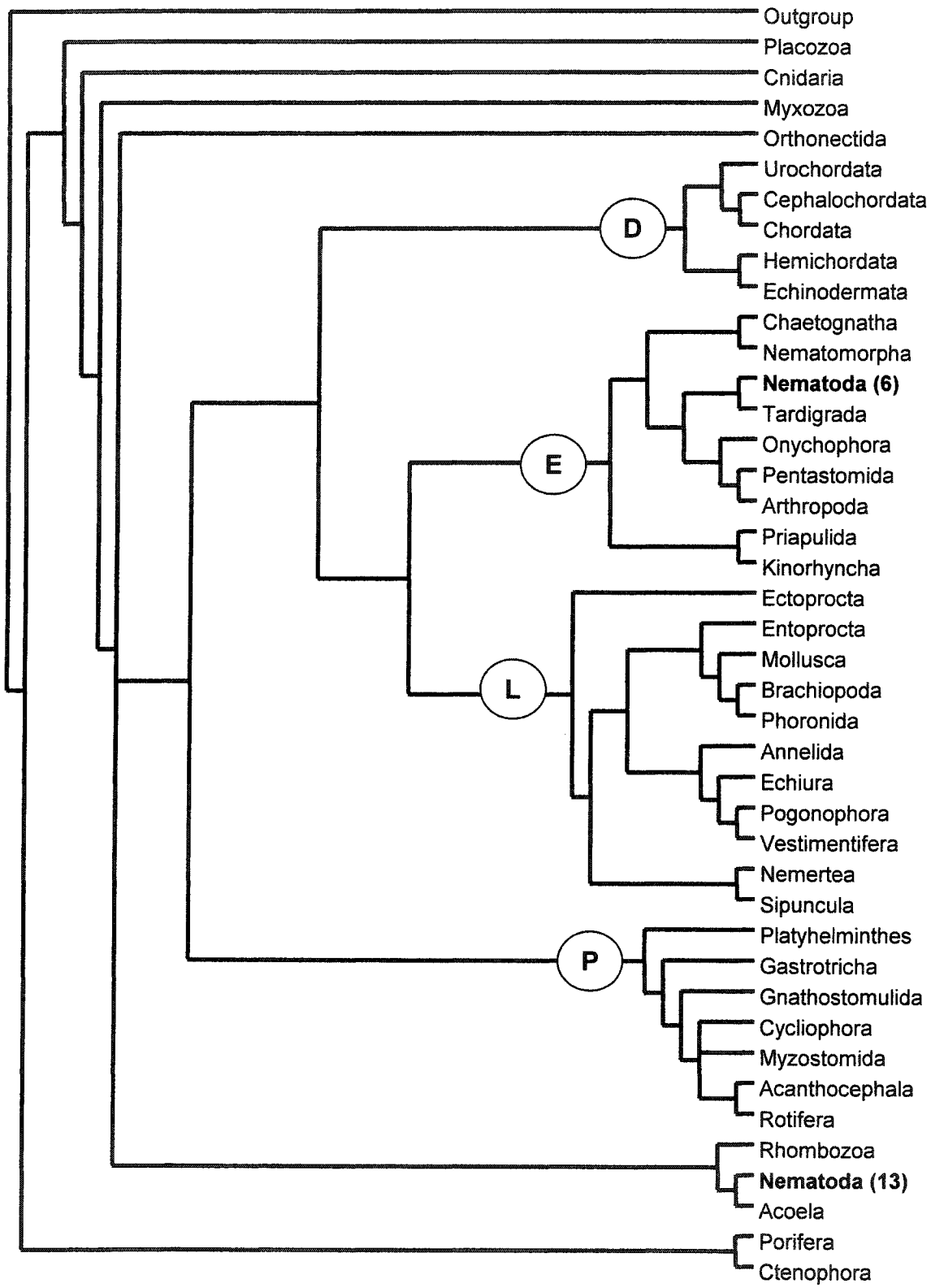

Figure 15: Phyla-grade molecular supertree allowing polyphyletic Nematoda
Relaxing monophyly of Nematoda (bold text) shifts the position of the Platyzoa (P). See text for details. Strict consensus of 4 MP trees, analysis as in fig. 14.

Orthonectida clades, clustering Rhombozoa with Acoela and the basal nematodes to the exclusion of Orthonectida. There are also minor changes within Ecdysozoa: Nematoda cluster with Tardigrada rather than Chaetognatha. This topology remains if the basal nematode taxa are eliminated from the analysis, however the relationships in the basal part of the tree return to that in the original tree.

Mollusca

As expected from the genera-level analysis, Mollusca is not supported as monophyletic when coded at the level of classes (fig. 16). The remainder of the tree retains its original topology, but within Lophotrochozoa relationships shift: Echiura + Pogonophora nest within the molluscan polytomy, forming the sister group to Brachiopoda + Phoronida. Ectoprocta remains the basal-most member of the Lophotrochozoa, while Annelida clusters with Nemertea + Sipuncula and Entoprocta.

Annelida

Coding the annelids as three separate classes: Oligochaeta, Hirudinae, and Polychaeta results in clustering Sipuncula with the monophyletic assemblage of annelids (fig. 17). This also collapses the node separating Sipuncula and Nemertea, creating a polytomy between Mollusca, Annelida, and Nemertea. There are no other changes in the topology of the tree.

Polychaeta

In the genera-level analysis, the different polychaete families do not form a monophyletic assemblage. When polychaete monophyly is not enforced, and polychaetes are coded as family level grades, they predominantly cluster with the other Annelids, along with Sipuncula, Echiura, Pogonophora + Vestimentifera, and Nemertea (fig. 18). Two polychaete families fall outside of this clade: Orbinidae and Chaetopteridae. However, this can be explained by the limited character data available for these taxa with which to place them reliably within the tree.

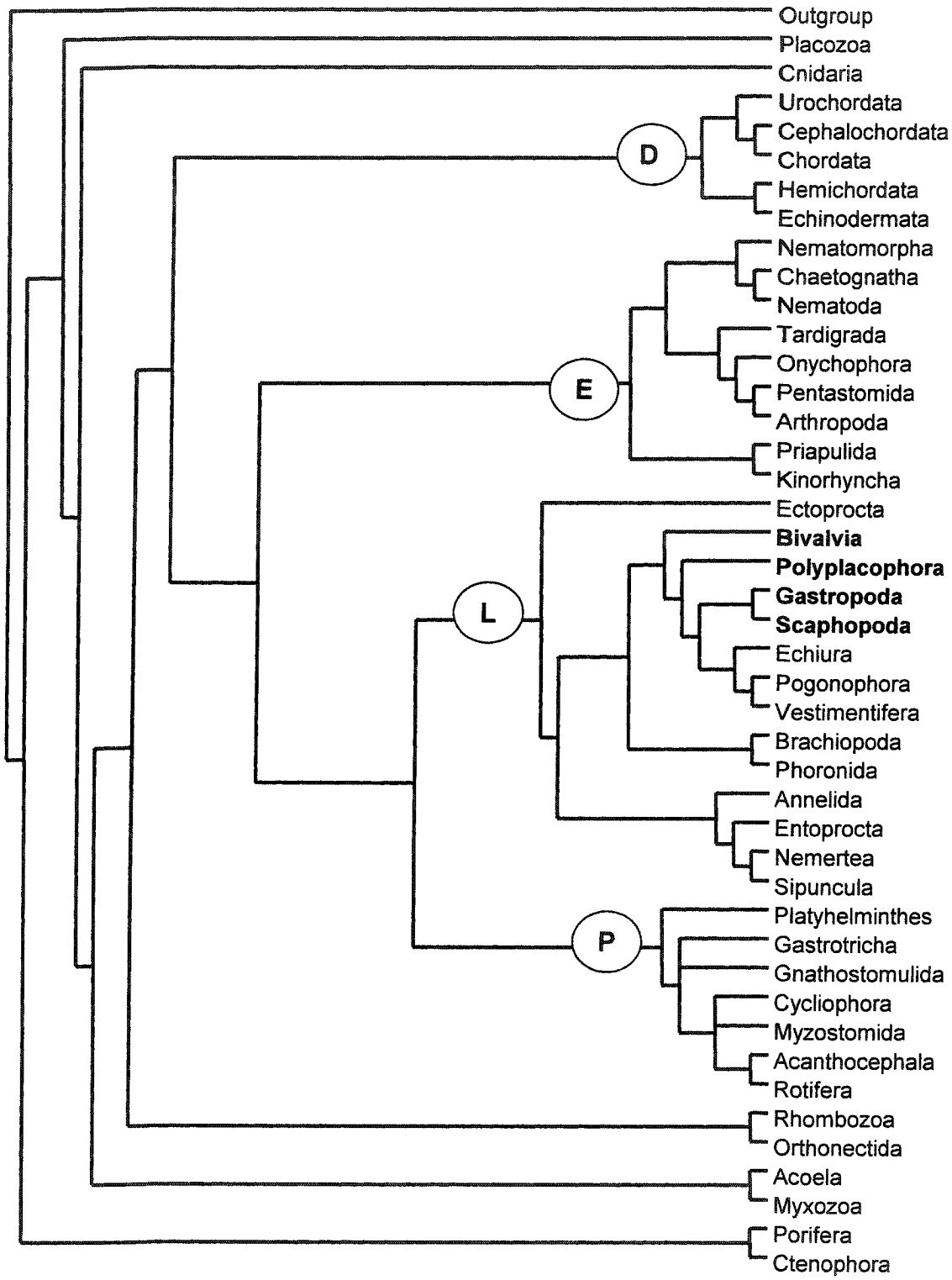

Figure 16: Phyla-grade molecular supertree allowing polyphyletic Mollusca
Relaxing monophyly of Mollusca (bold text) alters relationships within Lophotrochozoa (L). See text for details. Strict consensus of 4 MP trees, analysis as in fig. 14.

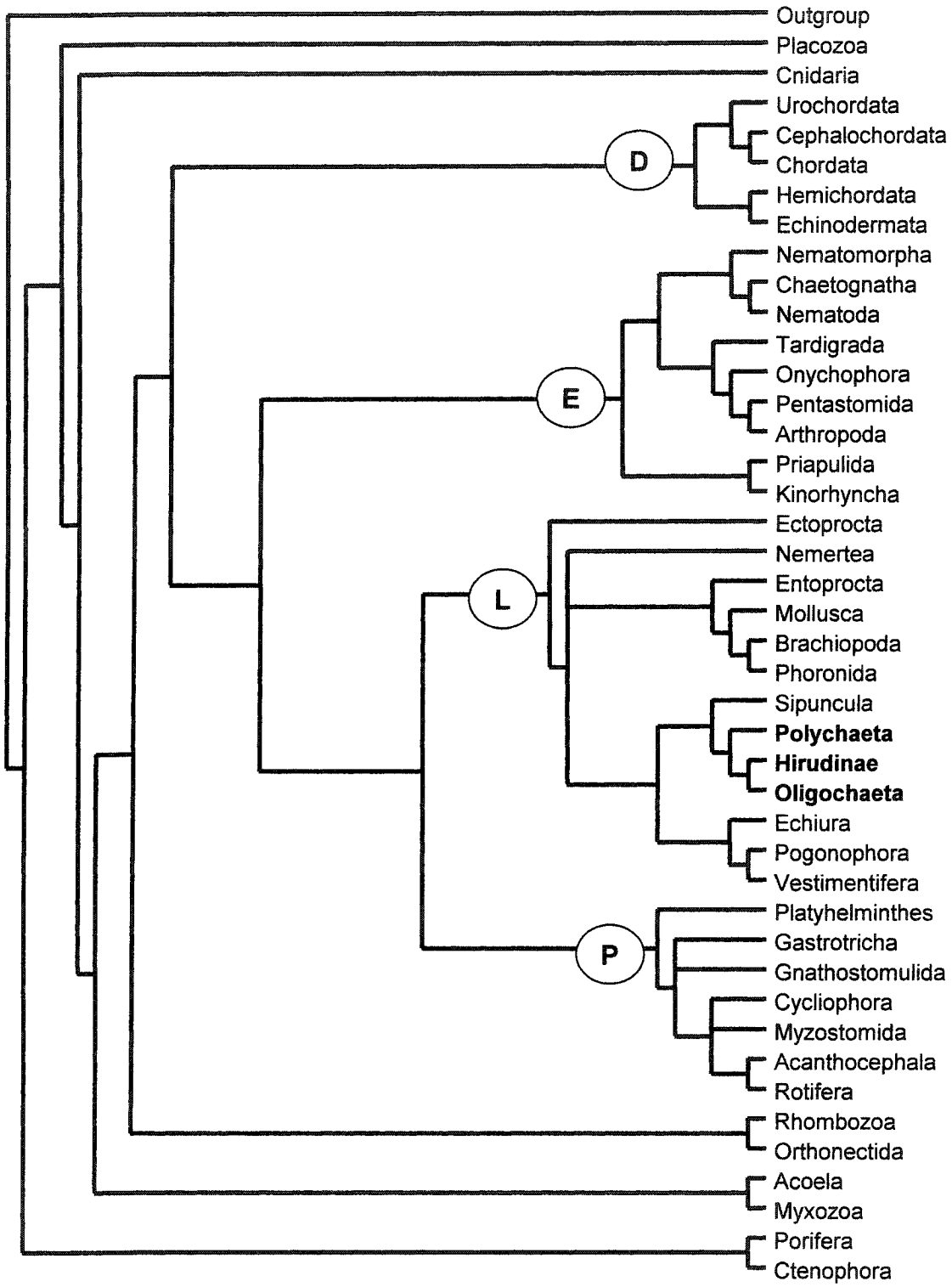

Figure 17: Phyla-grade molecular supertree allowing polyphyletic Annelida
Relaxing monophyly of Annelida (bold text) alters relationships within Lophotrochozoa (L). See text for details. Strict consensus of 8 MP trees, analysis as in fig. 4.

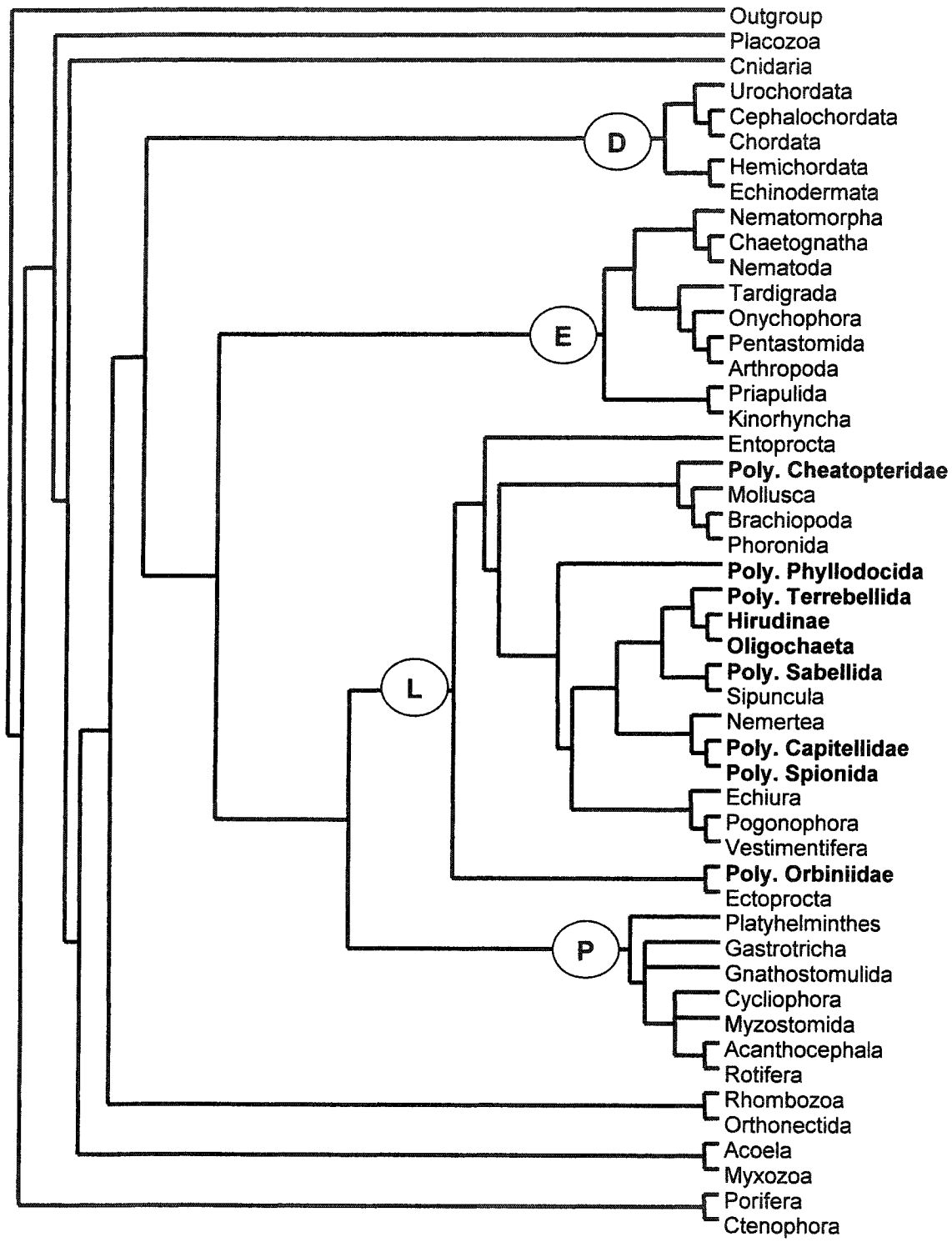

Figure 18: Phyla-grade molecular supertree allowing polyphyletic Polychaeta
Relaxing monophyly of Polychaeta and other annelid classes (bold text) alters relationships within Lophotrochozoa (L). See text for details. Strict consensus of 4 MP trees, analysis as in fig. 4.

Arthropoda

Like Mollusca, Arthropoda do not form a monophyletic assemblage when coded as traditional grades, forming a polyphyletic group with Chaetognatha, Nematoda, Nematomorpha, Onychophora, and Tardigrada (fig. 19). Within this assemblage, Onychophora form the sister group to a polychotomy consisting of Pentastomida, Crustacea, Insecta, and Collembola, which in turn forms the sister group to Myriapoda. Priapulida + Kinorhyncha form the sister group to this entire assemblage. The remainder of the tree remains unchanged. Relaxing crustacean monophyly in addition does not improve the resolution within Ecdysozoa.

3.3.5 Correction for non-independence of the data

Data used to create hypotheses represented in the source trees included in this study come predominantly from analysis of 18S sequences. Therefore characters derived from these source trees must be considered to be non-independent. To examine the effects of this 18S bias, data non-independence was corrected for by including alongside source trees derived from other data, only a single source tree representing hypotheses derived from 18S data, and a single tree representing elongation factor data.

Class-grade corrected analysis

Three major differences exist between the heavily 18S biased topologies and the topology shown here for the data independence corrected analysis, the first being the presence of a clade of diploblast animals at the base of the tree (fig. 20). The second involves the addition of Acoela, Rhombozoa, and Orthonectida (basal nematode taxa also nest within this clade) to Platyzoa. The third difference involves the relationships between the four bilaterian clades, all of which are present but their relative positions within the tree are unresolved in the strict consensus. Within the majority rule tree a clade of protostome animals is supported, in which Ecdysozoa form the sister group to Lophotrochozoa to the exclusion of Platyzoa + minor phyla. This protostome clade forms the sister group to Deuterostomia, with the diploblast clade as the outgroup. The position of

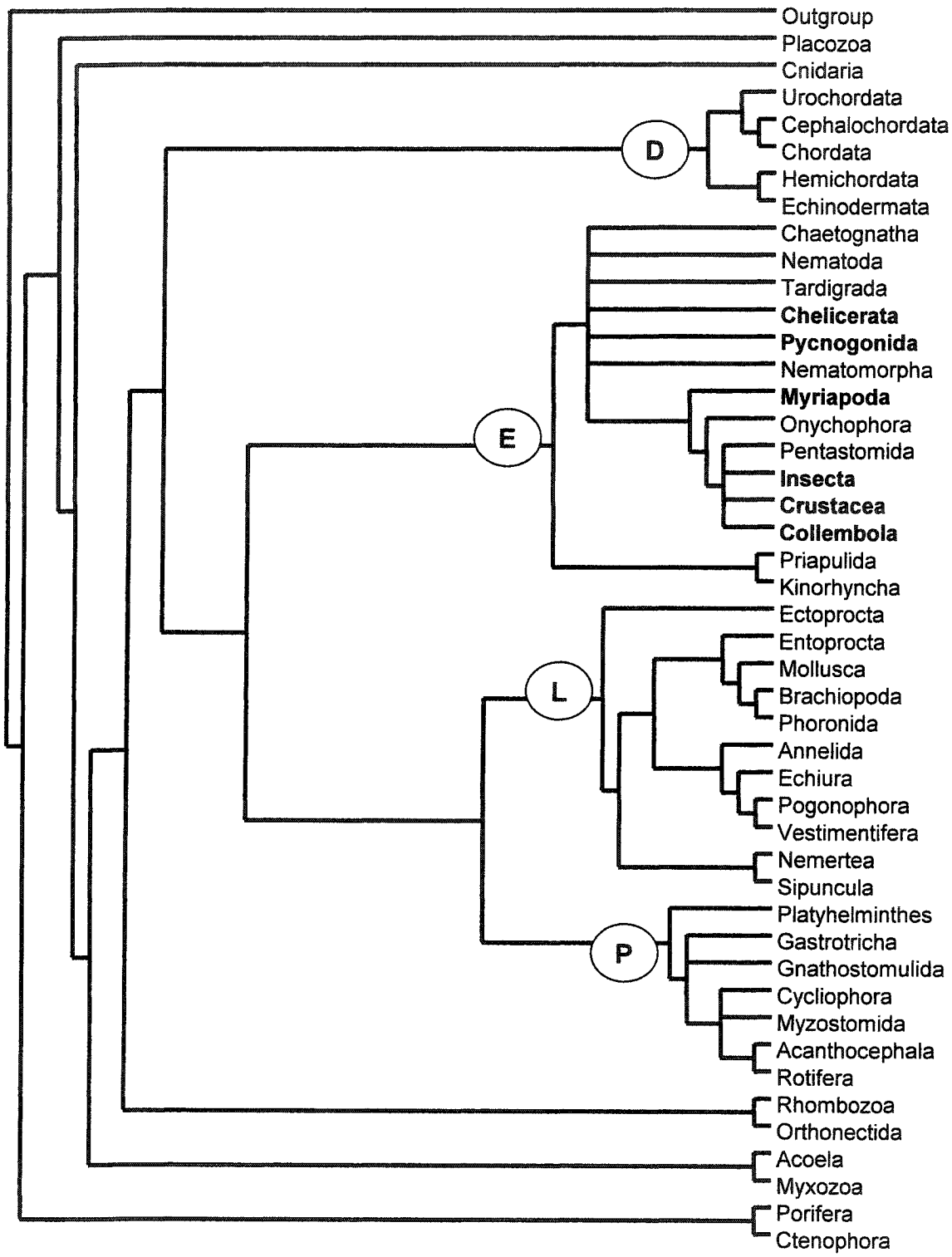

Figure 19: Phyla-grade molecular supertree allowing polyphyletic Arthropoda
Relaxing monophyly of Polychaeta and other annelid classes (bold text) alters relationships within Ecdysozoa (E). See text for details. Strict consensus of 32 MP trees, analysis as in fig. 4.

Myxozoa remains obscure, and a single group of sponges falls into the basal-most position within the tree.

There are subtle changes within each of the major bilaterian clades: within Deuterostomia the clade comprising Echinodermata + Hemichordata is lost; within Ecdysozoa, Arthropoda form a monophyletic assemblage including Pentastomida, excepting for Pycnogonida and Nematoda, which form an unresolved polytomy with the remaining arthropod groups; topology within Platyzoa remains unchanged; within Lophotrochozoa two main clades exist, one including the molluscan lineages and the other including the annelid lineages, with Ectoprocta forming the outgroup.

A monophyletic Mollusca is not supported; the molluscan lineages form an unresolved polytomy with Brachiopoda, Entoprocta, and Nemertea. There are also two polychaete families represented here, as seen earlier in the relaxed polychaete analysis of the phyla-grade tree. Greater resolution exists within the clade containing the annelid lineages, showing Pogonophora + Vestimentifera nested deep within polychaete families and Sipuncula and Terrebellidae (Polychaeta) as outgroups to the rest of the Annelida (Hirudinae + Oligochaeta).

Phyla-grade corrected analysis

Compressing the independence-corrected class grade matrix to reflect phyla grade relationships (fig. 21) gives similar results to the uncompressed analysis (fig. 20), differences being that Orthonectida shifts basally, and the clade of diploblast animals does not resolve in the phyla-grade analysis, nor do the two clades within Lophotrochozoa.

3.4 Discussion

3.4.1 Benefits and Pit-falls of compressing nodes

The rationale for collapsing source tree nodes is as follows: supertree analysis at the level of the individual (as is the case for all source trees included) involves three levels of computing power:

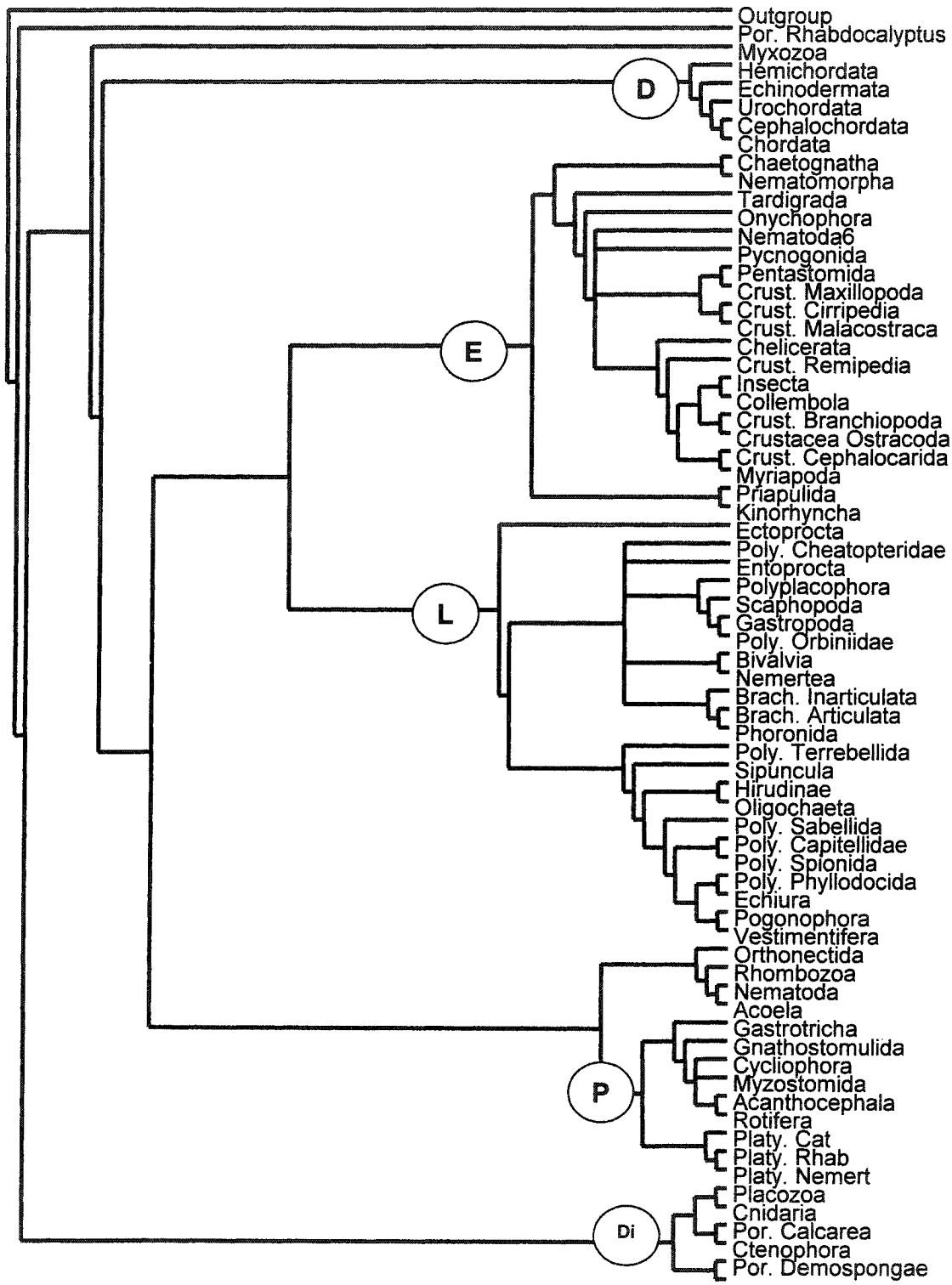

Figure 20: Class- and Phyla-grade molecular supertree after data non-independence correction

Data correction reveals the presence of a clade of diploblast taxa (Di). See text for details. 50% MR of 10,000 MP trees derived from 10 molecular source trees.

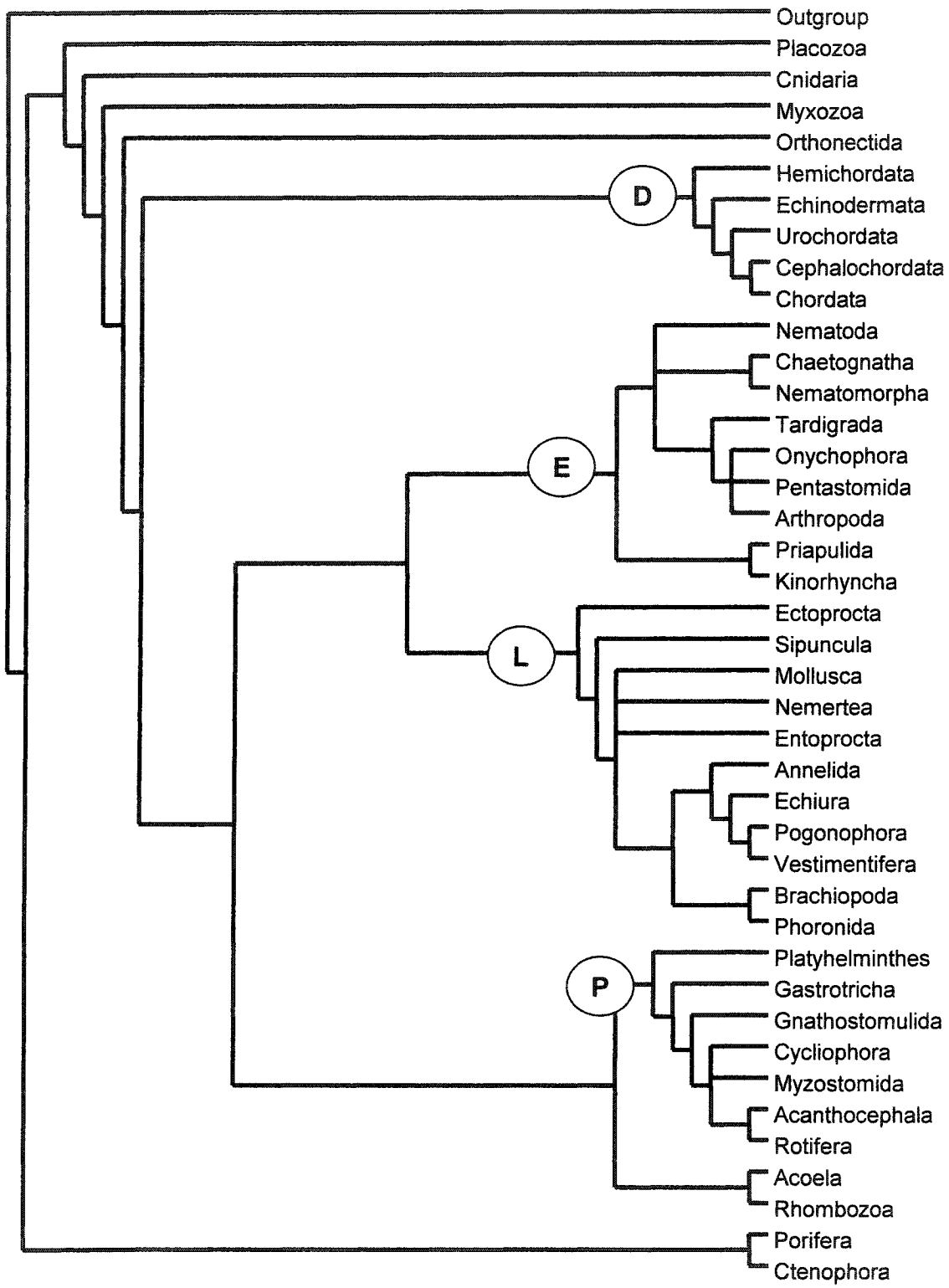

Figure 21: Phyla-grade molecular supertree, data non-independence corrected
Using supraspecific taxa representing phyla eliminates the diploblast clade illustrated in figure 20. The other bilaterian clades are represented. 50% MR of 10,000 MP trees, derived from 10 molecular source trees.

1. grouping taxa into monophyletic clades
2. sorting out relationships *between* these clades
3. sorting out the relationships *within* these clades

Although all of these relationships are important, the primary interest in this study is relationships *between* these clades (point #2). Collapsing terminal nodes into supraspecific taxa eliminates both points (1) and (3) from the analysis, resulting in a much simpler computational task. A similar approach was taken for investigating angiosperm phylogeny by Davies *et al.* (2004), wherein terminal taxa reflect family-level clades.

Collapsing source tree nodes into supraspecific taxa necessarily implies the assumption of monophyly. Within individual source trees this holds little significance for the outcome of the analysis because the collapsed nodes represent monophyletic groupings (with few exceptions), and the resultant character state is, by the very nature of the matrix, the ancestral character state – i.e. inclusion within the monophyletic clade. Bininda-Emonds *et al.* (1998) have shown that the possibility for errors derived from including supraspecific taxa in phylogenetic analyses are significantly decreased by using the ancestral character state for the clade represented by the supraspecific taxon.

A benefit of using supraspecific taxa in this analysis is that representation of terminal taxa within source trees is increased, leading to an overall increase in informative characters. This is both the greatest strength of this method, and perhaps its greatest weakness because the possibility exists that the clade of exemplar species represented by terminal supraspecific taxa may not be supported, and possibly even contra-indicated, within individual source trees.

This is significant, given that incidences of polyphyletic supraspecific taxa increase the degree of potential error in phylogenetic hypotheses (Bininda-Emonds *et al.*, 1999). Although this is most significant when considering hypotheses derived from primary data, it likely also holds true for the supertree analyses presented here. As such, confidence in the monophyly of terminal supraspecific taxa is of significance. Contradictions of the monophyly assumptions were not present within the class-grade analysis. However they became an issue for the phyla-grade analysis. To minimize misrepresentation of

the source data these nodes were given the character state "0&1" to indicate that the group may or may not be affiliated with that node.

Despite these few inconsistencies within the source trees, there remains little doubt of the monophyly of most phyletic lineages based upon morphology (Nielsen, 2003). Molecular systematics has suggested that in some cases recognized phyletic grades may reside nested within other more inclusive phyletic grades (e.g. Phoronida may be nested within the clade Brachiopoda, making Brachiopoda paraphyletic with respect to Phoronida, but together forming a monophyletic clade; Cohen *et al.*, 1998; Cohen, 2000). Forcing monophyly of all individual exemplars into morphologically supported phyletic grades increases the data available for sorting out the nodes connecting these higher-level taxonomic assemblages. Admittedly though, it cannot be used to test for paraphyly of terminal taxa. The degree of resolution present within the phyla-grade analyses reflects this increase in phylogenetically informative characters.

3.4.2 Major differences in topology given by different methods.

The phyla-grade analysis most closely resembles the topology suggested by the genera-grade analysis, including the resolution of four bilaterian groups: Deuterostomia, Ecdysozoa, Platyzoa, and Lophotrochozoa. Interestingly, although Deuterostomia, Ecdysozoa, and Lophotrochozoa are all supported as monophyletic clades, the relationship between these major bilaterian clades was not resolved in the equivalent class-grade analysis (prior to non-independence correction). All of these analyses are heavily biased towards 18S data.

Changes in tree topology in the phyla-grade analysis when monophyly was relaxed for different groups illustrates that the relationships depicted within the major bilaterian clades are not robust. In contrast, because relaxing monophyly of any taxon had little effect on tree topology outside of the clade to which that taxon belongs suggests that although relationships within the clade may be uncertain, the existence of the four bilaterian clades is well supported by analyses of molecular data.

Additionally, the breakdown of clades when monophyly is not imposed suggests the molecular data do not show strong support for a united Mollusca or Arthropoda, and questions the clustering of Polychaeta within Annelida. The existence of two clades of Nematoda has been shown to be an artifact of long-branch attraction (Aguinaldo, *et al.*, 1997).

3.4.3 Significance of non-independence of the data

Correction for data non-independence appears to increase overall tree resolution, revealing a clade of diploblast animals and adding Acoela, Orthonectida, and Rhombozoa as sister taxa to Platyzoa. Neither relationship is present in the 18S-biased analyses, highlighting both the importance of correcting for data non-independence (if one wished to use supertrees as a phylogenetic hypothesis in and of itself) and increasing the diversity of molecular data available for addressing metazoan systematics.

Most supertree analyses have been criticized for not correcting for non-independence of the data (Gatesy *et al.*, 2002), simply stating the bias (for example Davies *et al.*, 2004). However, proponents of supertrees have acknowledged this criticism, and are more rigorously pushing to account for this data non-independence (Bininda-Emonds *et al.*, 2002). Here, I use data independence correction to illustrate the overwhelming lack of multiple molecular data sets from which to draw phylogenetic conclusions.

3.4.4 Implications for metazoan phylogeny

Non-systematists with interests in metazoan phylogeny have a tendency to use phylogenies reproduced in review articles where systematists produce summary cladograms reflecting what they feel is the current view of phylogenetic relationships (e.g. Balavoine, 1998; Adoutte *et al.*, 2000; Peterson *et al.*, 2000). In this study I use supertree methods to objectively quantify the current status of molecular systematics of the metazoa. Data independence correction reveals that only 10 independent molecular sources exist, the majority of which are derived from ribosomal RNA sequences, and taxon sampling is extremely poor for non-18S sources.

Phylogenies derived from 18S data have revealed that this molecule is insufficient for resolving all metazoan relationships, especially those within Lophotrochozoa (Adoutte *et al.*, 2000). This fact is reflected in the poor decay indices obtained within this clade in the phyla-grade analysis. The paucity of other molecular data available by which to derive phylogenetic hypotheses leaves the systematic community at a loss for a robust resolution. Deriving phylogenetic hypotheses with analysis of sequence data from a single molecule can be prone to errors related to the separate evolution of genes and gene families (Page and Charleston, 1997; Page, 2000; Martin, 2002). This highlights the importance of increased collection, from phylogenetically informative exemplar species, of molecular data derived from molecules other than 18S, in order to best estimate metazoan phylogeny.

3. 5 Conclusions

In summary, molecular data supports the existence of four major clades of bilaterian animals. However, the relationships between these groups remain obscured by the predominant use of one molecule (18S rRNA). When all sources are given equal weight, regardless of data independence, and thereby resulting in an 18S-biased topology, the tree is similar to that currently accepted by molecular systematists, illustrating the existence of two major bilaterian clades: the deuterostomes and protostomes. Within the protostomes a clade comprising Lophotrochozoa and Platyzoa (= Spiralia) is also supported. However, taking data independence into account reveals that other non-18S molecular data do not support the existence of this clade, and may be able to more reliably place minor phyla within the context of these four major bilaterian clades. Furthermore, correcting for data independence illustrates that the molecular data available supports the presence of a clade of diploblastic animals as outgroup to the bilateria.

It is important to bear in mind that hypotheses of phylogenetic relationships presented here are only as robust as the source analyses from which they derive. The topologies depicted here are meant to serve as a summary of the

data presented by systematic biologists, and may be subject to change as the field of molecular systematics continues to evolve. As such, one must realize that inference about character evolution between phyla must be made with caution, and those interested in character evolution must be prepared to re-evaluate their data in light of new data bearing on metazoan phylogeny. Nonetheless, despite the lack of congruence in strict consensus in supertree analyses derived at the level of taxonomic genera, the relationships depicted here in the phyla- and class-grade analyses, particularly those in which data independence has been corrected for, represent the best estimate of metazoan phylogeny as derived from molecular hypotheses.

The next chapter uses the consensus phylogeny presented here, combined with the histology and distribution data presented in the previous chapters to address the evolution of cartilage as a tissue type.

Chapter 4: Evolution of Cartilage

4.1 Evolution of Tissues[4]

The presence of cartilaginous tissues amongst invertebrate taxa holds evolutionary significance, suggesting that cartilage, as a tissue, appeared prior to the origin, divergence, and diversification of the vertebrates. This speculation about the early appearance of cartilage is strengthened by the fact that many similar types of molecules are used to build cartilage in vertebrates and invertebrates (see Chapter 1). However, it could equally be argued that there is only one way to build cartilage, and similarities in histology and biochemical properties between the various cartilaginous tissues indicate convergent evolution.

Recent attempts to examine the evolution of tissue types address the evolution of specific gene products, the rationale being that molecular evolution of tissue-specific genes should directly reflect the evolution of the tissue. Large-scale molecular analyses of many tissue-specific isoforms have indeed revealed a link between diversification of these different molecular isoforms and the associated radiation of vertebrate morphologies (Miyata *et al.*, 1994; Iwabe *et al.*, 1996).

This brings into question the relevance of deriving phylogenetic hypotheses at a level of analysis that differs from the data collected. The most familiar example of this problem is analysis of metazoan phylogeny (see Chapter 3), where investigators seek to determine the tree of life from the evolution of a single molecule, 18S rRNA (Field *et al.*, 1988; Winnepenninckx *et al.*, 1998a). The relationship between molecularly derived hypotheses of gene evolution and the "true" phylogenetic tree has been addressed by Page (2000) and Page and Charleston (1997) in what has been called *reconciliation tree reconstruction*, used to compare gene trees and a species tree or even to create a species tree

---

[4] Portions of the following are in press as part of: Cole, A.G. and Hall, B.K. 2004. Cartilage is a metazoan tissue; integrating data from invertebrate sources. – *Acta Zoologica* (Stockholm) **xx**:xxx-xxx

from gene trees[5]. The basic premise behind this methodology is that there are often cases of duplication and subsequent divergence or loss of many genes and gene products, making the creation of species trees from gene trees less straightforward than a 1:1 relationship. A reconciliation tree is the topology created to reflect these duplications and losses within the gene tree, resulting in a tree that reflects the actual relationships, albeit with two identical trees that are connected at the node where duplication occurred.

4.1.1 Genes and tissues

The relationship between genes and tissues is therefore not necessarily straightforward. OOta and Saito (1999) categorize the relationship between gene duplications and the differentiation of tissues into three cases, only two of which are informative with regards to tissue evolution. The first case, which is non-informative about tissue evolution, concerns the duplication of a structural gene where a single regulatory region is retained. This is significant, but non-informative for the purposes here, because the regulatory regions of the gene are thought to be responsible for tissue-specific expression of gene products (Arnosti, 2003). These paralogous genes show the same expression patterns. To be informative in terms of tissue evolution, a duplication of the regulatory region is required, either alone, or accompanied by duplication of the structural gene. Because of changes in the regulatory region, the expression pattern of the structural gene or paralogous gene pair may differ. Such changes in expression patterns are the connection between the evolution of the gene and the evolution of the tissue, allowing the latter to be inferred from the former (OOto and Saitou, 1999).

4.1.2 An example: evolution of muscle

OOta and Saitou (1999) address evolution of muscle tissues using molecular data to create gene trees of muscle-specific structural proteins, superimposing these gene trees onto one-another to create a cladogram depicting the evolution

---

[5] Page (1998) developed software [GeneTree] to create these reconciled trees, available as freeware from: http://taxonomy.zoology.gla.ac.uk/rod/genetree/genetree.html

of muscle. Their results suggest vertebrate muscle types form two distinct clades, one including skeletal and cardiac muscle, the other clustering smooth muscle with non-muscle cells (OOta and Saitou, 1999). Extending the analysis to non-vertebrate cell types reveals that arthropod skeletal muscle cells cluster with vertebrate skeletal and cardiac muscle, and that non-muscle clusters with non-muscle from both clades (OOta and Saitou, 1999). These results suggest that skeletal muscle, *as a tissue type*, evolved before the separation of vertebrate and arthropod lineages. That smooth muscle is more closely related to non-muscle indicates that muscle, *as a cell type*, evolved more than once in the vertebrate lineage.

OOta and Saitou's (1999) study on muscle evolution may hold interesting parallels with the evolution of cartilage. Unfortunately, the lack of published molecular data on invertebrate cartilages makes addressing the evolution of cartilage using molecular phylogenetic approaches unrealistic at this time. Since cartilage is found in both vertebrates and invertebrates, like muscle, cartilage must also pre-date the divergence of vertebrates and invertebrates.

Cartilages throughout the various metazoan lineages should best be thought of as a family of tissues. Similar to evolution that occurs within large gene families, where the closest relationships do not necessarily reflect taxonomic relationships (Iwabe *et al.*, 1996), similarities in cartilage features need not reflect taxonomic relationships, but rather reflects the evolution of cartilage as a tissue type. The degree of homology that exists between vertebrate and the various invertebrate cartilages depends largely on the level at which they are analyzed (Hall, 2003). A number of interesting connective tissues found amongst invertebrate lineages also need to be considered in order to determine the level of homology most appropriate for the family of cartilage tissues.

4.2 Invertebrate Connective Tissues

4.2.1 Chondroid connective tissue

Most metazoan phyla possess extracellular connective tissues composed of both fibrous protein and mucopolysaccharide ground substance, thereby qualifying as chondroid connective tissue. Chondroid connective tissue is common within bilaterian lineages (see Chapter 2) where it serves as a skeletal support, as in Nemertea where the chondroid connective tissue is continuous underneath the epithelia and constitutes a "continuous matrix skeleton" (McClintock Turbellville, 1991). Tissues that can be called chondroid connective tissues have also been described in basal metazoan lineages (e.g. "chondrochyme" of sponges: Minchin, 1900; Cowden and Harrison, 1976; Harrison and De Vos, 1991). The broad distribution of chondroid connective tissues in many distantly related clades (fig. 22) demands that early in metazoan history connective tissue began to organize with chondroid properties (fibrous protein + mucopolysaccharide ground substance). By extension, all metazoans should be able to form chondroid connective tissue under appropriate circumstances.

There are other ways by which animals can find the mechanical support offered by chondroid connective tissues, and so this tissue has been reduced or eliminated in some lineages. Examples of this reduction include groups with small body size such as Rotifera wherein an intracytoplasmic lamina serves as the major skeletal component (Clément and Wurdak, 1991), and Gastrotricha in which the external cuticle is the only well-developed extracellular matrix (Ruppert, 1991). Often thick sheets of collagenous extracellular matrix between epithelial layers provide the majority of the mechanical support, as in Chaetognatha (Shinn, 1997) and Hemichordata (Benito and Pardos, 1997; Chapter 2)

Given the commonalities between the extracellular matrices of both tissues, chondroid connective tissue is distinguishable from cartilage by the lack of a distinct cell population (Cole and Hall, 2004; Chapter 2). Within the metazoa, the structural support offered by chondroid connective tissue can be accomplished

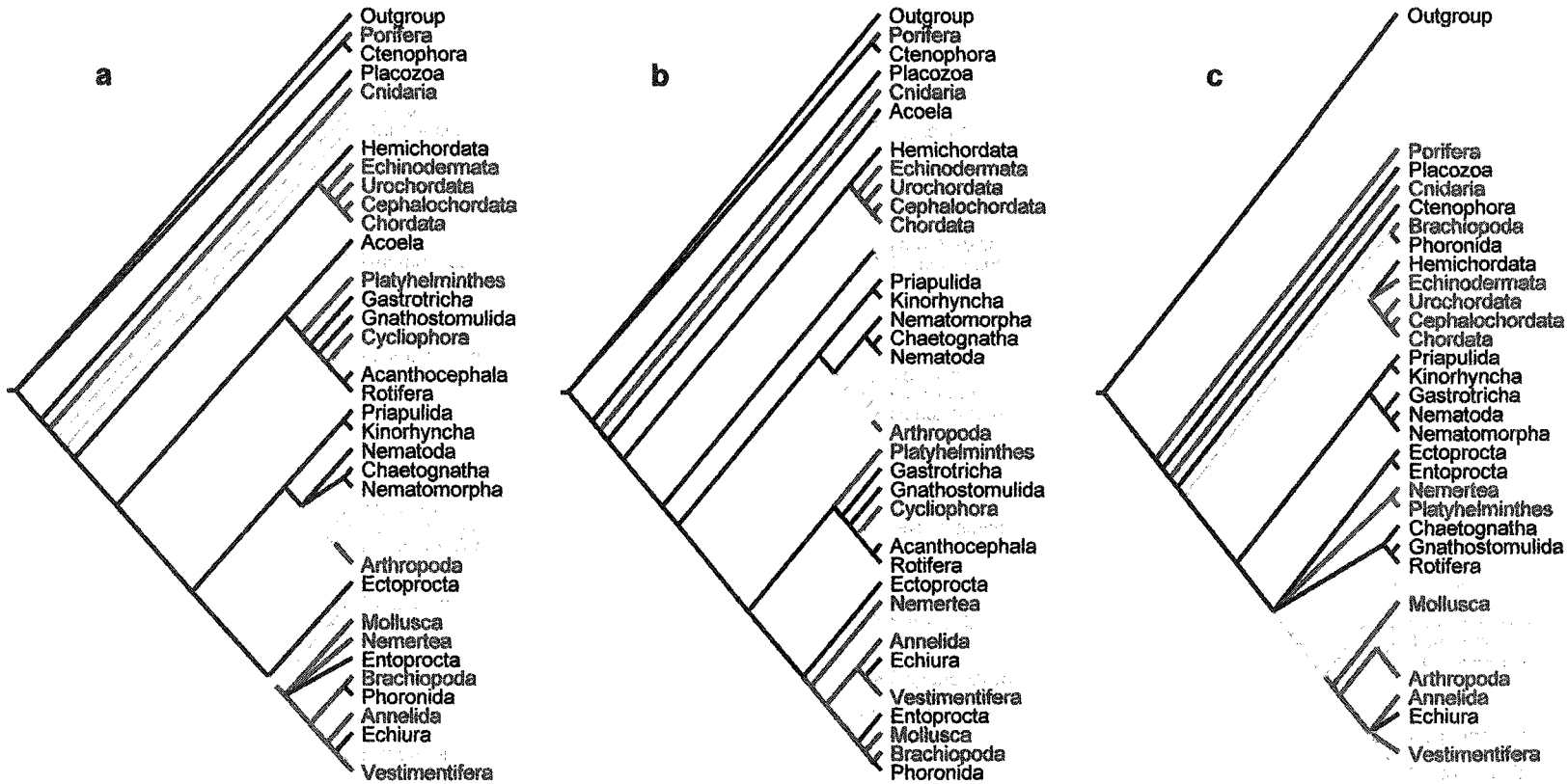

Figure 22: Distribution of chondroid connective tissue

Chondroid connective tissues (cct) are found in a number of metazoan lineages, nested throughout the tree. Data regarding lineages not directly examined in this study are derived from the Microscopic Anatomy of Invertebrates (Harrison, 1991). Lineages possessing cct are represented in blue, without are represented in black, and lineages for which no data was located are shown in grey. **a** Topology of tree reflects data independence correction molecular supertree from Chapter 3. Parsimony suggests 7 independent derivations, and 3 losses. **b** Data independence not corrected, from Chapter 3. Parsimony suggests 6 independent derivations and 3 losses. **c** Topology of Nielsen (2001), derived from cladistic analysis of morphological data. Parsimony suggests 5 – 6 independent derivations and 1 – 9 losses.

not only by modifications to the extracellular matrix, but also by cellular modifications independent of the extracellular matrix. Two trends can be identified: elaboration of the cytoskeleton (as seen within Rotifera), and the addition of large vacuoles within the cells, thereby producing turgid cells that can withstand compression. Within Platyhelminthes, large vacuoles occupy significant proportions of the cell volume within some epithelial and mesenchymal cells (Rieger *et al.*, 1991). When cells with these modifications are concentrated into an identifiable structure, the resulting tissues are most often referred to as "*chordoid*", owing to the fact that they bear resemblance to many vertebrate notochords; both tissue types contain vacuolated cells.

4.2.2 Chordoid tissue

As a tissue type, chordoid tissues consist of vacuolated connective tissue cells containing varying amounts of cytoplasmic myofilaments. The vacuolated chordoid cells are surrounded by an acellular fibrous sheath, which is secreted by these cells. Tissues referred to as chordoid can be grouped into two different types: those in which the predominant feature of the cells is that they are vacuolated, and those that contain extensive myofilaments. Chordoid tissue has been described in a number of lineages (fig. 23).

Cephalochordata

The cephalochordate notochord contains vacuolated cells in which the cytoplasm is full of myofilaments surrounding a large vacuole. Myofilaments become the predominant feature of notochord cells in adults. The high number of myofilaments within the cephalochordate notochord has been suggested to be a derived feature, a specialization for burrowing (Guthrie, 1975 as cited in Gans, 1989). In addition to the notochord, cephalochordates have skeletal elements within the oral cirri that exhibit similar chordoid properties, with vacuolated cells surrounded by a thick extracellular sheath (Ruppert, 1997). This tissue is considered to be cartilage, and its extracellular matrix stains with Verhoeff's reagent, indicating an elastin-like component (Wright *et al.*, 2001).

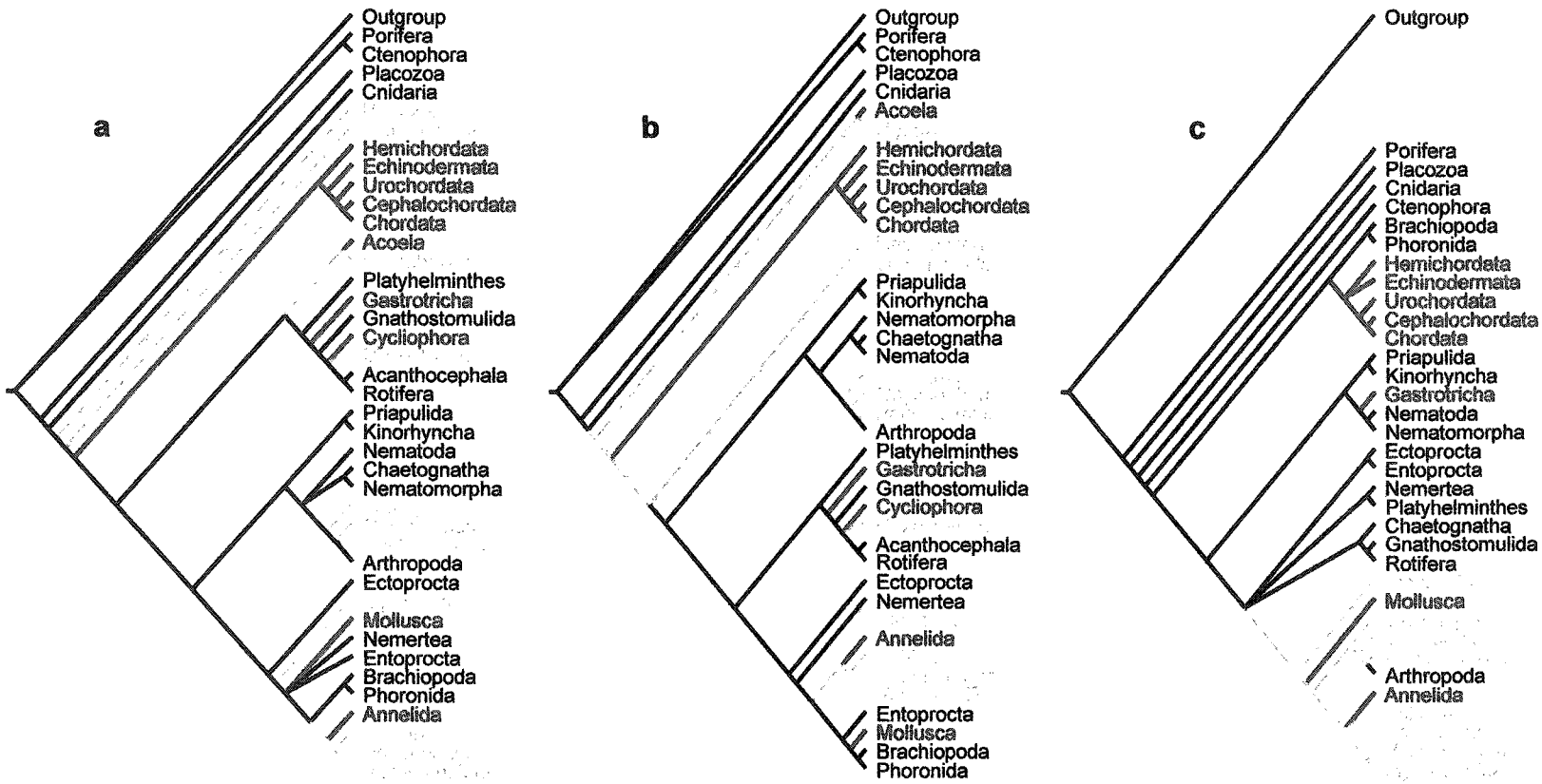

Figure 23: Distribution of chordoid tissues

Chordoid connective tissues are found in a number of metazoan lineages, nested throughout the tree. Data regarding lineages not directly examined in this study are derived from the Microscopic Anatomy of Invertebrates (Harrison, 1991). Lineages possessing chordoid tissues are represented in blue, without are represented in black, and lineages for which no data was located are shown in grey. **a** Data independence correction molecular supertree from Chapter 3. Parsimony suggests 6 independent derivations, no losses. **b** Data independence not corrected, from Chapter 3. Parsimony suggests 6 independent derivations and no losses. **c** Topology of Nielsen (2001). Parsimony suggests 4 independent derivations and no losses.

Urochordata

Schaffer (1930) describes connective tissues within tunicate mantels as superficially similar to chordoid tissues, with a basophilic extracellular matrix and cells containing large vacuoles.

Hemichordata

Homologies between the hemichordate stomochord and chordate notochord have oft been speculated, and it is from the chordoid tissue (stomochord) that hemichordates derive their name (Benito and Pardos, 1997). The structure of the stomochord differs within the two major hemichordate clades (Pterobranchia and Enteropneusta; Benito and Pardos, 1997). Pterobranch hemichordates lack vacuolated cells within the stomochord, which derives its structural properties primarily from its surrounding fibrous sheath, whereas vacuolated cells found within the enteropneust hemichordate stomochord contribute to the skeletal functions (Benito and Pardos, 1997). The vacuolated cells connect to one another apically by "zonulae adhaerentes" (Benito and Pardos, 1997).

Echinodermata

The paradental tongues of regular urchins, such as *Paracentrotus lividus*, are described as "whitish, gelatinous and club-shaped bodies" and are supported by the paradental axis (Bonasoro and Carnevali, 1994a). Histological analysis of this supporting tissue reveals that it is high in glycogen and glycosaminoglycans, and contains numerous large irregularly shaped cells that are connected to one another via hemidesmosomes and junctional complexes (Bonasoro and Carnevali, 1994a,b). Based upon this analysis the authors conclude these are chordoid tissues.

Acoela

Many acoels have chordoid tissues comprised of vacuolated cells. The chordoid cells are irregularly shaped, with many cell processes and a large vacuole (Rieger *et al.*, 1991).

Gastrotricha

In some species of gastrotrichs there are vacuolated epidermal cells, and a cellular connective tissue comprised of vacuolated "Y-cells", which serve a skeletal function. In other species there is an axial rod, or "chordoid organ", extending the length of the animal that has been likened to the chordate notochord. The cells of this tissue have a high cytoplasmic concentration of myofilaments (Ruppert, 1991).

Cycliophora

The chordoid larva of Cycliophora is named for one of its most prominent features, the chordoid organ, which is a ventrally located skeletal structure that spans the length of the larva (Funch, 1996). Much like the cells of the cephalochordate notochord, cells of the chordoid organ contain a large vacuole that is surrounded by cytoplasmic myofilaments. The entire organ is surrounded by a thick basal lamina (Funch and Kristensen, 1997).

The presence of chordoid tissues in these numerous invertebrate groups suggests that formation of axial support by means of vacuolated epithelial cells surrounded by an acellular fibrous matrix may be very ancient. Chordoid organs, with their extracellular sheath and mucopolysaccharide rich vacuoles, might qualify as central cell-rich vesicular cartilage.

4.2.3 Chordoid tissue as cartilage

The chordate notochord, in particular, is an interesting tissue worth further mention. It provides skeletal support, is cellular, and the large vesicular cells are surrounded by an extracellular sheath containing both polysaccharides (including chondroitin sulphate – Welsch *et al.*, 1991) and types I and II collagen (Eikenberry *et al.*, 1984). Despite these characteristics, most vertebrate researchers would not consider the notochord to be cartilaginous, but rather to be epithelial; the large vacuolated cells are connected to one-another by desmosomes and gap-junctions, surrounded by a basement membrane sheath, and no extracellular matrix separates the cells (Schmitz, 1998). The extracellular

matrix molecules produced by the notochordal cells are restricted to the acellular sheath surrounding the notochord itself, and to the large vacuoles within the cell bodies.

Whether or not the notochord and other chordoid tissues can be considered to be cartilage depends largely upon the acceptance of features that are not common to vertebrate hyaline cartilage, such as vacuolated cells and the presence of cell-cell connections. Two major obstacles to overcome in achieving acceptance of this idea are that there is no extracellular matrix between the cells of vertebrate notochords, and that the notochord is derived from an epithelium whereas cartilage is mesenchymal.

Cell-cell connections

Amongst the available invertebrate cartilages, cell-cell connections have been documented with electron microscopy in cephalopods (Bairati *et al.*, 1998), and cellular extensions between cells are seen with light microscopy in *Limulus* endosternite cartilage (Chapter 2). Whether or not the chondrocytes of sabellids also show cell-cell connections awaits electron microscopical studies. It is clear however, that such connections are by no means rare amongst the invertebrate cartilages, and therefore the presence of cell-cell junctions within chordoid organs is insufficient to abandon them as potential cartilages.

Extracellular matrix

Notochords found in cephalochordates and urochordates contain extracellular matrix derived from the notochordal cells. The vacuolated cells of the cephalochordate notochord are surrounded by an acellular collagenous sheath and extracellular metachromatic material is present between the cells (Ruppert, 1997); urochordate notochords have a mucopolysaccharide-rich lumen, which is formed by polarized secretion from notochordal cells. Although notochords within Urochordata are claimed frequently to be composed of vacuolated notochord cells (e.g. Gans, 1989), Burighel and Cloney (1997) point out that this speculation has never been supported by evidence from electron microscopy, furthermore demonstrating that urochordate notochord cells are indeed *not*

vacuolated. The fully formed notochord of urochordates is a tubular structure in which the cell bodies are located at the periphery and are bound by an acellular sheath (Burighel and Cloney, 1997). Notochord cells secrete extracellular matrix within the fibrous sheath. As the matrix accumulates cells become concave and eventually fuse at their apical ends to form fenestrated cells that surround the matrix-filled lumen (Burighel and Cloney, 1997). These features suggest that the lack of extracellular matrix between the notochordal cells of vertebrates may be a derived feature, and that secretion of mucopolysaccharides within the sheath of the notochord could be the ancestral condition. However, if all chordoid tissues are homologous, then retention within the vacuoles is more likely ancestral because none of the other invertebrate chordoid tissues have extensive amounts of extracellular matrix between the cells.

Chordoid cartilage

Can chordoid tissues, including the vertebrate notochord, be considered cartilage? Cartilage by definition has its glycosaminoglycans secreted into the extracellular matrix and not withheld in vacuoles. Although vesicular cell-rich cartilage has a certain amount of matrix product contained within large vacuoles, it also has a large amount of extracellular matrix (thereby qualifying as cartilage) whereas most chordoid tissues do not, and thus most chordoid tissues cannot be considered as cartilage.

However, enough similarities exist between cartilages and chordoid tissues for both of these tissues to be considered members of the same family of tissues derived from a chondroid connective tissue. It could be proposed that intercellular connections, as seen in many invertebrate cartilages, are remnants of an epithelial origin of the mesenchymal cells that gave rise to chondrocytes in these lineages. Epithelial to mesenchymal transitions are considered to be an important cell strategy arising during metazoan evolution; mesenchyme that does not return to an epithelial state often differentiates into connective tissues (Pérez-Pomares and Muñoz-Chápuli, 2002).

Cartilage may have been independently derived multiple times throughout the course of metazoan evolution, and one cannot rule out the possibility of epithelially derived cartilages such as the hemichordate skeleton. Similarities in histological structure between the various chordoid organs, early chordate notochords, and sabellid polychaete cartilage, furthermore suggest that central cell-rich vesicular cartilage may be the ancestral cellular cartilage condition.

4.3 Cartilage Evolution

4.3.1 Cartilage origins

As cartilage is found in a number of invertebrate taxa, cartilage, or at least the ability to form cartilage, arose either early in metazoan evolution or evolved more than once. Despite the interesting parallels between and within cartilages and chordoid tissues, these two classes of connective tissue should be regarded as independent tissue types. Thus, given the limited distribution of cartilage (fig. 24), it is most parsimonious to assume that cartilage arose independently multiple times over the course of metazoan evolution. This holds true even if chordoid tissues are considered cartilage (fig. 25).

The limited distribution of cartilage within polychaetes, being restricted to a single lineage, is a strong argument for independent evolution of cartilage within polychaetes. If not independently derived, one would expect to find cartilage within other polychaete lineages. However even in closely related polychaetes, with similar morphologies and life-history strategies, cartilage is absent (see Chapter 6).

Likewise, molluscan cartilage is most parsimoniously explained as an independently evolved tissue – presence of cartilage within other Lophotrochozoa lineages would otherwise be expected. Similarly, cartilage likely has two independent origins within arthropods: vesicular *Zellknorpel* cartilage within the horseshoe crab opisthosoma, and the fibro-hyaline cell rich cartilage found within the endosternite, which likely also exists amongst the crustaceans. Assuming a single origin within vertebrates, cartilage appears to have evolved independently a minimum of five times throughout the history of the metazoa.

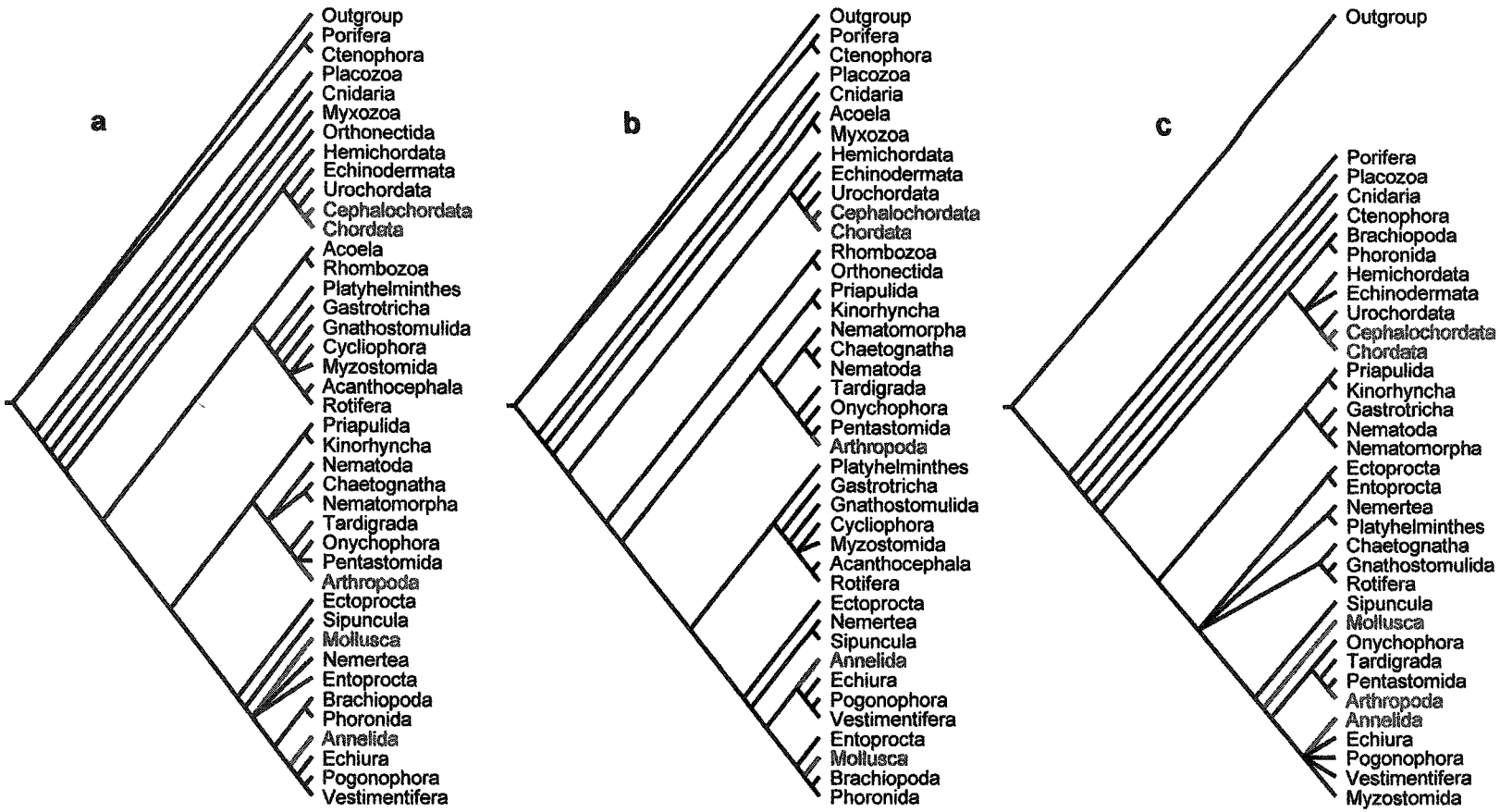

Figure 24: Distribution of cartilage

Cartilage is restricted to 4 metazoan lineages, nested throughout the tree. Lineages possessing cartilage are represented in blue, without are represented in black, and lineages for which no data was located are shown in grey. **a** Data independence correction molecular supertree from Chapter 3. Parsimony suggests 4 independent derivations, no losses. **b** Data independence not corrected, from Chapter 3. Parsimony suggests 4 independent derivations, no losses. **c** Topology of Nielsen (2001). Parsimony suggests 4 independent derivations and no losses.

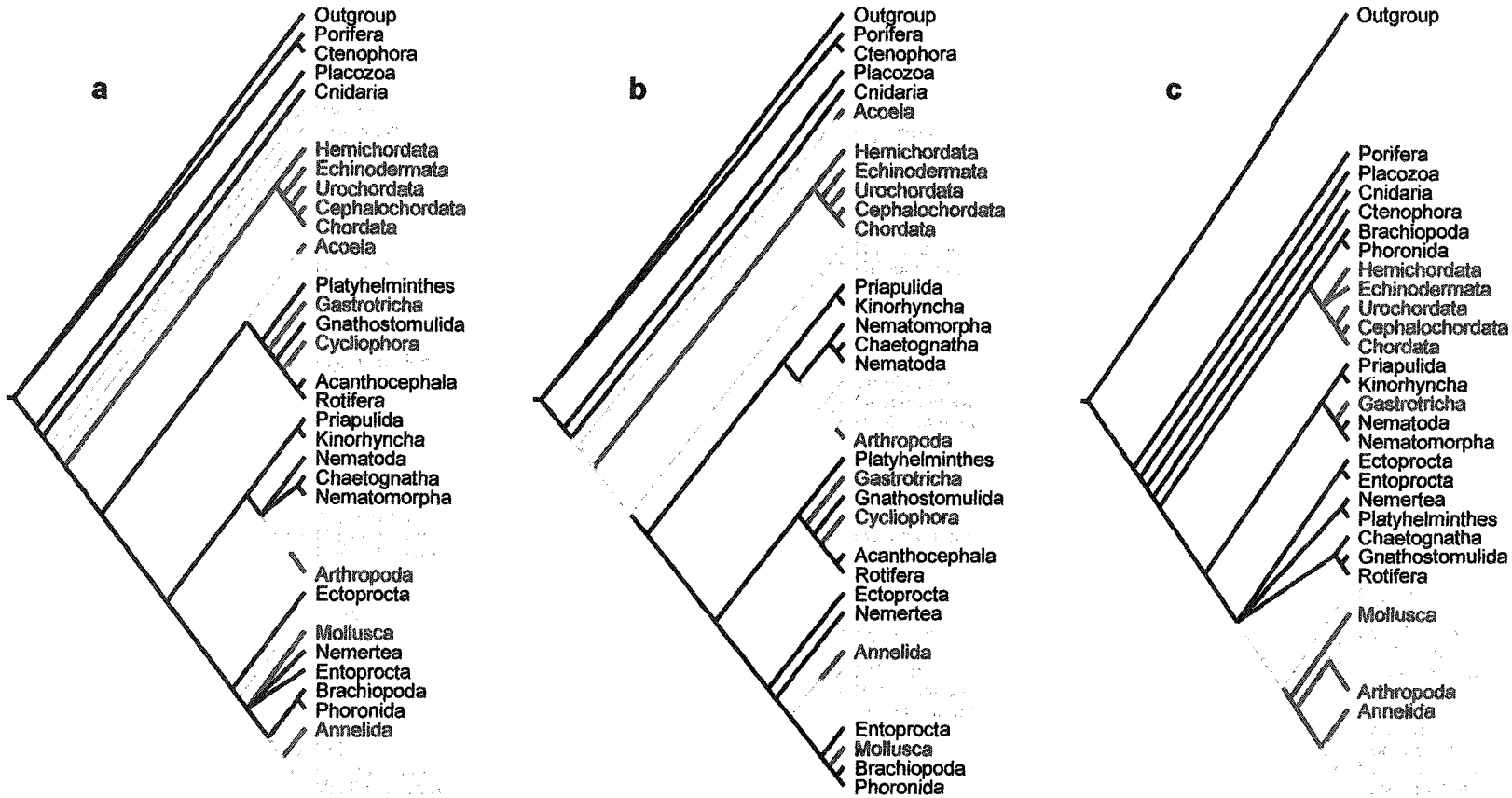

Figure 25: Distribution of cartilage and chordoid tissues

Considering chordoid tissue as a type of cartilage increases distribution to include members of the Platyzoa. Lineages possessing cartilage are represented in blue, without are represented in black, and lineages for which no data was located are shown in grey. **a** Data independence correction molecular supertree from Chapter 3. Parsimony suggests 7 independent derivations, no losses. **b** Molecular supertree, data independence not corrected, from Chapter 3. Parsimony suggests 7 independent derivations, no losses. **c** Topology of Nielsen (2001); Parsimony suggests 3 independent derivations and 0 – 7 losses, depending upon missing data.

However, the presence of cartilages amongst each of the major invertebrate clades – Lophotrochozoa (molluscs and sabellid polychaetes), Ecdysozoa (chelicerate arthropods), and Deuterostomia (vertebrates) – may be more significant than its limited distribution within each clade. Although it is most parsimonious to suggest that each cartilage is independently derived, loss of complex characters (such as an entire tissue type: cartilage) within the metazoa is far more prevalent than the independent multiple origins of such characters (discussed in Budd and Jensen, 2000). Therefore, although not parsimoniously suggested by the distribution of cartilage alone, it is reasonable to suggest that all metazoan cartilages evolved from a common ancestral connective tissue (discussed further below) and thus can be considered to be homologues as tissues.

4.3.2 Scenario reconstruction

Given the data presented in this thesis on the nature and distribution of connective tissues within invertebrates, it is possible to reconstruct a scenario regarding the evolution of cartilage. Although predominantly an exercise in speculation, Gans (1989) argues that scenario construction "forces us to look at organisms in new ways and to ask questions about systems that would otherwise be ignored" (pp. 223). Furthermore, he writes:

> "Phylogenetic scenarios are viewed as representing a second set of evolutionary hypotheses complementing the primary cladograms, which provide the initial basis for analysis. Clearly, biology must be more than the testing of hypotheses about phylogenetic pattern; it must also test hypotheses about the historical process responsible for the observed phenotypes. Notation that some phenotypic aspect has been 'gained' or 'lost' between two phylogenetic stages does not do so... Several basic rules let one establish scenarios. First, scenarios must derive from a phylogenetic scheme. Secondly, they should be based upon the best possible information about the biology of the extant members of the groups being considered." (Gans, 1989, pp. 222)

In the text that follows, I speculate on the origin of cartilage from a chondroid connective tissue precursor, and present hypotheses on the degree of homology between cartilages from different lineages.

Evolution of cartilage

Extracellular matrix

One could imagine that the origin of the ability to organize connective tissues into a cartilaginous tissue arose only once in the history of the metazoa if one accepts the hypothesis that extant bilaterian metazoa derive from large bodied ancestors (discussed in Budd and Jensen, 2000). After the origin of connective tissues in the form of elaborated extracellular matrix secreted by epithelial cells (as exists in sponges) would have appeared the ability to organize this matrix into chondroid connective tissues, thereby conferring greater stiffness and thus a mechanical advantage for embryos and adults. As we have already seen, chondroid connective tissues are found throughout the metazoa, except in cases where its absence can be explained by presence of other structures to confer the mechanical support provided by chondroid connective tissues (see section 4.2.1).

During the course of evolution, this ancestral chondroid connective tissue has diverged to give rise not only to the various vertebrate and invertebrate cartilages, but also to other related connective tissues (extant chondroid connective tissues, chordoid tissues, and vertebrate bone). Thus the similarities between invertebrate cartilages and vertebrate bone can be considered indicative of their descent from a common connective tissue precursor. Conversely, because cartilages within different metazoan lineages likely have arisen independently from this chondroid connective tissue (see section 4.3.1), the striking similarity between vertebrate cartilage and cephalopod cartilage is probably a result of convergence.

It is likely that the path taken by different lineages leading from chondroid connective tissue to cartilage is similar. In response to functional pressures, undifferentiated mesenchyme could become regionally differentiated, with different concentrations of extracellular molecules (chondroid connective tissue). These selective pressures could include both skeletal and protective functions, the need to withstand compression and tension generated by musculature, and the need to protect a centralized nervous system. Beresford (1993) discusses

these and other scenarios in the context of speculation on how invertebrate cells may have developed skeletal cell behaviours contributing to the evolution of the neural crest. Given time and persistence of the original functional pressures, the production of this regionally differentiated extracellular matrix would become ingrained in the genetic architecture of the animal through regional specialization of the matrix-producing cells.

Chondrocytes

These matrix-producing cells were ancestrally epithelial cells, and the transition from epithelia to mesenchyme likely played an important role in the diversification and subsequent evolution of chondroid connective tissues. Within many smaller-bodied lineages these cells retained their epithelial characters, giving rise to chordoid tissues. Among larger-bodied animals mesenchymal cells would be incorporated into the extracellular matrix, and it is these cells that become the presumptive pre-chondrocytes.

The presumptive pre-chondrocyte would likely be morphologically similar to fibroblasts: presumptive vertebrate secondary chondrocytes derive from mesenchymal cells of periostea (Beresford, 1983); chondroid connective tissue cells often also are fibroblastic, for example those described by Andersen *et al.* (2001) supporting the obteraculum of the vestimentiferan *Riftia pachyptila*. It can be envisioned that presumptive pre-chondroblasts, like all chondroblasts, required some cue from the external or extracellular environment to undergo this specialization, a cue such as induction by a mechanical stimulus transmitted through the extracellular matrix.

Within this matrix, the previously undifferentiated cells (fibroblasts) have specialized into a novel cell type (chondroblast), which produce the molecules of the extracellular matrix. In the course of this cellular specialization different phylogenetic lineages could have utilized different cell populations. In this case chondrocytes may not be considered as homologous, but cartilages (tissues derived from the same chondroid connective tissue precursor) are. The key concept that distinguishes cartilage from other chondroid connective tissues amongst vertebrates and invertebrates is that the cells secreting the cartilage

extracellular matrix are *distinct* from other connective tissue cells. Thus, cartilage as a tissue is *both* the extracellular matrix with fibrous protein and water absorbing mucopolysaccharides, *and* the chondrocytes that secrete this rigid matrix.

4.4 Conclusions

The most parsimonious scenario for the evolution of cartilage demands it be independently derived multiple times from chondroid connective tissue. The possibility that vertebrate and invertebrate cartilages share a latent homology cannot be dismissed, especially given the intuitive rationale that it is easier to lose a complex structure than it would be to re-invent it. Examples of convergent organization of other complex structures exist, such as the vertebrate and cephalopod eye. Eye evolution nicely illustrates the role functional constraints play in the evolution of complex organ systems, as well as providing evidence that the machinery for creating these systems independently may be homologous (i.e. all photoreceptor systems are specified by the *Pax-6* gene, regardless of their complexity; Gehring and Ikeo, 1999). The molecular specification of vertebrate cartilage is slowly being unravelled (Hall and Miyake, 2000; Buxton *et al.*, 2003), and investigations into the cellular and genetic basis of invertebrate cartilage development will be an important avenue to explore in determining the extent of homology between the various metazoan cartilages.

The final portion of this thesis addresses further the similarities between vertebrate skeletal tissues and invertebrate cartilage with reference to their development, focusing on representatives from two major invertebrate lineages: cephalopods (Chapter 5) and polychaetes (Chapter 6).

Chapter 5: Differentiation and Evolution of Cephalopod Cartilage

5.1 Introduction

One important feature of vertebrate cartilage, which has been used for both classification and discussions of its evolution, is embryologic origin (Hall, 1978, 2004; Beresford, 1983). Vertebrate cartilage can derive from either mesoderm or ectoderm (neural crest). Differences between chondrocytes from either germ layer exist, both morphologically and physiologically (Hall, 1971; Fyfe and Hall, 1979), but these have gone largely unexplored. Cartilage from either germ layer possesses similar molecular constituents and specification pathways (Hall and Miyake, 2000), supporting the notion of homology of vertebrate cartilages regardless of embryological origin. Thus, investigations into the development of invertebrate cartilages should provide valuable information that can be used to assess the homology of cartilage amongst the different metazoan lineages. Despite the significance of developmental data for assessing issues of homology and evolution of cartilages, little developmental data is available from invertebrate sources.

Cephalopod cartilages represent an excellent starting point for developmental studies because adult cephalopod cartilages are the best studied of the invertebrate cartilages (Chapter's 1 & 2) and they are most similar to vertebrate cartilage histologically (see Cephalopoda, section 2.3.2), yet nothing is known of their development.

5.1.1 Cephalopod cartilages

Thorough descriptions of the adult anatomy, including the location of cartilaginous endoskeletal elements, are available for the European cuttlefish *Sepia officinalis* (Tompsett, 1939) and the common squid *Loligo pealeii* (Williams, 1909). These descriptions form the foundation for investigations into the development of cartilage by indicating where to expect cartilage formation within the embryo, based upon its locations within the adult. Tompsett (1939) describes the location and morphology of 13 different cartilage-like structures in adult *Sepia officinalis*, including cartilages associated with the circulatory system (branchial

and diaphragm), mantle (dorsal, pallial, and fin), funnel musculature (funnel and nuchal), and those within the head (radular, brachial, and cranial) and eye (scleral, equatorial, and horseshoe).

5.1.2 Current study

I investigate the development of these reported cartilages in the cuttlefish *Sepia officinalis*, and compare these data with the distribution and degree of differentiation of cartilages at the time of hatching from five additional cephalopod species representing four major cephalopod taxonomic orders: Sepiida (*Sepia officinalis* and *S. pharaonis*), Sepiolida (*Euprymna scolopes*), Teuthida (*Loligo pealeii, Illex illecebrosus*), and Octopoda (*Octopus bimaculoides*).

The histology of all cartilaginous elements in the cuttlefish has never been described, thus I first investigate the histology of these tissues from adult specimens to confirm they are indeed cartilage. Many of these elements show remarkable histological convergence with vertebrate hyaline cartilage. I investigate the early onset of cartilage formation for cephalopod hyaline cartilages using serial histology of sequential embryological stages. These cartilages arise from mesenchyme during the last stages of embryonic development, although the exact timing of appearance of the different cartilaginous elements varies.

To assess the transferability of these data to other cephalopod species, I examine the distribution and degree of differentiation of cartilages in four additional species, including the common squid *Loligo pealeii*. In all species examined the scleral cartilage of the eye is well formed at hatching, suggesting this tissue is functionally important. Unlike in the cuttlefish, squid cartilages do not form until sometime after hatching. In other members of the Sepiida and Sepiolida cartilages are well developed at hatching, especially the funnel cartilage, suggesting they may form by similar means during embryogenesis.

I also assess the phylogenetic relationships between these major cephalopod clades by creating a supertree based upon molecular source trees (see Chapter

3), and use the resultant tree to discuss the evolution of cartilage within cephalopod molluscs.

5.2 Methods

5.2.1 Animals:

All animals were purchased from the National Resource Center for Cephalopods, in Galveston, Texas, unless specified otherwise. Investigations of *Sepia* cartilage development include analysis of a developmental series from stage 24 through hatching (Lemaire, 1970) and a growth series from hatching to 3 cm mantle length (ML) in 5 mm increments. Embryos were removed from the egg capsule and staged according to Lemaire (1970; table 5, fig. 26). Newly hatched juveniles of the following species also were collected: *Sepia pharaonis*, *Octopus bimaculoides*, and *Euprymna scolopes*. Fertilized egg strings of *Loligo pealeii* were obtained from the Marine Resources Center at the Marine Biological Laboratories, Woods Hole, MA. Embryos were collected in daily increments until hatching, and staged according to Arnold (1965). All animals were anaesthetized in 7.5% $MgCl_2$, fixed and stored in 10% neutral buffered formal saline. Fixed specimens of *Illex illecebrosus* were obtained from the collection of Dr. R. O'Dor at Dalhousie University.

5.2.2 Whole mount staining

Whole mount Alcian Blue staining of juvenile cuttlefish and squid was modified from Klymkowsky and Hanken (1991). Fixed specimens were immersed for 2-4 hours in 0.2% Alcian Blue dissolved in 30% glacial acetic acid and 70% EtOH, rehydrated in an ascending ethanol series and cleared in 0.5% KOH followed by an ascending glycerol series. Digestion with trypsin, as per Klymkowsky and Hanken (1991), resulted in rapid degradation of the specimens and separation of the head from the mantle cavity and therefore was omitted from the protocol. Addition of Alizarin Red to the protocol stained only the cuttlefish cuttlebone and the statocysts. The cuttlebone staining interfered with visualization of the Alcian Blue staining, and thus was omitted from the protocol.

Table 5: Staging table for *Sepia intestinalis*

Embryos were isolated from their egg capsules and staged according to Lemaire (1970; translated here from the original French manuscript).

Stage	Features	Mantle Length (mm)
1	**Fertilization**	na
2 – 7	2 – 64 cell stage	na
8	Morula	na
9	Blastula	na
10	**Gastrulation begins** ▪ endomesodermic ring	na
11	▪ extension of endomesodermic "strings"	na
12	▪ Embryonic and extra-embryonic areas distinguishable	na
13	▪ Shell gland becomes visible as a small circular spot in the center of the shell sac ▪ Beginning of growth of the extra-embryonic tissues over the yolk.	na
14	▪ Dorso-lateral thickenings form lateral part of the head and eyes ▪ Ventral thickenings indicate origin of arms and gills	na
15	▪ Outlines of arms begin separation ▪ Buccal funnel and gill thickenings appears around the shell sac	na
16	▪ Invagination of the stomodeum ▪ Formation of the primary optic vesicle	na
17	▪ Optic vesicle is closed half-way ▪ Yolk plug 5/6 covered by extra-embryonic ectoderm	na
18	**Onset of Organogenesis** ▪ Yolk sac is fully formed (vitellum + syncitial vitelline + extra-embryonic ectoderm) ▪ Primary optic vesicle is closed ▪ Mouth is well delimited ▪ Gills are pedicularized ▪ Edge of the mantle is thickened	na
19	▪ Constriction between the embryo and the external yolk sac ▪ Closure of the shell sac ▪ The folds of the funnel tube fuse with the folds corresponding to the base and the retractor muscles of the siphon ▪ Outlines of the 10 arms are paired ▪ Invagination of the statocysts ▪ Salivary glands visible at the bottom of the stomodeum.	na
20	▪ Separation of the embryo and yolk sac is very visible ▪ Shell sac is closed ▪ Statocysts have invaginated, but are still open to the exterior ▪ Arm outlines start to grow blurred • B3 is reduced • B4, much more developed than the others ▪ Funnel tube folds meet at midline ▪ Optic lobes form prominent mass behind the eyes ▪ The mantle continues its progression and covers the base of the gills ▪ Appearance of the fins	na

Stage	Features	Mantle Length (mm)
21	▪ Arms 5,4,3,2 are brought back ventrally while the arms dorsal remain near the mouth ▪ Appearance of the folds of the iris ▪ Funnel folds come together at the anterior extremities. ▪ Edges of crystalline lens and the suction cups of the arms ▪ Differentiation of the gills: two to three branchial filaments appear in the form of small transverse folds compared to the axis of the gills. ▪ The optic lobes are prominent behind the eyes	na
22	▪ Funnels fuse at their internal face and anterior ends ▪ Crystalline lens forms a refringent rod. ▪ The mantle covers about half of the gills	0.8 +/- 0.1
23	▪ The anterior edges of the funnel are totally fused to form the siphon. The posterior part of the funnel (base and siphon muscles) leaves between them a triangular opening. ▪ Gills have 6-7 layers ▪ Appearance of Hoyle's organ (hatching gland)	1.1 +/- 0.1
24	▪ The funnel is fully formed ▪ Edge of the mantle covers the base of the funnel and anal papillae, leaving the extremities of the gills uncovered. ▪ Spherical crystalline lens ▪ First sign of pigmentation of the retina – yellow/orange	1.5 +/-0.2
25	▪ The mantle totally covers the gills and the muscles of the funnel ▪ Retina is orange	2 +/- 0.2
26	▪ Ink sac is visible on the ventral surface ▪ Retina is dark orange ▪ Appearance of the secondary cornea ▪ Appearance of some yellow-orange dorsal and lateral chromatophores ▪ Hoyle's organ is visible in the form of an anchor	3+/- 0.3
27	▪ Secondary cornea covers half of the eye ▪ Retina is red-orange ▪ Dorsal chromatophores are more numerous and dark orange	4 +/- 0.3
28	▪ Eye is entirely covered by the secondary cornea ▪ Retina is maroon	4.7 +/- 0.3
29	▪ Secondary ventral eyelid ▪ Ventral chromatophores	5.5 +/- 0.4
30	▪ "W"-shaped pupil ▪ Yolk sac resorbed ▪ Hatching occurs	7+/- 1.0

Figure 26: Embryogenesis of the European cuttlefish *Sepia officinalis*
Cuttlefish embryos develop within individual egg sacs for ~40 days at 20°C. Specimens shown in l, n, o, q, r, v and w were first fixed in neutral buffered formalin, all others were photographed live. Scale bars: a-d = 5 mm; e-w = 1 mm. **a-d** Isolation of embryos from the egg sac: **a** Egg sac; **b** Egg sac with half the chorionic layers removed; **c** Egg sac with only the outer few chorionic layers intact, revealing the developing embryo within; **d** Developing embryo removed from the egg sac. **e** Stage 11; Higher magnification of the embryo shown in (d). Gastrulation has commenced, with the extension of the endomesodermic strings visible (*arrows*). **f** Lateral view of the same embryo shown in (a-e). **g,h** Stage 12; Embryo imaged from the top (g) and lateral views (h). **i** Stage 14/15; growth of extra-embryonic tissues over the yolk is underway. **j** Stage 16; Mesodermal thickenings are visible, the stomodeum has invaginated (*arrow*) and the optic vesicles are visible (*). **k** Stage 17-18; Lateral view, showing the embryo beginning to be elevated off the yolk. **l** Stage 18; Onset of organogenesis. **m** Stage 18-19; Ventral view showing the pedicularization of the gills and thickening of the mantle, the shell sac is beginning to close (*arrow*). **n** Stage 20; Dorsal view, the constriction between the embryo and the yolk sac is apparent. The shell sac is closed, the optic lobes are prominent behind the eyes and the fins are visible. **o** Stage 22; Ventral view, separation between the embryo and yolk sac is complete, the mantle covers half of the gills. **p** Stage 22; Dorsal view illustrating the first appearance of the developing lens within the eyes (*arrows*). **q** Stage 23; Dorsal view. **r** Stage 24; Dorsal view showing the spherical lens and beginnings of calcification of the cuttlebone (*bright white*). Light yellow-orange pigment is visible in the retina surrounding the lens within the eyes. **s** Stage 25; Dorsal view showing the retina is bright orange. **t** Stage 26; Dorsal view showing the dark orange pigmentation of the retina and appearance of dorsal chromatophores. **u** Stage 27; Dorsal view showing red-orange pigmentation of the eye. **v** Stage 28; Dorsal view. **w** Hatchling; Dorsal view.

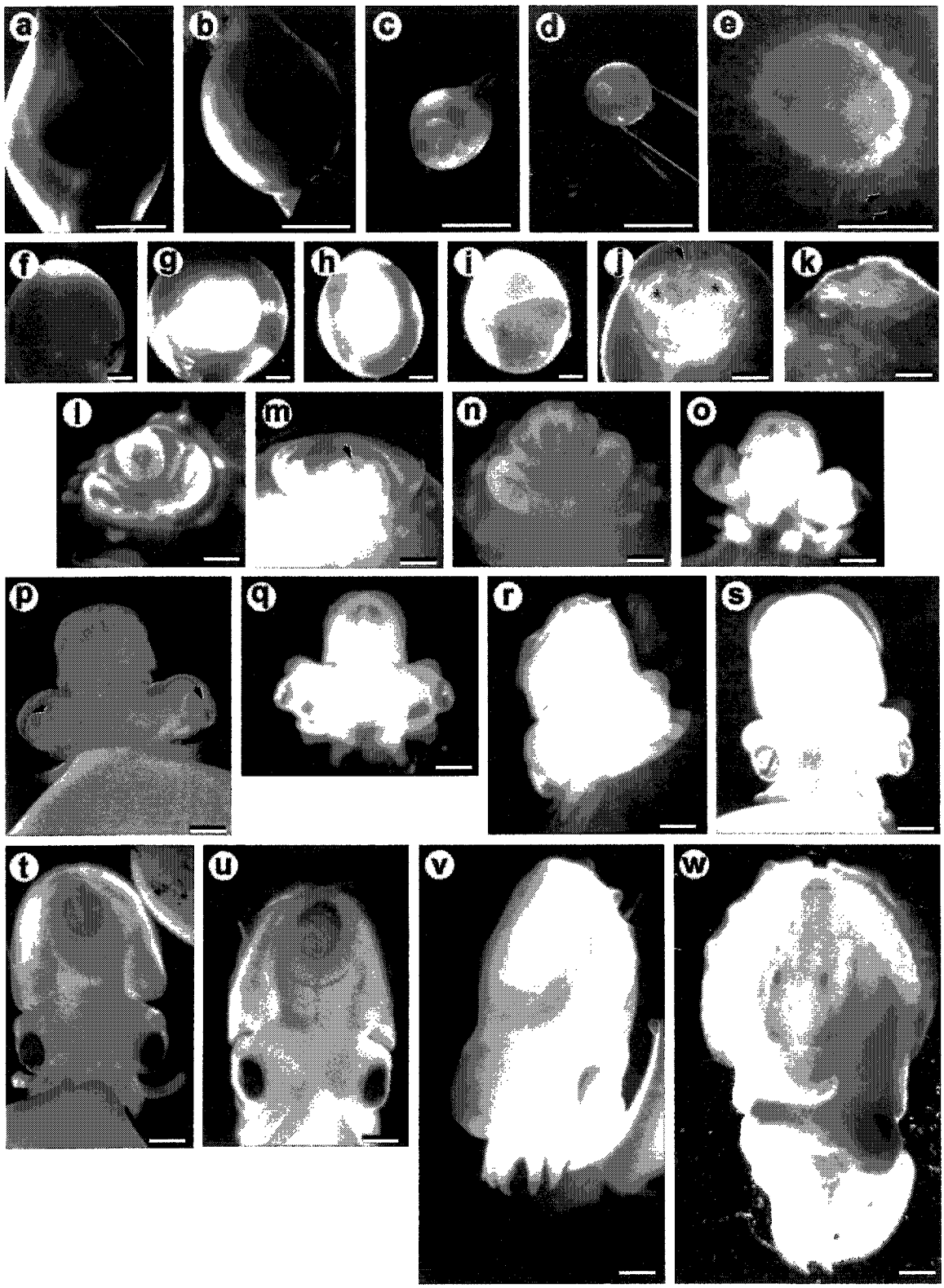

Figure 26

Although consistent staining was achieved using juvenile squids, staining of cuttlefish embryos and hatchlings was unreliable.

5.2.3 Histology

Fixed specimens were dehydrated in ethanol, cleared in hemo-D, and embedded in low melting point paraffin for sectioning. To facilitate sectioning of the yolk, blocks were immersed in water and re-frozen as necessary (as in Bourque *et al.*, 1993). Blocks were sectioned at 5-7 μm, and sections were mounted on Haupt's coated slides.

Sectioned specimens were stained using one of three histological protocols: Hall-Brunt Quadruple stain (Hall, 1986) to show onset of sulphated mucopolysaccharide deposition; Masson's trichrome to show onset of collagen deposition; my cartilage and connective tissue stain designed to show distribution of elastin, collagen, and mucopolysaccharides (see section 2.3.1).

5.2.4 Phylogeny

The phylogenetic relationships between cephalopod species were determined by creating a supertree from published molecular analyses (see Appendix 2.4), as described in Chapter 3. To determine the best estimate of cephalopod phylogeny, terminal taxa were reduced to the accepted major grades of cephalopod taxonomy (see Appendix 2.5). The distribution of cartilaginous elements was then plotted onto the resulting phylogeny.

5.3 Results

5.3.1 Cuttlefish staging

In staging cuttlefish embryos, degree of pigmentation is by far the easiest character to score for fresh material. However, fixation alters pigmentation patterns making pigmentation markers within the staging table less reliable for fixed tissue. As such, with fixed material total mantle length and size of the yolk sac are the more reliable staging characters for later stages of embryonic development.

5.3.2 Cartilaginous elements in cuttlefish

The cuttlefish has many different cartilages (fig. 27a), which have been described in detail by Tompsett (1939). I investigate the histological properties of each of these tissues and find that of the thirteen "cartilages" described therein, all except the branchial skeleton are cartilage. The branchial skeleton is made up of an acellular fibrous protein matrix, lacking mucopolysaccharides (fig. 27b) and thus is not a true cartilage. The radular cartilage shows the highest amount of mucopolysaccharide staining (fig. 27d), and the chondrocytes within this tissue are distinct from those forming the remaining cartilage in that they possess a large vesicle or vacuole, as previously described (Raven, 1958). Cartilages resembling vertebrate hyaline cartilage include the cranial cartilage surrounding the brain (fig. 27e), brachial cartilage supporting the ventral arms and tentacles, the interlocking funnel (fig. 27f) and pallial cartilages, the dorsal and nuchal cartilages, and the diaphragm and fin cartilages. These cartilages vary in amount of mucopolysaccharide staining, with the diaphragm (not shown) and pallial (fig. 27c) cartilages showing the lowest concentration of staining. The development of only these cartilages confirmed to show histological similarity to vertebrate hyaline cartilage is examined in this study.

5.3.3 Onset of cartilage differentiation

Whole mount Alcian Blue staining

In vertebrates it is possible to analyze the onset of cartilage formation utilizing whole-mount Alcian Blue staining (Klymkowsky and Hanken, 1991). However, although this technique works well to stain cartilage in juvenile squid, it also stains non-cartilaginous structures such as the pen (fig. 28a), and fails to pick up the earliest signs of cartilage formation in cuttlefish (fig. 28b,c). Therefore it was necessary to analyze the onset of cartilage formation using histological sections. From these sections I have reconstructed the initial differentiation of cartilages found within *S. officinalis* (fig. 29).

Figure 27: Distribution of cartilaginous elements from *Sepia officinalis*
Thirteen different cartilaginous structures have been described in the adult cuttlefish. Of these, all are found here to be cartilaginous, with the exception of the branchial skeleton. Scale bar = 100 µm; *hc* = hyaline cartilage; *og* = optic ganglion **a** Tissues previously reported to be cartilage are highlighted blue in a figure modified from the original description (Tompsett, 1939). **b** The branchial skeleton is acellular, and does not contain any mucopolysaccharides, as indicated by light green staining using my new cartilage and connective tissue protocol. **c** The pallial cartilage (*hc*) within the mantle wall is restricted to a layer underlying the epidermis (*inset*), developing from individual cells (*arrows*) in hatchlings. **d** The radular cartilage shows extensive mucopolysaccharide staining, with vesiculated chondrocytes. **e** Chondrocytes within the orbital portions of the cranial cartilage are large spherical cells. **f** This same spherical chondrocyte morphology is found in the funnel cartilage, where the overlying epithelial layer (*left*) remains distinct from the underlying cartilage.

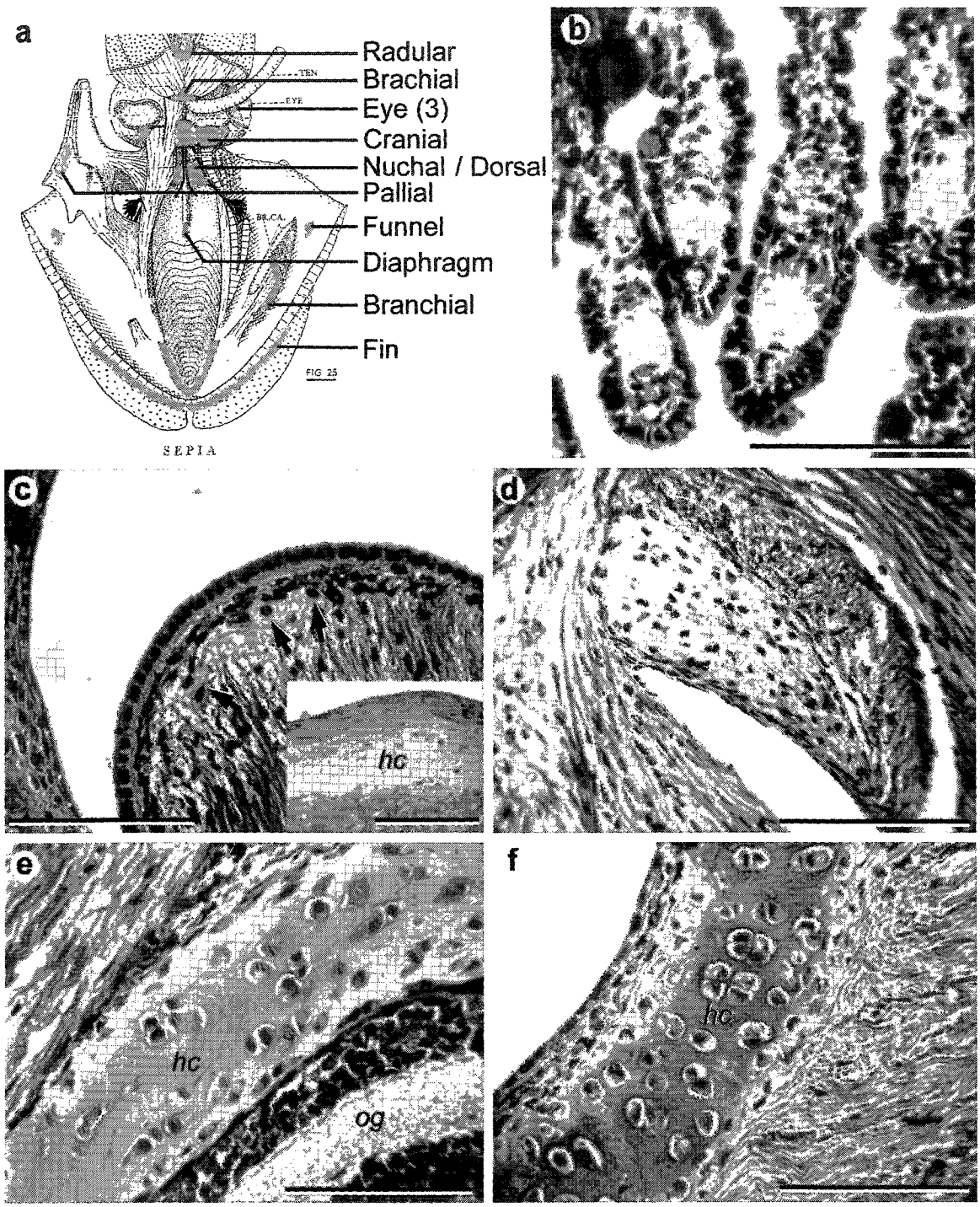
a
Radular
Brachial
Eye (3)
Cranial
Nuchal / Dorsal
Pallial
Funnel
Diaphragm
Branchial
Fin
FIG 25
SEPIA
b
c
hc
d
e
hc
og
f
hc

Figure 27

Onset of Cartilage Formation

The first cartilages visible in the embryo are the interlocking funnel and pallial complex. The funnel cartilages form as indentations in the ventral wall of the developing funnel, first appearing just after the funnel folds have fused (fig. 29a-i). In the adjacent mantle wall, protrusions that will form the pallial cartilages are visible. The morphology of these two cartilages can be seen in embryos with the aid of a dissecting microscope.

As development proceeds, a portion of the cranial cartilage (the orbital cartilages; see fig. 28d-g) differentiates between the funnel musculature and the brain (fig. 29j-l), in part filling portions of the extensive cranial blood sinus that exists within the head in these early embryos. Although the cranial cartilage in adult cuttlefish is a single structure (fig. 28d-g), the orbital cartilages form from two separate centres of chondrification and are later fused together by the statocyst and bridge cartilages. This fusion occurs near the end of embryogenesis, at stage 28, when the remaining bilaterally symmetrical portions of the cranial cartilage form (fig. 29m-o). At hatching, more of the cranial cartilage is present (fig. 29p-r), however in places such as the bridge between the orbital cartilages, little more than a fibrous connective tissue exists.

Also at stage 28, the fin and brachial cartilages differentiate from connective tissue. At this point all the future cartilages have begun differentiation and are recognizable as cartilage in histological section (fig. 29m-o), the last of which being the diaphragm and pallial cartilages (fig. 29p-r).

5.3.4 Mechanisms of cartilage differentiation

In order to determine the mechanism of cartilage differentiation in the cuttlefish, regions of cartilage formation were analyzed in section prior to the onset of chondrogenesis. Despite the fact that the individual cartilages are histologically indistinguishable after differentiation, the mechanism of formation is variable between the individual cartilages.

In all cases of cartilage formation, the secreted extracellular matrix becomes reactive to Alcian Blue (HBQ staining: indicating mucopolysaccharides) prior to

Figure 28: Whole-mount Alcian Blue staining of cephalopods
Alcian Blue staining reveals structure of cartilaginous elements in juvenile cephalopods, but fails to pick up earliest signs of differentiation. *BC* – branchial cartilage; *CC* – cerebral cartilage; *cb* – cuttlebone; *cr* – cranial cartilage; *do* – dorsal cartilage; *fi* – fin cartilage; *fu* – funnel cartilage; *hs* – horseshoe cartilage; *nu* – nuchal cartilage; *pa* – pallial cartilage; *sc* – scleral cartilage; *SC* – statocyst cartilage; *TR* – trochlear cartilage. Scale bar = 1 cm. **a** Alcian Blue can be used to identify cartilage in young squid (*Illex illecebrosus*, ~25 mm ML), however staining is not restricted to cartilage, as indicated by blue staining of the pen (*pen*). Cartilages associated with the eye (scleral (*sc*) and horseshoe (*hs*)), the cranial (*cr*), funnel (*fu*), nuchal (*nu*), and fin (*fi*) cartilages can be visualized. **b,c** Although some cartilages can be visualized in hatchling (**b**) and juvenile (**c**) cuttlefish, not all elements that are differentiated histologically as cartilage at this stage can be distinguished from Alcian Blue wholemounts. **d-g** Drawings of the cranial cartilage from the adult cuttlefish, as presented as figures 26-29 in Tompsett (1939). The cranial cartilage can be divided into a number of bilateral components: orbital cartilage (*OC*), trochlear cartilage (*TR*), statocyst cartilage (*SC*), cerebral cartilage (*CC*), and the central bridge cartilage (*bridge*). Also shown is the location of the brachial cartilage (*BC*) relative to the cranial cartilage. In all but (**f**) ventral is to the top. **d** posterior view; **e** right lateral view; **f** ventral view; **g** anterior view.

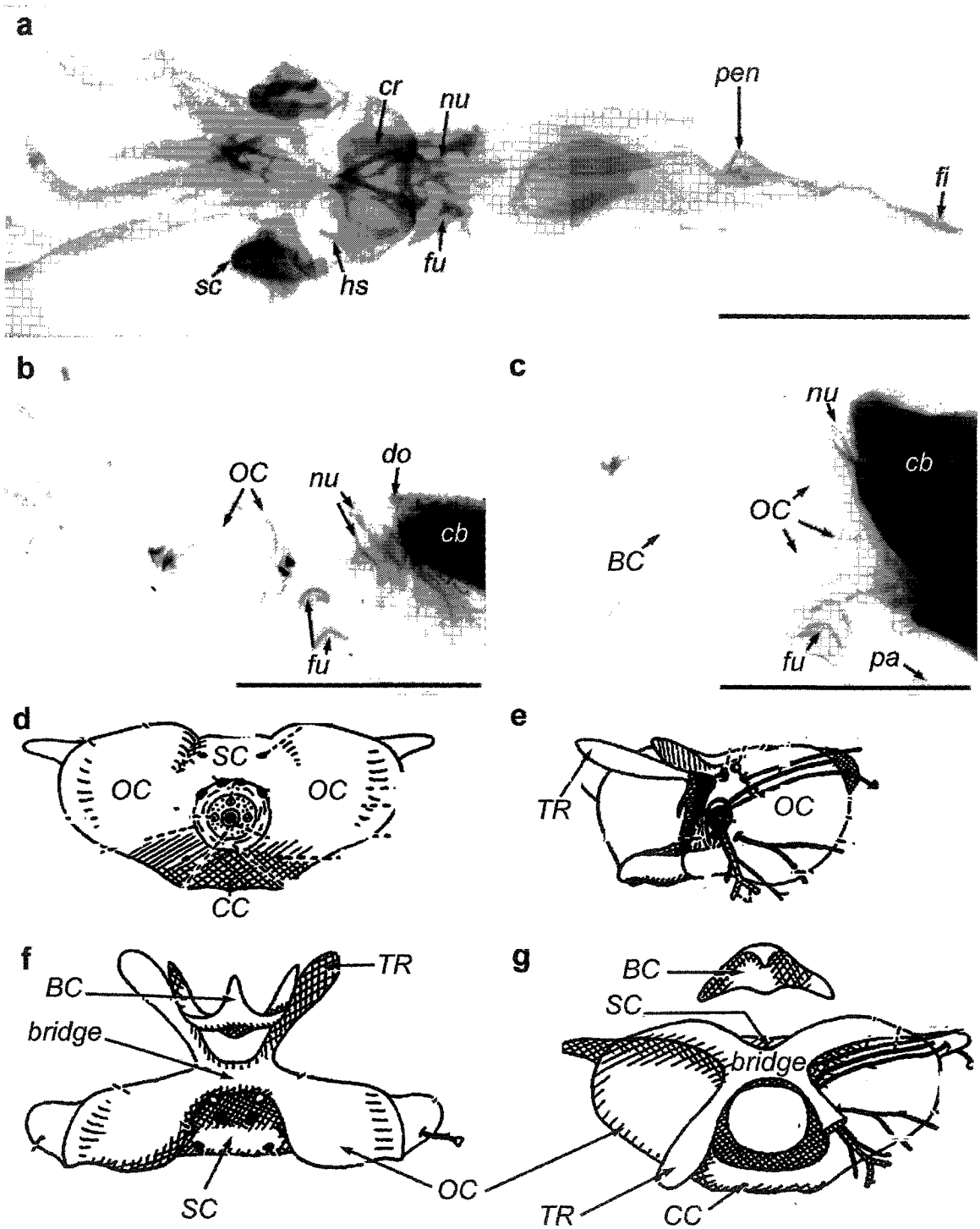
a
cr
nu
pen
fi
sc
hs
fu
b
OC
nu
do
cb
fu
c
nu
cb
OC
BC
fu
pa
d
SC
OC
OC
CC
e
TR
OC
f
BC
TR
bridge
SC
OC
g
BC
SC
bridge
TR
CC

Figure 28

Figure 29: Onset of cartilage formation within *Sepia officinalis*
The onset of cartilage formation was reconstructed from histological sections (see figure 30), and is illustrated schematically in ventral (second column) and lateral view (third column), drawn to scale with the yolk sac included. Embryos isolated from their egg case and removed from the yolk sac were photographed from the ventral surface using dark-field illumination (shown in the first column). Initial signs of cartilage formation are indicated by light blue, differentiating cartilages dark blue. **a-c** Stage 24 (st24); the funnel cartilage is already differentiated as a cellular condensation. **d-f** Stage 25 (st25) **g-i** Stage 26 (st26); cells of the funnel cartilage have begun to differentiate. **j-l** Stage 27 (st27); the orbital portion of the cranial cartilage is distinguishable. **m-o** Stage 28 (st28); the fin, brachial, and the rest of the cranial cartilage first appear. **p-r** Stage 29 (st29); all remaining cartilages are differentiated, including the nuchal/dorsal complex.

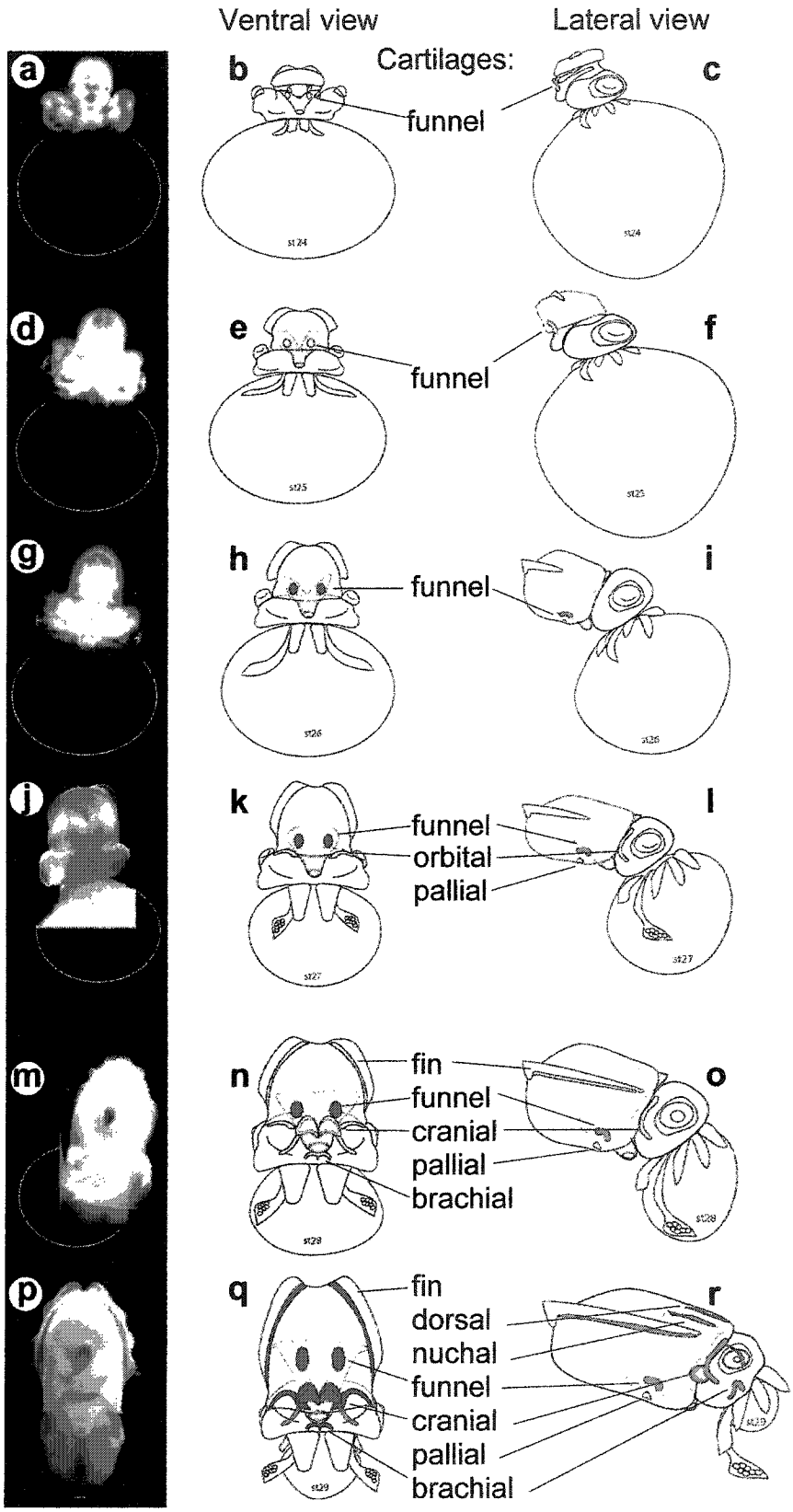
Ventral view
Lateral view
Cartilages:
a
b
c
funnel
d
e
f
funnel
g
h
i
funnel
j
k
l
funnel
orbital
pallial
m
n
o
fin
funnel
cranial
pallial
brachial
p
q
r
fin
dorsal
nuchal
funnel
cranial
pallial
brachial

Figure 29

staining with Light Green (Masson's trichrome: indicative of collagen), suggesting that the first molecules to be deposited are the mucopolysaccharides as in vertebrates during cartilage formation. Most cartilages in the cuttlefish form at stage 28 by direct differentiation from loose mesenchyme, without showing any signs of cellular condensation formation. This mode of differentiation is illustrated for fin cartilage formation in figure 30.

Funnel Cartilage

As soon as the surface depression on the funnel folds is visible, a distinct cuboidal epithelial layer overlying the presumptive funnel cartilage can be identified (fig. 30c). Underlying this epithelial layer is a mesenchymal condensation of cells, not unlike those typical of vertebrates. The cells of this condensation become spherical and cease mitotic activity, as evidenced by the large size and diffuse chromatin of the nuclei (fig. 30g). This is followed by a period where cells are separated by a small amount of matrix, which is not yet reactive with histological stains. I will refer to this stage as the *proto-cartilage* stage (fig. 30j). By stage 28 the matrix between the chondrocytes reacts with histological stains, indicating maturation of the extracellular matrix components (fig. 30r). As development proceeds, the extracellular matrix between the chondrocytes continues to expand (fig. 30v). In adult animals, this matrix is extensive and contains large amounts of mucopolysaccharides centrally, while retaining a high collagenous component peripherally (see fig. 8e,f in Chapter 2).

Pallial Cartilage

In direct contrast to the funnel cartilage, the corresponding pallial cartilages do not chondrify during early embryogenesis. When this structure is visible as a protrusion of the mantle wall, there exists a well-defined epithelial layer overlying a mesenchymal condensation (fig. 30c). As development proceeds this condensation disappears; a proto-cartilage stage is never seen and although the morphological protrusion is still evident, and more defined, the tissue underlying the epithelium is loose mesenchyme. It is not until hatching that individual cells

Figure 30: Ontogeny of cartilage differentiation from *Sepia officinalis*
Embryos were sectioned from stage 24 (st24; first row, **a-d**) until just prior to hatching (st29; last row, **t-w**). The level of the sections are indicated on the diagram (first column) by arrows (1), (2), and (3) correspond to histological sections illustrated in columns for the fin, funnel, and orbital cartilages respectively. Arrowheads indicate the region of cartilage formation in all sections. Scale bar = 100 µm; *bs* = blood sinus; *cc* = cartilage condensation; *e* = epithelium; *m* = mesenchyme; *og* = optic ganglia; *pc* = proto-cartilage.

a-d Stage 24 (st24): **b** There is no cartilage formation at the base of the developing fin, although there is a space between the developing cuttlebone and mantle. **c** The funnel and pallial cartilages are visible morphologically as a protrusion (pallial) and indentation (funnel), both lined with a distinct cuboidal epithelial layer overlying a cellular condensation of mesenchymal cells (*m*). **d** A condensation of cells can be seen within the developing funnel musculature where this tissue abuts the cranial blood sinus (*bs*) surrounding the optic ganglia.

e-g Stage 25 (st25), due to processing difficulties, images of the orbital cartilage are not available for this stage: **f** There is still no sign of cartilage formation at the base of the developing fin. **g** Cells within the funnel cartilage condensation (*cc*) have ceased cell division, as indicated by the large size and diffuse nature of the nuclei.

h-k Stage 26 (st26): **i** The fin cartilage still has not formed, however deposition of extracellular matrix (ECM) forming the cuttlebone has begun (*white arrowheads*). **j** The cells of the developing funnel cartilage have become spherical, and have begun to deposit ECM which does not yet react with histochemical stains. At this stage, the developing cartilage is referred to as proto-cartilage (*pc*). **k** The condensation of cells forming the orbital cartilage (*cc*) is still visible at the edge of the cranial blood sinus (*bs*).

l-o Stage 27 (st27): **m** There is still little change at the base of the developing fin. **n** The ECM of the developing funnel cartilage has increased and the spherical morphology of the chondrocytes is more apparent. **o** The condensation of cells of the developing orbital cartilage have begun to differentiate as a proto-cartilage (*pc*). The proto-cartilage is convoluted, and fills the space formerly occupied by the cranial blood sinus so that it abuts the optic ganglia.

p-s Stage 28 (st28): **q** The fin cartilage has begun to differentiate from the mesenchyme at the base of the developing fin as indicated by extensive deposition of cartilage matrix (green) surrounding large spherical chondrocytes. **r** The ECM of the funnel cartilage stains strongly for collagen (green). **s** The developing orbital cartilage also stains for collagen (green), and is less convoluted.

t-w Stage 29 (st29), just prior to hatching: **u** The fin cartilage continues to expand and deposit more ECM. **v** The funnel cartilage is well differentiated, with the amount of ECM between individual chondrocytes expanding. **w** The orbital cartilage is no longer convoluted, and cells continue to deposit ECM.

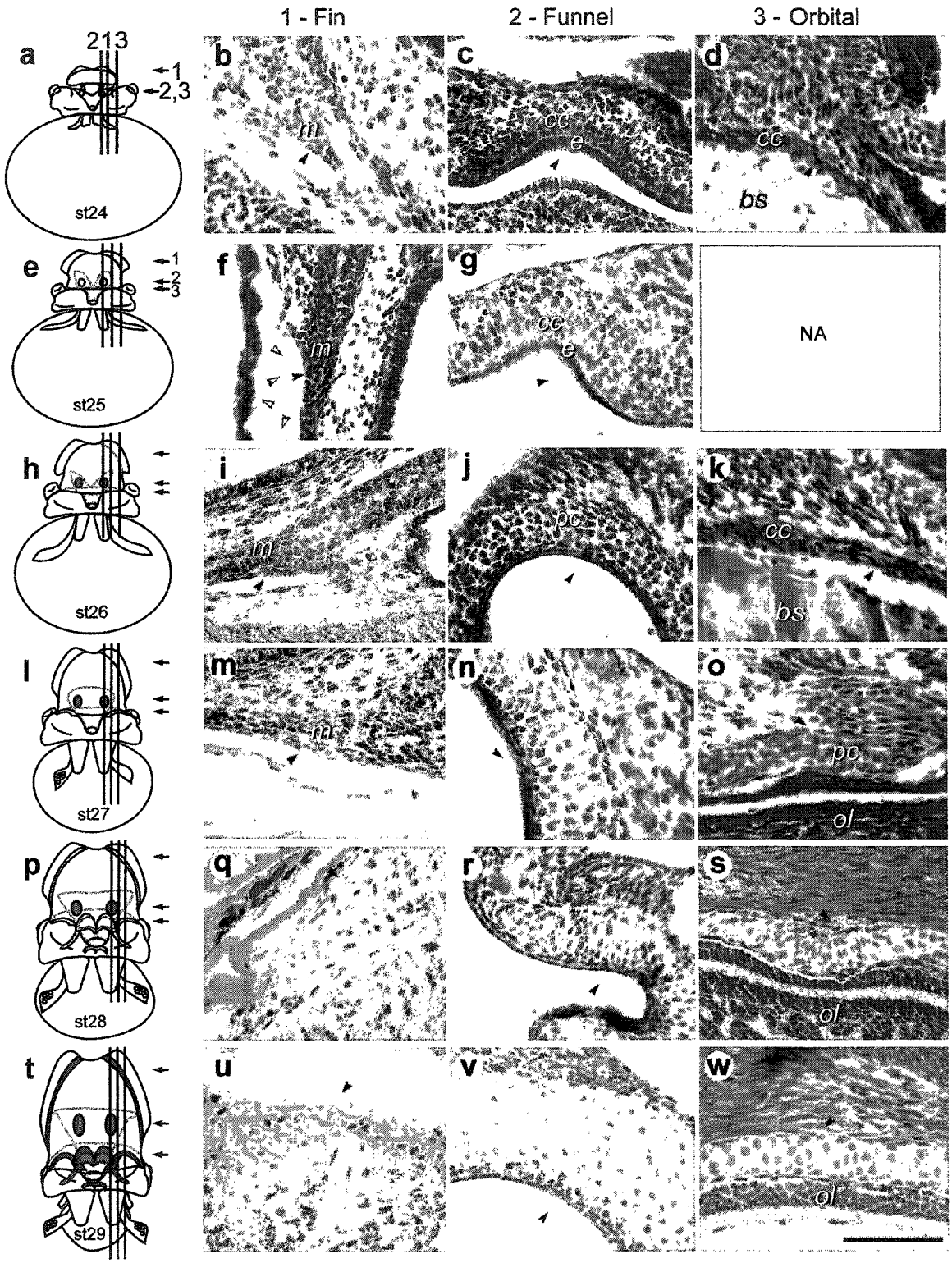
1 - Fin
2 - Funnel
3 - Orbital
a
213
1
2,3
st24
b
m
c
cc
e
d
cc
bs
e
1
2
3
st25
f
m
g
cc
e
NA
h
st26
i
m
j
pc
k
cc
bs
l
st27
m
m
n
o
pc
ol
p
st28
q
r
s
ol
t
st29
u
v
w
ol

Figure 30

within this mesenchyme become spherical and begin to deposit an extracellular matrix reminiscent of cartilage (see fig. 27c).

Orbital Cartilage

The only other cartilages found to go through a proto-cartilage stage are the orbital cartilages. As early as stage 24 a mesenchymal condensation can be seen forming at the edge of the cranial sinus (fig. 30d). By stage 26 this condensation has expanded, and the cells show the diffuse staining properties of proto-cartilage (fig. 30k). In the adult this cartilage is a smooth cup-like structure that in part houses the eyes and optic ganglia, but at this stage the edge of the condensation is folded upon itself (fig. 30o,s). As with the funnel cartilage, the extracellular matrix begins to react to histological stains by stage 28. By stage 29, just prior to hatching, all traces of the convolutions have disappeared (fig. 30w).

5.3.5 Comparisons with other Cephalopod species

The distribution and degree of differentiation of cartilages within four additional cephalopod species was investigated in order to assess the degree of transferability of the cuttlefish data to other cephalopod species (table 6; fig. 31).

Sepia pharaonis

Sepia pharaonis juveniles are slightly bigger at hatching than their *S. officinalis* counterparts, hatching at 7.5mm mantle length (ML). Similar to what is seen in the European cuttlefish, *S. pharaonis* hatchlings have all cartilages differentiated at the end of embryogenesis.

Euprymna scolopes

The Hawaiian bob-tail squid, *Euprymna scolopes* is comparatively much smaller at the end of embryogenesis, hatching at ~3.5 mm mantle length. At hatching, the funnel and fin cartilages are well differentiated. This species does not retract its head into the mantle cavity, and is missing the nuchal and dorsal cartilages. Additionally, *E. scolopes* does not have any remnant of the molluscan

Table 6: Cartilage distribution at hatching of selected cephalopods
Mantle length was measured medially from fixed specimens. Cartilage distribution was determined from histological section, wherein ++ = fully differentiated tissue; + = onset of cartilage differentiation; m = morphologically present, but not differentiated as cartilage; NA = structure not available in this species.

	Sepia officinalis	*S. pharaonis*	*Euprymna scolopes*	*Illex illecebrosus*	*Loligo pealeii*	*Octopus bimaculoides*
Mantle Length [mm]:	7	7.5	3.5	~3*	2	5.5
Cranial	++	++	+	++	-	+
Brachial	++	++	NA	NA	NA	NA
Scleral/Equatorial	++	++	++	++	+	++
Funnel articulating	++	++	++	++	-	NA
Pallial articulating	m	m	m	m	-	NA
Nuchal	++	++	NA	++	m	NA
Dorsal mantle	++	++	NA	++	-	NA
Fin attachment	++	++	++	?	-	NA

* The juvenile specimens of *Illex illecebrosus* examined are significantly larger than hatchlings, which measure ~1mm ML (O'Dor *et al.*, 1982)

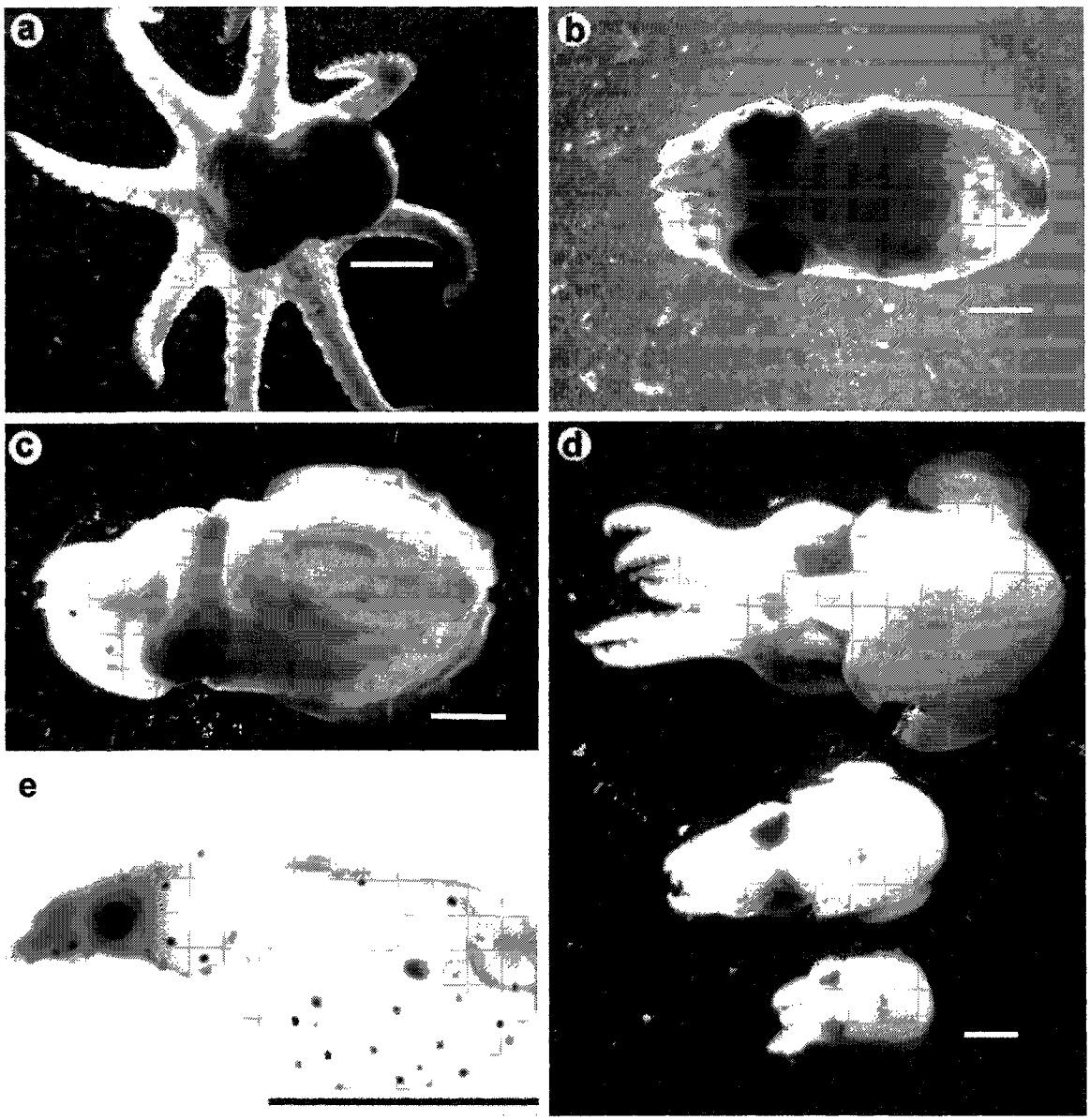

Figure 31: Juvenile cephalopods examined in this study
Cephalopod molluscs show size variability at hatching. Specimens illustrated were first fixed in formalin and then photographed with a stereomicroscope, except (**e**), which was photographed live with a compound microscope. Scale bar = 2 mm. **a** *Octopus bimaculoides*; **b** *Sepia pharaonis*; **c** *Sepia officinalis*; **d** *Euprymna scolopes*, shown are all three size classes examined; **e** *Loligo pealeii*.

shell. In its place, the fin cartilages extend not only laterally supporting the fins, but also medially, providing the mechanical support otherwise conferred by the pen or cuttlebone (fig. 32a). At hatching this species also has a cartilaginous hatching spine, composed of 5-6 chondrocytes. This tissue is comparatively poor in mucopolysaccharide content, and disappears shortly after hatching.

The cranial cartilage is present at hatching as a collagen-rich deposit surrounding the ganglia (fig. 32b), more prominent surrounding the statocysts than the optic lobes. As the animal ages, the extracellular matrix expands, and more cells are incorporated (fig. 32d). Similar to the sepiids, *Euprymna* has a well-developed scleral cartilage at hatching (fig. 32c).

Loligo pealeii

Embryos of the pelagic common squid *Loligo pealeii* are significantly smaller than those of *S. officinalis*, measuring only ~2.5 mm mantle length at hatching. The scleral cartilage is recognizable in hatchlings (fig. 32e), and its development can be followed in unfixed whole-mount preparations with Alcian Blue staining (fig. 33). Mucopolysaccharide deposition begins distally at stage 26 (fig. 33a,b), and continues until hatching (fig. 33g,h).

The cranial cartilage is little more than a collagenous layer surrounding the ganglia (figure 32f), and the beginnings of the nuchal cartilage can be seen as an elevated epithelial layer overlying the pen. No indications of funnel cartilage are present, including the absence of an epithelial layer, mesenchymal condensation, and morphological indentation, nor is there any indication that cartilage will form at any of the other sites described as cartilaginous in the adult (Williams, 1909).

Illex illecebrosus

Although hatchlings of *Illex illecebrosus* were not available for analysis, young juveniles (3 mm ML) were examined. Section preservation artefacts prevented me from distinguishing whether or not a fin cartilage is present, however the scleral, cranial, funnel, nuchal, and dorsal cartilages are all well differentiated at this stage.

Figure 32: Histology of cartilages from select cephalopod species
Comparative histological analysis of cephalopod hatchlings reveals variability in number and location of differentiated cartilages. New cartilage and connective tissue stain (a-d,g,h) and Masson's trichrome staining (e,f). Scale bar = 100 µm. **a-d** The Hawaiian bob-tail squid *Euprymna scolopes*: **a** *Euprymna* hatchlings lack any remnant of the pen. In its place the fin cartilages extend dorso-medially (*arrows*). **b** At hatching the cranial cartilage is little more than a sheet of collagenous material (*arrows*). **c** The scleral cartilage within the eyes is well formed (*arrows*). **d** Within juveniles that are 4.5 mm mantle length the extracellular matrix of the cranial cartilage has expanded (*arrows*), and chondrocytes can be identified embedded in the matrix. **e,f** The common squid *Loligo pealeii* hatchlings: **e** *Loligo* hatchlings also have an identifiable scleral cartilage at hatching (*arrows*). **f** The cranial cartilage exists as only a thin acellular collagenous layer surrounding the ganglia (*arrows*). **g,h** *Octopus bimaculoides* hatchlings: **g** Juvenile *Octopus* also have a well developed scleral cartilage within the eyes (*arrows*). **h** The cranial cartilage (*cc*) is also well formed at hatching in this species.

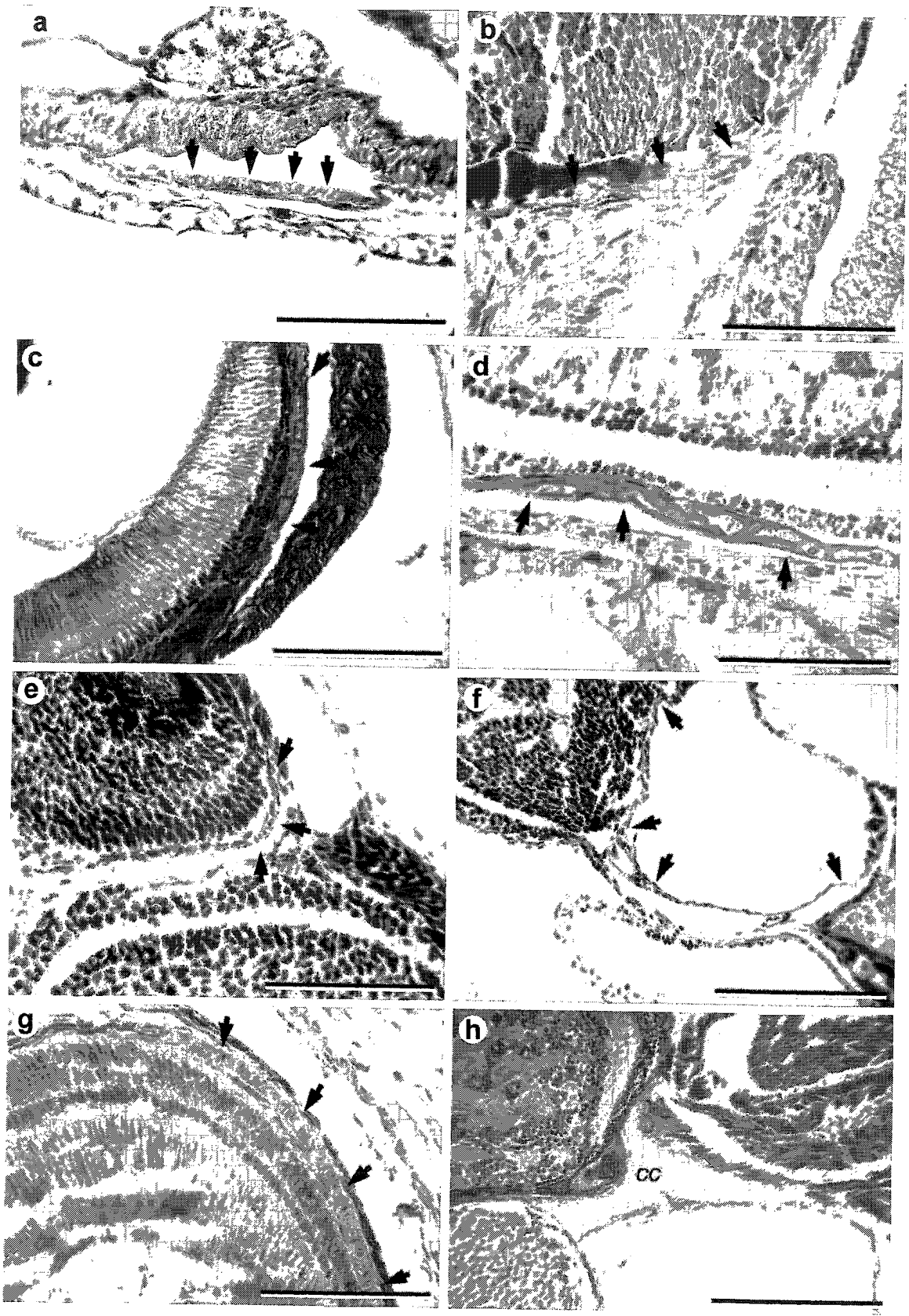

Figure 32

Figure 33: Eye cartilage formation of embryonic *Loligo pealeii*
Whole mount Alcian Blue staining of embryos fixed in the staining solution (95% EtOH containing 2% Alcian Blue) reveals early mucopolysaccharide deposition associated with the development of the eye and scleral cartilages. Scale bars = 1 mm. **a,b** Stage 26; mucopolysaccharide deposition (*blue staining*) begins at the distal-most portions of the developing sclera. **c,d** Stage 27; **e,f** Stage 28; **g,h** Stage 29; mucopolysaccharide deposition of the sclera is nearly complete (*blue staining*).

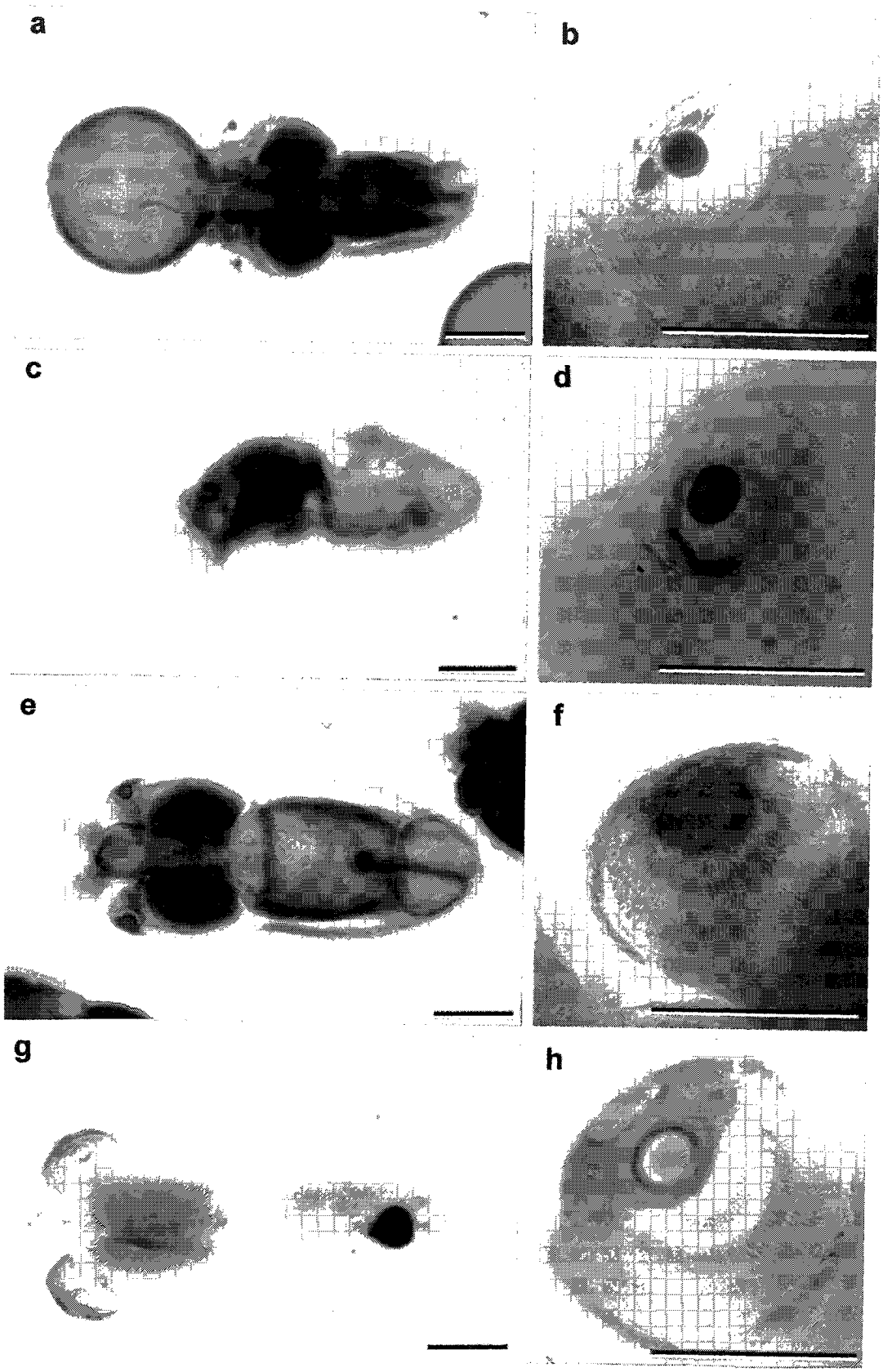

Figure 33

Octopus bimaculoides

Newly hatched *Octopus* hatch at ~5.5 mm mantle length, and have well-developed cartilages within the eye (fig. 32g). The cranial cartilage is present as a collagen-rich single layer of cells, similar to *Euprymna* hatchlings, except where the statocyst cartilages connect medially (fig. 32h). No other cartilages are present, nor are they expected on the basis of adult anatomy (Robson, 1929).

5.3.6 Cephalopod phylogeny

To put this comparative data into the appropriate phylogenetic context, I created a supertree of cephalopod phylogeny (fig. 34). The five cephalopod species examined here fall into four major cephalopod orders: Sepiida (*Sepia officinalis* and *S. pharaonis*), Sepiolida (*Euprymna scolopes*), Teuthida (*Loligo pealeii*), and Octopoda (*Octopus bimaculoides*) (see Appendix 2.5). Taxon compression (see Chapter 3) into the currently recognized nine cephalopod super-clades results in a single fully resolved tree (fig. 34a). The Sepiida, Sepiolida, and Teuthida belong to the clade Decapodaformes, characterized by having 10 brachial appendages, whereas the Octopoda belong to the clade Octopodoformes, having only 8 brachial appendages. These two clades are confirmed as monophyletic in all analyses, as indicated by the supertree (fig. 34b), however the relationships between the major grades (orders), and the monophyly of these groups remain obscure.

5.4 Discussion

5.4.1 Cephalopod phylogeny and cartilage evolution

As a result of molecular phylogenetics, cephalopod taxonomy will likely undergo further revision in the near future. At present cephalopod phylogenetics, particularly with regards to the decapodoformes, is largely unresolved, and therefore statements with regards to character evolution must be made with caution. Additionally, the distribution of cartilaginous elements was investigated here in only a select few members of these major cephalopod grades. More data

a

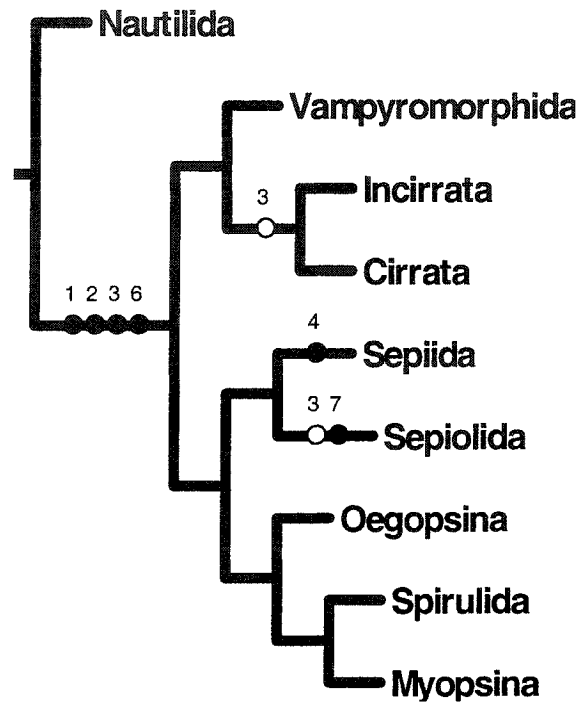

Figure 34: Phylogeny of cephalopods
Distribution of cartilages within cephalopods is related to phylogeny. Cephalopod phylogeny was determined by a supertree analysis of molecular hypotheses, see text for details. Origin and loss of cartilaginous elements have been plotted onto this phylogeny, on the basis of the analysis of a select few taxa analyzed in the current study. Characters are as follows: 1 = Cranial cartilage; 2 = Funnel/Pallial cartilages; 3 = Nuchal/Dorsal cartilages; 4 = Brachial cartilage; 5 = Scleral cartilage; 6 = Fin cartilages; 7 = Dorsal extension of the fin cartilage. Scleral cartilage (5) is not depicted in the figure because its presence/absence within *Nautilus* is unknown at present, making the origin of these structures uncertain. Closed circles indicate gains of structures; open circles indicate losses. **a** Forcing monophyly of major cephalopod taxonomic grades results in a single best estimate of cephalopod phylogeny. Brachial cartilages (4) evolved within Sepiida; Dorsal extension of the fin cartilages (7) evolved within Sepiolida. The nuchal/dorsal cartilage complex has been lost independently at least twice: once within Sepiolida and again within Octopoda (Incirrata + Cirrata). **b** Analysis of cephalopod phylogeny at the level of genera results is inconclusive. The separation of the Octopodoformes and the Decopodoformes is well supported by all analyses, however monophyly of the major grades within these groups is not. Consensus trees (strict and 50% majority rule) of 30,000 best fit trees.

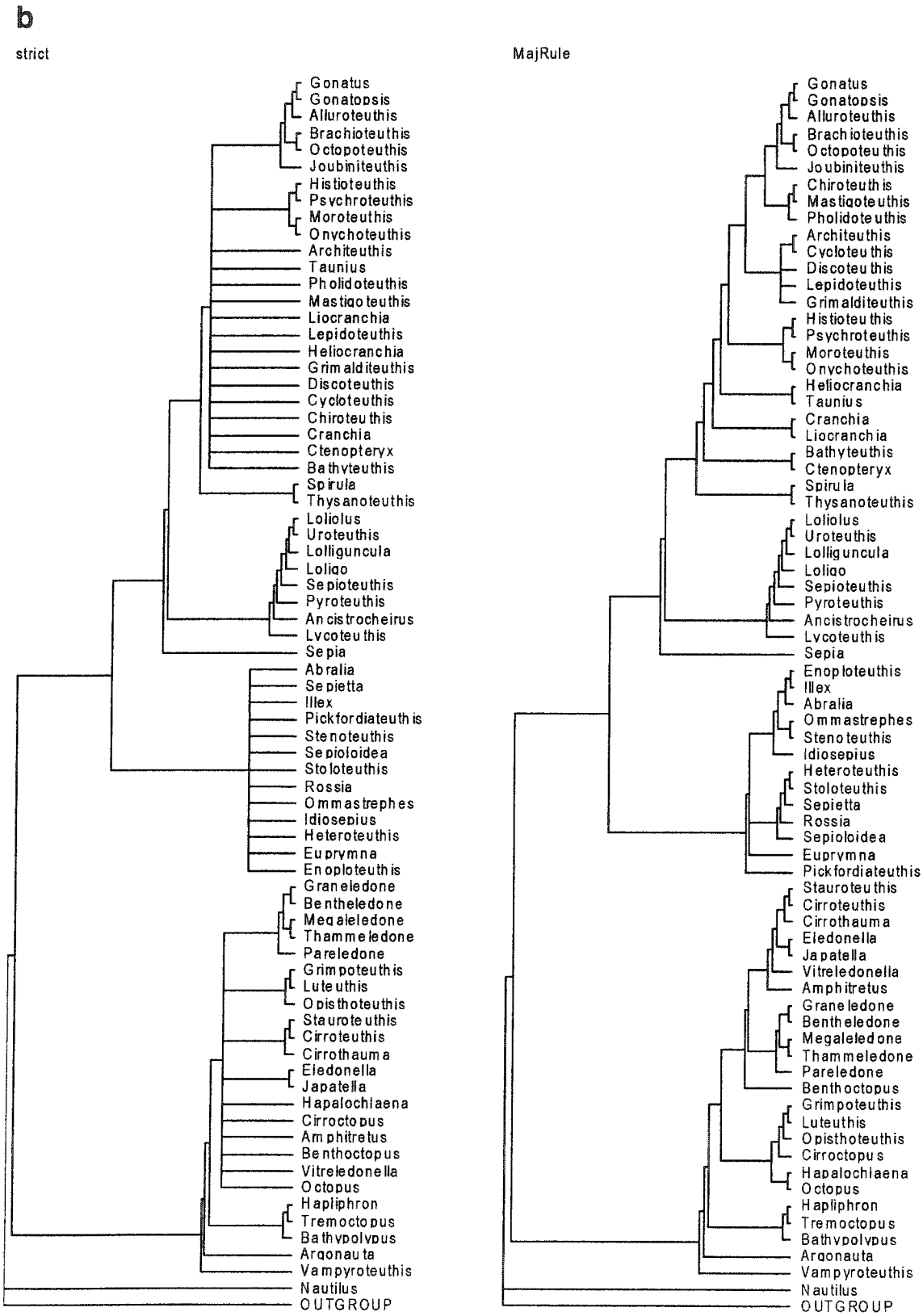
b
strict
Gonatus
Gonatopsis
Alluroteuthis
Brachioteuthis
Octopoteuthis
Joubiniteuthis
Histioteuthis
Psychroteuthis
Moroteuthis
Onychoteuthis
Architeuthis
Taunius
Pholidoteuthis
Mastigoteuthis
Liocranchia
Lepidoteuthis
Heliocranchia
Grimalditeuthis
Discoteuthis
Cycloteuthis
Chiroteuthis
Cranchia
Ctenopteryx
Bathyteuthis
Spirula
Thysanoteuthis
Loliolus
Uroteuthis
Lolliguncula
Loligo
Sepioteuthis
Pyroteuthis
Ancistrocheirus
Lycoteuthis
Sepia
Abralia
Sepietta
Illex
Pickfordiateuthis
Stenoteuthis
Sepioloidea
Stoloteuthis
Rossia
Ommastrephes
Idiosepius
Heteroteuthis
Euprymna
Enoploteuthis
Graneledone
Bentheledone
Megaleledone
Thammeledone
Pareledone
Grimpoteuthis
Luteuthis
Opisthoteuthis
Stauroteuthis
Cirroteuthis
Cirrothauma
Eledonella
Japatella
Hapalochlaena
Cirroctopus
Amphitretus
Benthoctopus
Vitreledonella
Octopus
Hapliphron
Tremoctopus
Bathypolypus
Argonauta
Vampyroteuthis
Nautilus
OUTGROUP
MajRule
Gonatus
Gonatopsis
Alluroteuthis
Brachioteuthis
Octopoteuthis
Joubiniteuthis
Chiroteuthis
Mastigoteuthis
Pholidoteuthis
Architeuthis
Cycloteuthis
Discoteuthis
Lepidoteuthis
Grimalditeuthis
Histioteuthis
Psychroteuthis
Moroteuthis
Onychoteuthis
Heliocranchia
Taunius
Cranchia
Liocranchia
Bathyteuthis
Ctenopteryx
Spirula
Thysanoteuthis
Loliolus
Uroteuthis
Lolliguncula
Loligo
Sepioteuthis
Pyroteuthis
Ancistrocheirus
Lycoteuthis
Sepia
Enoploteuthis
Illex
Abralia
Ommastrephes
Stenoteuthis
Idiosepius
Heteroteuthis
Stoloteuthis
Sepietta
Rossia
Sepioloidea
Euprymna
Pickfordiateuthis
Stauroteuthis
Cirroteuthis
Cirrothauma
Eledonella
Japatella
Vitreledonella
Amphitretus
Graneledone
Bentheledone
Megaleledone
Thammeledone
Pareledone
Benthoctopus
Grimpoteuthis
Luteuthis
Opisthoteuthis
Cirroctopus
Hapalochlaena
Octopus
Hapliphron
Tremoctopus
Bathypolypus
Argonauta
Vampyroteuthis
Nautilus
OUTGROUP

Figure 34

on the distribution of cartilaginous elements amongst different cephalopod taxa are required in order to fully resolve trends in cephalopod cartilage evolution.

Nonetheless, a number of trends can be identified here by plotting the presence and absence of cartilages, on the basis of the taxa examined here, onto the best estimate of major taxonomic relationships derived from supertree analysis of molecular hypotheses (fig. 34a). Cranial cartilage appears basal within these lineages because it is present in all taxa examined. Presence of the funnel/pallial and nuchal/dorsal articulating cartilages appear to be common to all decapodaformes, and has likely been lost in the octopods because the nuchal cartilage is present in *Vampyroteuthis*, the sister group to the clade of octopods, leading Vecchione *et al.* (2000) to suggest its presence in the neocoleoid ancestor. *E. scolopes* has also lost the nuchal/dorsal complex, but has gained a dorsal extension of the fin cartilages which replaces the pen. Brachial cartilage is restricted to the Sepiid lineage.

5.4.2 Trends in cephalopod cartilage development

The adult European cuttlefish possesses many distinct cartilaginous structures. Most of these tissues serve as attachment sites for major muscle groups (Tompsett, 1939), and thus are presumed to be functionally very important to the animal. I have shown that these tissues arise early in embryonic development, supporting the notion that they serve a necessary function in hatchlings. This is further supported by comparisons with cartilage distribution at hatching in other species, at least in those with primarily benthic life histories, where cartilages are well developed in hatchlings.

Scleral cartilages

The cartilages of the eye (scleral, equatorial, and horseshoe) form during embryogenesis in all species examined. The presence of eye cartilages, and their early formation, suggests that these are required for proper function of the eye. This is significant to cephalopods, all of which are visual predators throughout their life. Within vertebrates, the scleral elements are thought to provide protection for the eye (Curtis and Miller, 1938; Nakamura and

Yamaguchi, 1991). The cartilaginous sclera of the cuttlefish eye is not sufficiently rigid to keep the shape of the eye when isolated from the animal, and is the site of most ocular muscle attachments (Tompsett, 1939). This suggests that the role of the cuttlefish sclera may be less of protection and more for increased vision, facilitating accommodation and allowing rotation of the eye within the orbit.

Nuchal/Dorsal cartilage complex

In the cuttlefish, the collar and retractor muscles attach to the nuchal cartilage, and this cartilage intercalates with the overlying dorsal cartilage of the mantle (Tompsett, 1939). The nuchal/dorsal cartilage complex provides a means for keeping the dorsal mantle cavity closed during funnel expulsion (Tompsett, 1939), and provides a smooth surface between the mantle and funnel that may facilitate retraction of the head. *Euprymna* and members of the Octopodoformes clade do not have the ability to retract their head, and the epithelium of the dorsal mantle is continuous with the dorsal epithelium of the head, thereby eliminating the need for a cartilaginous nuchal/dorsal complex. Although the cartilage has not yet formed, this complex is morphologically distinguishable as an epithelial layer in *Loligo* hatchlings, indicating its functional importance within lineages that retain this head-retraction ability.

Absence of cartilage within Loligo pealeii *embryos*

The absence embryonic cartilage formation in the pelagic squid *Loligo pealeii* may be indicative of developmental constraints and/or historical contingency. This species hatches at the smallest size of any of the cephalopods investigated. It is possible that a minimal size requirement for cartilage formation exists, below which *L. pealeii* falls. Cartilages are present in small juvenile *I. illecebrosus* (~3 mm ML), but whether or not this species hatches with fully formed cartilages remains to be seen. That the fin and funnel cartilages are so well developed in *E. scolopes* hatchlings, which are only ~1 mm ML larger than *L. pealeii*, calls into question: *how small is too small?* This question will be further explored in the next chapter, wherein data derived from polychaete studies will also be considered.

The early formation of cartilage within *E. scolopes*, and lack thereof within *L. pealeii*, may also be a product of historical contingency. Funnel cartilage formation within *S. officinalis* begins early in embryological development, and by different means than most other cartilages, through cellular condensation and proto-cartilage formation. The heterochronic shift in funnel cartilage formation with reference to other cartilages within this taxon may have evolved in response to selective pressures experienced by hatchlings, suggesting that the funnel cartilage is functionally very important to the juvenile. Because *E. scolopes*, and other Sepiolids, are thought to be the sister group to the Sepiids (see fig. 34a), it is possible that early formation of the funnel cartilage evolved in the common ancestor of these two clades, whereas delayed onset of funnel cartilage formation is characteristic of pelagic species, the Teuthids. This is not to say that Teuthids cannot show embryonic development of funnel cartilages. However, if this were to occur it would likely be found in species that hatch at a large size, such as the oval squid *Sepioteuthis lessoniana* (Shigeno *et al.*, 2001), representing a second, separate evolution of a heterochronic shift in early funnel cartilage formation. Whether or not all Sepiids and Sepiolids undergo early funnel cartilage formation remains to be seen, with the pygmy squid *Idiosepius*, who's adults do not exceed ~15 mm ML (Shigeno and Yamamoto, 2002), being the ideal candidate taxon to test these ideas.

5.4.3 Comparisons with vertebrate cartilage formation

Inductive cues - Mechanical

Amongst vertebrates, primary cartilages require induction from overlying epithelia whereas secondary cartilages form from periostea largely in the absence of epithelial – mesenchymal interactions (Hall, 1983). The role for mechanical stimulation as the inducing factor has been well established in chickens; applying mechanical stimulation in culture leads to cartilage formation (Hall, 1967, 1978) and neuromuscular paralysis blocks secondary cartilage formation but not bone formation (Hall, 1979). A role for mechanical stimulation inducing cephalopod cartilage differentiation is suggested by the fact that many

cuttlefish cartilages do not differentiate until the latter part of embryonic development, stage 28, when all of the major organ systems have formed and the animal shows extensive muscle contraction (personal observation).

Inductive cues - Epithelial

The cephalopod funnel cartilage supports the funnel retractor musculature in the adult, and thus is also subject to extensive mechanical stimulation during embryogenesis. However, in the benthic cephalopods examined here, the funnel cartilage begins to develop prior to the time when this musculature becomes functional, thereby eliminating the possibility of induction by mechanical stimulus for this particular cartilage. In order to maintain cartilage formation in the absence of mechanical stimulus, the inductive signal must be otherwise transmitted. In this case, the overlying epithelial layer is an obvious possibility. It is currently unknown whether or not the epithelium in these structures is sending out an inductive signal regulating funnel cartilage formation in the cuttlefish, an area that merits further investigation.

Cranial cartilage is unique amongst the cuttlefish cartilages in that it does pass through condensation and proto-cartilage phases prior to overt differentiation of the cartilage. If cellular condensations are indicative of induction via methods other than mechanical stimulation of mesenchyme, then the lack of an epithelial layer in the case of the orbital cartilage suggests the inductive influence must come from elsewhere. This cartilage forms from mesenchyme that is bathed in haemolymph within the cephalic sinus of the head (personal observation), suggesting that the inducing factors may be present within the circulatory system. If this were so, then the mesenchyme forming the orbital cartilages must exhibit competency to form cartilage that is not present in other mesenchymal regions that also make contact with the haemolymph. Alternatively the inductive influence may come from the brain itself, which is known to occur within vertebrates (Hall, 1971). Unfortunately distinguishing between these two alternatives may prove exceedingly difficult.

5.4.4 *Sepia officinalis* as a model system for invertebrate cartilage formation

Cuttlefish develop from large yolky eggs, resulting in highly modified discoidal cleavage, gastrulation, and organogenesis (Naef, 1928) compared to other spiralians. These features render cephalopods not particularly well suited to experimental manipulations, making *in vitro* experimental exploration of the mechanisms of cartilage formation in cephalopods challenging.

Examining germ layer origin; cell lineage studies

Cephalopod embryos do not develop well outside of the protective egg case (personal observation), making cell lineage studies nearly impossible. Therefore, the germ layer origin of cartilage within cephalopods remains undetermined at the present time. However, cuttlefish embryos may be amenable to studies on the mechanism of cartilage induction.

In vivo *experiments*

I have found that *S. officinalis* embryos can be manipulated to a limited extent within the egg sac by removing the outer chorionic layers, leaving only the innermost layer intact (see fig. 26c). This layer has elastic properties, enabling the embryo to be manipulated while still inside the egg sac. As long as this layer remains intact, the manipulated embryos will continue to survive and develop for some time, possibly even to hatching – although embryos in such manipulated egg sacs are prone to early hatching and loss of yolk sacs (personal observation), reducing juvenile survival rates (Naef, 1928). Thus there is potential in this system to examine the role of mechanical stimulation in funnel cartilage formation by severing the connection to the retractor muscles through the chorion.

In vitro *experiments*

Within vertebrates, much has been learnt about cartilage induction from tissue and organ culture studies. Growing excised tissues in cultures can yield information regarding autotomy of morphology – whether the cartilage retain their 'normal' shape when removed from influences of the rest of the embryo; the

effects of different chemical cues on cartilage differentiation of cultured mesenchyme can be determined; the role of epithelial-mesenchymal interactions can be elucidated by removing the epithelium, transplanting and co-culturing mesenchyme and epithelia. The benefits and limitations of these types of experimental embryological techniques for exploring vertebrate skeletal development may be found in Hall (1983).

There has been some success using cephalopod tissues for organ, tissue, and cell cultures, especially with reference to ganglion cells (Marthy, 1975, 1982, 1985; Marthy and Aroles, 1987). The funnel cartilage in the cuttlefish forms in association with an epithelium, develops early in embryonic development, and is easily accessible in embryos of most stages, thus offering excellent opportunities for studying the role of the epithelium in cartilage formation in culture, definitely warranting further exploration. Culture studies could also prove fruitful in defining the role of mechanical stimulation, wherein cultured mesenchymal cells could be subjected to externally applied mechanical stimulation, testing whether or not cartilage differentiation can be induced.

5.5 Conclusions

The presence of cartilage in many invertebrate groups suggests that cartilage as a tissue pre-dates the origin of vertebrates. Knowledge of the developmental mechanisms of cartilage formation amongst invertebrates is the first step in elucidating further commonalities between cephalopod and vertebrate cartilages. Here I offer the first detailed description of the onset and mechanism of cartilage differentiation in an invertebrate, identifying important trends in how cephalopod cartilage differentiates which may offer insights into the evolution of development in cartilage as a tissue type. If independently derived, the remarkable similarity of the funnel cartilage differentiation described here with vertebrate primary cartilage differentiation would signify convergent evolution of these tissues, and so similarities in developmental mechanisms highlight developmental constraints that organisms face in building a highly organized cartilaginous tissue. My data indicates that formation of cartilage through the process of cellular condensations

may be indicative of selection pressure to form cartilage early in development, before mechanical induction becomes an option within the embryos. As such, cartilage formation by means of a condensation could be considered to be an embryonic adaptation for cartilage formation, as per Romer, (1942), although not in the evolutionary sense originally implied.

Confirmation of this idea requires comparative data from other sources. I now turn to the development and regeneration of cartilage in another major invertebrate lineage, the polychaete annelids.

Chapter 6: Development and Regeneration of Sabellid Polychaete Cartilage

6.1 Introduction

Similar to studies of development, regeneration studies can yield valuable information regarding cellular plasticity and tissue differentiation. Many invertebrates possess remarkable regenerative abilities, which have been studied extensively within flatworms (planaria) leading to major advances in understanding axial patterning (i.e. Bayascas *et al.*, 1998).

Despite the fact that all cartilage-bearing invertebrates are known to possess some degree of regenerative capacity, the ability to regenerate cartilage has rarely been the focus of study. Exceptions include gastropod molluscs and polychaete annelids. Radular cartilages regenerate following proboscis amputation in *Urosalpinx* and *Eupleura*, with histologically differentiated cartilage, derived from mesenchyme which also gives rise to muscle cells, distinguishable 8 days post-amputation (Carriker *et al.*, 1972). In some sabellid polychaetes the branchial crown, including its cartilaginous internal support tissue, grows back in 11 – 14 days (*Sabella melanostigma*: Douglas-Hill, 1969; *Sabellastarte magnifica*: Person 1983; *Potamilla sp.*: personal observation), suggesting that these animals may also provide a good system for studying the regenerative capacities of cartilaginous tissues.

6.1.1 Sabellid polychaetes

Members of the Sabellidae are often referred to as feather-duster worms owing to the structure of their feeding apparatus (fig. 35a,b). They represent one of the most diverse polychaete assemblages, even including freshwater representatives (Rouse and Pleijel, 2001). The mouth is surrounded by a branchial crown of ciliated tentacles that when extended into the water column filters water by creating current flow towards the centre of the crown. The branchial crown has two main components: the radioles derived from the base of the crown, and pinnules that branch off the main axis of the radioles in a feather-like pattern (fig. 35a,b).

The cartilage within the branchial crown of sabellid polychaetes originates at the base of the crown, and extends distally through the radioles and into the pinnules (Fitzhugh, 1989). The branchial cartilage is comprised of two distinct histological regions: a cellular core of vacuolated chondrocytes and an acellular fibrous sheath surrounding the chondrocytes (Person and Mathews, 1967; Cowden and Fitzharris, 1975; Chapter 2). Whole mount Alcian Blue staining reveals the matrix associated with the cartilage in the radioles (fig. 35a), while decomposition of soft tissues in a magnesium chloride solution exposes the skeletal rods in fresh specimens (fig. 35b).

Within many species of sabellid polychaetes, the branchial crown is readily autotomized (separated from the rest of the body along a transverse groove located at the base of the tentacles) and re-grown throughout the life history of the animals, however no studies have investigated the organization and differentiation of the lost appendages. In contrast, the regeneration of anterior regions from fully bisected animals, including the skeletal components, has been studied in the sabellid polychaetes *Sabella pavonina* (Berrill, 1931; Berrill and Mees, 1936) and *Sabella melanostigma* (Douglas-Hill, 1969). During regeneration, sabellid polychaetes regenerate only three anterior segments: the anterior-most head segments including the branchial crown, the collar segment, and an initial thoracic segment. Subsequent thoracic segments are regenerated by morphollaxis (transdifferentiation) of abdominal segments adjacent to the newly formed anterior region, suggesting that the newly formed head acts as an organizer, re-patterning the anterior abdominal segments into thoracic ones (Berrill, 1931).

6.1.2 Current study

Here, I investigate the comparative histology of branchial tentacles in three sabellid genera, *Potamilla*, *Fabricia* and *Myxicola*, as well as in *Hydroides*, a member of the Serpulidae, which are thought to form the sister-group to the Sabellidae (Fitzhugh, 1989). My results indicate that cartilage is not found in either *Hydroides* or in *Fabricia*, and that the histology of *Myxicola* cartilage differs

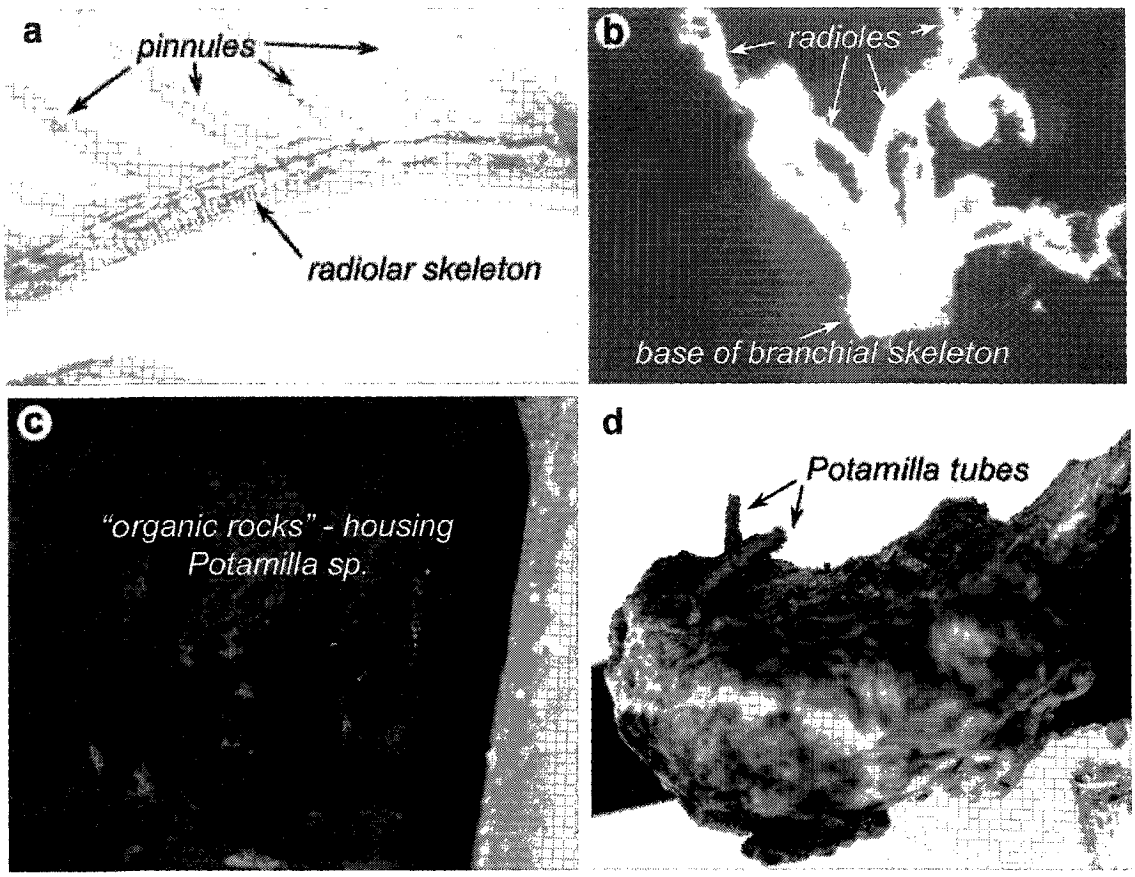

Figure 35: Sabellid polychaete (*Potamilla sp.*) examined in this study
Sabellid polychaetes have an internal skeleton supporting their branchial crown of feeding tentacles, composed of a series of pinnules coming off the main axis of the radioles. **a** The skeletal matrix can be stained with Alcian Blue. Note the compact row of skeletal cells within the radiole (*radiolar skeleton*). **b** The branchial skeleton can be isolated from the rest of the animal by prolonged exposure to magnesium chloride solution, showing the thicker skeleton at the base of the tentacles from which the radioles originate. **c,d** The sabellid polychaete *Potamilla sp.* lives embedded in organic rocks composed primarily of encrusting bryozoans, wherein they build soft tubes that extent into the water column (**d**).

from *Potamilla sp.* in its relative amount of cellular and acellular components.

Furthermore, in this chapter I describe the development of the cartilage-bearing polychaete *Potamilla sp.*, including a detailed chronology of metamorphosis and cartilage formation. Chondrocytes are the first mesenchymal cells to differentiate within the developing tentacles. Data collected regarding branchial crown development and cartilage differentiation are compared with cartilage differentiation during regeneration following autotomization of the branchial crown, testing the null hypothesis that regeneration of the branchial tentacles will follow the same pattern exhibited during development. The sequence of regenerating branchial radioles indeed mirrors their development.

Regeneration was examined in adults and newly metamorphosed juveniles in order to determine at what point after metamorphosis animals are able to regenerate lost body parts. Within adults, the circulatory system invades the developing crown prior to differentiation of cartilage cells from the mesenchyme. However, the circulatory system within the branchial tentacles of juveniles is not yet well developed, and chondrocytes are the first identifiable mesenchymal cell type.

6.2 Methods

6.2.1 Animals

Specimens of *Potamilla sp.* were examined from two populations, Pacific and Atlantic. These specimens were not identified to species level and may comprise two different species. They are therefore treated here separately as Pacific and Atlantic samples. *Potamilla sp.* (Pacific) specimens were collected from the dock pilings at Friday Harbor Laboratories, WA. Specimens of *Myxicola infundibulum* and *Fabricia sabella* were collected from the Bay of Fundy. *Potamilla sp.*, NS (Atlantic) and *Hydroides elegans* were purchased from the Marine Biological Station in Woods Hole, MA.

Potamilla sp. (Atlantic) and *Hydroides elegans* live alongside numerous other polychaete species embedded in extensive bryozoan colonies (fig. 35c,d), and require extensive excavation from this organic material. Polychaetes were

isolated from these "organic rocks" by first hitting the substrate with a hammer, thereby creating fissures along the embedded worm tubes. Sabellid polychaetes were then dissected free with blunt forceps under a stereomicroscope. Adult *Potamilla sp.* (Atlantic) ranging in size from 0.7 cm to 5.6 cm were collected in a similar manner. Once the animals and their tubes had been removed from the organic substrate, adults were held in ice cube trays and cultured in aerated seawater at room temperature. Filtered, autoclaved seawater was replaced daily to maintain salinity and water levels, and animals were fed a diet of cultured algae.

To collect data regarding cartilage differentiation within sabellid polychaetes, regeneration experiments (described below) were attempted in *Myxicola infundibulum*. No regeneration of the excised crown was observed over a period of 2 months, and animals showed extremely high mortality rates. In contrast, *Potamilla sp.* (Atlantic) will regenerate its branchial crown and its corresponding cartilage, and is gravid during the late summer season. Therefore this species was chosen to examine cartilage differentiation during development and regeneration.

Procuring gametes

Potamilla sp. (Atlantic) is dioecious, and eggs were found to be present in adults as small as 1.8 cm body length during the late summer – early autumn (Aug – Oct). Development and metamorphosis of this species has not been described, and so the chronology of developmental events including cartilage differentiation was investigated. Males and females can be easily distinguished by the colouration of the body wall: males appear yellow-orange whereas females are red-brown. Eggs obtained through dissection were found not to be viable, and so spawning of oocytes must be induced in females. Some animals will spawn eggs after being isolated from the substrate and placed in finger bowls of room temperature seawater. Only ~20% of animals spawn with this technique and no other method proved to be more successful to induce spawning. Viable sperm was obtained easily by puncturing the body wall.

6.2.2 Regeneration studies

To study the regeneration of the tentacle skeletal material, animals were induced to autotomize their feeding tentacles. Removal of tentacles in *Potamilla sp.* (Atlantic) was accomplished by holding the base of the tentacles with fine forceps for 5-10 seconds, while applying gentle tension on the worm with a second pair of forceps. The worms autotomize their tentacles in one piece with minimal additional tissue damage, reducing the risk of bacterial infection. Operated animals were then returned to their holding trays and treated with antibiotics to prevent bacterial infections [3 cc penicillin-streptomycin (SIGMA No. P3539) per litre of autoclaved seawater]. Experimental animals succumbed to bacterial infections in >80% of surgeries without antibiotics, but show complete recovery with antibiotic treatment.

Regeneration progress was monitored and photographed daily. Collections of animals at different stages were fixed for 24-48 hours in DENT's fixative [1 part dimethyl sulfoxide (DMSO) in 4 parts 100% methanol; Klymkowsky and Hanken, 1991], neutral buffered formalin or 4% paraformaldehyde.

6.2.3 BrdU incorporation

5-Bromodeoxyuridine (BrdU) incorporates into the DNA of dividing cells during S-phase in place of thymidine, and can be detected immunologically allowing visualization of cell division (Gratzner, 1982). To address when new cells of the regenerating cartilage are born, regenerating *Potamilla sp.* were incubated for 2 hours in 1 mg/ml BrdU dissolved in 4% EtOH in filtered seawater. Control worms were similarly treated with 4% EtOH without BrdU for 2 hours, resulting in 100% survival and regeneration in both treatments.

Sections from BrdU incorporated worms were stained for BrdU incorporation according to manufacturers instructions using a BrdU *in-situ* detection kit (BD Biosciences No. 550803), followed by counter-staining with Masson's trichrome. Unfortunately the BrdU incorporation experiments did not yield any useful information. BrdU immunoreactivity was present throughout the cytoplasm of

most cells in all stages examined, and so no data regarding the birth of target cells could be discerned.

6.2.4 Histology

Histology of the branchial crown was examined in representatives of the two major clades of Sabellid polychaetes, the Sabellinae (2 populations of *Potamilla sp.* and *Myxicola infundibulum*) and Fabriciinae (*Fabricia sabella*). The structure of the sabellid branchial crown was compared with representatives from their sister group, the Serpulidae (2 populations of *Hydroides elegans*). Fixed material was dehydrated, embedded into low melting point paraffin wax, sectioned at 5-7 µm, and mounted on Haupt's coated slides. Sections were stained with one of the following histological protocols: HBQ, Masson's trichrome, or my cartilage and connective tissue stain (see Chapter 2).

6.3 Results

6.3.1 Comparative branchial crown histology

Potamilla

Adult *Potamilla sp.* (Pacific) branchial cartilages have two histologically distinct regions: a central core of cells and a peripheral acellular region between the chondrocytes and the overlying epithelium (fig. 36a,b). The staining properties of these two regions in the Pacific samples are discussed in Chapter 2, and so will not be re-visited here.

The acellular matrix component of *Potamilla sp.* (Atlantic) is thinner than that of the Pacific sample. Otherwise the two *Potamilla sp.* samples are similar histologically. The number of radioles comprising the tentacles of *Potamilla sp.* (Atlantic) vary with size, and thus age, of the animal. The smallest animals investigated (0.7 cm body length, 0.13 cm collar width) have as few as 5 radioles, while larger animals (5.6 cm body length, 0.33 cm collar width) possess as many as 19 radioles. A thick piece of cartilage joins the two bilateral halves of the branchial crown across the mid-line (fig. 36d). Cartilages supporting the radioles

Figure 36: Branchial skeleton histology of sabellid and serpulid polychaetes
Within polychaetes, cartilaginous branchial skeletons are restricted to sabellids. Scale bars = 100 µm; *cc* = cellular cartilage; *cct* = chondroid connective tissue. **a,b** *Potamilla sp.* (Pacific): **a** Cartilage of the radioles are connected by acellular matrix (*white arrows*). **b** The cartilage within the distal part of the radioles is many cells wide. **c** The base of the tentacles in *Fabricia sabella* are supported by a thick acellular extracellular matrix (*green*), which is continuous with the basement membrane of the overlying epithelium. No chondrocytes are embedded within this tissue. **d,e** *Potamilla sp.* (Atlantic): **d** The two halves of the branchial crown are connected by a cellular cartilage (*cc*), which has only a thin acellular sheath (*black arrow*). **e** Within the pinnules, the cartilage core is 4 cells thick. **f** *Hydroides elegans*: Tentacles of the serpulid polychaete are supported by a fibrous outer cuticle (*black arrows*), with no internal cartilaginous support. **g,h** *Myxicola infundibulum*: **g** Cartilage at the base of the slime worm is composed of many tightly packed chondrocytes, surrounded by a thick acelluar matrix (*black arrows*). High tensile fibres (*red*) support regions between the pinnules. **h** Within the pinnules the cartilage is 4-5 cells wide. **i** *Hydroides elegans:* The operculum is supported by extensive chondroid connective tissue (*cct*), also showing an outer fibrous sheath.

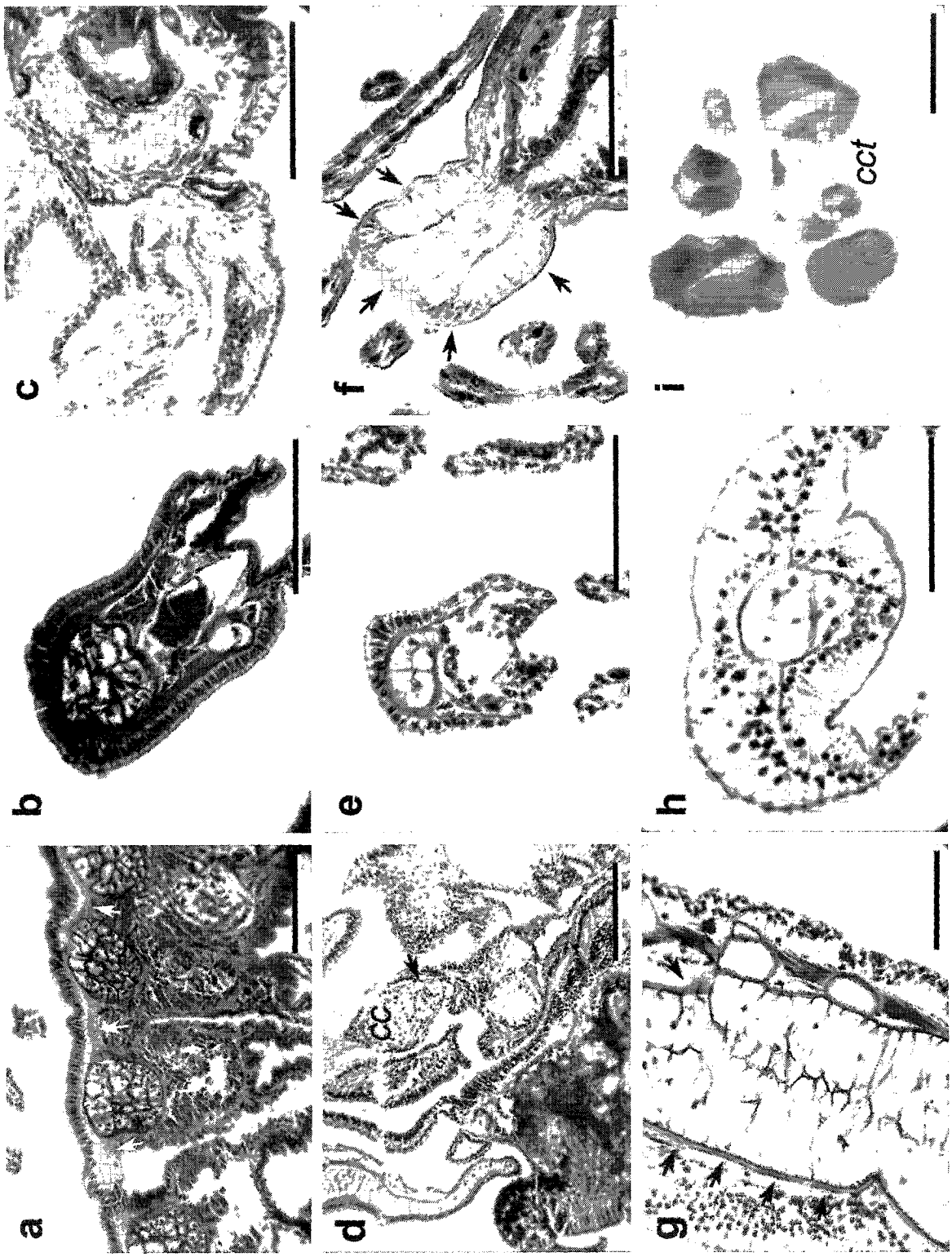

Figure 36

in mid-size animals (0.2 cm collar width) are 4-5 cells wide (fig. 36e), whereas at the tips of the pinnules the skeleton is only a single cell wide.

Fabricia

Fabricia sabella adults are amongst the smallest of the sabellid polychaetes measuring only ~0.2 cm body length. Within the branchial crown of the adult a thin acellular fibrous layer lies between the epithelium and the vasculature of the tentacles. The fibrous layer is thicker at the base of the crown, however no chondrocytes are present (fig. 36c).

Myxicola

Compared to *Fabricia*, at 6 cm body length *Myxicola infundibulum* is a giant amongst Sabellids. The acellular outer fibrous component of *Myxicola* cartilage is thinner than in *Potamilla sp.*, and is continuous with the basement membrane of the overlying epithelium. In *Myxicola* the connection with the radioles at the base of the pinnules is reinforced by high tensile fibres as indicated by Masson's trichrome stain (Flint *et al.*, 1975; fig. 36g).

Hydroides

The generic name "fan-worm" refers to members of the Serpulidae, worms whose general body plan is very similar to that of the Sabellidae. Although serpulid polychaetes also possess a branchial crown of feeding tentacles, there is no internal skeletal support. *Hydroides* branchial tentacles are supported by a thick acellular cuticular layer, located outside an epithelium whose cells are larger than those comprising the epithelium of sabellids examined here (fig. 36f). *Hydroides* also have an operculum that is supported internally by extensive chondroid connective tissue (fig. 36i).

6.3.2 Development of *Potamilla*

Embryology

Fertilization results in the formation of a fertilization membrane (fig. 37a). Development is rapid at 18°C, and larval morphogenesis fails at higher

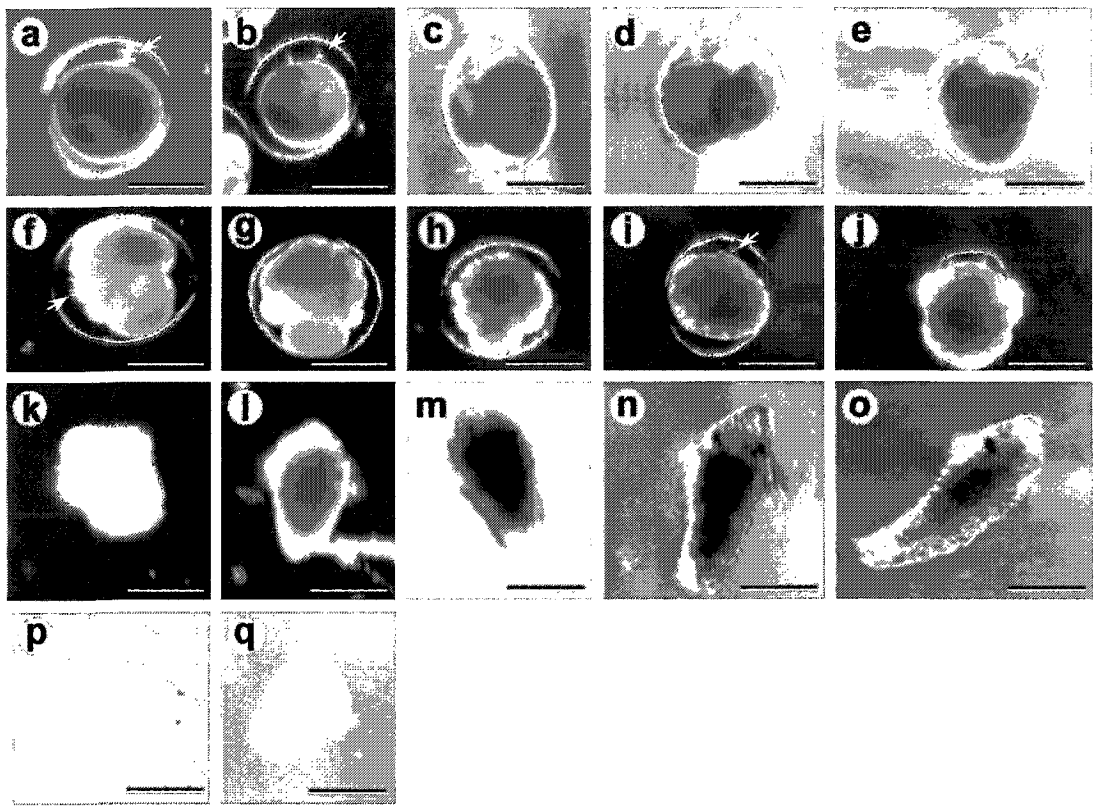

Figure 37: Embryogenesis of *Potamilla* (Atlantic)
Embryogenesis in *Potamilla* (Atlantic) is rapid, resulting in free-swimming trochophore larvae. Scale bars = 100 µm. **a** Fertilized egg showing elevated fertilization membrane and polar lobes (*white arrows*). **b** Onset of first unequal cleavage perpendicular to the polar bodies (top). **c** 2 cell stage; **d** Four cell stage; **e** 8 cell stage; **f** 16 cell stage; **g** 32 cell stage; **h** 32-64 cell stage; **i** Gastrulation; **j** Hatching of trochophore larva; **k** 4 hour trochophore; **l** 10 hour trochophore, showing onset of eyespot pigmentation; **m** 36 hour trochophore larva; **n,o** 120 hour trochophore, competent to metamorphose. **p,q** 10 hour trochophore larvae raised at 22°C showing abnormal morphogenesis, including extreme swelling of the body wall.

temperatures. The fertilized egg is large (150 µm) and yolk-rich, and thus opaque, with a small amount of orange pigmentation. The first cleavage occurs at 1-1.5 hr post-fertilization, with subsequent cleavages following at 30 minute intervals (table 7). The first cell division is unequal, likely due to spindle displacement because no polar lobe forms, and gives rise to a macromere (CD) and a mesomere (AB) (fig. 37b,c). The second cleavage is equal in the AB cell, and unequal in the CD cell, giving rise to three mesomeres (A, B, and C) and a macromere (D) (fig. 37d). Pigmentation is largely restricted to the macromere and one of the mesomeres. The third and subsequent cleavages are asymmetrical in all blastomeres giving rise to pigmented micromeres at the animal pole, mesomeres, and a single large macromere situated ventrally (fig. 37e-h). During gastrulation (fig. 37i) the macromere undergoes an equal cell division prior to being internalized.

After gastrulation the prototrochal cells become ciliated, and the trochophore larva hatches from the fertilization membrane at around 15 hours post-fertilization (fig. 37j,k). After hatching the head and anal vesicles differentiate, eye spot pigmentation appears at ~24h (fig. 37l), and the larva elongates with the formation of three protosegments by day 3 (metatrochophore larva) (fig. 37m-o). Metatrochophore larvae swim for at least 2 more days, but are able to remain at this stage for up to two weeks. Elevated temperatures (>19°C) lead to abnormal metatrochophore development and failure to metamorphose (fig. 37p,q).

Metamorphosis

The earliest metatrochophore settlement and metamorphosis was observed at 5 days post-fertilization, with many larvae settling between 5-7 days (table 8). In response to a thin bacterial layer on the bottom of the dish, competent larvae settle to the bottom and form a mucus tube. At this point the larva become dorso-ventrally flattened, and the anal and head vesicles disappear (Metamorphosis 1: fig. 38a). Branchial buds appear in the posterior part of the prostomium, between the eyespots and the prototroch (Metamorphosis 2: fig. 38b). A constriction appears anterior to the developing branchial buds, forming a "snout" at the

Table 7: Timetable of development at 18°C for *Potamilla sp.*
Adult female worms of the genus *Potamilla* were induced to spawn by elevated temperatures. Newly spawned oocytes were fertilized with sperm obtained by puncturing the body wall of adult male worms. Development was observed with a stereomicroscope, and major features of embryogenesis were recorded.

Time post-fertilization (hr)	Stage	Features
0	Fertilization	▪ Elevation of fertilization membrane
1	2	▪ Unequal cleavage
1.5	4	▪ Equal and unequal cleavage
2	8	▪ Spiral cleavage pattern
2.5	16	"
4.5	32	"
5	64	"
8-9	Gastrulation begins	▪ Epiboly of micromeres and mesomeres ▪ Macromere internalization
15	Hatching	
15-24	Trochophore I	▪ Head and anal vesicle formation
25	Trochophore II	▪ Eyespot pigmentation
48	Metatrochophore	▪ Segmental differentiation
120 (5d)	Competency	▪ First metamorphosis seen

Table 8: Metamorphosis and cartilage formation of *Potamilla sp.*
Embryos reared from artificial fertilization were kept in culture through metamorphosis and monitored daily. Metamorphosis was followed with a stereomicroscope, and major morphogenetic changes were recorded.

Time post-settlement (hrs)	Stage	Features
0	Metamorphosis 1	▪ Mucus tube created ▪ Dorso-ventral flattening
6-12	Metamorphosis 2	▪ Protrusion of tentacle buds ▪ Construction of prostomium "snout" ▪ Elaboration of tube
12-18	Metamorphosis 3	▪ Differentiation of pygidium ▪ Prostomium "snout" almost completely absorbed ▪ Branching of tentacle buds
18-24	Metamorphosis 4	▪ Prostomium "snout" gone ▪ Tentacles branched with three main radioles
24-36	Metamorphosis 5	▪ Cartilage differentiation within main axes of tentacles ▪ Appearance of fourth radiole ▪ Pinnule branching of dorsal radiole begins ▪ (termination of differentiation in non-settled individuals)
36-48	Juvenile	▪ Growth of tentacles ▪ Further growth and differentiation of body segments
14-21 days	Second size class Juvenile	▪ Doubling of body segments

Figure 38: Metamorphosis and branchial cartilage formation of *Potamilla sp.* *Potamilla sp.* larvae are relatively short lived, quickly settling onto a hard substrate and metamorphosing into a juvenile worm. Scale bars = 100 µm. **a** Metamorphosis 1: upon settlement, the trochophore larva settles onto the substrate and secretes a mucous tube (*white arrowheads*). **b** Metamorphosis 2: the branchial buds of the developing tentacles begin to protrude from the posterior prostomium, and the anterior prostomium begins to constrict at the base, forming the "*snout*". **c,d** Metamorphosis 3: the tentacles continue to elongate and begin to branch into three main axes, while the "*snout*" is absorbed. **e** Metamorphosis 4: the "*snout*" is completely absorbed, and differentiation begins within the main axis of the tentacles. **f** Metamorphosis 5: the branchial skeleton (*bc*) can be observed within the tentacles by the time the larvae begins to feed. **g,h** Fully metamorphosed juvenile within its tube (**g**), and protruding its branchial crown for feeding, in which the branchial cartilage can be imaged (*bc*) (**h**). **i** 2 week-old juvenile worm, illustrating the size increase compared to newly settled juveniles (**g,h**). **j** Histological section of a metamorphosing larva as in (**f**), showing the differentiating cartilage (*bc*) within the base of the tentacles. **k** The cartilage (*bc*) within the tentacles of fully metamorphosed juveniles, as in (**h**), is only a single cell wide.

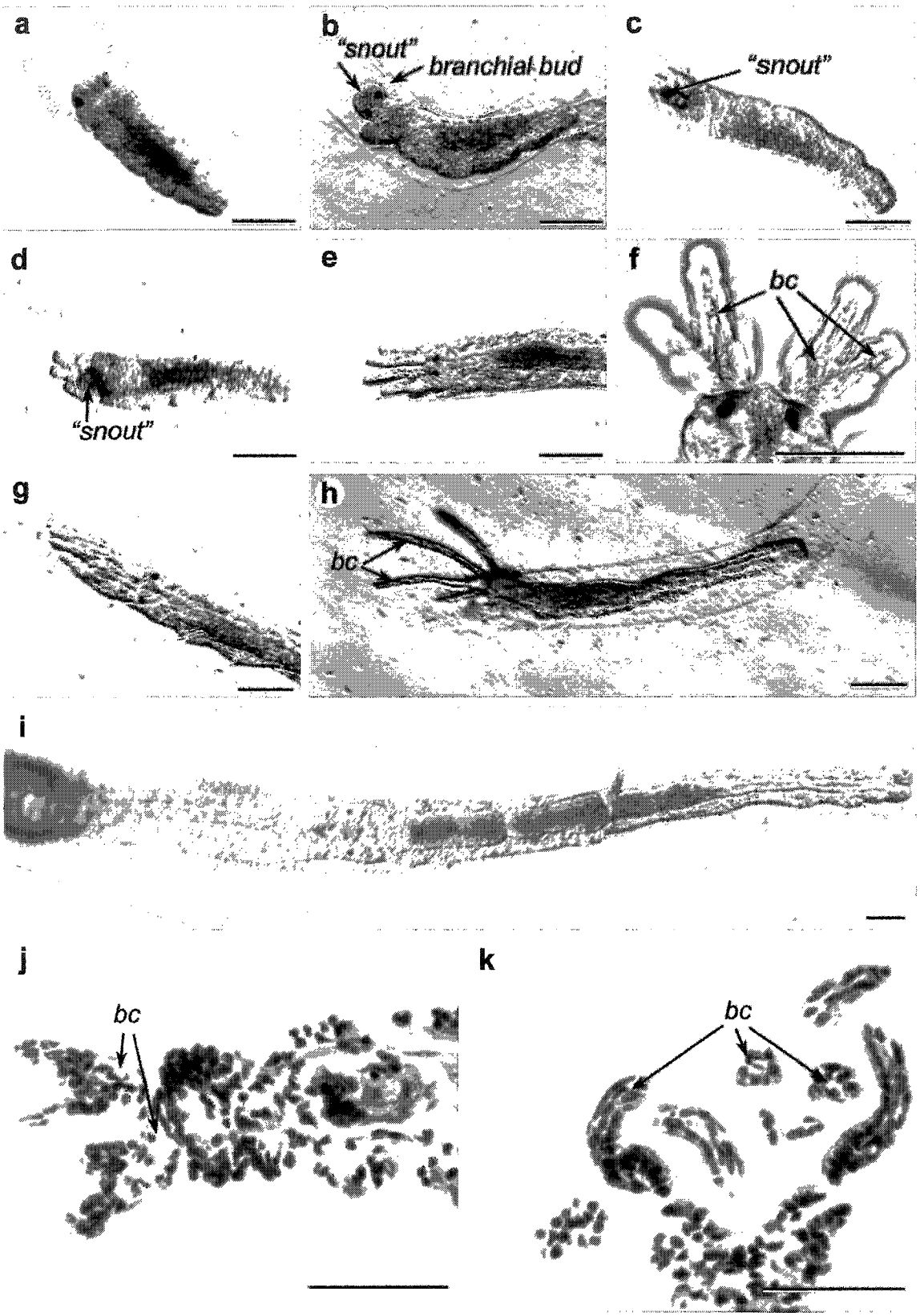

Figure 38

anterior-most end of the larval prostomium. The "snout" is filled with opaque, pigmented, yolky cytoplasm. As metamorphosis proceeds the "snout" is absorbed (Metamorphosis 3 & 4: fig. 38c-e).

Branchial bud growth is rapid following settlement, with a functional branchial crown present 2 days post-settlement. The first radioles of the developing crown appear dorsally, with subsequent radioles added in sequence along the dorso-ventral axis. After establishment of four main radioles the lateral buds of the pinnules begin to form (Metamorphosis 5: fig. 38f).

Larvae that remain in the water column for 14 days do not form a "snout" during metamorphosis, suggesting that this may be a site of yolk storage. Metatrochophore larvae that do not settle and build a mucous tube within two weeks undergo metamorphosis while still swimming in the water column. Upon losing their trochophore, these individuals can be seen crawling along the surface of the dish. Animals that do not build a tube die by 25 days post-fertilization.

Juveniles grow rapidly and will feed on algae added to the cultures, but also on bacteria present within the seawater. Around two weeks post-metamorphosis juvenile worms double in size and segment number overnight, forming a second size class of juveniles (fig. 38i).

Cartilage formation

Cartilage differentiates between the epithelial layers as outgrowth of the branchial buds proceeds. Differentiation begins proximally at the crown base, and proceeds distally as the cartilage grows. Just prior to pinnule bud formation, cartilage cells can be distinguished histologically at the base of the crown (Metamorphosis 5: fig. 38j,k), however at this time the acellular sheath that surrounds the cartilage in adults is not present.

Figure 39: Regeneration of newly metamorphosed *Potamilla sp.*
Recently settled juvenile *Potamilla* are able to completely regenerate anterior head regions following amputation. Scale bars = 100 µm; *white arrows* = region of regenerating branchial crown. **a** 0 days post-amputation; The wound in the anterior amputated region has not yet closed. **b** 1 day; The epithelium has closed over the amputation site. **c** 3 days; Branchial tentacle buds have formed within the anterior blastema, and begin to show outgrowth and branching. **d** 4 days; The branchial buds show three main radiole branches, which are beginning to elongate. **e** 5 days; Two additional radioles have been added to the branchial tentacles. **f** 7 days; The branchial tentacles have completely re-grown and the animal has re-commenced feeding. Note also the reappearance of the pigmented eyespots. **g-i** Second size-class juveniles will autotomize their feeding tentacles. **g** Immediately following autotomization. **h** 5 days; Branchial bud elongation is apparent, and pinnule buds have begun to form. **i** 21 days; The entire branchial crown has re-grown.

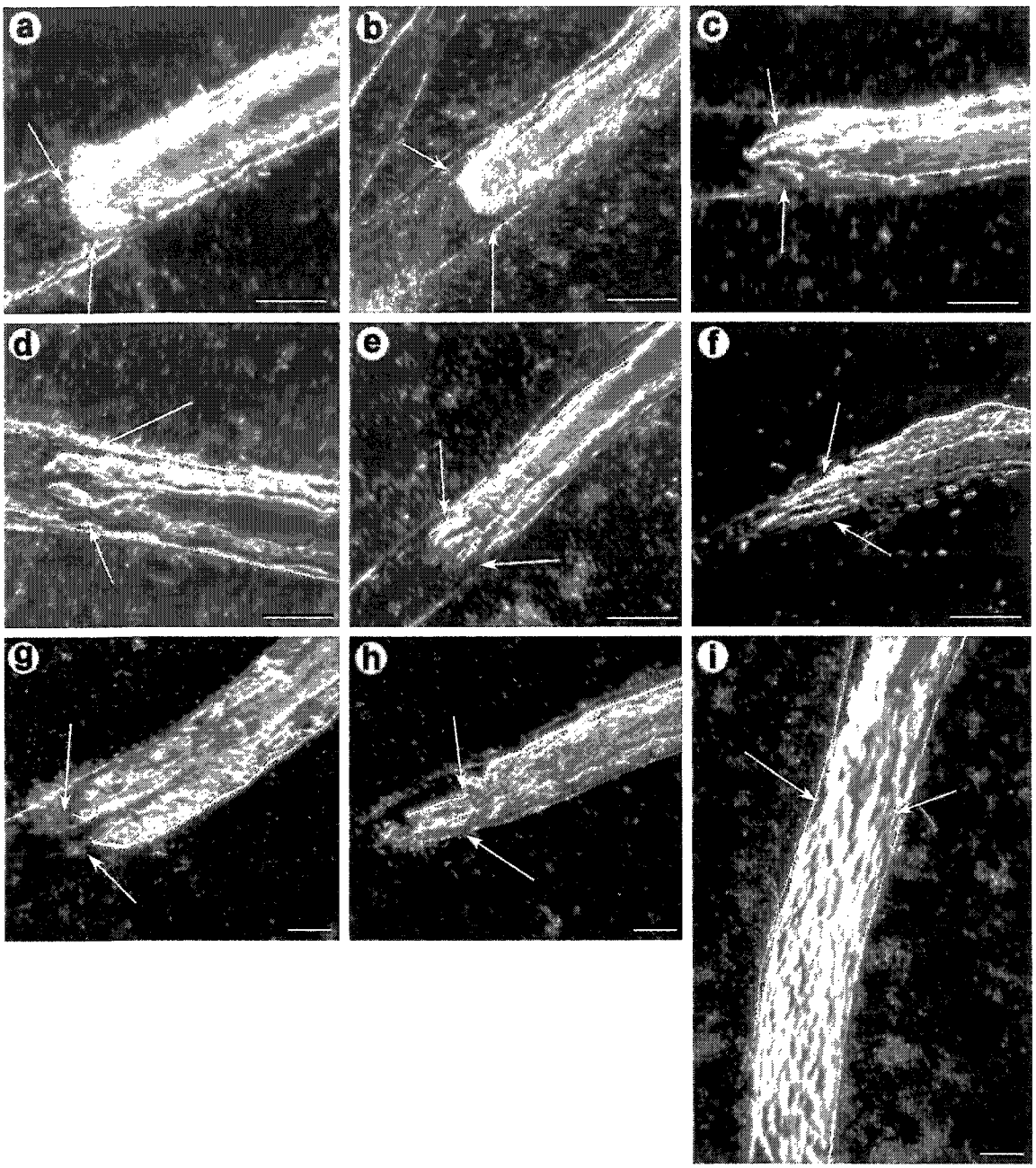

Figure 39

6.3.3 *Potamilla* tentacle regeneration

Juveniles

The regenerative abilities of adults, described below are present in newly metamorphosed juveniles. When severed at the thoracic segment, these juveniles will re-grow their heads within 10 days (fig. 39), similar to the time it takes severed adults to regenerate. Also similar to adult worms, juveniles within the second size class will autotomize their branchial crown when disturbed and re-grow a new set in as few as 5 days.

Adults

The branchial crown grows back rapidly after autotomization, and the animals show signs of feeding after only 8-9 days (table 9). Following autotomization of the crown, the branchial hearts and vessel feeding the branchial crown are visible (fig. 40a). A thickened ridge of tissue forms around the branchial vessel after the first 24 hours (day 1), and this ridge of tissue increases in size for the following 48 hours (day 2 and 3) (fig. 40b-d). The ridge of regenerating tissue initially forms three radiolar outgrowths (day 4), with subsequent radioles added ventrally (fig. 40e). The blood vessel extends within each of these branches as they elongate (day 5), allowing them to be extended and relaxed via hydrostatic pressure (fig. 40f-l). Pinnule bud formation begins after significant elongation of the radioles, between day 7 and 10 post-amputation (fig. 40m-o).

6.3.4 Cartilage differentiation during regeneration

Histological analysis shows that intact animals have a fibrous layer separating the branchial crown from the underlying tissues, including the brain, or ganglia (fig. 41a,b). The fibrous layer is continuous with the basement membrane of the overlying epithelium, and extends under the branchial cartilages that overlie the body wall musculature and ganglia. Between the cartilage and this fibrous layer are mesenchymal cells.

Table 9: Regeneration of branchial crown from adult *Potamilla sp.*
Animals were induced to autotomize their branchial crown and subsequent regeneration of branchial crown was monitored daily using a stereomicroscope.

Day post-autotomization	Progress of regeneration
0	Removal of tentacles
1	Epithelium completely healed over wound site
2	Small ridge of tissue forms laterally to branchial vessel
3	Branching pattern visible within branchial ridge, three small radiolar buds
4	Growth of radioles
5	More growth, addition of a fourth bud
6	More growth, addition of a fifth bud
7	More growth, addition of a sixth bud
8	Animal seen filtering algae: onset of feeding
9	Continued elongation of radioles
10	First appearance of lateral pinnule buds
11	Growth of lateral buds
12	First sign of pigment
13	Pigment has darkened significantly
14	Regeneration completed

Figure 40: Regeneration of feeding tentacles of adult *Potamilla sp.*
Adult *Potamilla* will re-grow fully functional branchial crowns in two weeks following autotomization. Adult worms were induced to autotomized their branchial crown, and the progress of regeneration was documented daily. Scale bar = 1 mm; *arrowheads* = regenerating branchial crown. Anterior view is shown on top, and ventral view is shown below. **a** 6 hrs following autotomization; pools of blood are visible within the branchial hearts at the base of the missing tentacles. **b** One day following autotomization: the wound has healed, but otherwise there are no visible changes. **c** Two days: a thickened ridge of tissue is visible in the region of the regenerating tissue. **d** Three days: the thickened ridge of tissue is further elevated, and first signs of branching of this tissue is evident. **e** Four days; significant growth of the first three regenerating radioles can be seen. **f-h** More growth, and addition of radioles ventrally: **f** Five days; **g** Six days;. **h** Seven days; **i-l** Continued elongation of radioles, vascularization can be identified within the developing radioles: **i** Eight days; **j** Nine days; **k** Ten days; **l** Eleven days; **m** Twelve days: pinnule buds appear equidistantly spaced along the radioles. **n** Thirteen days: continued elongation of radioles, and growth of pinnules can be seen. The tentacles are functional at this point, and the animal has re-commenced feeding. **o** Thirteen days: one individual succumbed to unilateral bacterial infection, however the contra-lateral tentacles regenerated in a similar time-frame as conspecifics.

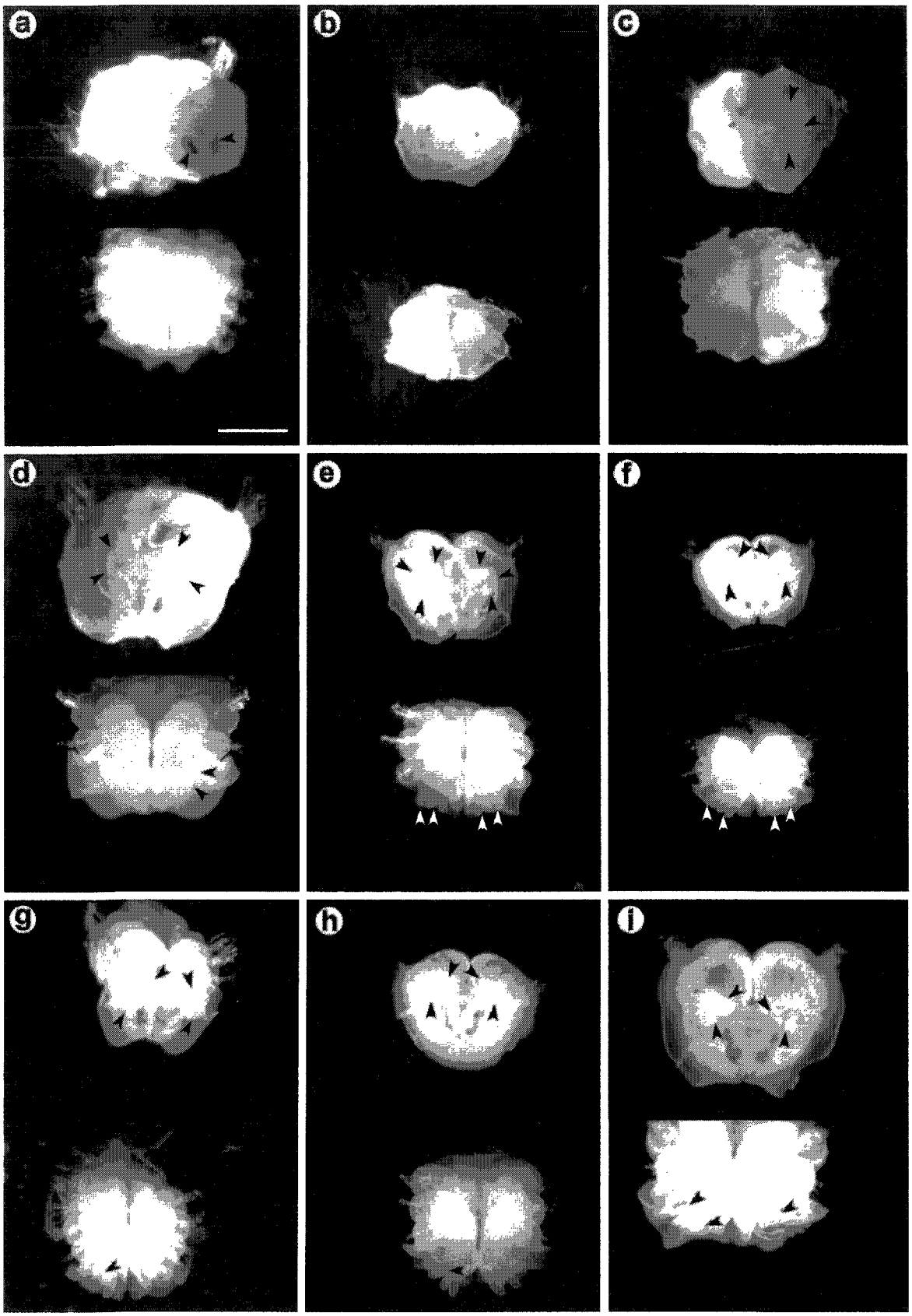

Figure 40

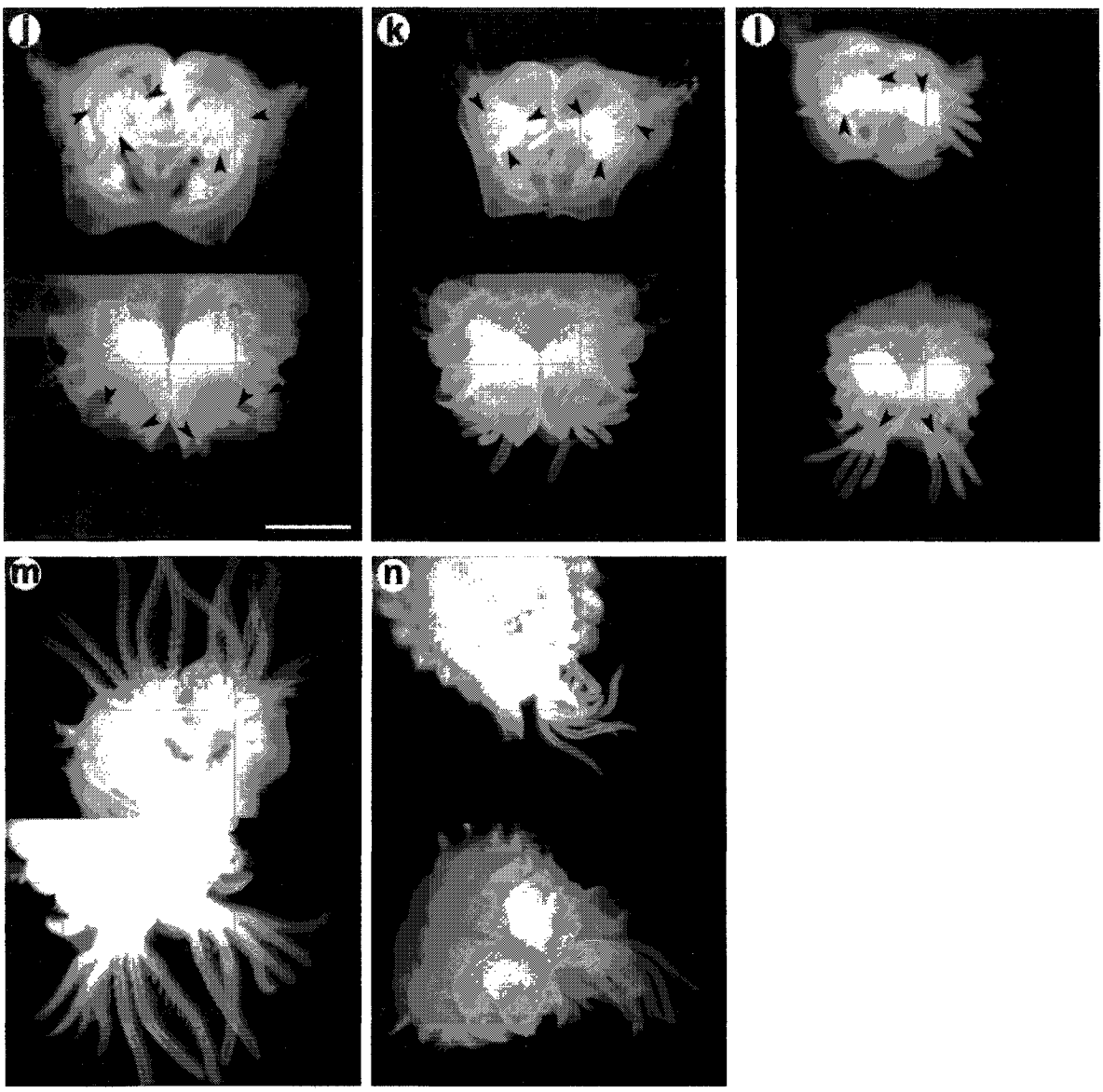

Figure 40: Continued

Figure 41: Chondrocyte differentiation during regeneration of adult *Potamilla sp.* Histological analysis of regenerating branchial tentacles in adult *Potamilla* reveals that chondrocyte differentiation is preceded by vascularization of tentacles. Chondrocytes first appear from mesenchyme within the radioles that is adjacent to vascular vessels. Animals were induced to autotomize their tentacles, and treated with 1 mg/ml BrdU for 2 hrs prior to fixation, embedding, and sectioning. Sections were stained with an anti-BrdU antibody, followed by counter-staining with Masson's trichrome. The BrdU antibody was found throughout the cytoplasm of all cells (*brown staining*), and thus did not yield any useful information. Scale bars = 100 µm; *bg* = branchial ganglia; *bv* = branchial blood vessel; *mc* = mesenchymal cells of adult; *m* = mesenchymal cells of regenerating blastema; *sm* = skeletal mesenchyme of regenerating branchial crown.

a-c Adult tentacles: **a** Medial section through adult tentacles illustrating position of cartilage relative to underlying branchial ganglia (*bg*). **b** Section illustrating the dorsal contact zone between the cartilage and the dorsal musculature. A number of mesenchymal cells (*mc*) are seen between the acellular region of the cartilage (*green staining*) and the membrane separating the tentacles from the musculature. **c** The fibrous protein of the cartilage within the adult radioles stains red, indicating higher tensile properties. The cartilage within the fully formed radioles is 4-5 cells thick.

d-o Histological analysis of regenerating branchial cartilages after autotomization:

d One day post autotomization, medial section: the epithelium is continuous across the apical surface of the worm. The basement membrane of the epithelium (*green staining*) is discontinuous in the region directly overlying the branchial ganglion (*bg*).

e Day 2, medial-lateral section: mesenchymal cells begin to accumulate between the epithelium and branchial ganglion. The basement membrane separating the epithelium from the underlying mesenchymal blastema is thick (*light green staining*).

f Day 3, medial section: mesenchymal cells continue to accumulate under the epithelium; the epithelial layer is columnar.

g-h Day 5: **g** Medial section illustrating bilateral growth of branchial buds. **h** Cross section through the developing radioles showing the centrally located vessel (*bv*) and adjacent presumptive skeletal mesenchyme (*sm*). There is no sign of chondrocyte differentiation within this mesenchyme at this point.

i-k Day 8: **i** Cross section through developing tentacles at the base of the developing radioles. Chondrocytes (*bc; arrows*) are seen differentiating within the mesenchyme adjacent to the blood vessel (*red staining*). **j** Medial section at the base of the tentacles illustrating the base of the five radioles in relation to the musculature (*red staining*) and branchial ganglia (*bg*). **k** Higher magnification of

the section shown in (j), illustrating the lack of chondrocyte differentiation within the base of the developing branchial crown at this stage.

l Day 9, medial section through a single radiole at the level of the blood vessel. An epithelial thickening can be seen where a pinnule bud will form (*arrow*). At this stage there is still no chondrocyte differentiation within the mesenchyme of at the base of the crown.

m Day 11, lateral section through the base of the tentacles showing the first signs of chondrocyte differentiation at the base of the radiole.

n,o Day 13: **n** Cross section through the base of the developing branchial crown. Mesenchymal cells underlying the epithelium have begun to deposit cartilage matrix material (*green staining*), and cells within the centre of the mesenchyme are becoming vacuolated. **o** Cross section through the distal portion of the radioles showing well-differentiated chondrocytes, 4-5 cells across. This is similar to the structure of the original adult radiole skeleton (see c).

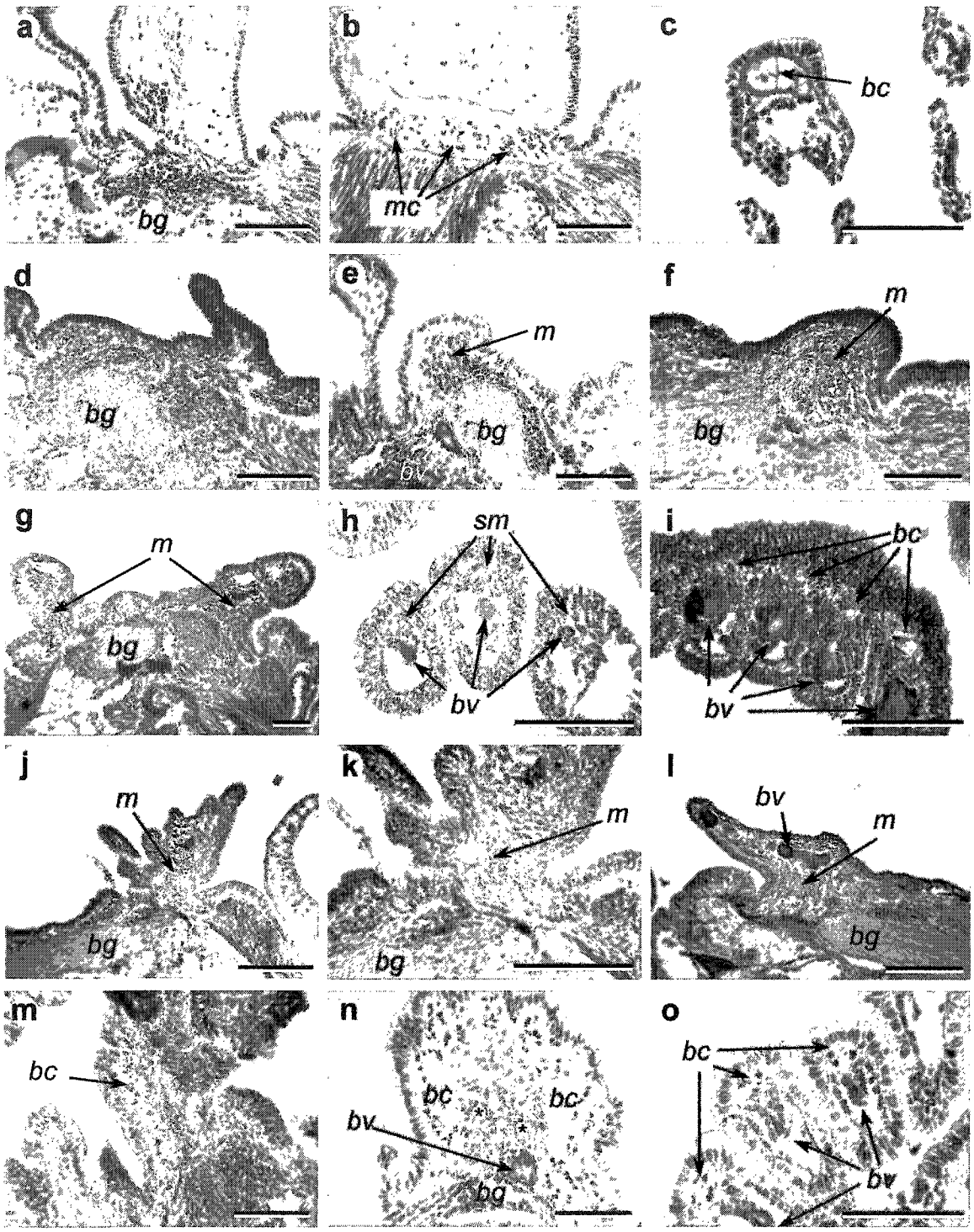
a
bg
b
mc
c
bc
d
bg
e
m
bg
f
m
bg
g
m
bg
h
sm
bv
i
bc
bv
j
m
bg
k
m
bg
l
bv
m
bg
m
bc
n
bc
bc
bv
bg
o
bc
bv

Figure 41

One day post-autotomy

After autotomization of the crown, an epithelial layer forms at the wound site overlying the fibrous layer (fig. 41d). In the region overlying the ganglia (where the regenerating branchial buds will form) the fibrous layer is discontinuous, suggesting that it may be being broken down in this region. At this time there are few mesenchymal cells between the ganglia and the epithelium.

Two – three days post-autotomy

A regeneration bud forms beneath the epithelium two days after the crown has been autotomized. Mesenchymal cells accumulate between the epithelium and the ganglia over the next 36 hours, leading to protrusion of the regeneration bud (fig. 41e,f).

Four – five days post-autotomy

By day four, the regeneration bud is clearly divided into three lobes, which are the initial radioles in the new crown. The circulatory system invades the mesenchyme of the developing branchial buds on day five (fig. 41g,h), followed by elongation of the radioles. Mesenchymal cells are clearly visible within the growing branchial radioles alongside the blood vessel, however there are no signs of chondrocyte differentiation.

Six – eight days post-autotomy

The radioles continue to elongate, with subsequent radioles added ventrally between days six and seven. By day eight, differentiation of a row of chondrocytes within the mesenchyme of the radioles can be detected histologically (fig. 41i). Chondrocyte differentiation within the radioles always occurs adjacent to the blood vessel, and there is no sign of chondrocyte differentiation at the base of the developing crown (fig. 41j,k). This is in contrast to the pattern of differentiation during development, where the first signs of chondrocyte differentiation occur basally within the developing crown.

Nine – eleven days post-autotomy

Radiole elongation and differentiation continues over the next few days, with still no sign of chondrocyte differentiation within the base of the crown, although differentiation of mesenchyme within the base of the radioles has begun (fig. 41m). New radioles continue to arise ventrally from the tentacle base, which can be visualised as a regional thickening of the epithelium (fig. 41l).

Twelve – fourteen days post-autotomy

By day twelve the mesenchyme within the base of the crown begins to show differentiation into chondrocytes. Differentiation occurs first in mesenchyme adjacent to the epithelium where the radioles join the base of the tentacles. By day thirteen, cells within the mesenchyme in the centre of the tentacle base begin to vacuolate, but do not yet deposit visible matrix products (fig. 41n). Within the radioles the branchial skeleton is now 3-4 cells wide (fig. 41o). At this point, nearly two weeks after autotomization of the crown, pigmented ocelli differentiate within the epithelium and the branchial crown is fully functional for feeding. However, the thickened acellular fibrous sheath and the cartilage bridge joining the two halves of the cartilage within the adult crown have yet to form. These last features of the fully differentiated sabellid cartilage will form as the crown continues to grow, as evidenced by examination of specimens four weeks post-autotomization, wherein both the sheath and the connecting cartilage have re-appeared.

6.4 Discussion

6.4.1 *Potamilla* cartilage development

Sabellid cartilage, a feature of the adult organism, first appears during metamorphosis. Despite the fact that metamorphosing larvae are small, chondrocytes are the first mesenchymal cells to differentiate within the developing branchial crown. This early differentiation of chondrocytes is contra-indicated if a minimal size threshold exists, as discussed below, and suggests that branchial cartilage production may be autotomously specified in this lineage.

Within adult *Potamilla sp.* the number of radioles are variable, with new radioles added to the crown ventrally. This pattern of adult radiole growth is mirrored by the development and regeneration of the crown, wherein the branchial bud begins elongation of the dorsal-most radiole first, with subsequent radioles developing from the ventral bud tissue. The sequential formation of radioles and their cartilage parallels the situation in horseshoe crabs, where the branchial appendages and their cartilages are added sequentially in development (table 10).

6.4.2 Regeneration

Unlike many invertebrates, vertebrates are unable to regenerate major portions of their body trunk; regeneration is restricted to appendages and portions of the internal organs. Much is known regarding vertebrate appendage regeneration, particularly the fins of fish and limbs of amphibians (i.e. Bryant *et al.*, 2002; Akimenko *et al.* 2003; Endo *et al.*, 2004). With regards to the regeneration of vertebrate cartilage, it is well established that in order to regenerate cartilage, a cartilage anlagen must remain at the sight of amputation (e.g. rabbit ear cartilage: Thouveny and Tassava, 1998). Within sabellids, cartilage is only found within the branchial crown and thus because no cartilage remains after autotomization, during regeneration the new cartilage arises *de novo* from mesenchymal cells.

During limb regeneration in amphibians, a blastema of undifferentiated cells (in which the cells are derived from de-differentiation of "stump" tissue) forms under the wound epithelium (Endo *et al.*, 2004). Within sabellids, a similar blastema forms during regeneration following bisection of the worm, with cells derived from both totipotent coelomocytes and dedifferentiation of remaining tissues, particularly from fragmentation and dedifferentiation of muscle (Douglas-Hill, 1969). Here I have shown that regeneration following autotomy of the branchial crown does not involve de-differentiation of remaining tissues. The implication being, cells contributing to the regeneration bud derive from mesenchyme residing between the cartilage and the fibrous layer (fig. 41a,b).

Table 10: *Limulus polyphemus* cartilage differentiation

The presence of cartilage is indicated as determined from histological sections (+) or whole mount Alcian Blue preparations (++) of the horseshoe crab *Limulus polyphemus*. Branchial cartilages are numbered from 1 through 6 in an anterior to posterior sequence. Specimens examined include embryonic stage 21 (Sekiguchi, 1988), hatchlings, first (H+1), second (H+2), and ninth (H+9) post-embryonic molt.

Cartilaginous element	Stage 21	Hatchling	H+1	H+2	H+9
Endosternite			+	+	++
Chilarium cartilages		+	+	+	++
Branchial cartilages (1)	+	+	+	+	++
Branchial cartilages (2)	+	+	+	+	++
Branchial cartilages (3)			+	+	++
Branchial cartilages (4)				+	++
Branchial cartilages (5)					++
Branchial cartilages (6)					++

Potamilla *cartilage regeneration*

The body walls of adult *Potamilla sp.* are very fragile, making them highly susceptible to damage. The regenerative ability of *Potamilla sp.* compensates for this fragility, and suggests that they would be able to reproduce asexually through fission. Asexual reproduction has never been documented for *Potamilla*, however paratomy (regeneration of terminal body regions within the body of the parent prior to fission) is reported to occur in other members of the Sabellinae (Rouse and Pleijel, 2001).

In contrast to the regenerative abilities exhibited by *Potamilla sp.*, no regeneration was seen following excision of the branchial crown in *Myxicola.* Additionally, *Myxicola* adults could not be induced to autotomize their branchial crown. It is possible that the large body size of *Myxicola* relaxes some of the predatory pressures on this animal and thus the ability to regenerate their head would serve no selective advantage. Studies on polychaete respiration have shown that the branchial crown is required for meeting the animal's respiratory requirements (Wells, 1952). This physiological requirement alone may be enough to account for both the loss of autotomization and inability to regenerate the lost structures.

6.4.3 *Potamilla* as a model system for cartilage formation

Cell lineage studies

Potamilla sp. is an ideal candidate for embryological studies, and should be amenable to cell lineage studies. Within two days of settling out of the water column *Potamilla sp.* larvae fully metamorphose into feeding juveniles. Upon metamorphosis, tentacle formation and subsequent cartilage differentiation is rapid and can be followed microscopically.

Induction of regenerating cartilage

The appearance of chondrocytes in newly metamorphosed juveniles, whose tentacles are only composed of an epithelium with a few mesenchymal cells, begs the question of whether this tissue is induced or autotomously specified. It is unlikely that the induction of cartilage formation derives from mechanical

stimuli, although the possibility that the epithelium is contractile and thereby transmits a mechanical signal cannot be dismissed because juvenile worms can expand and contract their feeding tentacles (personal observation). The branchial crown does not yet have a hydroskeleton (blood vessel), nor are any muscles present within the crown, thus a contractile epithelium is the most likely way that this mobility is achieved.

Autotomous specification is not supported by preliminary cell culture data. Dissociated cells from autotomized *Potamilla sp.* branchial crowns (dissociated using 1% trypsin in seawater) survive and proliferate in cell culture (personal observation). In preliminary trials, I have maintained cell cultures derived from tentacle cells for periods of weeks, in which time the composition of the cell culture changes from fibroblasts, chondrocytes, pigmented, ciliated, and granular cells (first two days), to a monolayer of undifferentiated spherical cells. After one week in culture these cells reach densities of 2-3 cell layers thick. These preliminary data indicate that this system may provide a fruitful avenue for investigating chemical induction of cartilage formation using various candidate molecules.

Vertebrate cartilage induction can be transmitted using a chemical signal, which amongst vertebrates often derives from an epithelial layer (e.g. bFGF signalling between otic epithelium and underlying mesenchyme forming the otic capsule: Frenz *et al.*, 1994). Given that *Potamilla sp.* cartilage forms from mesenchyme located between the epithelium of the branchial appendages, an epithelial origin for cartilage induction is possible. This possibility could be tested experimentally by removing the epithelium from regenerating branchial regions and culturing the underlying mesenchyme.

6.4.4 Comparative histology

The branchial skeleton within sabellid polychaetes varies in terms of relative contribution of the cellular and acellular regions. Specimens of *Potamilla sp.* examined possess cartilage with well-developed cellular and acellular components, whereas the highly cellular cartilage within the largest species

examined here (*Myxicola infundibulum*) has only a thin acellular region that is continuous with the basement membrane of the overlying epithelium. In contrast, the smallest species examined (*Fabricia sabella*) does not possess any cellular cartilage within the branchial crown, having instead only a thickened basement membrane. These results suggest that the acellular component of the branchial skeleton within larger sabellids may derive from the overlying epithelium and not from the chondrocytes themselves. The acellular fibrous sheath arises late in the differentiation of the cartilage, beyond the period examined here for either initial differentiation (post-metamorphosis) or differentiation following regeneration. Therefore, I have not determined whether this second histological territory derives from the chondrocytes themselves, or if it is secreted by the overlying epithelium – a possibility suggested by the comparative histological structure of different sabellid polychaetes.

6.4.5 Sabellid cartilage evolution

Influence of body size

Dwarf sabellid polychaetes (such as *Fabricia sabella*) lack cartilages that are found within larger members of sister taxa. Similarly, cartilage formation within cephalopods appears to be strongly influenced by body size, indicated by the lack of cartilages within *Loligo* hatchlings (Chapter 5). These data suggest that there may be a minimum body size requirement for cartilage formation. This postulation is further supported by data derived from analysis of vertebrates that have undergone miniaturization, wherein an overall reduction in number of cartilaginous elements within the limb is reported (Hanken, 1985). This observation could be explained by the fact that there is a minimum threshold number of cells required to form a functional cellular condensation, and with a decrease in size and accompanying reduction in overall cell number, fewer cartilage condensations form within the developing limb. However, the polychaete cartilage described here does not develop from a large condensation of cells, forming instead from individual mesenchymal cells within the developing tentacles. This cartilage formation occurs at a very small body size in *Potamilla*

sp., suggesting that in this lineage cartilage differentiation is not limited by body size.

Branchial cartilage as a cladistic character

Branchial skeletons have only rarely been used in cladistic analyses of polychaetes (Fitzhugh, 1989). This is somewhat surprising given that the branchial skeleton is the only known structure within polychaetes to be comprised of cartilage. Even within members of the Serpulidae, sister clade to the Sabellidae, there are no cartilages present, confirmed here from sections of two populations of *Hydroides elegans*. Fitzhugh recognized significance of the limited distribution of a cartilaginous endoskeleton, and uses it to argue for the inclusion of Caobangiidae within the Sabellidae based upon the shared presence of a cartilaginous skeleton – a relationship that has now been confirmed by a more rigorous cladistic analysis (G. Rouse, personal communication). The Caobangiidae are the only other polychaetes known to possess tentacle cartilage (Fitzhugh, 1989). The Caobangiidae would be an interesting lineage in which to investigate cartilages because they are one of a handful of freshwater polychaetes, however to my knowledge there have been no studies on these tissues.

Taxa within the Sabellidae fall into one of two major clades: the Sabellinae and the Fabriciinae. Sabellinae all have an internal radiolar skeleton, whereas members of Fabriciinae largely lack a cellular branchial skeleton (Fitzhugh, 1989). In those Fabriciinae where a skeleton is present it is never more than a single cell thick, and the chondrocytes are reported to be anucleate (Fitzhugh, 1998) – although these specimens have not been subject to any histological analysis (G. Rouse, personal communication). It is likely that the absence of a cellular cartilage within this lineage is a reflection of overall reduction in body size and thus can be considered to be a secondary loss. The lack of cartilage within any other polychaete lineage presents a strong argument for the independent evolution of cartilage within the Sabellid lineage.

6.5 Conclusions

The ability of some animals to regenerate entire body regions, often from previously differentiated cells, is remarkable in and of itself. Here, I provide the first data available regarding development of sabellid polychaete branchial cartilages. Cartilage first forms at metamorphosis from mesenchymal cells of the prostomium. I further examine the similarities between cartilage development and differentiation following tentacle autotomization and subsequent regeneration. In both cases chondrocytes differentiate from mesenchymal cells, uniformly secreting a pericellular cartilage matrix. Regeneration following autotomization does not appear to involve fragmentation and dedifferentiation of other tissues, as described previously for regeneration from partial body segments. The relative contributions of the acellular and cellular regions of the sabellid cartilage varies between species within the clade, and the presence of an acellular region, but not acellular component, within members of the Fabriciinae suggest that the acellular region may be derived from the overlying epithelium, and not the chondrocytes themselves. However, the formation of the acellular regions was not addressed in this study and thus is highlighted as a fruitful avenue for further investigations.

Chapter 7: Conclusions

7.1 Cartilage: definition, distribution, and classification

The relationship between different connective tissue types found amongst metazoan lineages is not fully understood. A continuum of histologically similar cartilage-like tissues exists. At one end of this continuum are tissues wherein the extracellular matrix predominates; at the other are tissues that have greatly reduced amounts of extracellular matrix:

- Chondroid connective tissues – defined as connective tissue composed primarily of extracellular matrix that is structurally similar to cartilage, but lacking well-defined chondrocytes (Chapter 2)
- Cartilage – defined as a cellular connective tissue composed of an extracellular matrix containing high amounts of fibrous protein and hydrophilic mucopolysaccharides, and chondrocytes that are distinct from other connective tissue cells (Chapter 1)
- Chordoid – defined as vacuolated cells surrounded by an acellular fibrous sheath, but lacking extensive intracellular matrix (Chapter 4)

7.1.1 Cartilage distribution

Cartilage is present outside vertebrates and therefore is a metazoan tissue type. This is not a new discovery, although its significance is often disregarded – possibly due to debate regarding what constitutes cartilage, and thus how widely distributed these tissues are. I have developed a new histology protocol – designed to distinguish within a single section: high and low tensile fibrous protein, elastin, and mucopolysaccharides – and have employed this protocol in a rigorous histological analysis of invertebrate connective tissues to assess the distribution of cartilage (Chapter 2).

I have found that not all tissues previously reported as cartilage warrant this designation. I have demonstrated that cartilage is found in chordates, sabellid polychaetes, arthropods, and molluscs, and that chondroid connective tissues

are widespread amongst the invertebrate metazoans. Furthermore, invertebrate cartilages exhibit a range of histological structure, in terms of the relative amount of extracellular matrix and the morphology of the chondrocytes, requiring the expansion of current cartilage classification schemes in order to account for this diversity.

7.1.2 Cartilage classification

Acellular cartilage

Although the lack of a cellular component is in direct contrast with the definition of cartilage presented in this thesis (Chapter 1), similarities in histological composition of cartilage matrices and the acellular matrix comprising the hemichordate skeleton suggest that this hemichordate tissue may be representative of a new category of cartilage, acellular cartilage. This tissue represents the completion of a full spectrum of cartilage histologies, from acellular to cell-rich cartilages (Chapter 2). Acellular cartilage parallels vertebrate acellular bone (common amongst the advanced teleosts; Moss, 1961; Witten *et al.*, 2004), which arises developmentally by polarization of extracellular matrix secretion from osteocytes (Ekanyake and Hall, 1987, 1988). Similarly, the hemichordate skeleton appears to derive from polarized secretion of matrix products from epithelial cells. The question of the relationship between cartilage and epithelia arises due to the similarity between matrices of these hemichordate acellular skeletons and cartilage matrix.

Epithelially-derived cartilage

One cannot rule out the possibility of epithelially derived cartilages such as the hemichordate skeleton. Some features of invertebrate cartilages described here suggest a close relationship between cartilage and epithelia: intercellular connections, as seen in cephalopod and arthropod cartilages (Chapter 2), may be remnants of an epithelial origin of the mesenchymal cells that gave rise to chondrocytes in these lineages; the acellular region of sabellid polychaete cartilages may be derived from the overlying epithelium rather than from chondrocytes (Chapter 6). Thus central cell-rich cartilage, described in sabellid

polychaetes, may be thought to represent an intermediate phenotype between epithelially derived acellular skeletal tissues and cellular skeletal supports.

Vesicular cartilage

Vacuolated chondrocytes are common within invertebrate cartilages, found in cartilages of all three invertebrate lineages, but not in all invertebrate cartilages. Consequently, I have instated a new category of cartilage within the current histological classification schemes: vesicular cartilage, described here within the opisthosomatic cartilages of chelicerate arthropods and forming the skeleton of sabellid polychaete branchial crowns (Chapter 2). In the context of this cartilage type – cartilage wherein the chondrocytes contain a large vesicle or vacuole that augments the structural and mechanical properties of the cartilage – one might also consider vertebrate notochords as cartilage. By extension, chordoid tissues of small metazoan lineages could be considered cartilage and thus might represent one of the earliest forms of cartilage. However, cartilage by definition contains extracellular matrix, which (aside from the surrounding fibrous sheath) is absent in most chordoid tissues thereby rendering them interesting cellular support tissues, but not cartilage. The similarities between chordoid cells and vesicular chondrocytes, and the use of type II collagen within vertebrate notochords and cartilage, do suggest a close relationship between cartilage and chordoid as tissue types.

7.2 Trends in cartilage evolution: insights from invertebrate taxa

7.2.1 Metazoan phylogenetics

Evaluation of cartilage evolution, or even simply relationships between various connective tissue types, relies on having a robust phylogeny onto which the distribution of these tissues can be mapped. Ideas regarding metazoan phylogeny have been changing in recent years, with discrepancies arising between morphologically derived phylogenies and those derived from molecular data. I have created a supertree of the metazoa based upon published molecular

hypotheses in order to objectively assess the consensus view of metazoan relationships (Chapter 3).

My results show that the presence of three main lineages of bilaterian animals is strongly indicated by recent molecular data. In addition, my results reveal that the use of supraspecific taxa increases the amount of information available for sorting relationships between multi-phyletic clades, and thus can increase the resolution of nodes separating these clades within supertree analyses. Correcting for data non-independence, which is not yet common practice for supertree construction, revealed the presence of a clade of diploblast taxa located basally within the tree. This result highlights the importance of increased collection of data from molecules other than 18S rRNA in order to maximize the resolution of metazoan relationships.

7.2.2 Cartilage tissue evolution

The distribution of chondroid connective tissues, mapped onto the tree topology derived from my supertree analyses, lead me to the conclusion that the ability to form chondroid connective tissue, with structural matrix properties similar to those seen in cartilage, arose before the divergence of vertebrates and invertebrates (Chapter 4). Cartilage can be envisioned to have arisen from this chondroid connective tissue independently in different lineages, forming a family of tissues. Thus, the remarkable similarities between vertebrate and cephalopod cartilage are convergent, otherwise the structure of cartilage within all lineages would be expected to be equally similar.

7.2.3 Connective tissue homology

Although it is most parsimonious (based solely upon distribution) to speculate that cartilage has been independently derived multiple times, the presence of these tissues in representatives of all three major bilaterian lineages should not be overlooked. Cartilages throughout all lineages may possess a deep homology at the level of tissue origin, connected to one another by their latent homologue: chondroid connective tissue (Chapter 4). Furthermore, shared properties between invertebrate cartilages and vertebrate bone (such as cell-cell

connections and use of similar molecular constituents: type I collagen, osteonectin, and bone sialoproteins; Chapter 2) suggest that vertebrate bone also derives from the same chondroid connective tissue as the invertebrate cartilages, although it is possible that these features may also be convergent – and therefore not indicative of a common origin from an ancestral chondroid connective tissue. To determine the extent of homology (beyond the level of tissue types) between the various metazoan cartilages, and indeed between cartilages and other similar connective tissues (bone, chordoid, and chondroid) much more data is needed with regards to the developmental mechanisms of cartilage development and the molecular constituents of cartilage in all invertebrate groups. Regardless of their level of homology, many similarities exist between these tissues and trends can be identified that are common to the development and evolution of cartilage in general.

7.2.4 Body-size requirements

My studies suggest that cartilage is not present, nor is it expected, in extremely small organisms. However, the presence of chordoid organs, sharing many structural and functional similarities with cartilage, is evidence that cellular skeletal tissues are possible in small-bodied taxa (Cycliophora, Gastrotricha, and Acoela). There is a clear trend within cephalopod molluscs (Chapter 5) and polychaete annelids (Chapter 6) towards reduction or loss of cartilages accompanying reduction in body size. For example, cellular cartilage is absent within the Fabriciinae (sabellid polychaete), replaced by an expanded fibrous layer underlying the epithelium.

At present, data are lacking with regard to the distribution of cartilage in miniature cephalopod species. However I have demonstrated that body size at hatching and the presence of differentiated cartilages are related. Cartilage is thus predominantly a cellular skeletal support tissue found in large-bodied animals, and chordoid tissues are a feature of small-bodied animals (Chapter 4). The only lineage that appears to have both tissue types are the vertebrates, wherein the chordoid tissue (notochord) is a feature of the small-bodied embryos,

and is often replaced by cartilage and other connective tissues as the animals increase in size.

7.2.5 Lineage specific cartilage evolution

My comparative studies on the distribution of cartilaginous elements amongst cephalopods and sabellid polychaetes have shown that within a lineage, gain and loss of cartilaginous structures has occurred. The large number of distinct cephalopod cartilages allowed for a more detailed phylogenetic analysis of lineage-specific cartilage evolution (Chapter 5). This analysis showed that the appearance of a large number of these structures is correlated with reduction of the external shell. This includes the appearance of cartilages surrounding the centralized ganglia, and those associated with fin and mantle function (funnel/pallial and nuchal/dorsal assemblages). Furthermore, the distribution of these structures indicated that mantle-related cartilages were lost independently within the octopods (both assemblages) and sepiolids (nuchal/dorsal), and that new cartilages appeared within the sepiids (branchial) and sepiolids (dorsal extension of the fin cartilage).

Within the sabellid polychaetes, as mentioned above, loss of cartilage within Fabriciinae can be explained by the overall reduction of body-size. Because sabellid polychaetes only possess a single cartilaginous element, loss of this element results in the loss of cartilage as a tissue type within that lineage. In contrast, the large number of independent cartilaginous elements found within cephalopods makes the disappearance of cartilage, as a tissue type, highly unlikely. This distributional bias indicates that it would be reasonably easy for cartilage to be eliminated from any lineage in which only a single cartilaginous element evolved. Thus, the widespread absence of reported cartilages amongst metazoan lineages may not represent a true reflection of the ancestral distribution of cartilages.

7.3 Trends in cartilage differentiation

I examined cartilage differentiation within representatives of two invertebrate lineages: *Sepia* (cephalopod: Chapter 5) and *Potamilla* (sabellid polychaete: Chapter 6). Both invertebrate lineages examined within this thesis offer opportunities for further increasing our understanding of mechanisms underlying cartilage differentiation.

7.3.1 Regeneration

The regenerative abilities of sabellid polychaetes, particularly the tendency of disturbed worms to autotomize and subsequently re-grow their branchial crown, allowed me to compare cartilage differentiation during development with that which follows autotomization (Chapter 6). Formation of the morphological structure of the branchial crown during regeneration mirrored their development, in that the initial branchial bud undergoes a tripartite division to from three initial radioles. Subsequent radioles are added ventrally during regeneration and development, as well as during normal growth of adult animals. Chondrocyte differentiation, the first cells to form during initial branchial development, occurs after vascularization of the regenerating tentacles, a reflection of their larger size and that the branchial tentacles are at least partially responsible for adult respiration.

7.3.2 Condensations

Whereas cartilage appears during metamorphosis within the indirect developing polychaete, cartilage formation occurred largely during embryogenesis within direct developing cephalopods. Differentiation from uncondensed mesenchyme was represented in both polychaetes and cephalopods. These data suggest that, ancestrally, formation of cartilage was accomplished via mechanisms more akin to those seen within formation of vertebrate secondary cartilage in terms of differentiation from uncondensed cells, possibly induced mechanically.

In contrast, the earliest appearing cartilages within the cephalopod developed from a cellular condensation, similar to primary cartilage formation within

vertebrates. The formation of a cellular condensation was shown to occur either in association with a cuboidal epithelial layer, or in the absence of close association with an epithelium. These cellular condensations occur before any muscular contractions of the associated mantle tissues. These data suggest that cartilage formation from cellular condensations is a derived feature that facilitates the development of cartilages prior to the establishment of functional neuromuscular complexes.

7.4 Last words

Invertebrate cartilages exist and represent substantial material imparting vast novel research opportunities, which has gone virtually untapped in recent decades. The work presented in this thesis provides the foundation for exploiting these tissues in order to gain valuable insights into the development and evolution of cartilaginous tissues throughout the Metazoa.

Literature Cited

Abele, L.G., W. Kim, and B.E. Felgenhauer. (1989). Molecular evidence for inclusion of the phylum Pentastomida in the Crustacea. *Molecular Biology and Evolution* **6,** 685-691.

Adoutte, A., G. Balavoine, N. Lartillot, O. Lespinet, B. Prud'homme, and R. de Rosa. (2000). The new animal phylogeny: Reliability and implications. *Proceedings of the National Academy of Sciences* **97,** 4453-4456.

Aguinaldo, A. A., J.M. Turbeville, L.S. Linford, M.C. Rivera, J.R. Garey, R.A. Raff, and J.A. Lake. (1997). Evidence for a clade of nematodes, arthropods and other moulting animals. *Nature* **387,** 489-493.

Aguinaldo, A.A., and J. Lake. (1998). Evolution of the Multicellular Animals. *American Zoologist* **38,** 878-887.

Akimenko, M., Mari-Beffa, M., Becerra, J., and Geraudie, J. (2003). Old questions, new tools, and some answers to the mystery of fin regeneration. *Developmental Dynamics* **226,** 190-201.

Andersen, A. C., Hamraoui, L., and Zaoui, D. (2001). The obturaculum of *Riftia pachyptila* (Annelida, Vestimentifera): Ultrastructure and function of the obturacular muscles and extracellular matrix. *Cahiers de Biologie Marine* **42,** 219-237.

Anderson, F.E. (2000). Phylogeny and historical biogeography of the loliginid squids (Mollusca: Cephalopoda) based on mitochondrial DNA sequence data. *Molecular Phylogenetics and Evolution* **15,** 191-214.

Arnold, J.M. (1965). Normal embryonic stages of the squid, *Loligo pealei* (Lesueur). *Biological Bulletin* **128,** 24-32.

Arnosti, D.N. (2003). Analysis and function of transcriptional regulatory elements: Insights from *Drosophila. Annual Revue of Entomology* **48,** 579-602.

Ayad, S., and Weiss, J.B. (1984). A new look at vitreous-humour collagen. *Biochemistry Journal* **218,** 835-40.

Ayad, S., Boot-Handford, R.P., Humphries, M. J., Kadler, K. E. and Shuttleworth, C. A. (1994). "The Extracellular Matrix Facts Book." Academic Press Limited, London.

Bairati, A., M. Comazzi, and M. Gioria. (1995). A comparative microscopic and ultrastructural study of perichondrial tissue in cartilage of *Octopus vulgaris* (Cephalopoda, Mollusca). *Tissue & Cell* **27,** 515-523.

Bairati, A., Comazzi, M., Cioria M., and Rigo, C. (1998). The ultrastructure of chondrocytes in the cartilage of *Sepia officinalis* and *Octopus vulgaris* (Mollusca, Cephalopoda). *Tissue and Cell* **30,** 340-351.

Bairati, A., Comazzi, M., Gioria, M., Hartmann, D.J., Leone, F., and Rigo, C. (1999). Immunohistochemical study of collagens of the extracellular matrix in cartilage of *Sepia officinalis*. *European Journal of Histochemistry* **43,** 211-225.

Balavoine, G. (1997). The early emergence of playthelminthes is contradicted by the agreement between 18S rRNA and *Hox* genes data. *Academie des sciences* **320,** 83-94.

Balavoine, G. (1998). Are platyhelminthes coelomates without a coelom? AN argument based on the evolution of *Hox* genes. *American Zoologist* **38,** 843-858.

Ballard, J.W.O., Olsen, G.J., Faith, D.P., Odgers, W.A., Rowell, D.M., and Atkinson, P.W.. (1992). Evidence from 12S ribosomal RNA sequences that Onychophorans are modified Arthropods. *Science* **258,** 1345-1348.

Bayascas, J. R., Castillo, E., and Salo, E. (1998). Platyhelminthes have a Hox code differentially activated during regeneration, with genes closely related to those of spiralian protostomes. *Development Genes and Evolution* **208,** 467-473.

Benito, J., and Pardos, F. (1997). Chapter 2: Hemichordata. *In* "Hemichordata, Chaetognatha, and the Invertebrate Chordates" (F. W. Harrison, and Ruppert, E.E., Ed.), Vol. 15, pp. 15-101. Wiley-Liss, New York.

Benjamin, M. (1990). The cranial cartilages of teleosts and their classification. *Journal of Anatomy* **169,** 153-172.

Benjamin, M., and Ralphs, J.R.. (1991). Extracellular matrix of connective tissues in the heads of teleosts. *Journal of Anatomy* **179,** 137-148.

Benjamin, M., C.W. Archer, and J.R. Ralphs. (1994). Cytoskeleton of cartilage cells. *Microscopy research and Technique* **28,** 372-377.

Beresford, W.A. (1981). "Chondroid Bone, Secondary Cartilage, and Metaplasia." Urban & Schwarzenberg, Baltimore.

Beresford, W. A. (1993). Cranial skeletal tissues: Diversity and evolutionary trends. *In* "The Skull: Patterns of structural and systematic diversity." (Hanken J., and Hall, B.K., Ed.), Vol. 2, pp. 69-130. The University of Chicago Press, Chicago and London.

Berney, C., Pawlowski, J., and Zaninetti, L. (2000). Elongation factor-alpha sequences do not support an early divergence of the Acoela. *Molecular Biology and Evolution* **17,** 1032-1039.

Berrill, N.J. (1931). Regeneration in *Sabella pavonina* (Sav.) and other sabellid worms. *Journal of Experimental Zoology* **58,** 495-523.

Berrill, N.J., and Mees, D. (1936). Reorganization and regeneration in *Sabella*. II. The influence of temperature. III. The influence of light. *The Journal of Experimental Zoology* **74,** 61-89.

Bininda-Emonds, O.R.P., Bryant, H.N., and Russell, A.P. (1998). Supraspecific taxa as terminals in cladistic analysis: implicit assumptions of monophyly and a comparison of methods. *Biological Journal of the Linnean Society* **64,** 101-133.

Bininda-Emonds, O.R.P., Gittleman, J.L., and Purvis, A. (1999). Building large trees by compiling phylogenetic information: a complete phylogeny of the extant Carnivora (Mammalia). *Biological Reviews* **74,** 143-175.

Bininda-Emonds, O.R.P., and Sanderson, M. (2001). Assessment of the accuracy of matrix representation with parsimony analysis supertree construction. *Systematic Biology* **50,** 564-579.

Bininda-Emonds, O.R.P., Gittleman, J.L., and Steel, M.A. (2002). The (super)tree of life: Procedures, problems, and prospects. *Annual Review of Ecology and Systematics* **33,** 265 - 289.

Bitsch, C., and Bitsch, J. (2002). The endoskeletal structures in arthropods: cytology, morphology and evolution. *Arthropod Structure and Development* **30,** 159-177.

Black, M.B., Halanych, K.M., Mass, P.A.Y., Hoeh, W.R., Hashimoto, J., Desbruyeres, D., Lutz, R.A., and Vrijenhoek, R.C. (1997). Molecular systematics of vestimentiferan tubeworms from hydrothermal vents and cold-water seeps. *Marine Biology* **130,** 141-149.

Bonasoro, F., and Candia Carnevali, M.D. (1994a). Atypical chordoid structure in the aristotle's lantern of regular echinoids. *Acta Zoologica* **75,** 89-100.

Bonasoro, F., and Candia Carnevali, M.D. (1994b). Chordoid structures in regular sea-urchins. *In* "Echinoderms through time" (B. David, Guille, A., Féral, J., and Roux, M., Ed.), pp. 581-587. A.A. Balkema, Rotterdam.

Boore, J.L., Collins, T.M., Stanton, D., Daehler, L.L., and Brown, W.M. (1995). Deducing the pattern of arthropod phylogeny from mitochondrial DNA rearrangements. *Nature* **376,** 163-165.

Boore, J.L., and Staton, J.L. (2002). The mitochondrial genome of the sipunculid *Phascolopsis gouldii* supports its association with Annelida rather than Mollusca. *Molecular Biology and Evolution* **19,** 127-137.

Boot-Handford, R. P., and Tuckwell, D.S. (2003). Fibrillar collagen: the key to vertebrate evolution? A tale of molecular incest. *Bioessays* **25,** 142-151.

Bourque, W.T., Gross, M., and Hall, B.K. (1993). A histological processing technique that preserves the integrity of calcified tissues (bone, enamel), yolky amphibian embryos, and growth factor antigens in skeletal tissue. *The Journal of Histochemistry and Cytochemistry* **41,** 1429-1434.

Bremer, K. (1988). The limits of amino-acid sequence data in angiosperm phylogenetic reconstruction. *Evolution* **42,** 795-803.

Bremer, K. (1994). Branch support and tree stability. *Cladistics* **10,** 295-304.

Bridge, D., Cunningham, C.W., DeSalle, R., and Buss, L.W. (1995). Class-level relationships in the phylum Cnidaria: Molecular and morphological evidence. *Molecular Biology and Evolution* **12,** 679-689.

Brooks, D.R., and McLennan, D.A. (1991). "Phylogeny, Ecology and Behavior: A research program in comparative biology." Chicago University Press, Chicago, IL.

Brusca, R.C., and Brusca, G.J. (2002). "Invertebrates." Sinauer Associates, Inc., Sunderland, Massachusetts.

Bryant, S.V., Endo, T., Gardiner, D.M. (2002). Vertebrate limb regeneration and the origin of limb stem cells. *Int. J. Dev. Biol.* **46,** 887–896.

Budd, G., and Jensen, S. (2000). A critical reappraisal of the fossil record of the bilaterian phyla. *Biological Reviews* **75,** 253-295.

Burighel, P., and Cloney, R.A. (1997). Urochordata: Ascidiacea. *In* "Microscopic anatomy of invertebrates" (F.W. Harrison, and Ruppert, E.E., Ed.), Vol. 15: Hemichordata, Chaetognatha, and the invertebrate chordates, pp. 221-347. Wiley-Liss, New York.

Buxton, P.G., Hall, B., Archer, C.W., and Francis-West, P. (2003). Secondary chondrocyte-derived *Ihh* stimulates proliferation of periosteal cells during chick development. *Development* **130,** 4729-4739.

Cameron, C.B., Garey, J.R., and Swalla, B.J. (2000). Evolution of the chordate body plan: New insights from phylogenetic analysis of deuterostome phyla. *PNAS* **97,** 4469-4474.

Carlini, D.B., Reece, K.S., and Graves, J.E. (2000). Actin gene family evolution and the phylogeny of coleoid cephalopods (Mollusca: Cephalopoda). *Molecular Biology and Evolution* **17,** 1353-1370.

Carranza, S., Baguna, J., and Riutort, M. (1997). Are the platyhelminthes a monophyletic primitive group? An assessment using 18S rDNA sequences. *Molecular Biology and Evolution* **14,** 485-497.

Carriker, M.R., Person, P., Libbin, R., and Van Zandt, D. (1972). Regeneration of the proboscis of muricid gastropods after amputation, with emphasis on the radula and cartilages. *Biological Bulletin* **143,** 317-331.

Cavalier-Smith, T., Allsopp, M.T.E.P., Chae, E.E., Boury-Esnault, N., and Vacelet, J. (1996). Sponge phylogeny, animal monophyly, and the origin of the nervous system: 18S rRNA evidence. *Canadian Journal of Zoology* **74,** 2031-2045.

Christen, R., Ratto, A., Baroin, A., Perasso, R., Grell, K.G., and Adoutte, A. (1991). An analysis of the origin of metazoans, using comparisons of partial sequences of the 28S RNA, reveals an early emergence of triploblasts. *The EMBO Journal* **10,** 499-503.

Clément, P., and Wurdak, E. (1991). Rotifera. *In* "Microscopic anatomy of invertebrates" (F.W. Harrison, and Ruppert, E.E., Ed.), Vol. 4: Aschelminthes, pp. 219-297. Wiley-Liss, New York.

Cohen, B.L., Stark, S., Gawthrop, A.B., Burke, M.E., and Thayer, C.W. (1998). Comparison of articulate brachiopod nuclear and mitochondrial gene trees leads to a clade-based redefinition of protostomes (Protostomozoa) and deuterostomes (Deuterostomozoa). *Proceedings o the Royal Society of London, Series B: Biological Sciences* **265,** 475-82.

Cohen, B.L. (2000). Monophyly of brachiopods and phoronids: reconciliation of molecular evidence with Linnaean classification (the subphylum Phoroniformea nov.). *Proceedings of the Royal Society of London, Series B: Biological Sciences* **267,** 225-231.

Cole, A., and Hall, B.K. (2004). Cartilage is a metazoan tissue; Integrating data from invertebrate sources. *Acta Zoologica,* in press.

Collins, A.G. (1998). Evaluating multiple alternative hypotheses for the origin of bilateria: an analysis of 18S rRNA molecular evidence. *Proceedings of the National Academy of Sciences USA* **95,** 15458-15463.

Conn, H.J. (1973). "Staining procedures used by the Biological Stain Commission." Williams & Wilkins, Baltimore.

Cowden, R.R. (1967). A histochemical study of chondroid tissue in *Limulus* and *Octopus*. *Histochemie* **9,** 149-163.

Cowden, R.R., and Fitzharris, T. (1975). The histochemistry and structure of tentacle cartilage tissues in the marine polychaete, *Sabella melanostigma*. *Histochemistry* **43,** 1-10.

Cowden, R.R., and Harrison, F.W. (1976). Cytochemical studies of connective tissues in sponges. *In* "Aspects of sponge biology" (F. W. Harrison, and Cowden, R.R., Ed.), pp. 69-82. Academic Press, New York.

Curtis , E.L., and Miller, R.C. (1938). The sclerotic ring in north american birds. **55,** 225-243.

Davies, T.J., Barraclough, T.G., Chase, M.W., Soltis, P.S., Soltis, D.E, and Savolainen, V. (2004). Darwin's abominable mystery: Insights from a supertree of the angiosperms. *Proceeding of the National Academy of Sciences* **101,** 1904-1909.

Delsman, H.C. (1912). Ontwikkelingsgeschiedenis van *Littorina obstusata*, Amsterdam.

Denison, R.H. (1963). The early history of the vertebrate calcified skeleton. *Clinical Orthopedics* **31,** 141-152.

Donoghue, P.C.J., and Sansom, I.J. (2002). Origin and early evolution of vertebrate skeletonization. *Microscopy Research and Technique* **59,** 352-72.

Douglas-Hill, S. (1969). Origin and development of the regeneration blastema in some species of sedentary polychaetes. *In* "Biology", pp. 168. University of Michigan.

Eeckhaut, I., McHug, D., Mardulyn, P., Tiedemann, R., Monteynes, D., Jangoux, M., and Milinkovitch, M.C. (2000). Myzostomida: a link between trochozoans and flatworms? *Proc. R. Soc. Lond. B* **267,** 1383-1392.

Eernisse, D.J., Albert, J.S., and Anderson, F.E. (1992). Annelida and Arthropoda are not sister taxa: A phylogenetic analysis of spiralian metazoan morphology. *Systematic Biology* **41,** 305-330.

Eikenberry, E.F., Childs, B., Sheren, S.B., Parry, D.A., Craig, A.S and Brodsky B. (1984). Crystalline fibril structure of type II collagen in lamprey notochord sheath. *Journal of Molecular Biology* **176,** 261-77.

Ekanayake, S. and Hall, B.K. (1987). The development of acellularity of the vertebrate bone of the Japanese Medaka, *Oryzias latipes* (Teleostei; Cyprinidontidae). *Journal of Morphology* **193,** 253-261.

Ekanayake, S. and Hall, B.K. (1988). Ultrastructure of the Osteodenesis of Acellular Vertebral Bone in the Japanese Medaka, *Oryzian latipes* (Teleostei, Cyprinidontidae). *The American Journal of Anatomy* **182,** 241-249.

Eliberg, R.G., and D.A. Zuckerberg. (1975). Mineralization of invertebrate cartilage. *Calcification Tissue Research* **19,** 85-90.

Endo, T., Bryant, S.V., and Gardiner, D.M. (2004). A stepwise model system for limb regeneration. *Developmental Biology* **270,** 135-145.

Erickson, G.R., Gimble, J.M., Franklin, D.M., Rice, H.E., Awad, H., and Guilak, F. (2002). Chondrogenic potential of adipose tissue-derived stromal cells in vitro and in vivo. *Biochemical and Biophysical Research Communications* **290,** 763-769.

Exposito, J.-Y., and Garrone, R. (1990). Characterization of a fibrillar collagen gene in sponges reveals the early evolutionary appearance of two collagen gene families. *Proceedings of the National Academy of Sciences, U.S.A.* **87,** 6669-6673.

Falshaw, R., Hubl, U., Olfman, D., Slim, G.C., Amjad Tariq, M., Watt, D.K. and Yorke, S.C.. (2000). Comparison of the glycosaminoglycans isolated from the skin and head cartilage of Gould's arrow squid (*Nototodarus gouldi*). *Carbohydrate Polymers* **41,** 357-364.

Field, K. G., Olsen, G.J., Lane, D.J., Giovannoni, S.J., Ghiselin, M.T., Raff, E.C., Pace, N.R., and Raff, R.A. (1988). Molecular phylogeny of the animal kingdom. *Science* **239,** 748-753.

Fitzhugh, K. (1989). A systematic revision of the Sabellidae-Caobangiidae-Sabellongidae complex (Annelida: Polychaeta). *Bulletin of the American Museum of Natural History* **192,** 1-104.

Fitzhugh, K. (1998). New fan worm genera and species (Polychaeta, Sabellidae, Fabriciinae) from the western Pacific, and cladistic relationships among genera. *Zoologica Scripta* **27,** 209-245.

Flint, M. (1972). Interrelationships of mucopolysaccharide and collagen in connective tissue remodelling. *Journal of Embryology and Experimental Morphology* **27,** 481-495.

Flint, M., Lyons, M., Meaney, M.F., and Williams, D.E. (1975). The Masson staining of collagen - an explanation of an apparent paradox. *Histochemical Journal* **7,** 529-546.

Fortey, R. A., Briggs, D.E.G., and Wills, M.A. (1996). The Cambrian evolutionary 'explosion': decoupling cladogenesis from morphological disparity. *Biological Journal of the Linnean Society* **57,** 13-33.

Frenz, D.A., Liu, W., Williams, J.D., Hatcher, V., Galinovic-Schwartz, V., Flanders, K.C., and Van de Water, T.R. (1994). Induction of chondrogenesis: requirement for synergistic interaction of basic fibroblast growth factor and transforming growth factor-beta. *Development* **120,** 415-424.

Friedrich, M., and Tautz, D. (1995). Ribosomal DNA phylogeny of the major extant arthropod classes and the evolution of myriapods. *Nature* **376,** 165-167.

Funch, P. (1996). The chordoid larva of *Symbion pandora* (Cycliophora) is a modified trochophore. *Journal of Morphology* **230,** 231-263.

Funch, P., and Kristensen, R.M. (1997). Cycliophora. *In* "Microscopic anatomy of invertebrates" (F.W. Harrison, and Woollacott, R.M., Ed.), Vol. 13: Lophophorates, Entoprocta, and Cycliophora, pp. 409-474. Wiley-Liss, New York.

Fyfe, D. M., and Hall, B.K. (1979). Lack of association between avian cartilages of different embryological origins when maintained *in vitro. American Journal of Anatomy* **154,** 485-496.

Gaill, F., Jamraoui, L., Sicot, F.X., and Timple, R. (1994). Immunological properties and tissue localization of two different collagen types in annelid and vestimentifera species. *European Journal of Cell Biology* **65,** 392-401.

Gans, C. (1989). Stages in the origin of vertebrates: Analysis by means of scenarios. *Biol. Rev.* **64,** 221-268.

Garey, J.R., Near, T.J, Nonnemacher, M.R, and Nadler, S.A. (1996). Molecular evidence for Acanthocephala as a subtaxon of Rotifera. *Journal of Molecular Evolution* **43,** 287-292.

Garey, J.R., and Schmidt-Rhaesa, A. (1998). The essential role of "minor" phyla in molecular studies of animal evolution. *American Zoologist* **38,** 907-917.

Garrone, R. (1998). Evolution of Metazoan Collagens. *Progress in Molecular and Subcellular Biology* **21,** 119-139.

Gatesy, J., Matthee, C., DrSalle, R., and Hayashi, C. (2002). Resolution of a supertree/supermatrix paradox. *Systematic Biology* **51,** 652-664.

Gehring, W. J., and Ikeo, K. (1999). Pax 6: mastering eye morphogenesis and eye evolution. *Trends in Genetics* **15,** 371-377.

Giribet, G., Carranza, S., Baguna, J., Riutort, M., and Ribera, C. (1996). First molecular evidence for the existence of a Tardigrada + Arthropoda clade. *Molecular Biology and Evolution* **13,** 76-84.

Giribet, G., and Ribera, C. (1998). The position of Arthropods in the animal kingdom: A search for a reliable outgroup for internal arthropod phylogeny. *Molecular Phylogenetics and Evolution* **9,** 481-488.

Giribet, G., Distel, D.L., Polt, M., Sterrer, W., and Wheeler, W.C. (2000). Triploblastic relationships with emphasis on the acoelomates and the position of Gnathostomulida, Cycliophora, Platyhelminthes, and Chaetognatha: A compinded approach of 18S rDNA sequences and morphology. *Systematic Biology* **49,** 539-562.

Gooden, M.D., Vernon, R.B, Bassud, J.A., and Sage, E.H. (1999). Cell cycle-dependent nuclear location of the matricellular protein SPARC: Association with the nuclear matrix. *Journal of Cellular Biochemistry* **74,** 152-167.

Gratzner, H.G. (1982). Monoclonal antibody to 5-bromo and 5-iododeoxyuridine: a new reagent for detection of CNA replication. *Science* **218,** 474-475.

Guralnick, R., and Smith, K. (1999). Historical and biomechanical analysis of integration and dissociation in mollscan feeding, with special emphasis on the true limpets (Patellogastropoda: Gastropoda). *Journal of Morphology* **241,** 175-195.

Guthrie, D.M. (1975). The physiology and structure of the nervous system of Amphioxus (the lancelet) *Branchiostoma lanceolatum* Pallas. *Zoologican Sciety of London Symposia* **36,** 43-80.

Haase, A., Stern, M., Wachtler, K., and Bicker, G. (2001). A tissue-specific marker of Ecdysozoa. *Development Genes and Evolution* **211,** 428-433.

Halanych, K.M. (1995). The phylogenetic position of the pterobranch hemichordates based on 18S rDNA sequence data. *Molecular Phylogenetics and Evolution* **4,** 72-76.

Halanych, K.M. (1996). Convergence in the feeding apparatuses of Lophophorates and Pterobranch Hemichordates revealed by 18S rDNA: an interpretation. *Biological Bulletin* **190,** 1-5.

Halanych, K.M. (1996b). Testing hypothesis of chaetognath origins: Long branches revealed by 18s ribosomal DNA. *Systematic Biology* **45,** 223-246.

Halanych, K.M. (1998). Considerations for reconstructing metazoan history: Signal, resolution, and hypothesis testing. *American Zoologist* **38,** 929-941.

Hall, B.K. (1967). The formation of adventitious cartilage by membrane bones under the influence of mechanical stimulation applied in vitro. *Life Sci.* **6,** 663-667.

Hall, B.K. (1970a). Differentiation of cartilage and bone from common germinal cells: I. The role of acidic mucopolysaccharide and collagen. *Journal of Experimental Zoology* **173,** 383-394.

Hall, B.K. (1970b). Cellular differentiation in skeletal tissues. *Biological Reviews* **45,** 455-484.

Hall, B.K. (1971). Histogenesis and morphogenesis of bone. *Clinical Orthopaedics* **71,** 249-268.

Hall, B.K. (1978). "Developmental and Cellular Skeletal Biology." Academic Press,

Hall, B.K. (1983). Cell-tissue interactions: A rationale and resume. *Journal of Craniofacial Genetics and Developmental Biology* **3,** 75-82.

Hall, B.K. (1986). The role of movement and tissue interaction in the development and growth of bone and secondary cartilage in the clavicle of the embryonic chick. *Journal of Embryology and Experimental Morphology* **93,** 133-152.

Hall, B.K., and Miyake, T. (2000). All for one and one for all: Condensations and the initiation of skeletal development. *BioEssays* **22,** 138-147.

Hall, B.K. (2002). Palaeontology and evolutionary developmental biology: A science of the nineteenth and twenty-first centuries. *Palaeontology* **45,** 647-669.

Hall, B.K. (2003). Descent with modification: the unity underlying homology and homoplasy as seen through an analysis of development and evolution. *Biological Revues of the Cambridge Philosophy Society* **78,** 409-433.

Hall, B.K. (2004). "Bones and Cartilage." Elsevier, London.

Ham, A.W., and Harris, W.R. (1950). Histological technique for the study of bone and some notes on the staining of cartilage. *In* "Handbook of Microscopical Technique" (R. M. Jones, Ed.), pp. 269-284. Hoeber, Inc., New York.

Ham, A.W., and Cormack, D.H. (1979). "*Histophysiology of cartilage, bone, and joints.*" J.B. Lippincott Company, Philadelphia and Toronto.

Hanelt, B., Van Schyndel, D., Adema, C.M., Lewis, L.A., and Loker, E.S. (1996). The phylogenetic position of *Rhopalura ophiocomae* (Orthonectida) based on 18S ribosomal DNA sequence analysis. *Molecular Biology and Evolution* **13,** 1187-1191.

Hanken, J. (1985). Morphological novelty in the limb skeleton accompanies miniaturization in salamanders. *Science* **229,** 871-874.

Harrison, F.W., and De Vos, L. (1991). Porifera. *In* "Microscoic anatomy of invertebrates" (F.W. Harrison, and Westfall, J.A., Ed.), Vol. 2: Placozoa, Porifera, Cniaria, and Ctenophora, pp. 29-89. Wiley-Liss, New York.

Harrison, F.W. (1991). Microscopic Anatomy of Invertebrates. Wiley-Liss, New York.

Hay, E.D. (1981). Extracellular Matrix. *The Journal of Cell Biology* **91,** 205s-223s.

Hayashi, M., Ninomiya, Y., Hayashi, K., Linsenmayer, T.F., Olsen, B.R. and Trelstad, R.L. (1988). Secretion of collagen types I and II by epithelial and endothelial cells in the developing chick cornea demonstrated by *in situ* hybridization and immunohistochemistry. *Development* **103,** 27-36.

Hedbom, E., Antonsson, P., Hjerpe, A., Aeschlimann, D., Paulsson, M., Rosa-Pimentel, E., Sommarin, Y., Wendel, M., Oldberg, A. and Heinegard, D. (1992). Cartilage matrix proteins. An acidic oligomeric protein (COMP) detected only in cartilage. *Journal of Biological Chemistry* **267,** 6132-6136.

Hendriks, L., C. Van Broeckhoven, A. Vandenberghie, Y. Van De Peer, and R. De Wachter. (1988). Primary and secondary structure of the 18S ribosomal RNA of the bird spider *Eurypelma californica* and evolutionary relationships amond eukaryotic phyla. *European Journal of Biochemistry* **177,** 15-20.

Holtrop, M.E. (1990). Light and electro microscopic structure of bone-forming cells. *In* "Bone: The osteoblast and osteocyte" (Hall, B.K. Ed.), Vol. 1, pp. 1-39. The Telford Press, New York.

Inoue, H., Otsu, K., Suzuki, S. and Nakanishi, Y. (1986). Difference between N-acetylgalactosamine 4-sulfate 6-O-sulfotransferases from human serum and squid cartilage in specificity toward the terminal and interior portion of chondroitin sulfate. *Journal of Biological Chemistry* **261,** 4470-5.

Ito, Y., and Habuchi, O. (2000). Purification and characterization of N-acetylgalactosamine 4-sulfate 6-O-sulfotransferase from the squid cartilage. *Journal of Biological Chemistry* **275,** 34728-36.

Iwabe, N., Kuma, K., and Miyata, T. (1996). Evolution of gene families and relationship with organismal evolution: Rapid divergence of tissue-specific genes in the early evolution of chordates. *Molecular Biology and Evolution* **13,** 483-493.

Jacenko, O., and Tuan, R.S. (1986). Calcium deficiency induces expression of cartilage-like phenotype in chick embryonic calvaria. *Developmental Biology* **115,** 215-232.

Jones, K.E., Purvis, A., MacLarnon, A., Bininda-Emonds, O.R.P., and Simmons, N.B. (2002). A phylogenetic supertree of the bats (Mammaila: Chiroptera). *Biological Revues of the Cambridge Philosophy Society* **77,** 223-259.

Junqueira, L.C.U., Toledo, O.M.S., and Montes, G.S. (1983). Histochemical and morphological studies on a new type of acellular cartilage. *Basic and Applied Histochemistry* **27,** 1-8.

Junqueira, L.C.U., Carneiro, J. and Kelley, R.O. (1998). "*Basic Histology.*" Appleton and Lange, Norwalk Connecticut.

Katayama, T., Yamamoto, M., Wada, H., and Satoh, N. (1993). Phylogenetic position of acoel turbellarians inferred from partial 18S rDNA sequences. *Zoological Science* **10,** 529-536.

Katayama, T., Wada, H., Furuya, H., Satoh, N., and Yamamoto, M. (1995). Phylogenetic position of the dicyemid mesozoa inferred from 18S rDNA sequences. *Biological Bulletin* **189,** 81-90.

Kimmel, C.B., Miller, C.T., Kruze, G., Ullmann, B., BrMiller, R.A., Larison, K.D., and Snyder, H.C. (1998). The Shaping of Pharyngeal Cartilages during Early Development of the Zebrafish. *Developmental Biology* **203,** 245-263.

Kimura, S., and Karasawa, K. (1985). Squid cartilage collagen: Isolation of type I collagen rich in carbohydrate. *Comparative Biochemistry and Physiology* **81B,** 361-365.

Kinoshita, A., Yamada, S., Haslam, S.M., Morris, J.R., Dell, A. and Sugahara, K. (1997). Novel tetrasaccharides isolated from squid cartilage chondroitin sulfate E containing unusual sulfated disaccharide units GlcA(3-*O*-sulfate)*b*1-3GalNAc(6-*O*-sulfate) or GlcA(3-*O*-sulfate)*b*1-3GalNAc(4,6-*O*-sulfate). *The Journal of Biological Chemistry* **272,** 19656-19665.

Kluge, A.G. (1989). A concern for evidence and a phylogenetic hypothesis of relationships among *Epicrates* (Boidae, Serpentes). *Systematic Zoology* **38,** 7-25.

Klymkowsky, M.W., and Hanken, J. (1991). Whole-mount staining of *Xenopus* and other vertebrates. *Methods in Cell Biology* **36,** 419-441.

Kobayashi, M., Takahashi, M., Wada, H., and Satoh, N. (1993). Molecular phylogeny inferred from sequences of small subunit ribosomal DNA, supports the monophyly of the metazoa. *Zoological Science* **10,** 827-833.

Kobayashi, M., Wada, H., and Satoh, N. (1996). Early evolution of the metazoa and phylogenetic status of diploblasts as inferred from amino acid sequence of elongation factor-1alpha. *Molecular Phylogenetics and Evolution* **5,** 414-422.

Koelliker, A. (1864/65). Weitere Beobachtungen über die Wirbel der Selachier. *Senckenbergsche Abh.* **5,** 51-99.

Kojima, S., Hashimoto, T., Hasegawa, M., Murata, S., Ohta, S., Seki, H., and Okada, N. (1993). Close phylogenetic relationship between Vestimentifera (tube worms) and Annelida revealed by the amino acid sequence of elongation factor-1alpha. *Journal of Molecular Evolution* **37,** 66-70.

Kowalewsky, A. (1867). Anatomie des *Balanoglossus* Delle Chiaje. *Memoires de l'Academie Imperiale des Sciences de St.-Petersburg* **7,** 10.

Kuettner, K.E., and Pauli, B.U. (1983). Vascularity of Cartilage. *In* "Cartilage: Structure, Function and Biochemistry" (B.K. Hall, Ed.), Vol. 1, pp. 281-312. Academic Press, New York.

Lake, J. A. (1990). Origin of the Metazoa. *Proc. Natl. Acad. Sci. USA* **87,** 763-766.

Lash, J. W., and Vasan, N.S. (1983). Glycosaminoglycans of Cartilage. *In* "Cartilage: Structure, Function and Biochemistry" (B. K. Hall, Ed.), Vol. 1, pp. 215-251. Academic Press, New York.

Lemaire, J. (1970). Table de développement embryonnaire de *Sepia officinalis* L. (Mollusque Céphalopode). *Bull. Soc. Zool. Fr.* **95,** 773-782.

Littlewood, D.T.J., Smith, A.B., Clough, K.A., and Emson, R.H. (1997). The interrelationships of the echinoderm classes: Morphological and molecular evidence. *Biological Journal of the Linnean Society* **61,** 409-438.

Littlewood, D.T., Telford, M.J., Clough, K.A., and Rohde, K. (1998). Gnathostomulida - An enigmatic metazoan phylum from both morphological and molecular perspectives. *Molecular Phylogenetics and Evolution* **9,** 72-79.

Littlewood, D.T.J., Rohde, K., and Clough, K.A. (1999). The interrelationships of all maloy groups of Platyhelminthes: Phylogenetic evidence from morphology and molecules. *Biological Journal of the Linnean Society* **66,** 75-114.

Liu, F., Miyamoto, M., Freire, N., Ong, P., Tennant, M., Young, T., and Gugel ,K. (2001). Molecular and morphological supertrees for eutherian (placental) mammals. *Science* **291,** 1786-1789.

Lorenzo, P., Bayliss, M.T. and Heinegard, D. (1998). A novel cartilage protein (CILP) present in the mid-zone of human articular cartilage increases with age. *The Journal of Biological Chemistry* **273,** 23463-23468.

Luckman, S.P., Rees, E., and Kwan, A.P. (2003). Partial characterization of cell-type X collagen interactions. *Biochemical Journal* **372,** 485-493.

Mackey, L.Y., Winnepenninckx, B., De Wachter, R., Backeljau, T., Emschermann, P., and Garey, J.R. (1996). 18S rRNA suggests that entoprocta are protostomes, unrelated to Ectoprocta. *Journal of Molecular Evolution* **42,** 552-559.

Maclean, N., and Hall, B.K. (1987). "*Cell Commitment and Differentiation.*" Cambridge University Press, Cambridge.

Maddison, W.P., and Maddison, D.R. (1992). "MacClade: Analysis of phylogeny and character evolution." Sinaur Associates, Inc., Sunderland, MA.

Marschall, F. (1907). Beitrage zur anatomie und histologie des tentakelapparates vo *Dasychone bombyx. In* "Zoology". Zool. Inst. Wien.

Marthy, H. (1975). Mise au point d'une culture primaire de cellules à partir du tissue embryonnaire de *Loligo vulgaris* L. (Céphalopode). *C. R. Acad. Sc. Paris* **280,** 291-294.

Marthy, H. (1982). The cephalopod egg, a suitable material for cell and tissue interaction studies. *Embryonic Development, Part B: Cellular aspects,* 223-233.

Marthy, H. (1985). Morphological bases for cell-to-cell and cell-to-substrate interaction studies in cephalopod embryos. *In* "Cellular and molecular control of direct cell interactions" (Marthy, H. Ed.), pp. 159-? Plenum Publishing Corporation.

Marthy, H., and Aroles, L. (1987). *In vitro* culture of embryonic organ and tissue fragments of the squid *Loligo vulgaris* with special reference to the establishment of a long term culture of ganglion-derived nerve cells. *Zool. Jb. Physiol.* **91,** 189-202.

Martin, A.P., and Burg, T.M. (2002). Perils of paralogy: Using HSP70 genes for inferring organismal phylogenies. *Systematic Biology* **51,** 570-587.

Martoja, R., and Bassot, J.M. (1965). Existence d'un tissue conjonctif de type cartilagineux chex certains instectes Orthopteres. *C.R. Hebd. Seances Acad. Sci.* **261,** 2954-2957.

McClintock Turbeville, J. (1991). Nemertinea. *In* "Microscopic anatomy of invertebrates" (F.W. Harrison, and Bogitsh, B.J., Ed.), Vol. 3, pp. 285-328. Wiley-Liss, New York.

McHugh, D. (1997). Molecular evidence that echiurans and pogonophorans are derived annelids. *Proceedings of the National Academy of Sciences USA* **94,** 8006-8009.

McHugh, D. (1998). Deciphering metazoan phylogeny: The need for additional molecular data. *American Zoologist* **38,** 859-866.

Minchin, E.A. (1900). Chapter III: Sponges. *In* "A treatise on zoology" (E.R. Lankaster, Ed.), Vol. 2, pp. 1-178. Adam & Charles Black, London.

Miyata, T., Kuma, K., Iwabe, N. and Nikoh, N. (1994). A possible link between molecular evolution and tissue evolution demonstrated by tissue specific genes. *Japanese Journal of Genetics* **69,** 473-480.

Moon, S.Y., and Kim, W. (1996). Phylogenetic position of the Tardigrada based on the 18S ribosomal RNA gene sequences. *Biological Journal of the Linnean Society* **116,** 61-69.

Moss, M. (1961). Studies of the acellular bone of teleost fish. *Acta Anatomica* **46,** 343-462.

Moss, M. L., and Moss-Salentijn, L. (1983). Vertebrate cartilages. *In* "Cartilage: Structure, Function and Biochemistry" (Hall, B.K. Ed.), Vol. 1, pp. 1-30. Academic Press, New York.

Myllyharju, J., and Kivirikko, J.I. (2004). Collagens, modifying enzymes and their mutations in humans, flies and worms. *Trends in Genetics* **20,** 33-43.

Naef, A. (1928). "Cephalopoda: Embryology." Smithsonian Institution Libraries, Washington, DC.

Nakamura, K., and Yamaguchi, H. (1991). Distribution of scleral ossicles in teleost fishes. *Mem. Fac. Fish. Kagoshima Univ.* **40,** 1-20.

Nefussi, J.R., Brami, G., Modrowski, D., Oboeuf, M., and Forest, N. (1997). Sequential expression of bone matrix proteins during rat calvaria osteoblast differentiation and bone nodule formation in vitro. *The Journal of Histochemistry & Cytochemistry* **45,** 493-503.

Nielsen, C. (2001). "Animal evolution. Interrelationships of the living phyla." Oxford University Press, New York.

Nielsen, C. (2003). Defining phyla: morphological and molecular clues to metazoan evolution. *Evolution & Development* **5,** 386-393.

O'Dor, R.K., Balch, N., Foy, E.A., Hirtle, R.W.M., Johnston, D.A. and Amaratunga, T. (1982). The embryonic development of the squid, *Illex illecebrosus*, and the effects of temperature on development rates. *J. Northwest Atl. Fish. Sci.* **3,** 41-45.

Odorico, D.M., and Miller, D.J. (1997). Internal and external relationships of the Cnidaria: Implications of primary and predicted secondary structure of the 5'-

end of the 23S-like rDNA. *Proceedings of the Royal Society of London B* **264,** 77-82.

Olsson, R. (1965). Comparative morphology and physiology of the *Oikopleura* notochord. *Israel Journal of Zoology* **14,** 213-220.

OOta, S., and Saitou, N. (1999). Phylogenetic relationship of muscle tissues deduced from superimposition of gene trees. *Molecular Biology and Evolution* **16,** 856-67.

Packard, A.S. (1880). "The anatomy, histology, and embryology of *Limulus polyphemus.*" Boston Society of Natural History, Boston.

Page, R. D. M., and Charleston, M.A. (1997). From gene to organismal phylogeny: Reconciled trees and the gene tree/species tree problem. *Molecular phylogenetics and evolution* **7,** 231-240.

Page, L., and Pedersen, R.V.K. (1998). Transformation of phytoplanktivorous larvae into predatory carnivores during the development of *Polinices lewisii* (Mollusca, Caenogastropoda). *Invertebrate Biology* **117,** 208-220.

Page, R.D.M. (1998). GeneTree: comparing gene and species phylogenies using reconciled trees. *BioInformatics* **14,** 819-820.

Page, R.D.M. (2000). Extracting species trees from complex gene trees: Reconciled trees and vertebrate phylogeny. *Molecular Phylogenetics and Evolution* **14,** 89-106.

Pawlowski, J., Montoya-Burgos, J., Fahrni, J.F., Wiiest, J., and Zaninetti, J. (1996). Origin of the metozoa inferred from 18S rRNA gene sequences. *Molecular Biology and Evolution* **13,** 1128-1132.

Person, P., and Mathews, M.B. (1967). Endoskeletal cartilage in a marine polychaete, *Eudistylia polymorpha. Biological Bulletin* **132,** 244-252.

Person, P., and Philpott, D.E. (1967). On the occurrence and the biologic significance of cartilage tissues in invertebrates. *Clinical Orthopedics* **53,** 185-212.

Person, P., and Philpott, D.E. (1969a). The nature and significance of invertebrate cartilages. *Biological Reviews* **44,** 1-16.

Person, P., and Philpott, D.E. (1969b). The biology of cartilage. I. Invertebrate cartilages: *Limulus* gill cartilage. *Journal of Morphology* **128,** 67-94.

Person, P. (1983). Invertebrate cartilages. *In* "Cartilage: Structure, Function and Biochemistry" (Hall, B.K., Ed.), Vol. 1. Academic Press, New York.

Peterson, K.J., Cameron, R.A., and Davidson, E.H. (2000). Bilaterian origins: significance of new experimental observations. *Developmental Biology* **219,** 1-17.

Peterson, K.J., and Eernisse, D.J. (2001). Animal phylogeny and the ancestry of bilaterians: inferences from morphology and 18S rDNA sequences. *Evolution & Development* **3,** 170-205.

Pérez-Pomares, J.M., and Muñoz-Chápuli, R. (2002). Epithelial-mesenchymal transitions: a mesodermal cell strategy for evolutive innovation in metazoans. *The Anatomical Record* **268,** 343-351.

Pisani, D., Yates, A.M., Langer, M.C., and Benton, M.J. (2002). A genus-level supertree of the Dinosauria. *Proceeding of the Royal Society, London. Series B Biological Sciences* **269,** 915-921.

Presnell, J.K., and Schreibman, M.P. (1997). "Humason's Animal Tissue Techniques." The Johns Hopkins University Press, Baltimore & London.

Rabinowitz, J.L., Tavares, C.J., Lipson, R., and Person, P. (1976). Lipid components and *in vitro* mineralization of some invertebrate cartilages. *Biological Bulletin* **150,** 69-79.

Rama, S., and Chandrakasan, G. (1984). Distribution of different molecular species of collagen in the vertebrate cartilage of shark (*Carcharius acutus*). *Connective Tissue Research* **12,** 111-118.

Raven, C.P. (1958). "Morphogenesis: the analysis of molluscan development." Pergamon Press,

Reed, C.G., and Cloney, R.A. (1977). Brachiopod tentacles: Ultrastructure and functional significance of the connective tissue and myoepithelial cells in *Terebratalia. Cell and Tissue Research* **185,** 17-42.

Regier, J.C., and Shultz, J.W. (1998). Molecular phylogeny of arthropods and the significance of the cambrian "explosion" for molecular systematics. *Amercan Zoologist* **38,** 918-928.

Rieger, R.M., Tyler, S., Smith, J.P.S., and Reiger, G.E. (1991). Platyhelminthes: Turbellaria. *In* "Microscopic anatomy of invertebrates" (F. W. Harrison, and Bogitsh, B.J., Ed.), Vol. 3, pp. 7-140. Wiley-Liss, New York.

Rigo, C., and Bairati, A. (2002). A new collagen from the extracellular matrix of *Sepia officinalis* cartilage. *Cell & Tissue Research* **310,** 253-256.

Roach, H.I. (1994). Why does bone matrix contain non-collagenous proteins? the possible roles of osteocalcin, osteonectin, osteopontin and bone sialoprotein in bone mineralisation and resorption. *Cell Biology Inernational* **18,** 617-628.

Robson, G.C. (1929). "Monograph of the recent Cephalopoda: Pt. 1 Octopodinae." Richard Clay & Sons, Ltd., Bungay, Suffolk.

Robson, P., Wright, G.M., and Keeley, F.W. (2000). Distinct non-collagen based cartilages comprising the endoskeleton of the Atlantic hagfish, *Myxine gluinosa*. *Anatomy and Embryology* **202,** 281-290.

Rodrigo, A.G. (1993). A comment on Baum's method for combining phylogenetic trees. *Taxon* **45,** 631-666.

Rodrigo, A.G. (1996). On comparing cladograms. *Taxon* **45,** 267-274.

Romer, A.S. (1942). Cartilage an embryonic adaptation. *American Naturalist* **76,** 394-404.

Rouse, G.W., and Fauchald, K. (1997). Cladistics and polychaetes. *Zoologica Scripta* **26,** 139-204.

Rouse, G.W., and Pleijel, F. (2001). "Polychaetes." Oxford University Press, New York.

Ruiz-Trillo, I., Tiutort, M., Littlewood, D.T.J., Herniou, E.A., and Baguna, J. (1999). Aceol flatworms: Earliest extant bilaterian metazoans, not members of platyhelminthes. *Science* **283,** 1919-1923.

Ruppert, E.E. (1991). Gastrotricha. *In* "Microscopic anatomy of invertebrates" (F. W. Harrison, and Ruppert, E.E., Ed.), Vol. 4: Aschelminthes, pp. 41-109. Wiley-Liss, New York.

Ruppert, E.E. (1997). Cephalochordata (Acrania). *In* "Microscopic anatomy of invertebrates" (F. W. Harrison, and Ruppert, E.E., Ed.), Vol. 15: Hemichordata, Chaetognatha, and the invertebrate chordates, pp. 349-504. Wiley-Liss, New York.

Sanderson, M.J., Purvis, A., and Henze, C. (1998). Phylogenetic supertrees: assembling the trees of life. *Trends in Ecology and Evolution* **13,** 105-109.

Schaffer, J. (1930). Die stutzgewebe. *In* "Hanbuck der mikroskopischen anatomie des menschen" (W. v. Mollendorf, Ed.), pp. 390, Berlin.

Schlegel, M., Lom, J., Stehmann, A., Bernhard, D., Leipe, D., Dykova, I., and Sogin, M.L. (1996). Phylogenetic analysis of complete small subunit ribosomal RNA coding region of *Myxidium lieberkuehni*: Evidence that myxozoa are metazoa and relation to the bilateria. *Archiv fur protisten kunde* **147,** 1-9.

Schmidt-Rhaesa, A., Bartolomaeus, T., Lemburd, C., Ehlers, W., and Garey, J. (1998). The position of the Arthropoda in the phylogenetic system. *Journal of Morphology* **238,** 263-285.

Schmitz, R.J. (1998). Comparative ultrastructure of the cellular components of the unconstricted notochord in the sturgeon and the lungfish. *Journal of Morphology* **236,** 75-104.

Schutze, J., Krasko, A., Custodio, M.R., Efremova, S.M., Muller, I.M., and Muller, W.E.G. (1999). Evolutionary relationships of Metazoa within the eukaryotes based on molecular data from Porifera. *Proceeding of the Royal Society of London B* **266,** 63-73.

Scott-Savage, P. and Hall, B.K. (1979). The timing of the onset of osteogenesis in the tibia of the embryonic chick. *Journal of Morphology* **162,** 453-464.

Sekiguchi, K. (1988). "Biology of Horseshoe Crabs." Science House Co., Tokyo.

Shigeno, S., Tsuchiya, K, and Segawa, S. (2001). Embryonic and paralarval development of the central nervous system of the loliginid squid (*Sepioteuthis lessoniana*). *Journal of Comparative Neurology* **437,** 449-475.

Shigeno, S., and Yamamoto, M. (2002). Organization of the nervous system in the pygmy cuttlefish, *Idiosepius paradoxus* Ortmann (Idiosepiidea, Cephalopoda). *Journal of Morphology* **254,** 65-80.

Shinn, G.L. (1997). Chaetognatha. *In* "Microscopic anatomy of invertebrates" (F. W. Harrison, and Ruppert, E.E., Ed.), Vol. 15: Hemichordata, Chaetognatha, and the invertebrate chordates, pp. 103-220. Wiley-Liss, New York.

Shultz, J. (2001). Gross muscular anatomy of *Limulus polyphemus* (Xiphosura, Chelicerata) and its bearing on evolution in the Arachnida. *The Journal of Arachnology* **29,** 283-303.

Siddall, M.E., Martin, D.S., Bridge, D., Desser, S.S., and Cone, D.K. (1995). The demise of a phylum of protists: phylogeny of myxozoa and other parasitic cnidaria. *Journal of Parasitology* **81,** 961-967.

Sivakumar, P., and Chandrakasan, G. (1998). Occurrence of a novel collagen with three distinct chains in the cranial cartilage of the squid *Sepia officinalis*: comparison with shark cartilage collagen. *Biochimica et Biophysica Acta* **1381,** 161-169.

Sivakumar, P., Suguan, L., and Chandrakasan, G. (2003). Similarity between the major collagens of cuttlefish cranial cartilage and cornea. *Comparative Biochemistry and Physiology Part B* **134,** 171-180.

Smith, S.E., Douglas, R., Burke da Silva, K., and Swalla, B.J. (2003). Morphological and molecular identification of *Saccoglossus* species (Hemichordata: Harrimaniidae) in the Pacific Northwest. *Canadian Journal of Zoology* **84,** 133–141.

Smothers, J.F., von Dohlen, C.D., Smith Jr., L.H., and Spall, R.D. (1994). Molecular evidence that the myxozoan protists and metazoans. *Science* **265,** 1719-1721.

Springer, M.S., and de Jong, W.W. (2001). Phylogenetics. Which mammalian supertree to bark up? *Science* **291,** 1709-1711.

Stricker, S.A., and Reed, C.G. (1985). Development of the pedicle in the articulate brachiopod *Terebratalia transversa* (Brachiopoda, Terebratulida). *Zoomorphology* **105,** 253-264.

Sugahara, K., Tanada, Y., Yamada, S., Seno, N., and Kitagawa, H. (1996). Novel sulfated oligosaccharides containing 3-*O*-Sulfated glucuronic acid from king crab cartilage chondroitin sulfate K. *The Journal of Biological Chemistry* **271,** 26745-26754.

Swalla, B.J. (2004). Evolution of the chordates: Worms or squirts? I*n* "Society for Integrative and Comparative Biology", pp. Abs. 12.3, New Orleans, Louisiana.

Swofford, D.L., and Maddison, W.P. (1992). Parsimony, character-state reconstructions, and evolutionary inferences. *In* "Systematics, Historical Ecology, and North American Freshwater Fishes" (R.L. Mayden, Ed.). Stanford University Press, Stanford, California.

Symonds, M.R. (2002). The effects of topological inaccuaracy in evolutionary trees on the phylogenetic comparative method of independent contrasts. *Systematic Biology* **51,** 541-553.

Taylor, L.H., Hall, B.K., Miyake, T. and Cone, D.K. (1994). Ectopic ossicles associated with metacercariae of *Apophallus brevis* (Trematoda) in yellow perch, *Perca flavescens* (Teleostei): development and identification of bone and chondroid bone. *Anatomy and Embryology* **190,** 29-46.

Telford, M.J., and Holland, P.W.H. (1993). The phylogenetic affinities of the chaetognaths: A molecular analysis. *Molecular Biology and Evolution* **10,** 660-676.

Thouveny, Y., and Tassava, R.A. (1998). Regeneration through phylogenesis. *In* "Cellular and molecular basis of regeneration: From invertebrates to humans" (P. Ferretti, and Géraudie, J., Ed.), pp. 9-43. John Wiley & Sons Ltd., New York.

Tillet, E., Franc, J. M., Franc, S., and Garrone, R. (1996). The evolution of fibrillar collagens: A sea-pen collagen shares common features with vertebrate type V collagen. *Comparative Biochemistry and Physiology* **113B,** 239-246.

Tompsett, D.H. (1939). "Sepia." The University Press of Liverpool, Liverpool.

Tsilemou, A., Giannicopoulou, P., and Vynois, D.H. (1998). Identification of a protein in squid cranial cartilage with link protein properties. *Biochimie* **80,** 591-594.

Turbeville, J.M., Pfeifer, D.M., Field, K.G., and Raff, R.A. (1991). The phylogenetic status of arthropods, as inferred from 18S rRNA sequences. *Molecular Biology and Evolution* **8,** 669-686.

Turbeville, J.M., Field, K.G., and Raff, R.A. (1992). Phylogenetic position of phylum Nemertini, inferred from 18S rRNA sequences: Molecular data as a test of morphological character homology. *Molecular Biology and Evolution* **9,** 235-249.

Turbeville, J.M., Schulz, J.R., and Raff, R.A. (1994). Deuterostome phylogeny and the sister group of the chordates: Evidence form molecules and morphology. *Molecular Biology and Evolution* **11,** 648-655.

Vecchione, M., Young, R.E., and Clarini, D.B. (2000). Reconstruction of ancestral character states in neocoleoid cephalopods based on parsimony. *American Malacological Bulletin* **15,** 179-193.

Vynios, D.H., Aletras, A., Tsiganos, C.P., Tsegenids, T., Antonopoulos, C.A., Hjerpe, A., and Engfeldt, B. (1985). Proteoglycans from squid cranial cartilage: Extraction and characterization. *Comparative Biochemistry and Physiology* **80B,** 761-766.

Vynios, D.H., and Tsiganos, C.P. (1990). Squid proteoglycans: Isolation and characterization of three populations from cranial cartilage. *Biochimie & Biophys. Acta* **1033,** 139-47.

Vynios, D.H., Morgelin, M., Papageorgakopoulou, N., Tsilemou, A., Spyracopoulou, G., Zafira, M. and Tsiganos, C.P. (2000). Polydispersity and heterogeneity of squid cranial cartilage proteoglycans as assessed by immunochemical methods and electron microscopy. *Biochimie* **82,** 773-782.

Vynios, D.H., Papageorgakopoulou, N., Sazakli, H., and Tsiganos, C.P. (2001). The interactions of cartilage proteoglycans with collagens are determined by their structures. *Biochimie* **83,** 899-906.

Wada, H., and Satoh, N. (1994). Details of the evolutionary history from invertebrates to vertebrates, as deduced from the sequences of 18S rDNA. *Proceedings of the National Academy of Sciences, USA* **91,** 1801-1804.

Wagele, J.W., and Stanjek, G. (1995). Arthropod phylogeny inferred from partial 12SrRNA revisited: monophyly of the Tracheata depends on sequence alignment. *Journal of Zoological Systematics and Evolution Research* **33,** 75-80.

Wells, G.P. (1952). The respiratory significance of the crown in the polychaete worms *Sabella* and *Myxicola. Proceedings of the Royal Society, London, Series B* **140,** 70-82.

Welsch, U., Erlinger, R., Potter, I.C. (1991). Proteoglycans in the notochord sheath of lampreys. *Acta Histochem* **91,** 59-65.

Welsch, U., Chiba, A., and Honma, Y. (1998). The notochord. *In* "The biology of hagfishes" (J. Jorgensen, ., Lomholt, J.P., Weber, R.E., and Malte, H., Ed.), pp. 145-159. Chapman & Hall, London.

Wilkinson, M. (1995). Coping with abundant missing entries in phylogenetic inference using parsimony. *Systematic Biology* **44,** 501-514.

Williams, L.W. (1909). "The anatomy of the common squid, *Loligo pealii*, Lesueur." E.J. Brill, Leiden, Holland.

Windholtz, M., Budavari, S., Stroumtsos, L.Y., and Noether Fertic, M. (1976). The Merck Index. Merck & Co., Inc., Rathway, NJ.

Winnepennickx, B., Backeljau, T., van de Peer, Y., and De Wachter, R. (1992). Structure of the small ribosomal subunit RNA of the pulmonate snail, *Limicolaria kambeul,* and phylogenetic analysis of the metazoa. *Federation of European Biochemical Societies* **309,** 123-126.

Winnepenninckx, B., Backeljau, T., and De Wachter, R. (1995). Phylogeny of protostome worms derived from 18S rRNA sequences. *Molecular Biology and Evolution* **12,** 641-649.

Winnepenninckx, B., Backeljau, T., Mackey, L.Y., Brooks, J.M., De Wachter, R., Kumar, S., and Garey, J.R. (1995b). 18S rRNA data indicate that aschelminthes are polyphyletic in origin and consist of at least three distinct clades. *Molecular Biology and Evolution* **12,** 1132-1137.

Winnepenninckx, B.M.H., Backeljau, T., and Kristensen, R.M. (1998a). Relations of the new phylum Cycliophora. *Nature* **393,** 636-638.

Winnepenninckx, B., Steiner, G., Backeljau, T., and DeWachter, T. (1998b). Details of gastropod phylogeny inferred from 18S rRNA sequences. *Molecular Phylogenetics and Evolution* **9,** 55-63.

Witten, P.E., and Hall, B.K. (2002). Differentiation and growth of kype skeletal tissues in anadromous male Atlantic Salmon (*Salmo salar*). *International Journal of Developmental Biology* **46,** 719-730.

Witten, P.E., Huysseune, A., Franz-Odendaal, T., Fedak, T., Vickaryous, M., Cole, A., and Hall, B.K. (2004). Acellular teleost bone: dead or alive, primitive or derived? *The Palaeontology Newsletter* **56?,** in press.

Wood, A., Ashhurst, D.E., Corbett, A., and Thorogood, P. (1991). The transient expression of type II collagen at tissue interfaces during mammalian craniofacial development. *Development* **111,** 955-68.

Wright, G.M., F.W. Keeley, and M.E. DeMont. (1998). Hagfish cartilage. *In* "The Biology of Hagfishes" (J. P. L. Jorgon Morup Jorgensen, Roy Weber, and Hans Malte, Ed.), pp. 160-170. Chapmand & Hall, London.

Wright, G.M., Keeley, F.W., and Robson, P. (2001). The unusual cartilaginous tissues of jawless craniates, cephalochordates and invertebrates. *Cell and Tissue Research* **304,** 165-74.

Yan, Q., and Sage, E.H. (1999). SPARC, a matricellular glycoprotein with important biological functions. *The Journal of Histochemistry & Cytochemistry* **47,** 1495-1505.

Zrzavy, J., Hypsa, V., and Tietz, D.F. (2001). Myzostomida are not annelids: Molecular and morphological support for a clade of animals with anterior sperm flagella. *Cladistics* **17,** 170-198.

Appendix 1: Source trees used in supertree analysis

A supertree matrix was constructed from previously published hypotheses, derived from analysis of only molecular data. Source papers in which more than a single viable hypothesis was represented had both topologies included in the matrix; see text for details. References not included in the original genera-grade analysis are highlighted in bold typeface.

Source	Figure	Data
Giribet 96	1	18S
Moon 96	1a,c	18S
Turbeville 91	5	18S
Winnepenninckx 95a	1,2	18S
Wada 94	1	18S
Collins 98	2,3	18S
Katayama 95	2	18S
Kobayachi 93	1	18S
Pawlowski 96	2	18S
Ruiz-Trillo 99	2	18S
Winnepenninckx 95b	1,2	18S
Garey 96	1	18S
Balavoine 97	3	18S
Katayama 93	3	18S
Winnepenninckx 98a	1	18S
Halanych 96a	1b	18S
Turbeville 94	2a	18S
Field 88	2	18S
Halanych 96b	2a,4b	18S
Telford 93	2,4	18S
Halanych 95	1	18S
Turbeville 92	3a	18S
Hendriks 88	3	18S
Boore 95	1	18S
Abele 89	2a	18S
Littlewood 98	1	18S
Schmidt-Rhaesa 98	2	18S
Aguinaldo 97	2,3	18S
Halanych 95	1	18S
Hanelt 96	1	18S
Smothers 94	1	18S
Bridge 95	2	18S
Winnepennickx 92	2	18S
Lake 90	3	18S
Giribet 98	(pg484)	18S
Mackey 96	1,2	18S
Cavalier-Smith 96	(pp2035,37, 38)	18S
Carranza 97	3,4,5,6	18S
Siddal 95	3a,c	18S
Cameron 00	2	18S
Littlewood 99	4a	18S
Halanych 98	3	18S
Winnepennickx 98b	5	18S
Peterson 01	2	18S
Zrzavy 01	2c,d,3,4	18S
Giribet 00	2	18S
Kojima 93	2	EF-α
Kobayachi 96	1,3,4	EF-α
McHugh 97	1	EF-α
Regier 98	4	EF-α
Eeckhaut 00	4	EF-α
Berney 00	3	EF-α
Wagele 95	5	12S
Ballard 92	3	12S
Schlegel 96	3	16S
Odorico 97	2	23S
Littlewood 97	4,5	28S
Friedrich 95	1	18S+28S
Christen 91	3	28S
Black 97	2	COI
Boore 02	4	COX
Schutze 99	1	HSP70;
	2	protein
	4	kinase; β-tubulin

Appendix 2: Electronic material

A2.1 Genera-grade matrix

Name: 1-Genera-grade.nex
File type: text file
Description: Nexus file, readable with MaClade, PAUP*, or any word processing program

A2.2 Class- and Phyla-grade matrix

Name: 2-Class_Phyla-grade.nex
File type: text file
Description: Nexus file, readable with MaClade, PAUP*, or any word processing program

A2.3 Full genera-grade supertree

Name: 3-Genera-grade_tree.rtf
File type: Rich text file
Description: Readable with any word processing program

A2.4 Cephalopod supertree matrix

Name: 4a-Cephalopoda_Genera.nex; 4b-Cephalopoda_Order.nex
File type: text files
Description: Nexus files, readable with MaClade, PAUP*, or any word processing program

A2.5 Classification of Cephalopoda

Name: 5-cephclassification.pdf
File type: Adobe PDF document
Description: Available from ceph-base (http://www.cephbase.utmb.edu/): lists classification of current cephalopod taxa current as of May, 2001